NASA TECHNICAL MEMORANDUM

NASA TM X-2569

NASA TM X-2569

SUPERSONIC AERODYNAMIC CHARACTERISTICS OF A TWO-STAGED SPACE-SHUTTLE MODEL HAVING A DELTA-WING ORBITER MATED ATOP A WINGED BOOSTER

by Ernald B. Graves

Langley Research Center
Hampton, Va. 23365

NATIONAL AERONAUTICS AND SPACE ADMINISTRATION • WASHINGTON, D. C. • SEPTEMBER 1972

1 Report No	2 Government Accession No	3 Recipient's Catalog No
NASA TM X-2569		

4 Title and Subtitle	5 Report Date
SUPERSONIC AERODYNAMIC CHARACTERISTICS OF A TWO-STAGED SPACE-SHUTTLE MODEL HAVING A DELTA-WING ORBITER MATED ATOP A WINGED BOOSTER	September 1972
	6 Performing Organization Code

7 Author(s)	8 Performing Organization Report No
Ernald B. Graves	L-8300
	10 Work Unit No
9 Performing Organization Name and Address	117-07-01-03
NASA Langley Research Center Hampton, Va. 23365	11 Contract or Grant No
	13 Type of Report and Period Covered
12 Sponsoring Agency Name and Address	Technical Memorandum
National Aeronautics and Space Administration Washington, D.C. 20546	14 Sponsoring Agency Code

15 Supplementary Notes

16 Abstract

An investigation has been conducted in the Langley Unitary Plan wind tunnel to determine the static aerodynamic characteristics of a two-staged space-shuttle system consisting of a delta-wing orbiter mated atop ("piggy-back") a winged booster. The tests were performed at Mach numbers from 2.30 to 4.60 at a Reynolds number of 8.2×10^6 per meter (2.50×10^6 per ft).

17 Key Words (Suggested by Author(s))	18 Distribution Statement
Space shuttle Booster Orbiter Delta wing Supersonic aerodynamic characteristics	Unclassified – Unlimited

19 Security Classif (of this report)	20 Security Classif (of this page)	21 No of Pages	22 Price*
Unclassified	Unclassified	259	$3.00

*For sale by the National Technical Information Service, Springfield, Virginia 22151

SUPERSONIC AERODYNAMIC CHARACTERISTICS OF A TWO-STAGED SPACE-SHUTTLE MODEL HAVING A DELTA-WING ORBITER MATED ATOP A WINGED BOOSTER

By Ernald B. Graves
Langley Research Center

SUMMARY

An investigation has been conducted in the Langley Unitary Plan wind tunnel to determine the static aerodynamic characteristics of a two-staged space-shuttle system consisting of a delta-wing orbiter mated atop ("piggy-back") a winged booster. The tests were performed at Mach numbers from 2.30 to 4.60 at a Reynolds number of 8.2×10^6 per meter (2.50×10^6 per ft).

The test results of the ascent (mated) configuration indicated nonlinear pitching-moment variations with lift coefficient and only limited aileron and rudder-control effectiveness. The orbiter configuration also exhibited nonlinear pitching-moment characteristics and indicated stable trim capability for only a relatively low angle-of-attack range. The data also indicated that the orbiter rudder was ineffective at high angles of attack and at the higher test Mach numbers. The booster configuration (with vertical fins) also produced nonlinear pitching moments and, because of pitch-up, indicated stable trim only up to angles of attack of about 4° at Mach numbers to 2.96. At higher Mach numbers low-angle instability occurred but with second stable trim points of about 25° at a Mach number of 3.95 and about 50° at 4.60. Use of ventral fins on the booster eliminated the pitch-up but increased the negative pitching-moment values near zero lift.

INTRODUCTION

The National Aeronautics and Space Administration is currently conducting studies of several space-shuttle systems designed to provide low-cost reusable space-flight vehicles. One of the configurations being developed is a two-staged system wherein a delta-wing orbiter is mated atop a winged booster designed for vertical launch. Each stage is planned to have the capability of landing on conventional airport runways. As a part of this configuration study, tests have been performed in the Langley Unitary Plan wind tunnel at Mach numbers from 2.30 to 4.60 to determine the static aerodynamic char-

acteristics of the booster and orbiter vehicles as well as of the mated system. The tests were performed at a Reynolds number of 8.2×10^6 per meter (2.50×10^6 per ft).

SYMBOLS

Aerodynamic coefficients are referenced to the body-axis system except for lift and drag which are referenced to the stability-axis system. For the ascent (mated) configuration the moment reference is at 71.3 percent of the body length of the booster; for the booster the moment reference is at 67.1 percent of the body length of the booster; and for the orbiter the moment reference is at 67.0 percent of the body length of the orbiter. Values are given in SI units and the equivalent values are given parenthetically in U.S. Customary Units. Measurements were made in U.S. Customary Units. The symbols are defined as follows:

b	reference wing span
C_A	axial-force coefficient, $\frac{\text{Axial force}}{qS_w}$
C_D	drag coefficient, $\frac{\text{Drag}}{qS_w}$
$C_{D,o}$	zero-lift drag coefficient
C_L	lift coefficient, $\frac{\text{Lift}}{qS_w}$
C_{L_α}	lift-curve slope per degree (near $\alpha = 0^o$)
C_l	rolling-moment coefficient, $\frac{\text{Rolling moment}}{qbS_w}$
C_{l_β}	effective dihedral parameter per degree, $\left(\frac{\Delta C_l}{\Delta \beta}\right)_{\beta=0^o,3^o}$
C_{l_δ}	roll-control parameter per degree at $\alpha \approx 0^o$, $\frac{\Delta C_l}{\Delta \delta}$
C_m	pitching-moment coefficient, $\frac{\text{Pitching moment}}{q\bar{c}S_w}$
C_{m_δ}	pitch-control parameter per degree at $\alpha \approx 0^o$, $\frac{\Delta C_m}{\Delta \delta}$
$C_{m,o}$	pitching-moment coefficient at zero lift

C_N normal-force coefficient, $\frac{\text{Normal force}}{qS_w}$

C_n yawing-moment coefficient, $\frac{\text{Yawing moment}}{qbS_w}$

C_{n_β} directional-stability parameter per degree, $\left(\frac{\Delta C_n}{\Delta \beta}\right)_{\beta=0^o,3^o}$

C_{n_δ} yaw-control parameter per degree at $\alpha \approx 0^o$, $\frac{\Delta C_n}{\Delta \delta}$

$C_{p,b}$ base-pressure coefficient, $\frac{p_b - p}{q}$

$C_{p,c}$ chamber-pressure coefficient, $\frac{p_c - p}{q}$

$C_{p,n}$ nozzle-pressure coefficient, $\frac{p_n - p}{q}$

C_Y side-force coefficient, $\frac{\text{Side force}}{qS_w}$

C_{Y_β} side-force parameter per degree, $\left(\frac{\Delta C_Y}{\Delta \beta}\right)_{\beta=0^o,3^o}$

- reference chord of wing

.g. center of gravity

./D lift-drag ratio

L/D)$_{max}$ maximum lift-drag ratio

I free-stream Mach number

free-stream static pressure

b base static pressure

c chamber static pressure

n nozzle static pressure

free-stream dynamic pressure

S_b base area

S_c chamber area

S_n nozzle area

S_w reference area of wing

x_{ac}/l aerodynamic-center location from body nose, percent body length

α angle of attack, degrees

β angle of sideslip, degrees

δ control-surface angle, accompanied by subscript denoting surface or surface rudder deflected (positive, trailing edge down or left when viewed from downstream)

Model nomenclature:

B_b booster body

B_o orbiter body

E orbiter elevon

e booster elevon

L5 combination of booster body, wing, canard, and vertical fins (basic booster configuration)

L8 combination of booster body, wing, canard, and ventral fins

02 combination of orbiter body, wing, and vertical tail (basic orbiter configuration)

R orbiter vertical tail

U booster ventral fin

V, V_b booster vertical fin

W_b booster wing

W_o orbiter wing

APPARATUS AND METHODS

Tunnel

The investigation was conducted in the high Mach number test section of the Langley Unitary Plan wind tunnel which is a variable-pressure, continuous-flow facility. The test section is about 1.22 meters (4 ft) square and 2.13 meters (7 ft) long, and the nozzle leading to the test section is of the asymmetric sliding-block type which permits a continuous variation in Mach number from about 2.3 to 4.7.

Models

Drawings of the models are shown as figure 1, and photographs of the models are presented as figure 2.

Booster-alone configuration.- The booster model consisted of a body, a high aft-mounted wing with tip fins, and a low-mounted jet canard. The wing had NACA 0010-64 airfoil sections with 3° of incidence and 7.7° dihedral. The leading-edge sweep of the wing was 44°. Elevons were provided on the wing trailing edge with the capability of deflecting $\pm 20^\circ$ in 10° increments. Wing-tip fins were provided for both vertical and ventral positions. These fins had 25° of rollout and trailing-edge rudders which deflected 0° outboard in the vertical position (L5 configuration) and 10° inboard in the ventral position (L8 configuration). The rudders could be positioned from 10° to -20° in 10° increments. Unless otherwise noted, booster data presented in this paper will be for the L5 configuration. The canard was rectangular in planform and had NACA 63-018 airfoil sections and 3° of incidence.

Orbiter-alone configuration.- The orbiter model had a low delta wing that was blended into the body and had wing sections that consisted of NACA 0012-64 at the root tapering to NACA 0010-64 at the tip. The wing had 10° dihedral, 2° incidence, and 55° leading-edge sweep. Trailing-edge elevons were furnished in the wing with deflection capability from 0° to -45° in 15° increments. A center-line vertical tail including a rudder was also provided with rudder deflections of 0° and 10°.

Launch configuration.- The launch or ascent configuration consisted of the orbiter mounted atop the booster with 0° incidence. Wing-tip fin rudders were positioned at 0° deflection. The orbiter was balance-mounted to a strut that was rigidly fastened to the

booster model. Only a minimum of clearance was maintained between the two models to prevent fouling.

Test Conditions

The tests were performed at the following conditions:

Mach number	Stagnation temperature		Stagnation pressure	
	K	^{o}F	kN/m^2	lb/ft^2
2.30	338.7	150	91.690	1915
2.96	338.7	150	129.803	2711
3.95	352.6	175	231.214	4829
4.60	352.6	175	321.133	6707

Configuration	Range of α, deg
Launch (mated)	-10 to 10
Orbiter	-10 to 35
Booster	-10 to 60

The Reynolds number was held constant at 8.2×10^6 per meter (2.50×10^6 per ft) except where model loads exceeded the balance limits. Test-section dewpoint temperature was maintained sufficiently low so as to assure negligible condensation effects.

Transition strips composed of single-spaced No. 45 sand grit placed three diameters apart were affixed to the wing and fin surfaces 1.0 centimeter (0.4 in.) aft of the leading edges in a streamwise direction and around the nose of each model 3.05 centimeters (1.2 in.) aft of the nose apex.

Measurements and Corrections

Forces and moments were measured on each model by means of internally mounted six-component strain-gage balances which, in turn, were rigidly fastened to an aft sting-support system. For the launch configuration, the balance in the orbiter was fastened to a strut which emerged from the underside of the orbiter and was rigidly fastened to the booster model.

Pressures were measured in the balance chamber and at the base of each model. For the booster model, the pressure was also measured at the base of the nozzle.

Angles of attack and sideslip have been corrected for sting-balance deflection due to aerodynamic loads on the model. In addition, angles of attack have been corrected for tunnel airflow misalinement.

The axial-force and drag-coefficient data have been adjusted to correspond to free-stream conditions acting over the base, chamber, and nozzles (where applicable) of each model. For the launch configuration, no adjustments were made for the base and chambe

pressures acting on the orbiter model. Typical values of base, chamber, and nozzle pressure coefficients for the various configurations are shown in figure 3.

DATA-REDUCTION CONSTANTS

Coefficient data presented in this paper are based on the following reference quantities:

Ascent and booster configurations:

$S_w = 0.046\ m^2$ $(0.490\ ft^2)$
$b = 0\ 4267\ m$ $(16.80\ in)$
$\bar{c} = 0.4267\ m$ $(16.80\ in)$

} Dimensions are not consistent with booster-model dimensions. (See fig. 1(c).)

$S_b = 0.00167\ m^2$ $(0.017986\ ft^2)$
$S_c = 0.00155\ m^2$ $(0.01667\ ft^2)$
$S_n = 0.00057\ m^2$ $(0.00618\ ft^2)$

Orbiter configuration:

$S_w = 0.0252\ m^2$ $(0.2716\ ft^2)$
$b = 0.22936\ m$ $(9.030\ in.)$
$\bar{c} = 0.1314\ m$ $(5.174\ in.)$
$S_b = 0.00136\ m^2$ $(0.01469\ ft^2)$
$S_c = 0.00067\ m^2$ $(0.00721\ ft^2)$

PRESENTATION OF RESULTS

The results of the tests are presented in the following figures:

	Figure
Ascent configuration:	
Effect of booster components on longitudinal characteristics	4
Effect of orbiter components on longitudinal characteristics	5
Effect of booster vertical-fin rudder deflection on longitudinal characteristics	6
Effect of booster-elevon deflection-in-roll on longitudinal characteristics	7
Lateral characteristics in sideslip	8
Booster vertical-fin rudder-control effectiveness	9
Booster-elevon roll-control effectiveness	10
Lateral-stability parameters	11
Summary of characteristics	12
Effect of booster components on longitudinal characteristics of orbiter	13
Effect of orbiter components on longitudinal characteristics of orbiter	14
Lateral characteristics of orbiter in sideslip	15

Figure

Orbiter configuration:
Elevon pitch-control effectiveness 16
Effect of elevon deflection-in-roll on longitudinal characteristics 17
Effect of vertical-tail rudder deflection on longitudinal characteristics 18
Lateral characteristics in sideslip 19
Effect of elevon deflection-in-pitch on lateral characteristics 20
Elevon roll-control effectiveness 21
Effect of vertical-tail rudder deflection on lateral characteristics 22
Lateral-stability parameters 23
Summary of characteristics 24

Booster configuration:
Elevon pitch-control effectiveness 25
Effect of vertical location of wing-tip fins on longitudinal characteristics 26
Effect of elevon deflection-in-roll on longitudinal characteristics 27
Effect of vertical-fin rudder deflection on longitudinal characteristics 28
Effect of ventral-fin rudder deflection on longitudinal characteristics 29
Lateral characteristics in sideslip 30
Effect of vertical location of wing-tip fins on lateral characteristics 31
Effect of elevon deflection-in-pitch on lateral characteristics 32
Elevon roll-control effectiveness 33
Effect of vertical-fin rudder deflection on lateral characteristics 34
Effect of ventral-fin rudder deflection on lateral characteristics 35
Lateral-stability parameters 36
Summary of characteristics 37

DISCUSSION

Ascent Configuration

It should again be noted that the reference dimensions used in presenting both booster and launch data are greater than those dictated by model geometry. The control-effectiveness parameters presented would be somewhat greater when using the actual dimensions of the model.

The variation of pitching-moment coefficient with lift coefficient is relatively nonlinear (fig. 4). The lateral data are reasonably linear with angle of sideslip at angles of attack near 0° and 10° (fig. 8). Rudder-control effectiveness (fig. 9) is limited and is accompanied by adverse rolling moments. Booster-aileron control (fig. 10) also appears limited, especially at the higher test Mach numbers, and adverse yawing moments are encountered. The summary data (fig. 12) show a general decrease in C_{L_α}, $C_{D,o}$, C_{l_δ},

and C_{n_δ} with increase in Mach number. In addition, a large forward movement in aerodynamic-center location with increase in Mach number occurs and the static margin decreases rapidly for this test range investigated. It is felt that the unstable characteristics of the model seen in figure 4 are a result of the moment reference location for the configuration being well aft of a realistic center-of-gravity location. A realistic center-of-gravity variation for the vehicle in this Mach number range may be noted in figure 12.

Orbiter Configuration

The pitching-moment variations with lift coefficient (fig. 16) are nonlinear to the extent that, for the center-of-gravity location of these tests, the orbiter model can achieve stable trim only up to $\alpha \approx 15^\circ$ at $M = 2.30$ with $\delta_E = -45^\circ$. This trim range reduced to $\alpha \approx 12^\circ$ at $M = 2.96$, to about 8° at $M = 3.95$, and to about 3° at $M = 4.63$. The elevon did produce positive pitching moments, but the large negative $C_{m,o}$ and the nonlinearities precluded the achievement of high trim angles of attack. Values of $(L/D)_{max}$ vary from about 3.0 to 2.5 with increasing Mach number (fig. 24).

Roll control is provided by the elevons throughout the test angle-of-attack and Mach number ranges (fig. 21); however, unfavorable yawing moments are encountered at the higher test angles of attack. The yaw-control capability of the vertical-tail rudder decreases markedly with increasing Mach number and angle of attack such that at the highest Mach numbers and angles of attack the rudder becomes ineffective (fig. 22) and slightly adverse rolling moments are encountered.

Booster Configuration

The variation of pitching moment with lift is quite nonlinear, indicating low-angle stable trim only up to $\alpha \approx 4^\circ$ at $M = 2.30$ and 2.96 with second trim points occurring at higher angles of attack. Second trim points occurred between $\alpha \approx 25^\circ$ at $M = 3.95$ and $\alpha \approx 50^\circ$ at $M = 4.60$ with instability occurring at low angles of attack (fig. 25). A comparison of wing-tip ventral fins (L8) with wing-tip vertical fins (L5; see fig. 26) shows that the ventral-fin configuration has a more negative $C_{m,o}$ but provides a slightly higher C_{L_α} and maximum C_L. Although the stability level of the two configurations is essentially the same at low angles of attack, the pitch-up characteristics of the booster are considerably improved through the addition of the ventral fins. Pitch-control effectiveness was not investigated for the configuration with the ventral fins. However, an examination of both the data obtained with the vertical fins in combination with the basic data (L5) and the data obtained with the ventral fins (L8) indicates that, in spite of the more negative values of pitching-moment coefficient at zero lift, the L8 configurations should achieve higher trim angles of attack because of the improved linearity.

The elevons are effective in producing rolling moment (fig. 33); and although this effectiveness decreases with Mach number at low angles of attack, there is an increase

in effectiveness with increasing angle of attack, particularly with increasing Mach number. However, adverse yawing moments are associated with elevon roll control. The vertical-fin rudder is effective in producing yawing moment (fig. 34) and some adverse roll although these moments tend to decrease with increasing Mach number and angle of attack. The ventral-fin rudders are much less effective than the vertical-fin rudders in producing yawing moment and even cause some yaw reversal and large positive increments of roll (fig. 35).

The lateral stability characteristics for the booster configuration (fig. 36) are quite nonlinear; and the directional stability, in general, appears to be inadequate for the moment reference point of these tests.

CONCLUDING REMARKS

An investigation has been conducted in the Langley Unitary Plan wind tunnel to determine the static aerodynamic characteristics of a two-staged space-shuttle system consisting of a delta-wing orbiter mated atop ("piggy-back") a winged booster designed for vertical launch. The tests were performed at Mach numbers from 2.30 to 4.60 at a Reynolds number of 8.2×10^6 per meter (2.50×10^6 per ft).

The test results of the ascent (mated) configuration indicated nonlinear pitching-moment variations with lift coefficient and only limited aileron and rudder-control effectiveness. The orbiter configuration also exhibited nonlinear pitching-moment characteristics and indicated stable trim capability for only a relatively low angle-of-attack range. The data also indicated that the orbiter rudder was ineffective at high angles of attack and at the higher test Mach numbers. The booster configuration (with vertical fins) also produced nonlinear pitching moments and, because of pitch-up, indicated stable trim only up to angles of attack of about 4° at Mach numbers to 2.96. At higher Mach numbers low-angle instability occurred but with second stable trim points of about 25° at a Mach number of 3.95 and about 50° at 4.60. Use of ventral fins on the booster eliminated the pitch-up but increased the negative pitching-moment values near zero lift.

Langley Research Center,
National Aeronautics and Space Administration,
Hampton, Va., July 13, 1972.

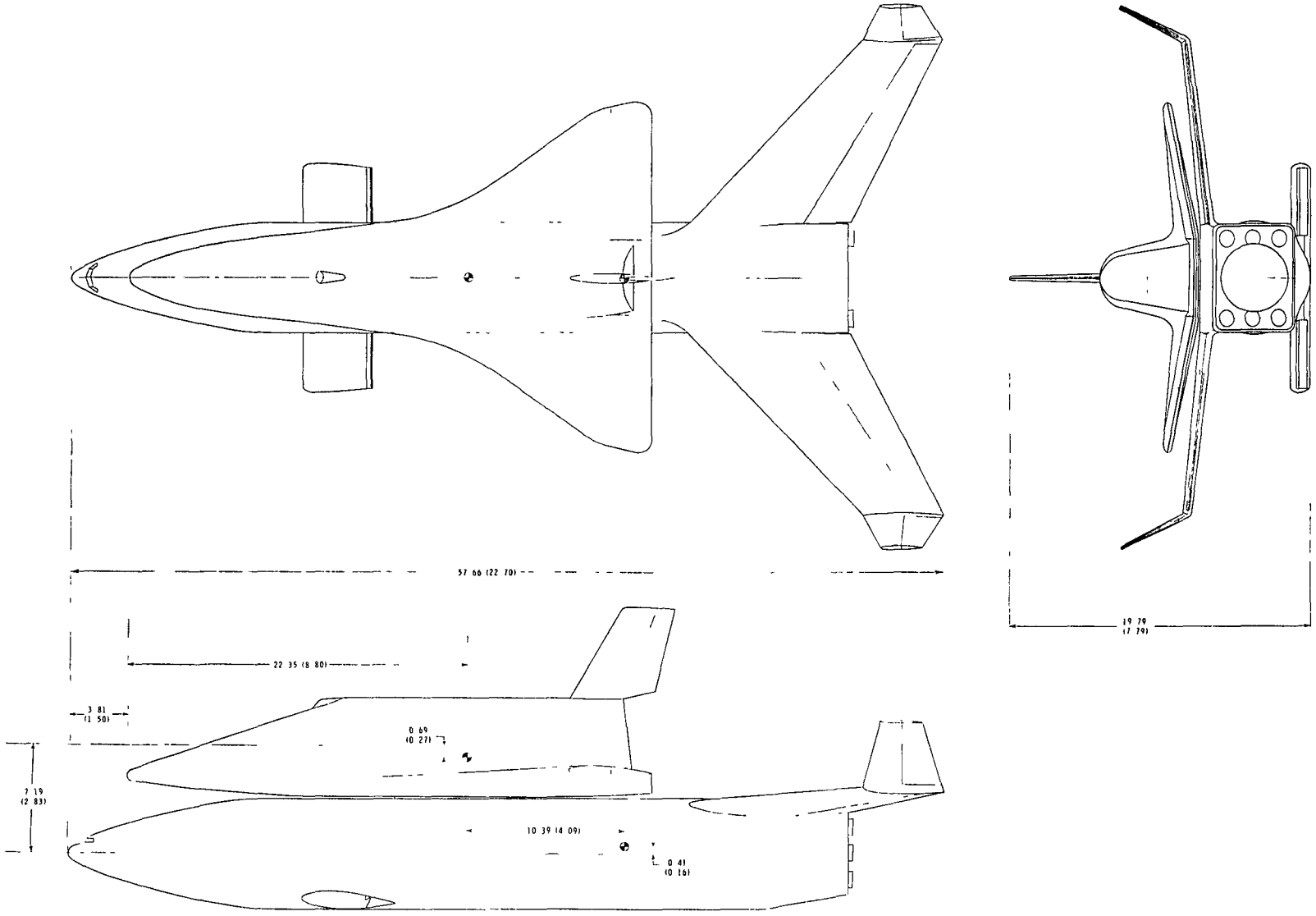

(a) Ascent configuration.

Figure 1.- Drawings of models. Unless otherwise noted, all dimensions are in centimeters (in.).

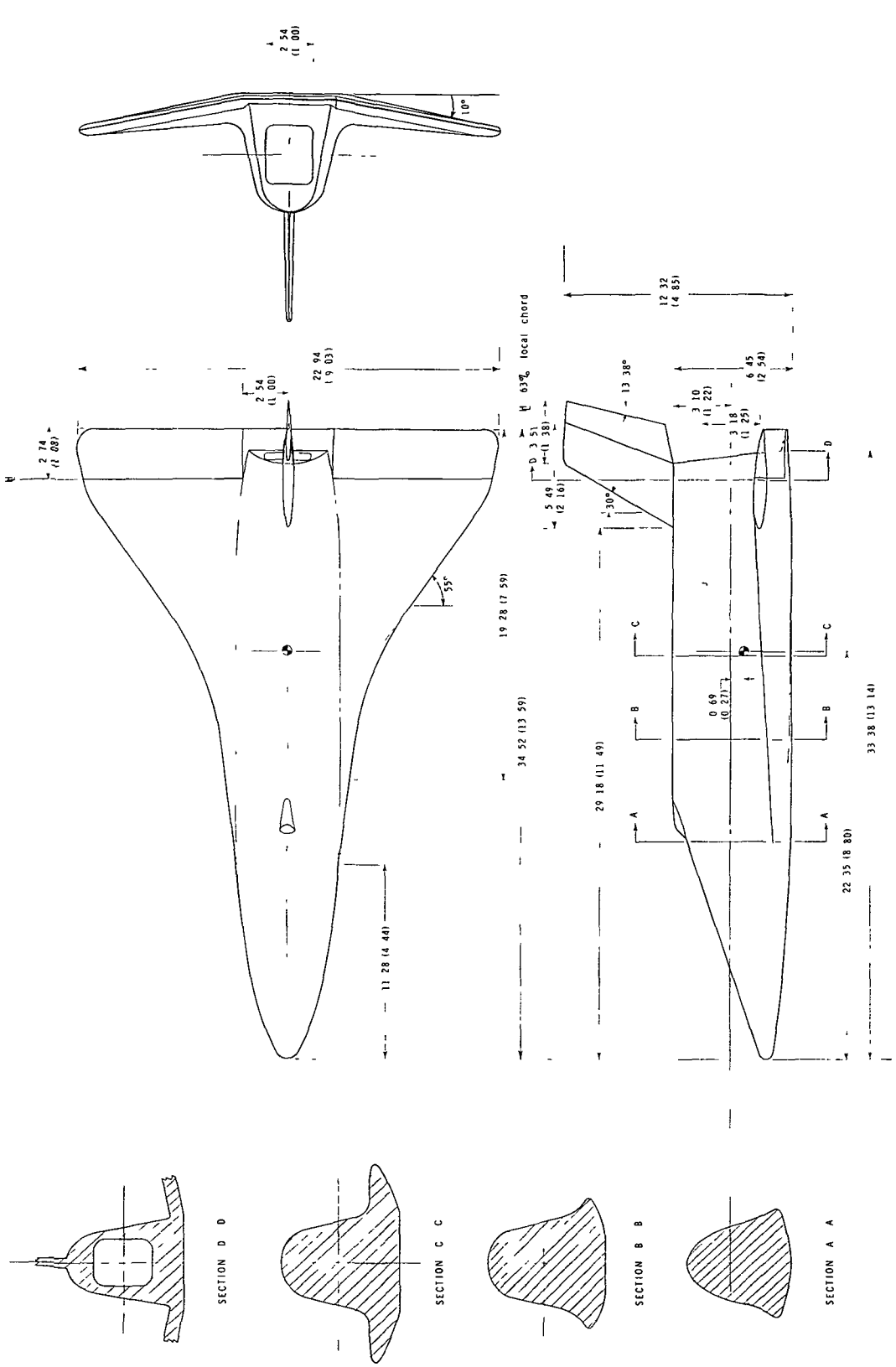

(b) Orbiter model.

Figure 1.- Continued.

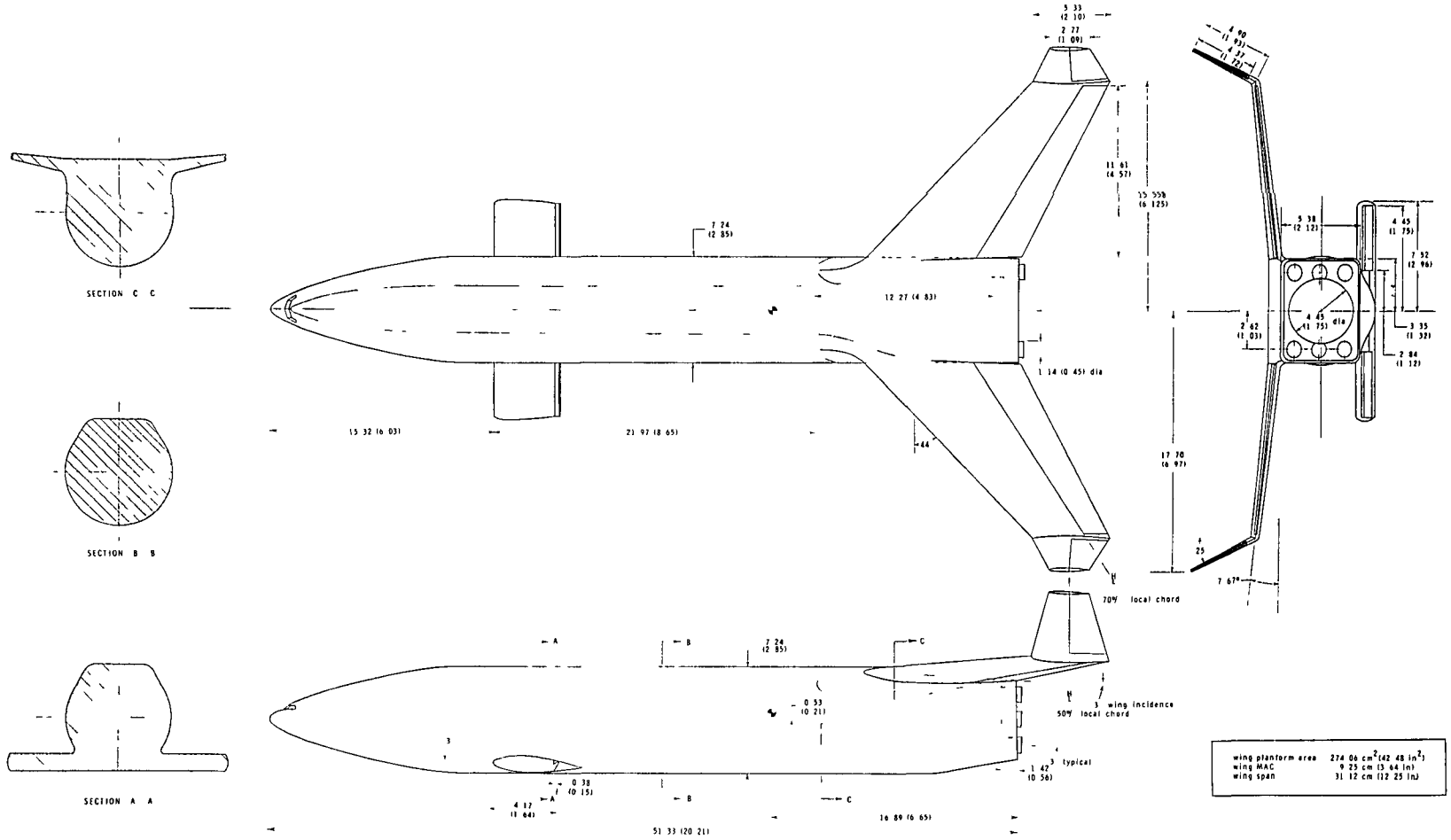

(c) Booster model.

Figure 1.- Continued.

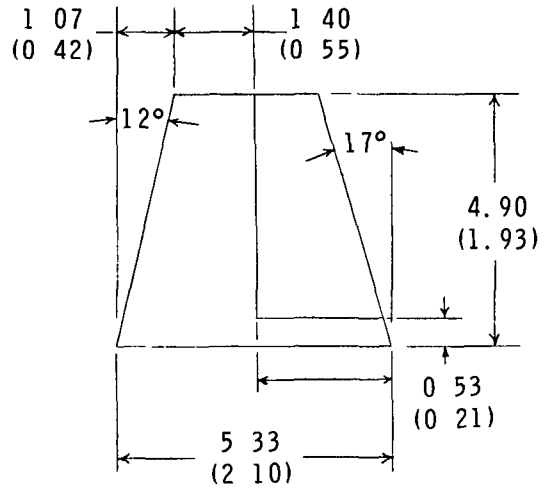

vertical fin

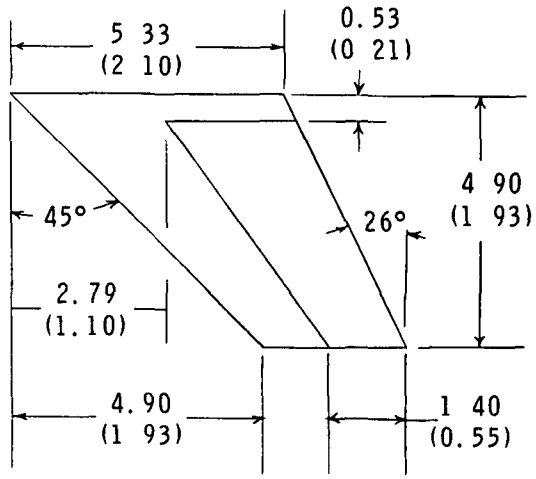

ventral fin

(d) Details of booster wing-tip fins.

Figure 1.- Concluded.

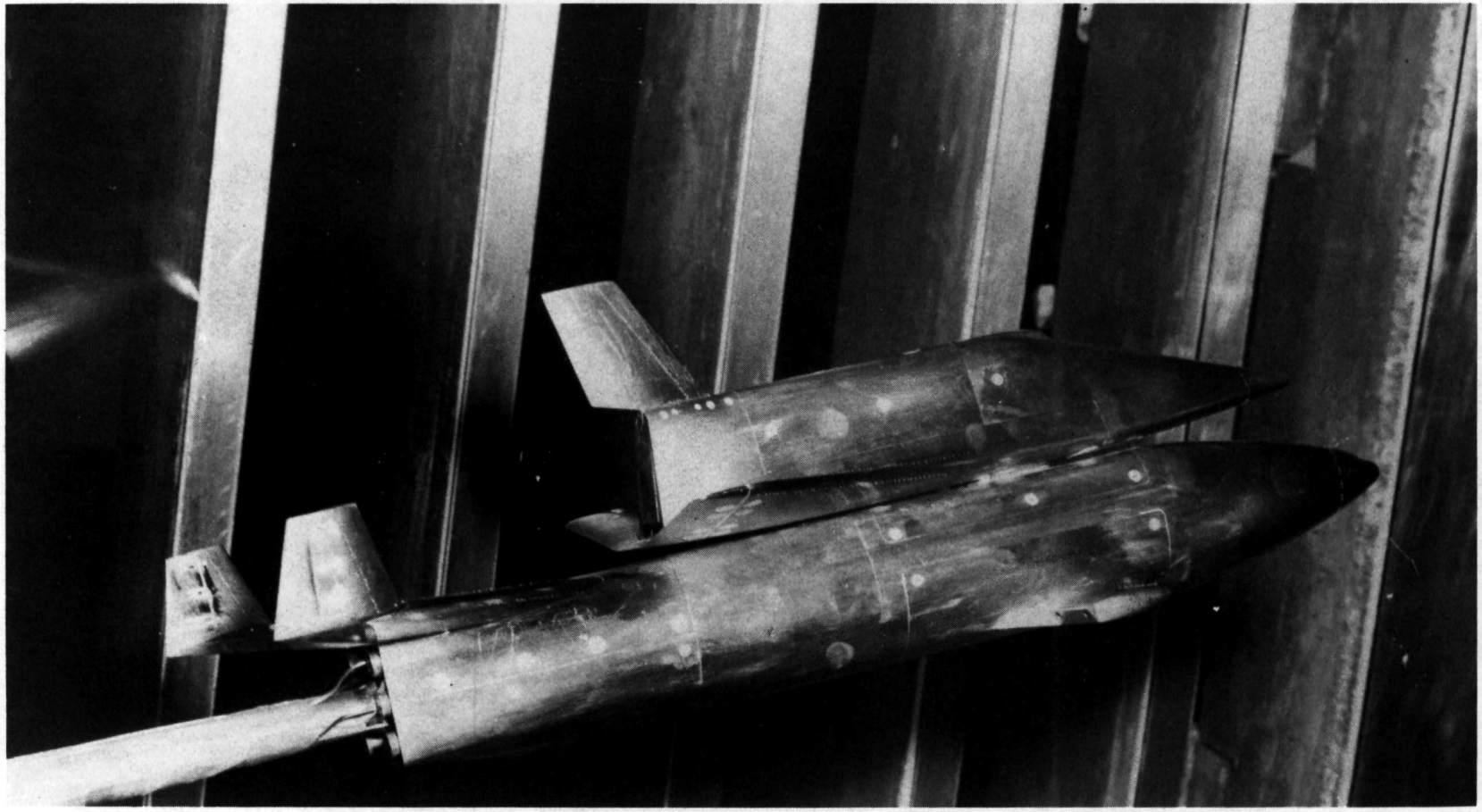

L-71-4432

(a) Ascent configuration.

Figure 2.- Photographs of models.

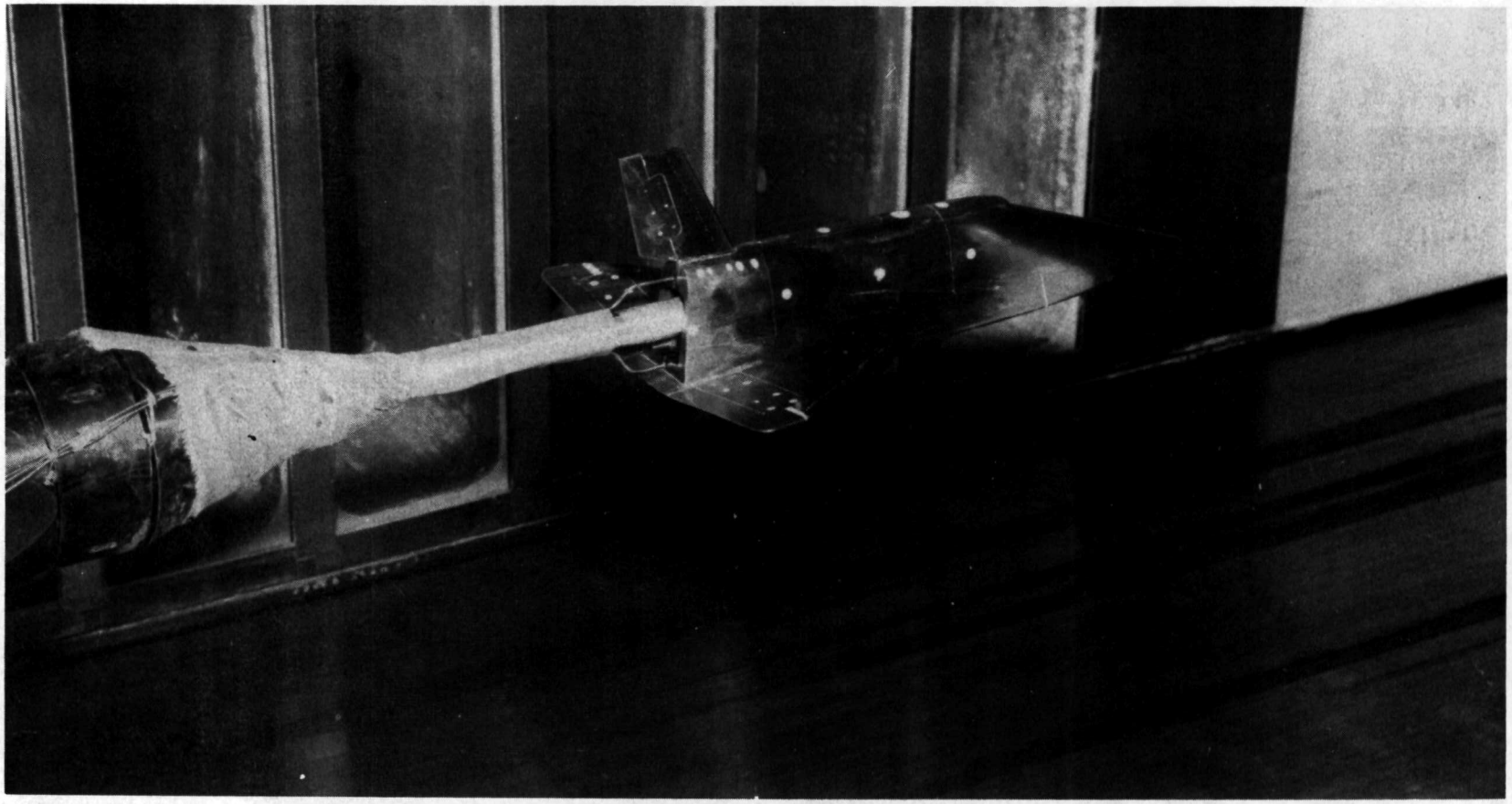

L-71-4506

(b) Orbiter model.

Figure 2.- Continued.

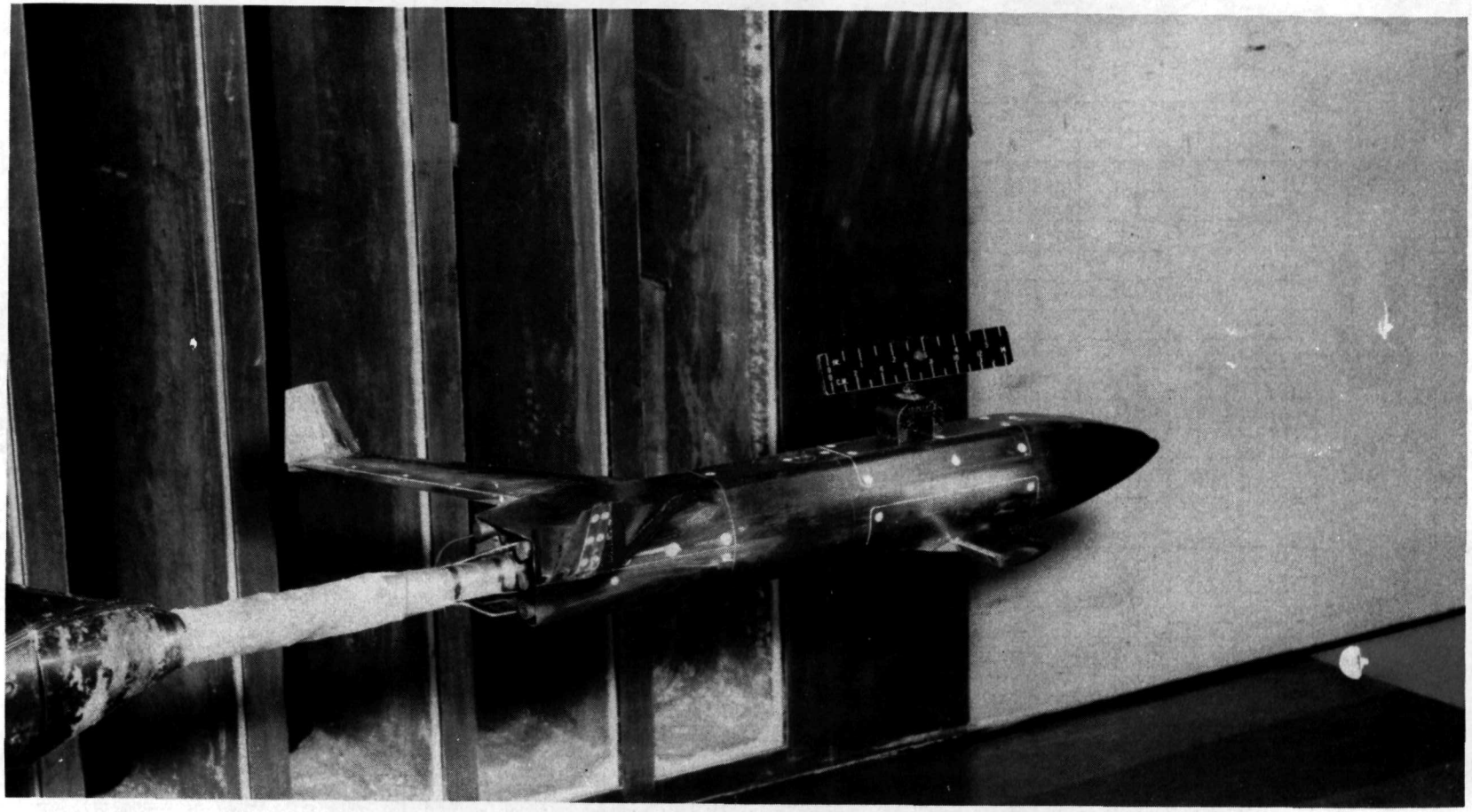

L-71-4430

(c) Booster model.

Figure 2.- Concluded.

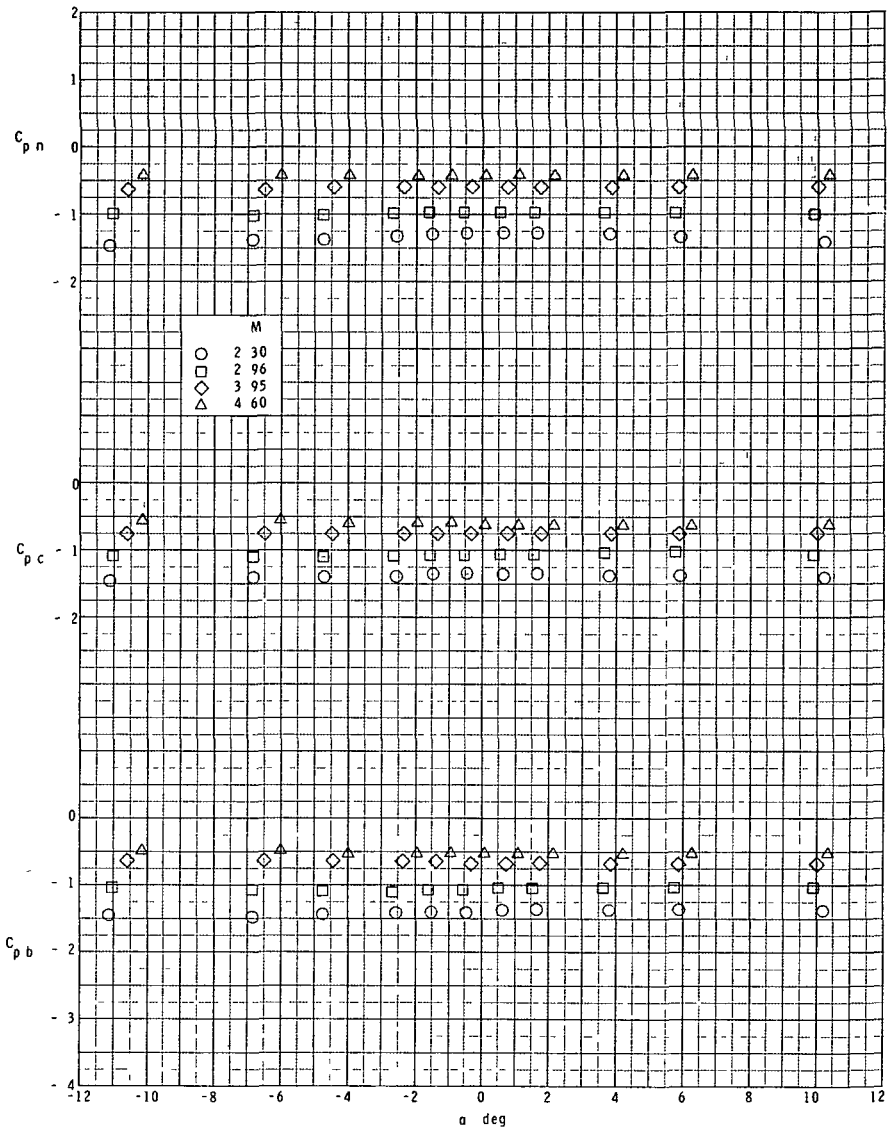

(a) Ascent configuration (booster only).

Figure 3.- Typical variation of pressure coefficients with angle of attack.

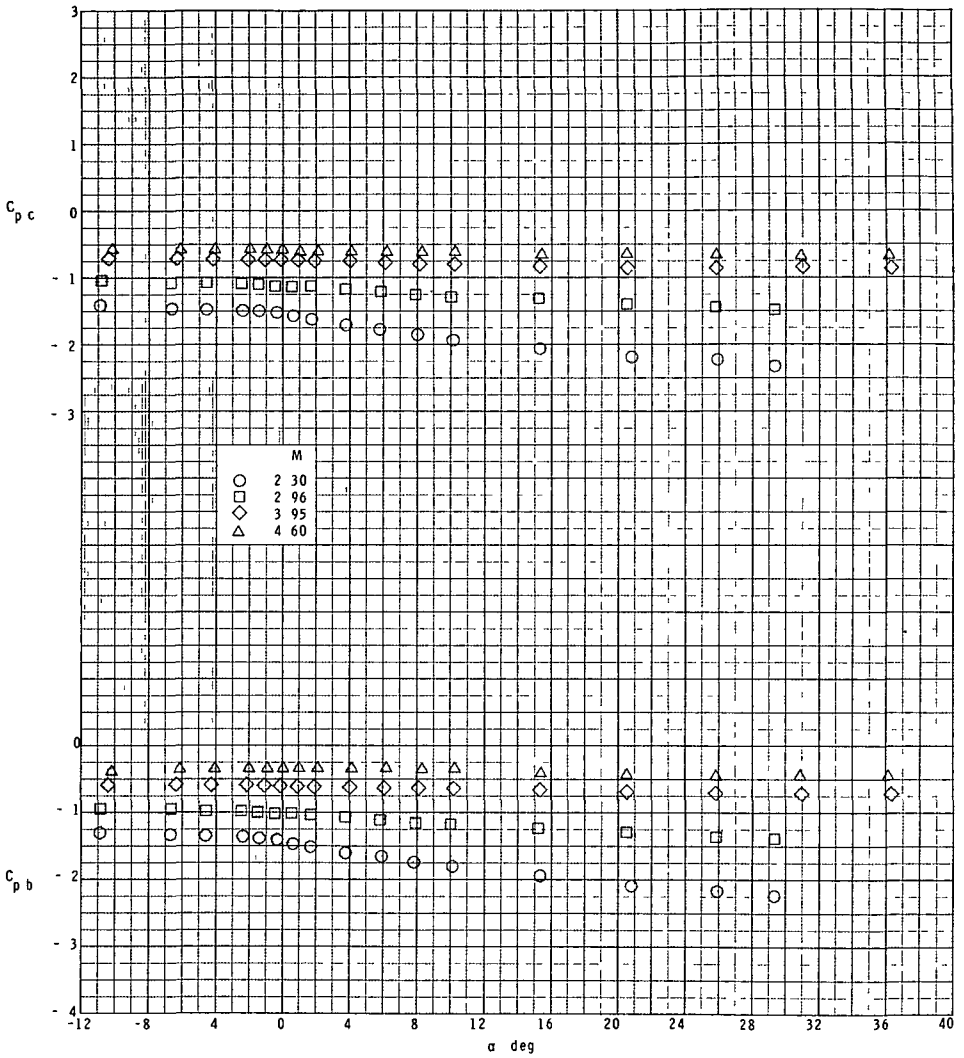

(b) Orbiter configuration.

Figure 3.- Continued.

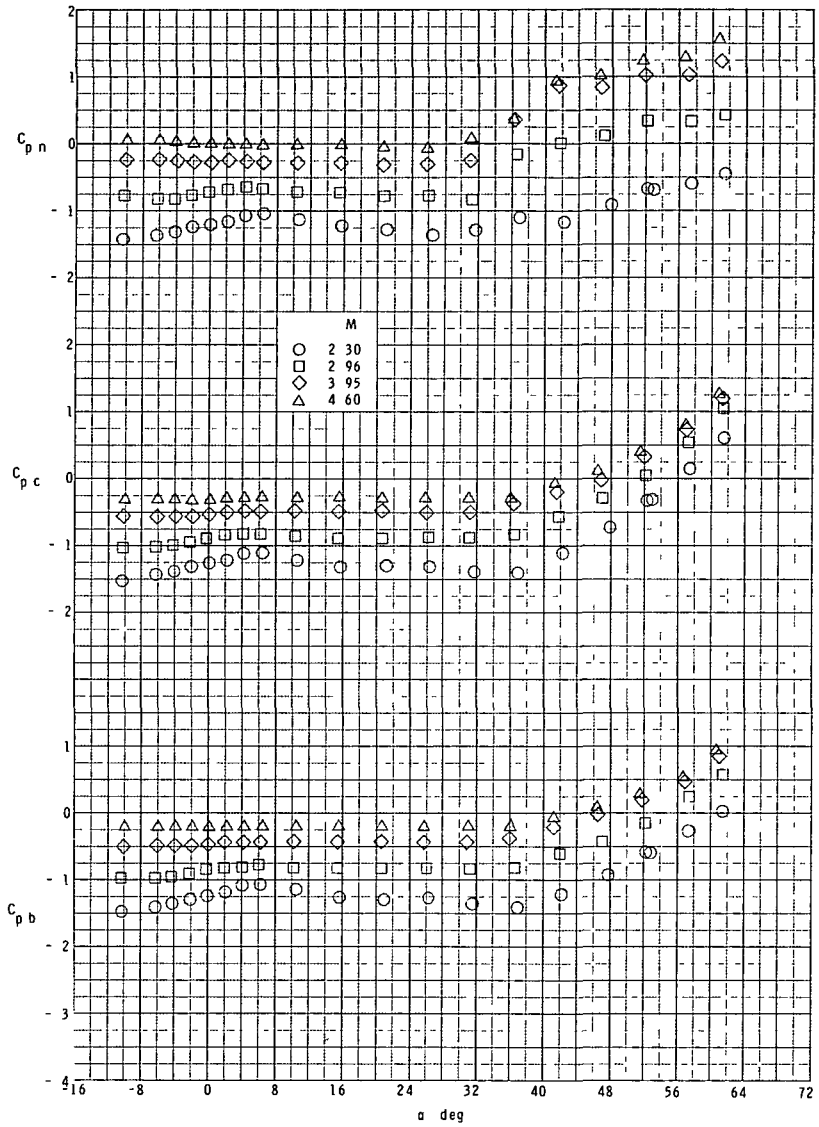

(c) Booster configuration.

Figure 3.- Concluded.

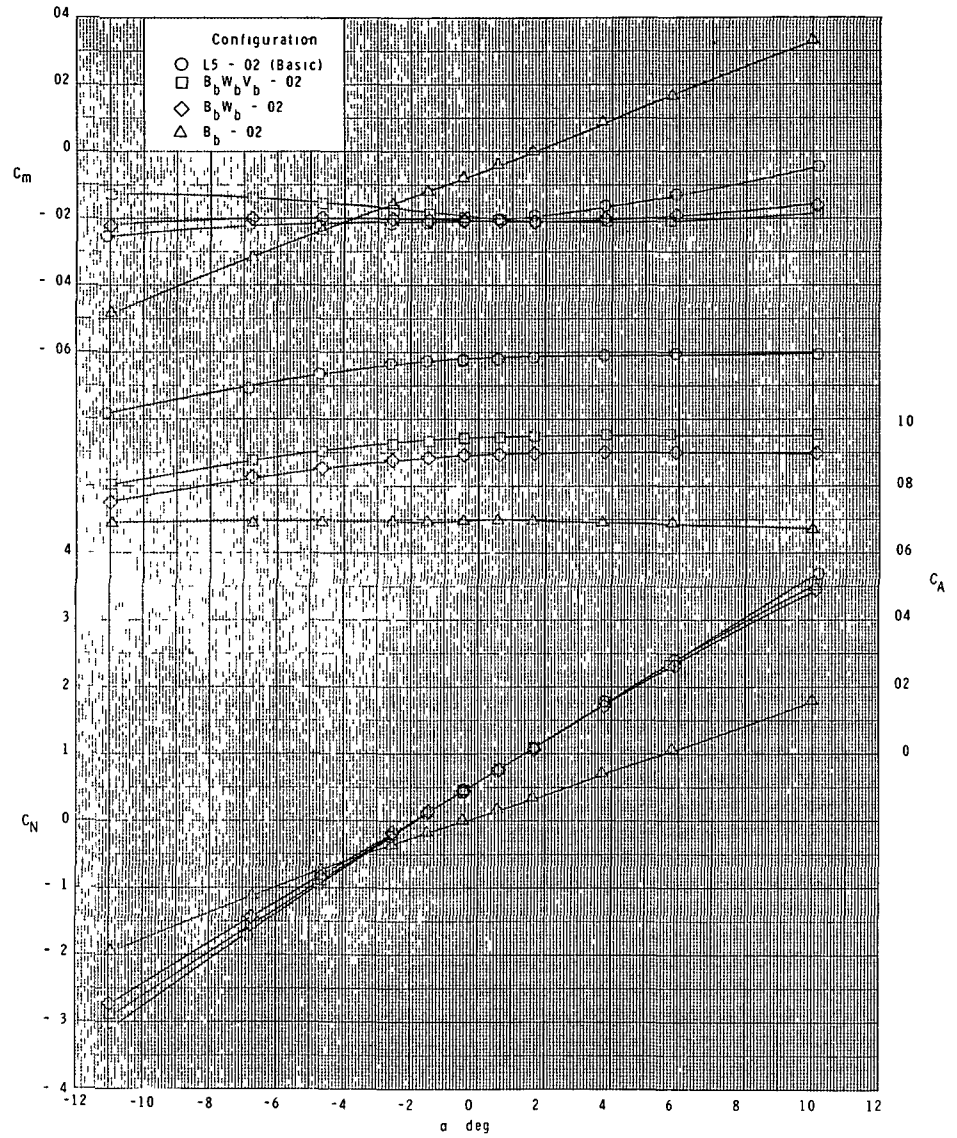

(a) M = 2.30.

Figure 4.- Effect of booster components on longitudinal characteristics. Ascent configuration.

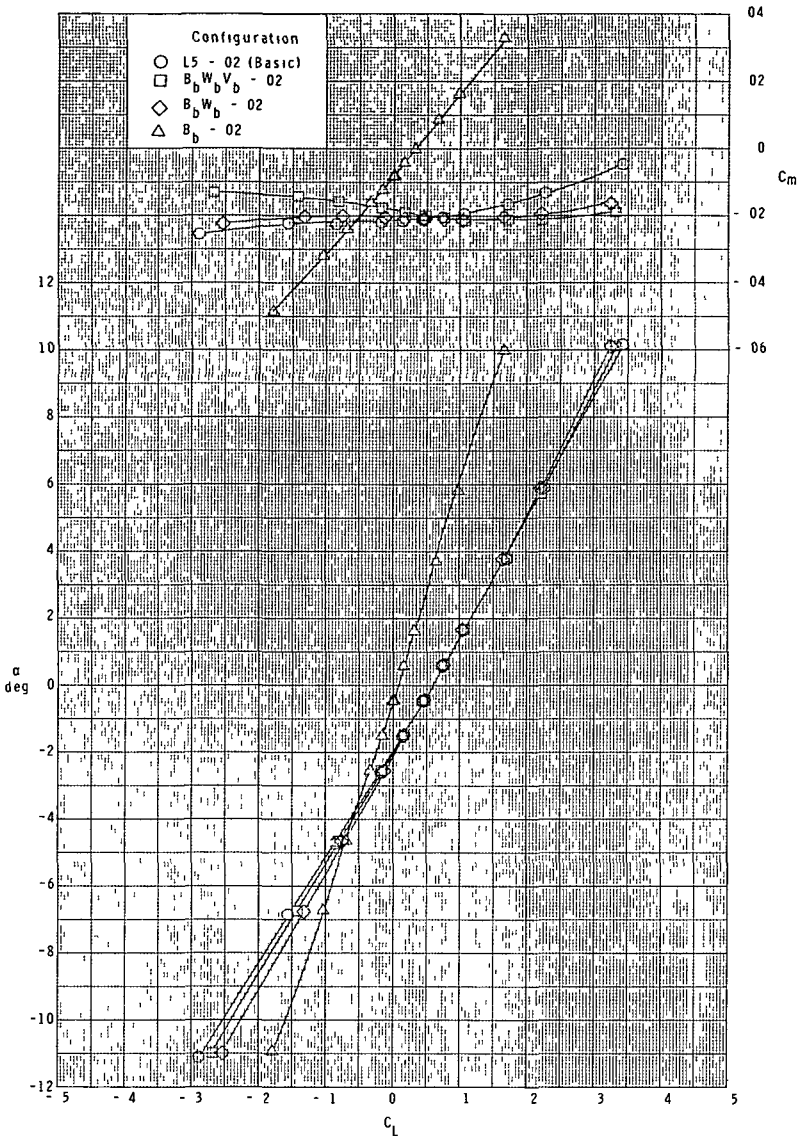

(a) Continued.

Figure 4.- Continued.

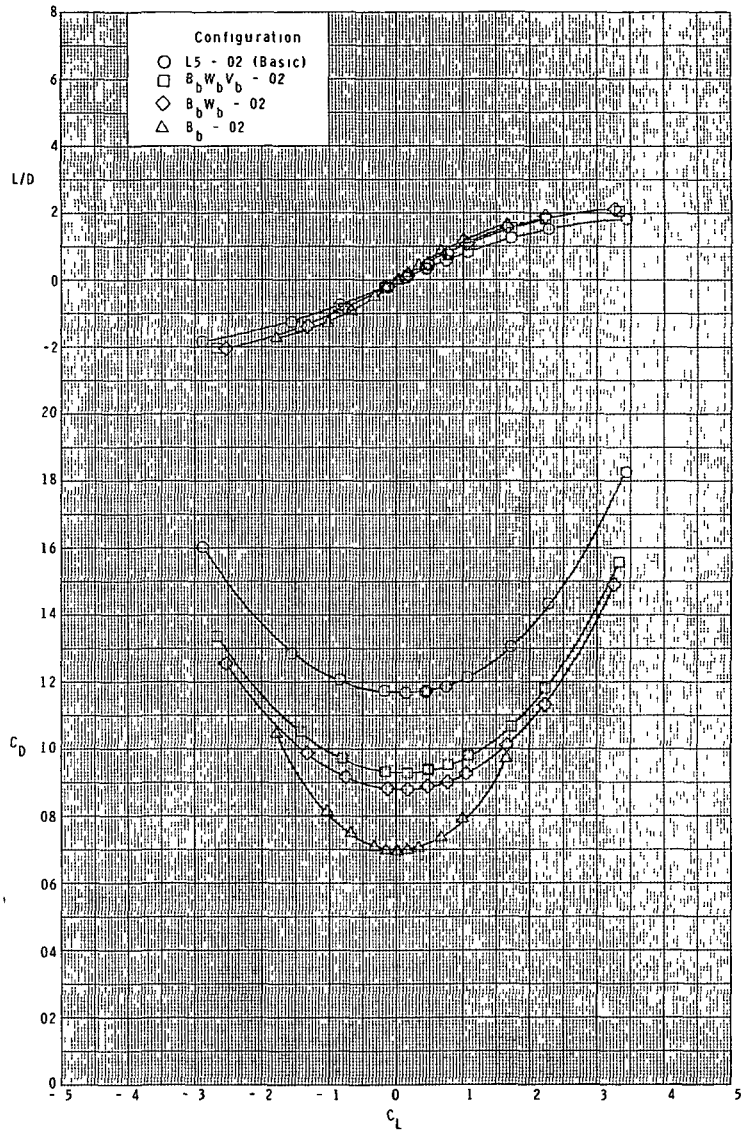

(a) Concluded.

Figure 4.- Continued.

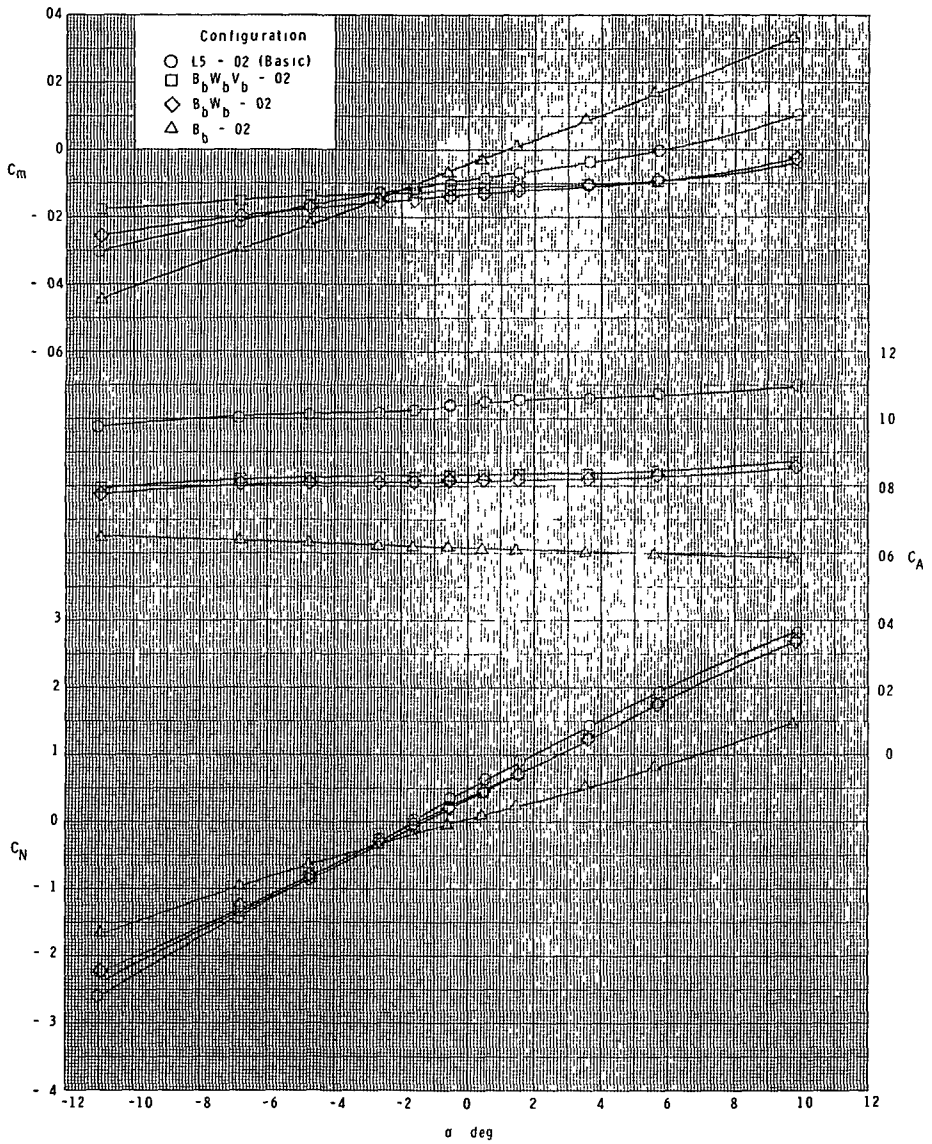

(b) M = 2.96.

Figure 4.- Continued.

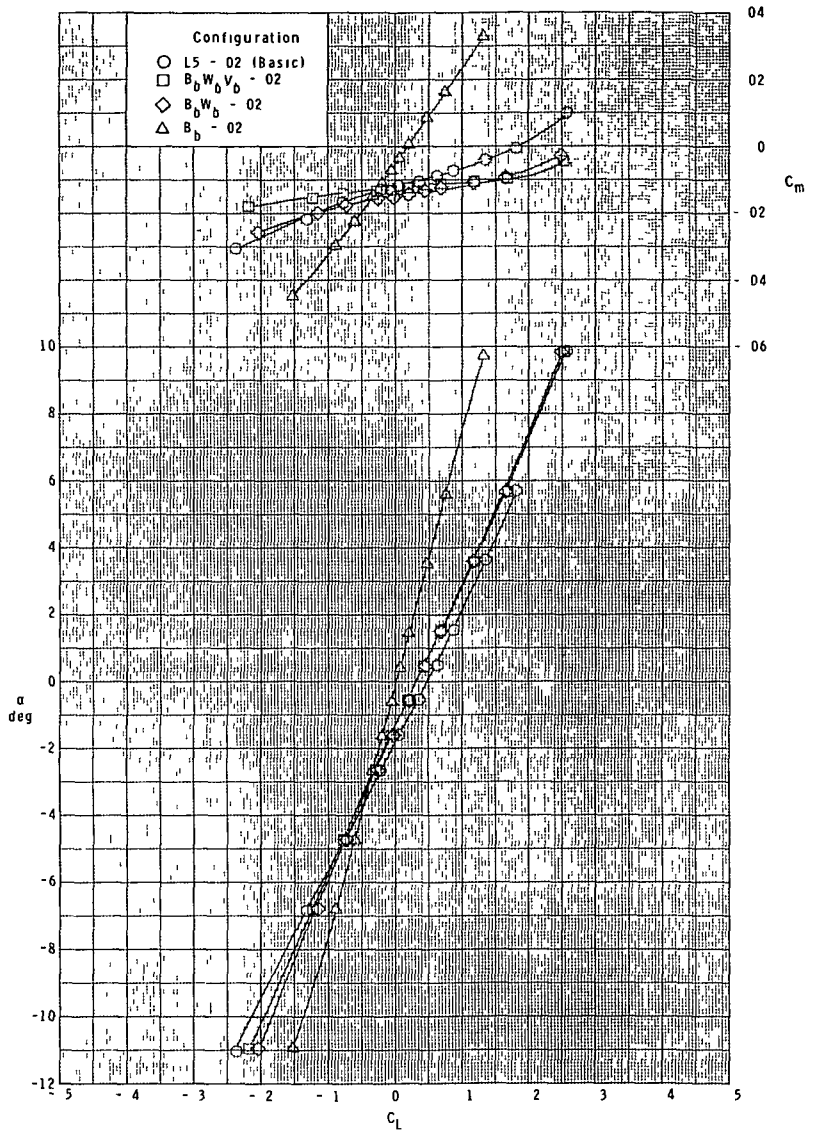

(b) Continued.

Figure 4.- Continued.

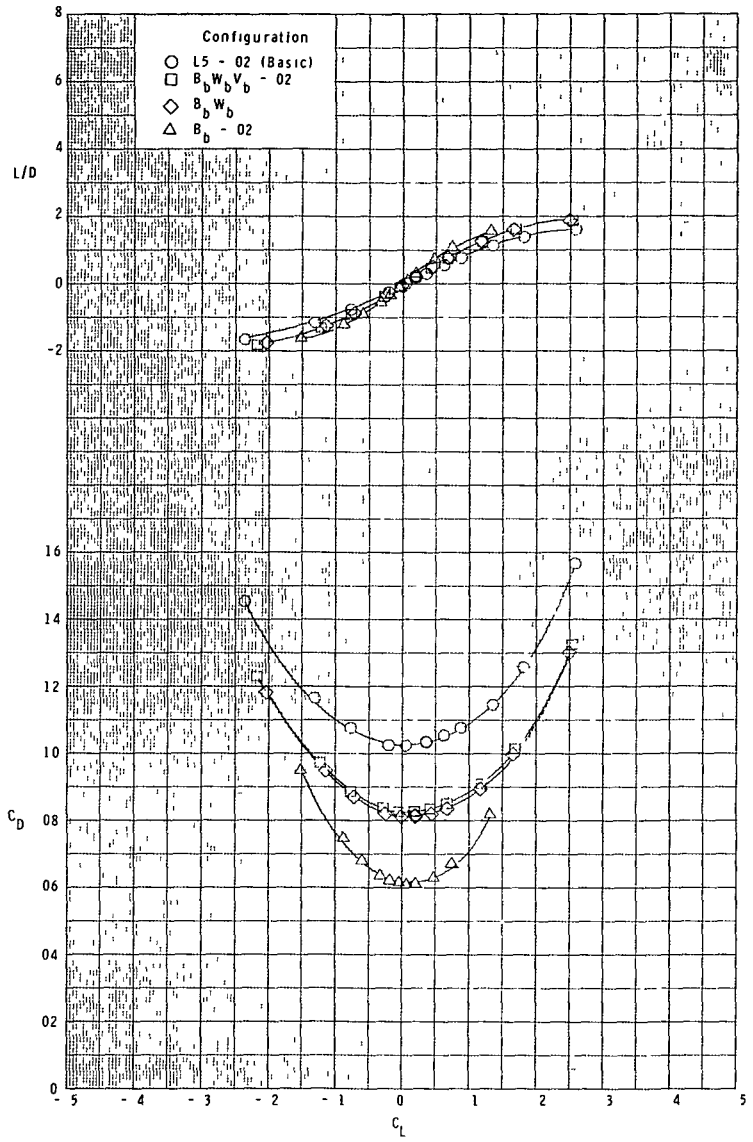

(b) Concluded.

Figure 4.- Continued.

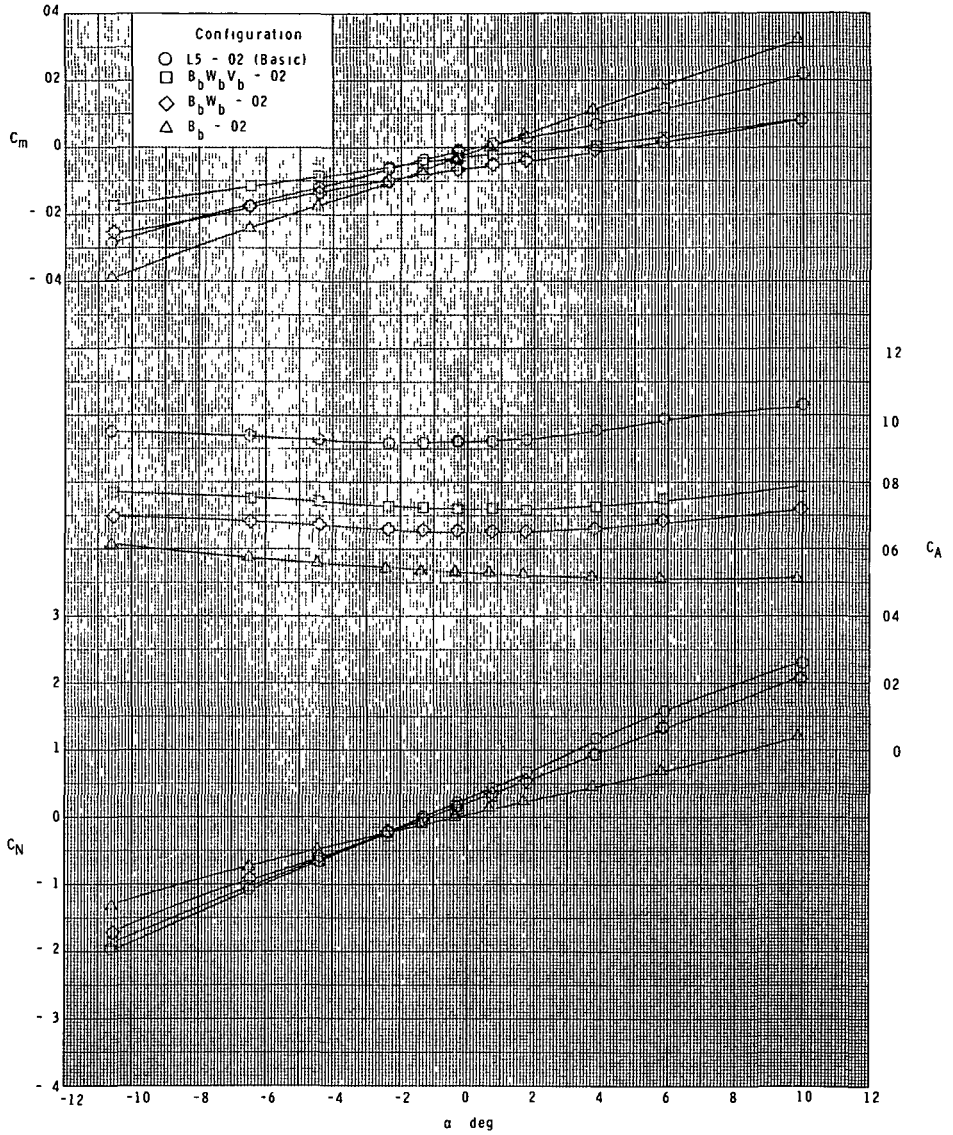

(c) M = 3.95.

Figure 4.- Continued.

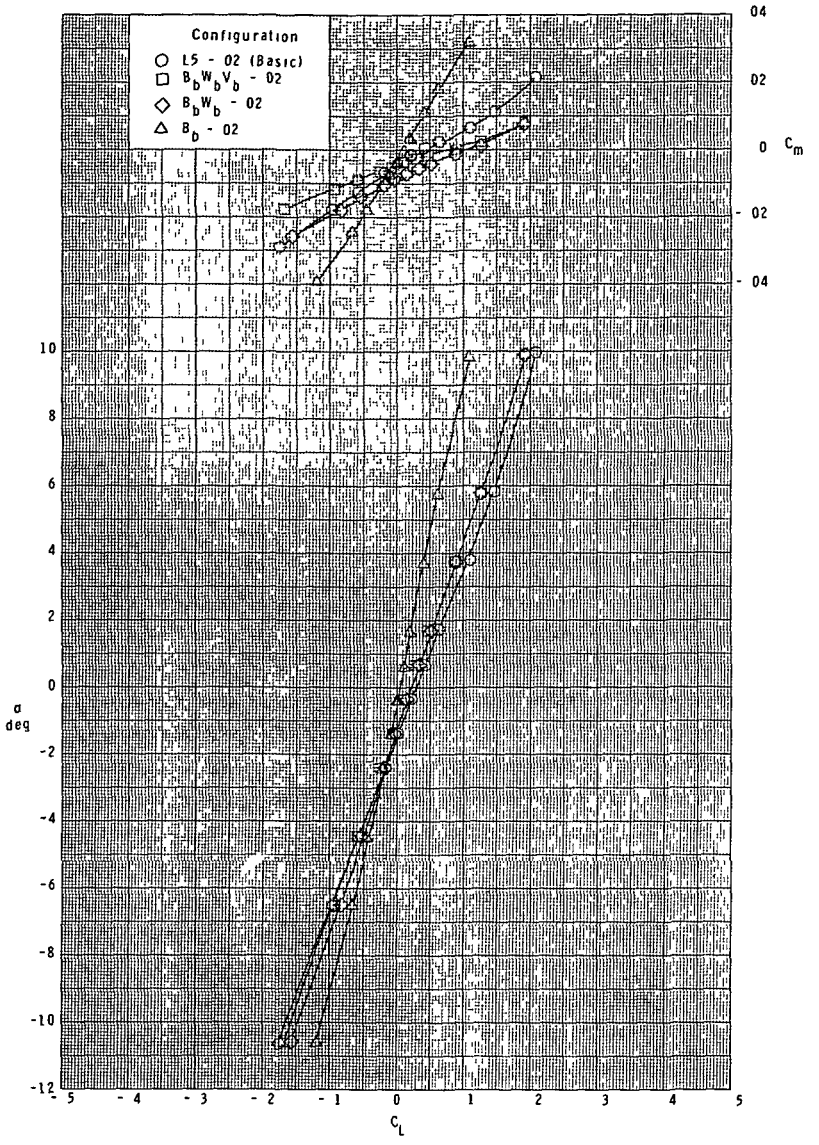

(c) Continued.

Figure 4.- Continued.

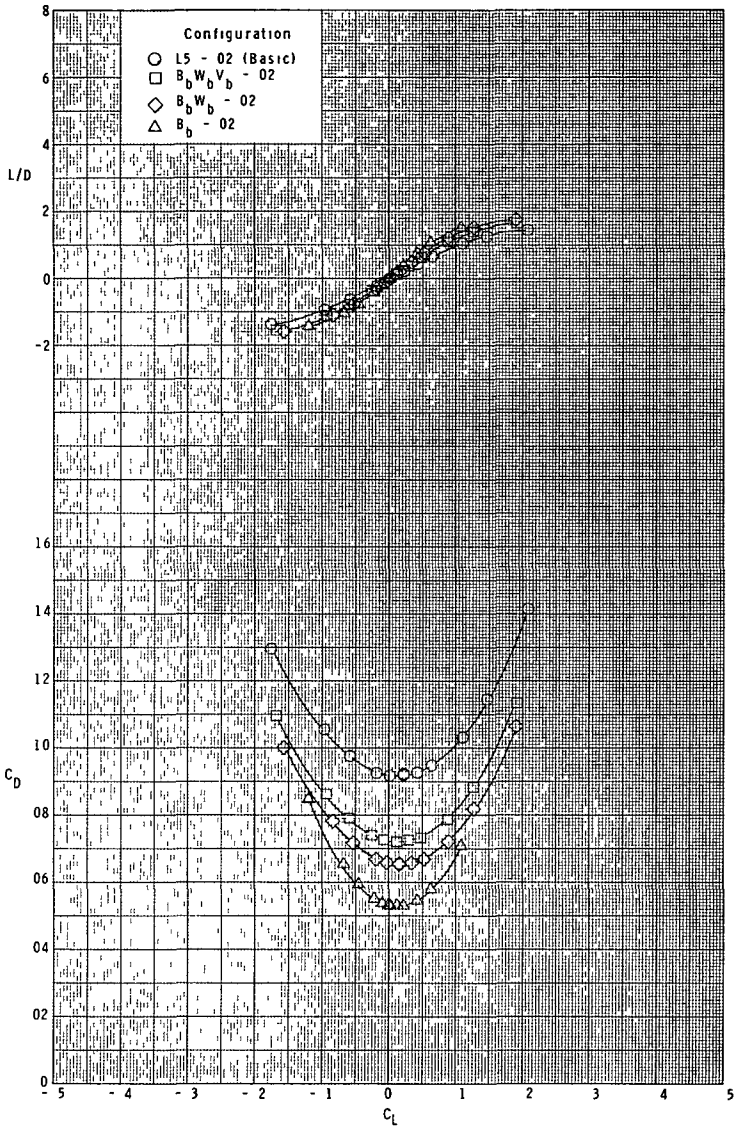

(c) Concluded.

Figure 4.- Continued.

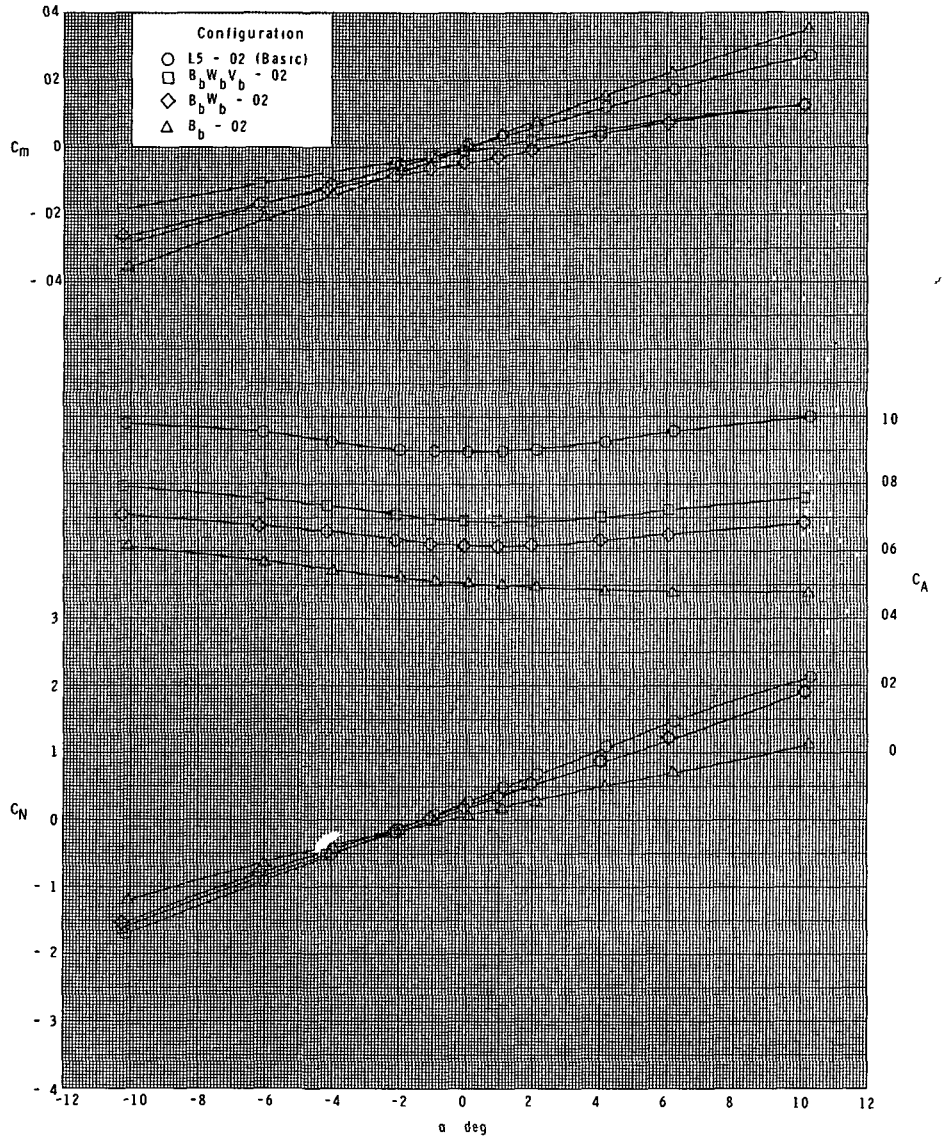

(d) M = 4.60.

Figure 4.- Continued.

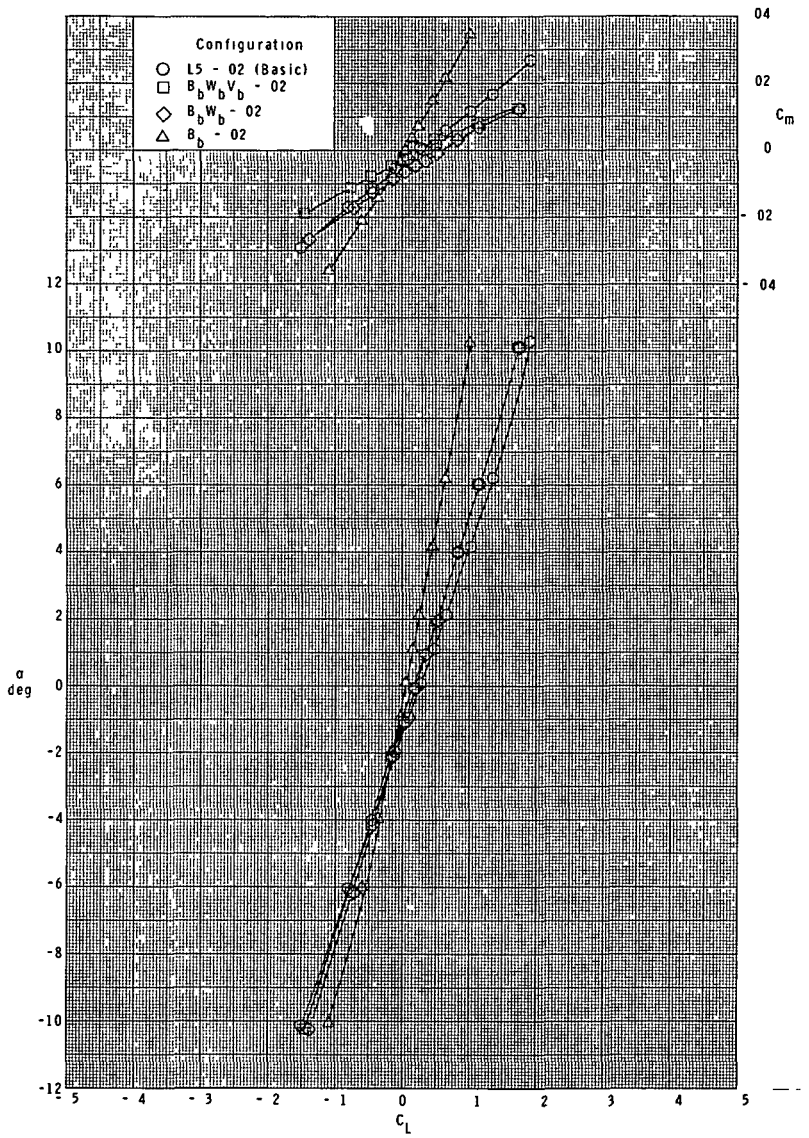

(d) Continued.

Figure 4.- Continued.

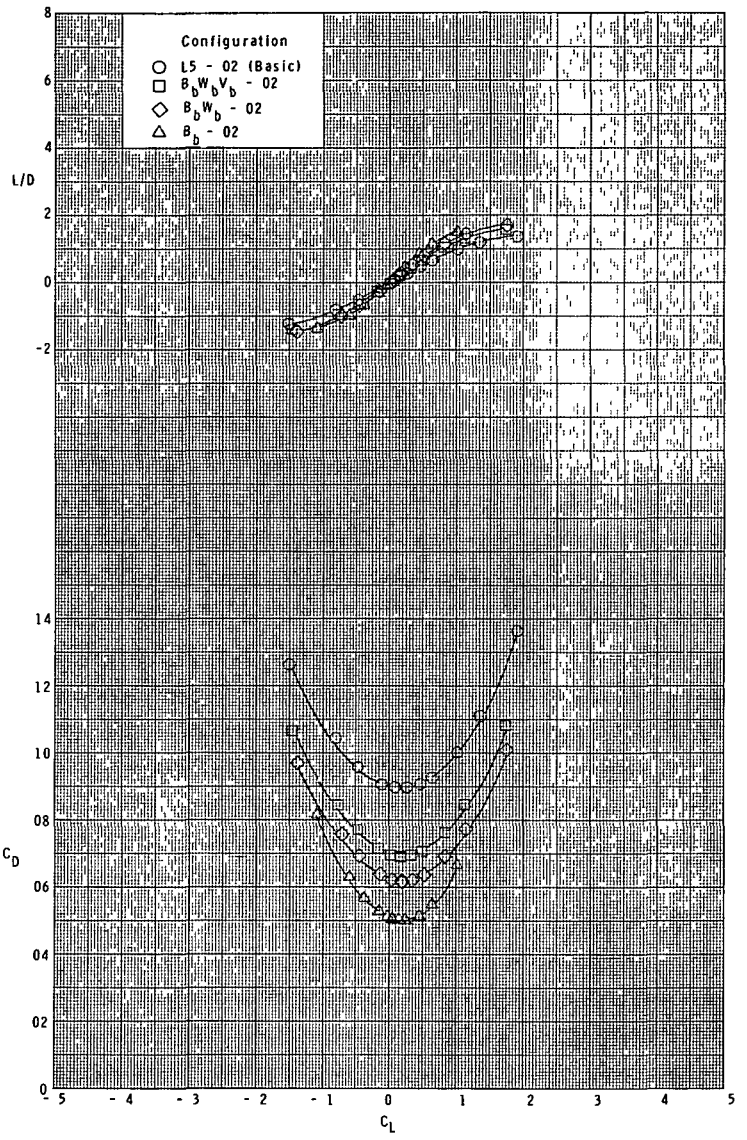

(d) Concluded.

Figure 4.- Concluded.

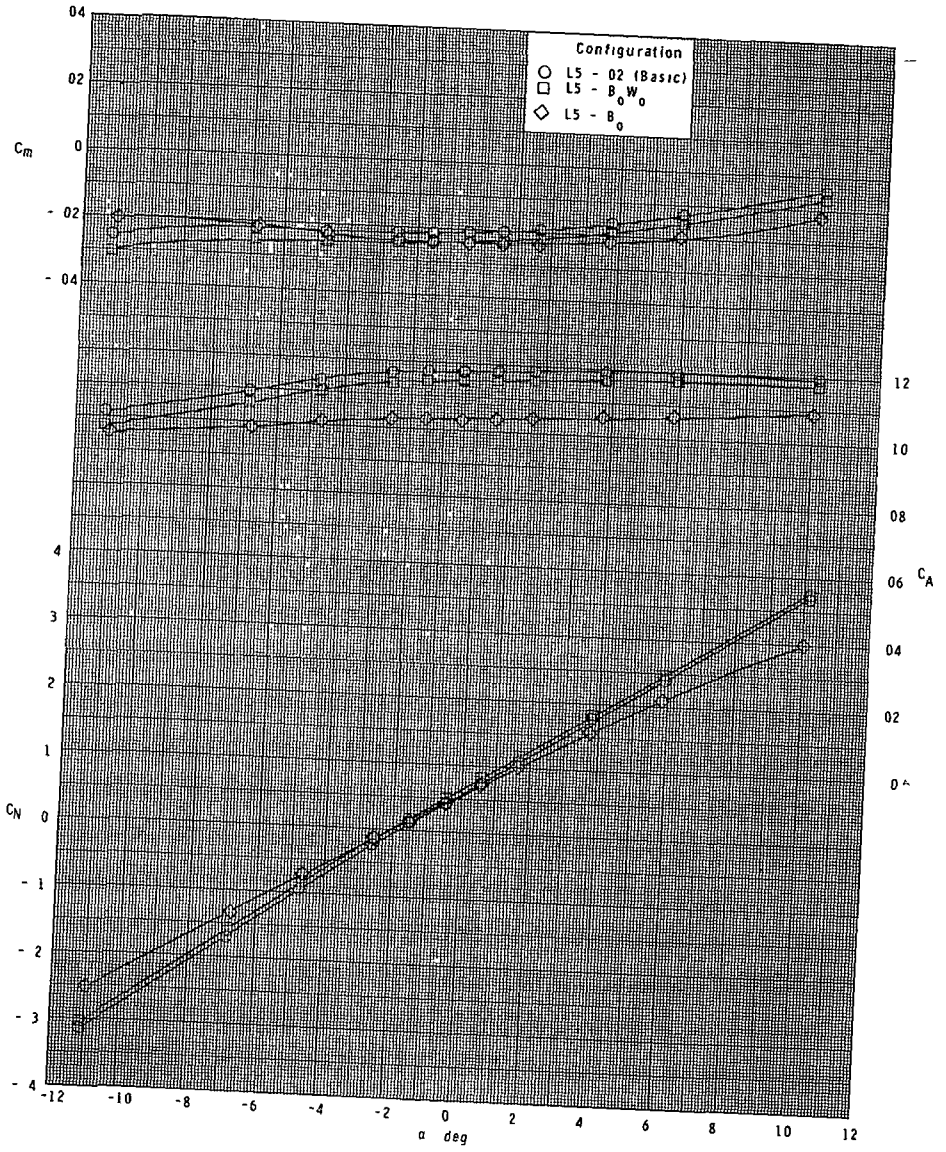

(a) M = 2.30.

Figure 5.- Effect of orbiter components on longitudinal characteristics. Ascent configuration.

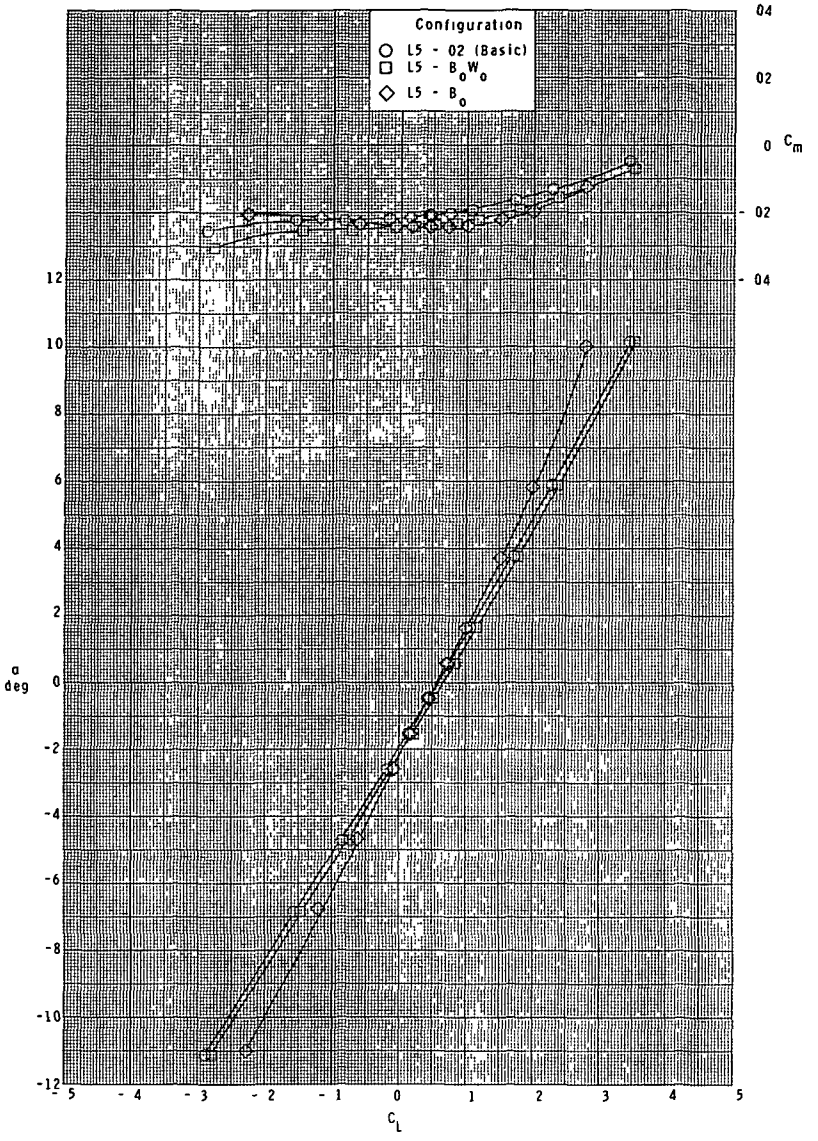

(a) Continued.

Figure 5.- Continued.

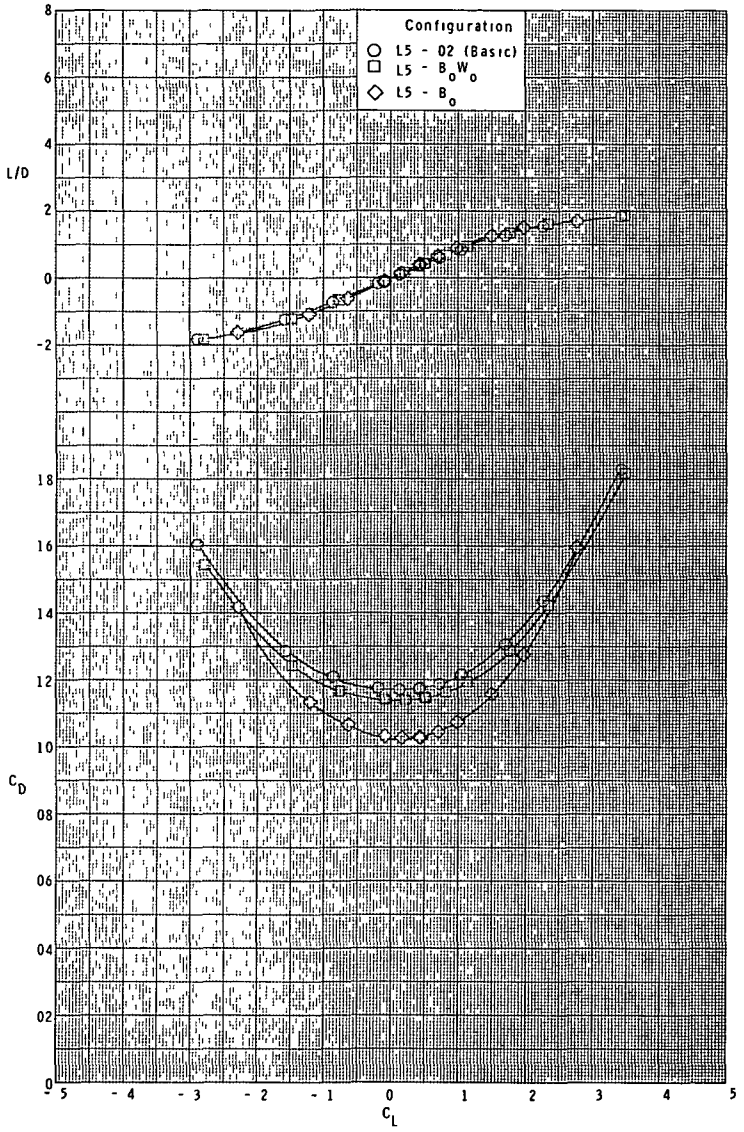

(a) Concluded.

Figure 5.- Continued.

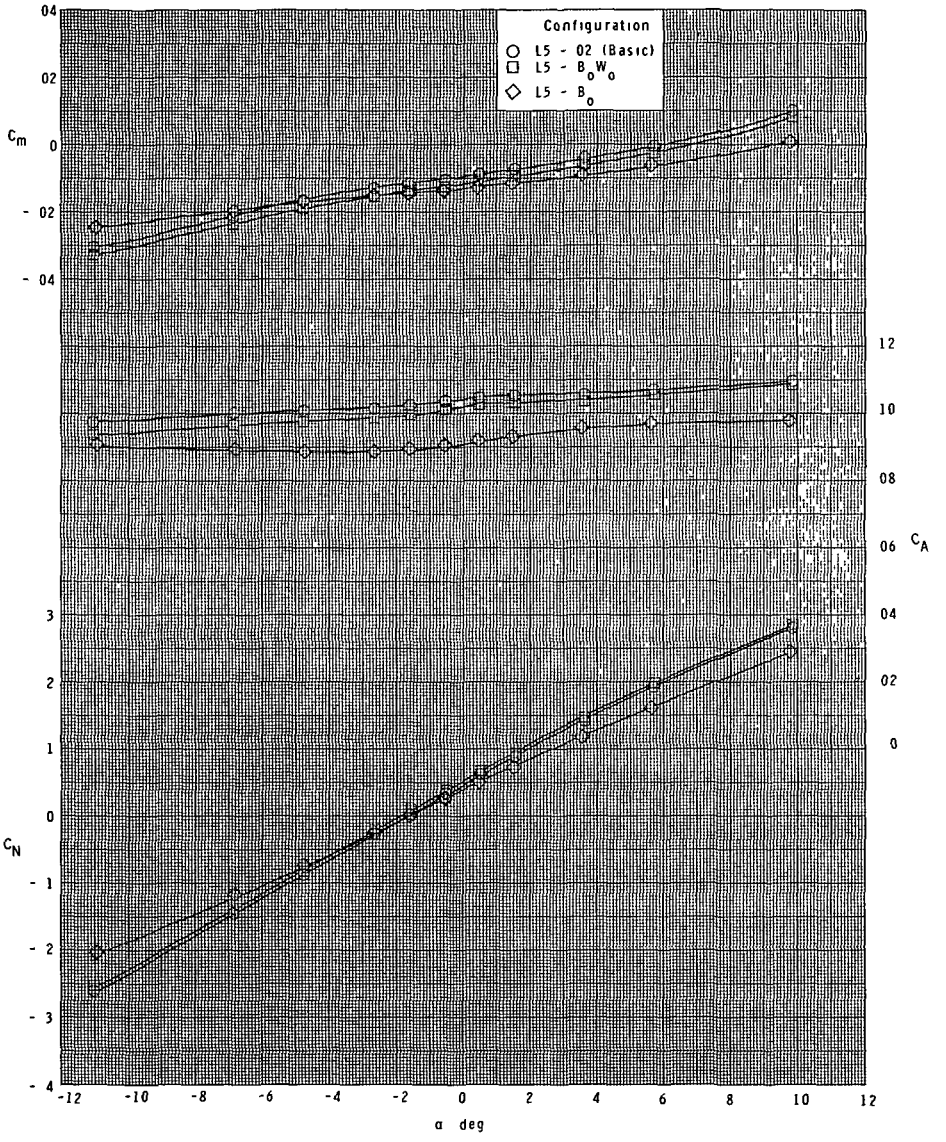

(b) M = 2.96.

Figure 5.- Continued.

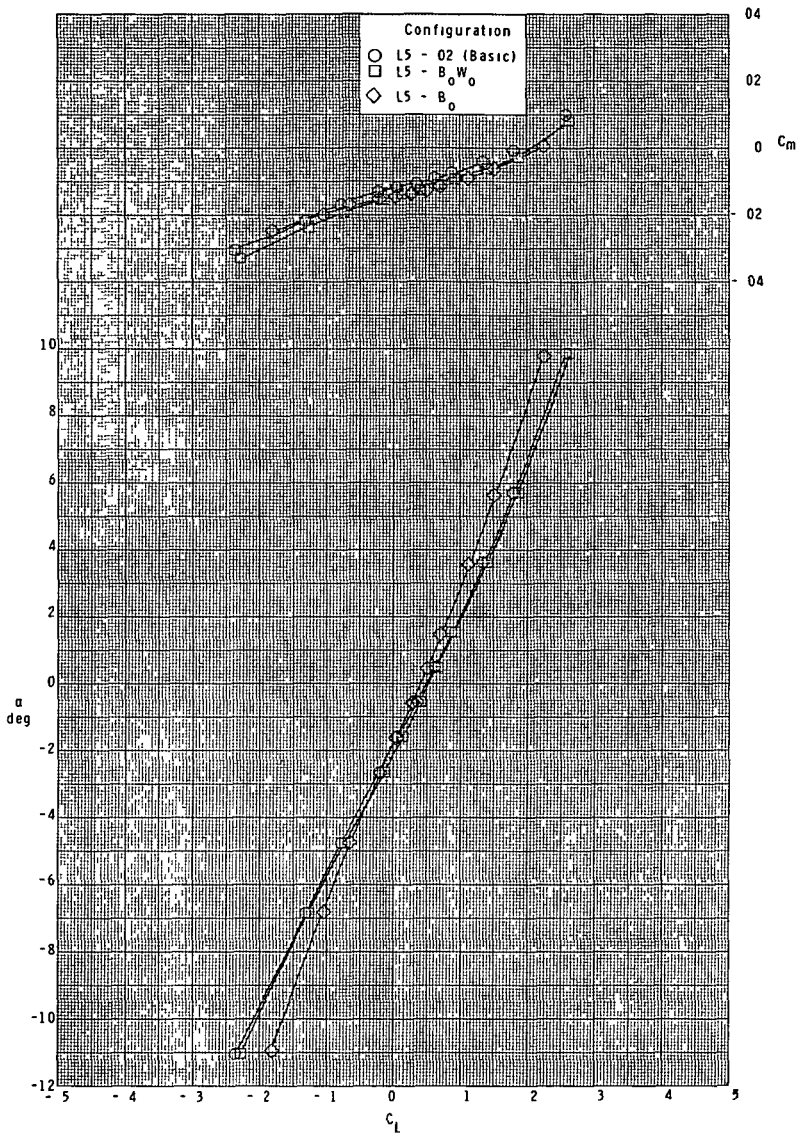

(b) Continued.

Figure 5.- Continued.

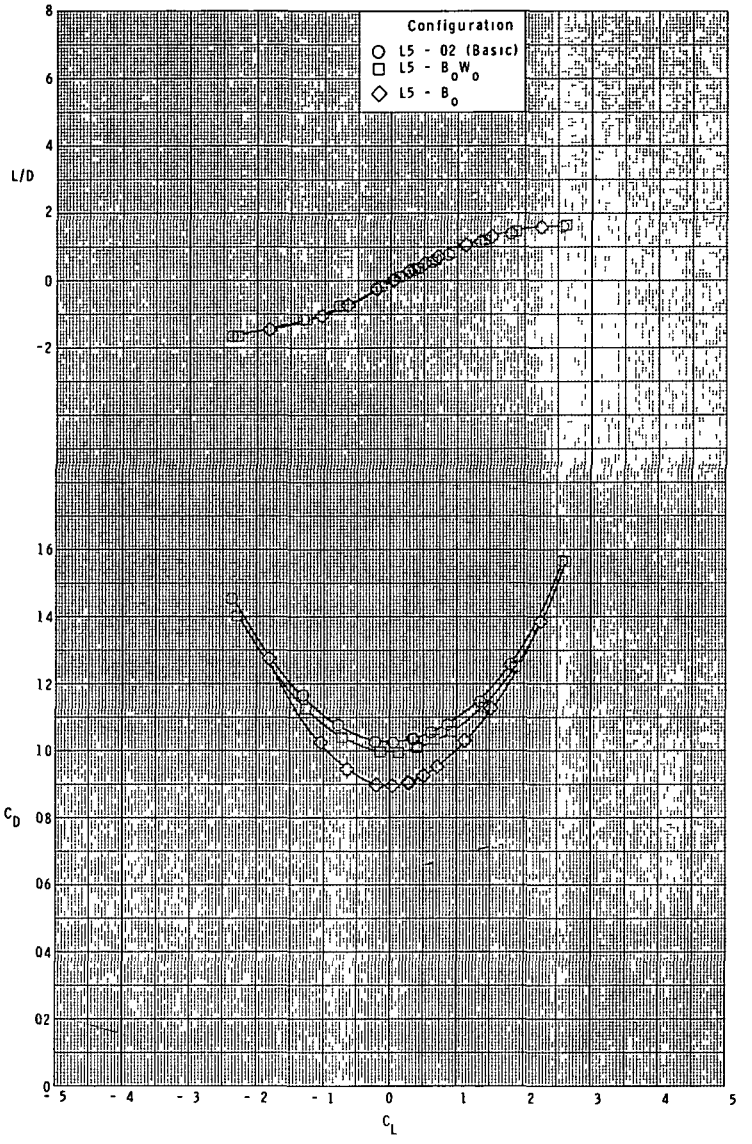

(b) Concluded.

Figure 5.- Continued.

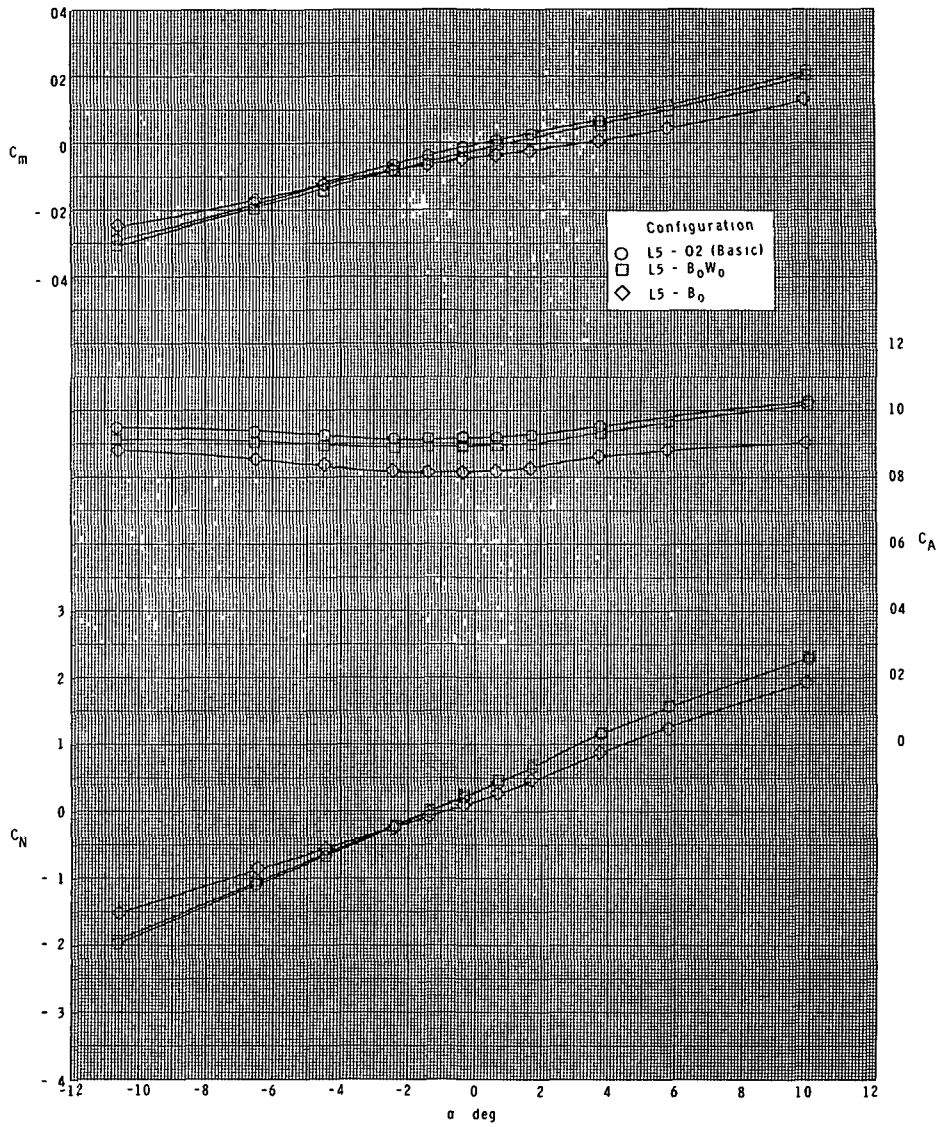

(c) M = 3.95.

Figure 5.- Continued.

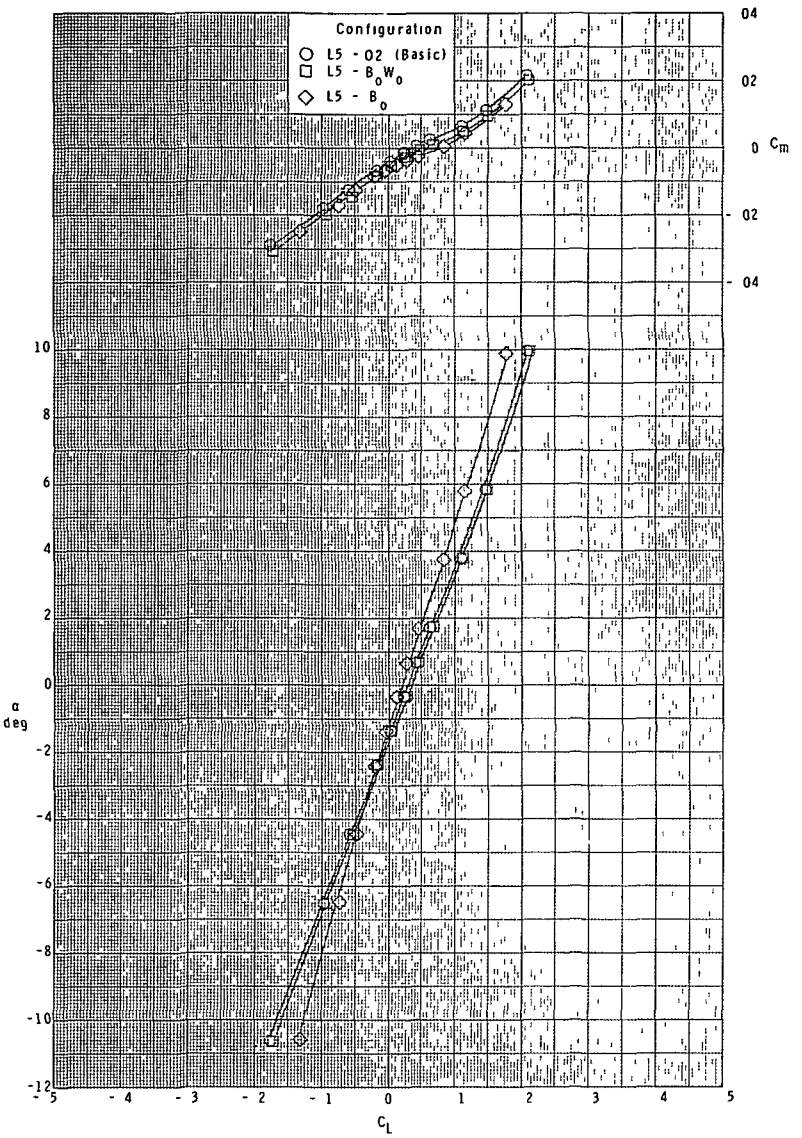

(c) Continued.

Figure 5.- Continued.

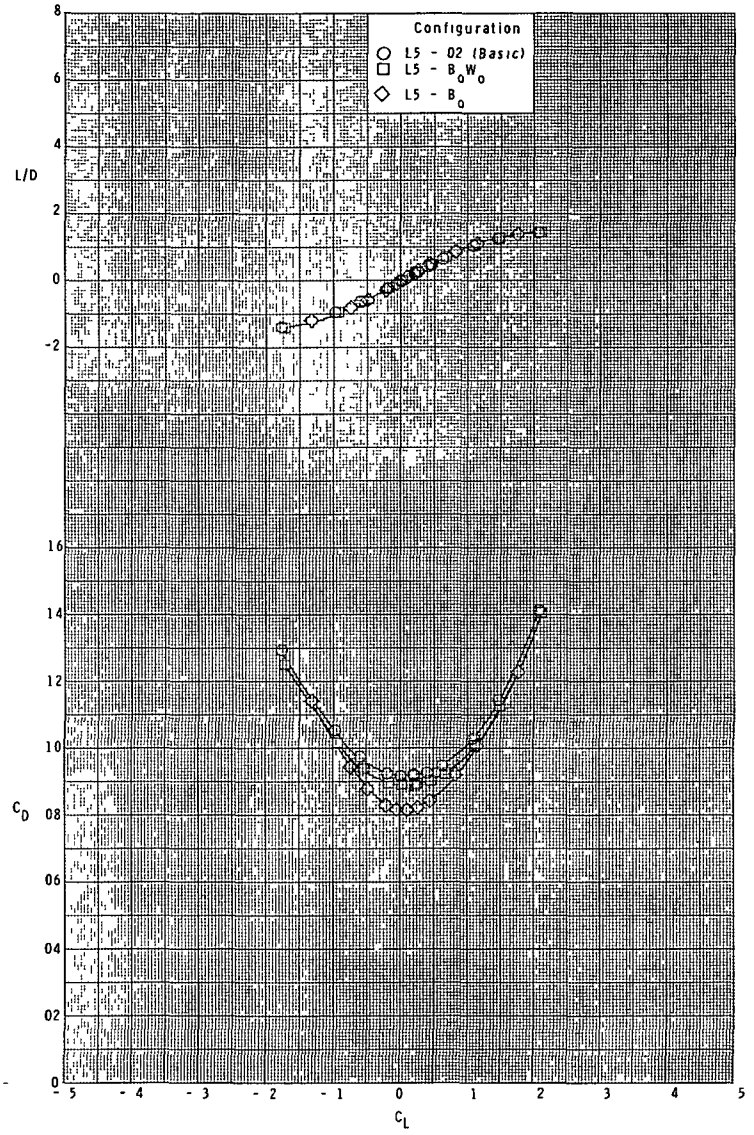

(c) Concluded.

Figure 5.- Continued

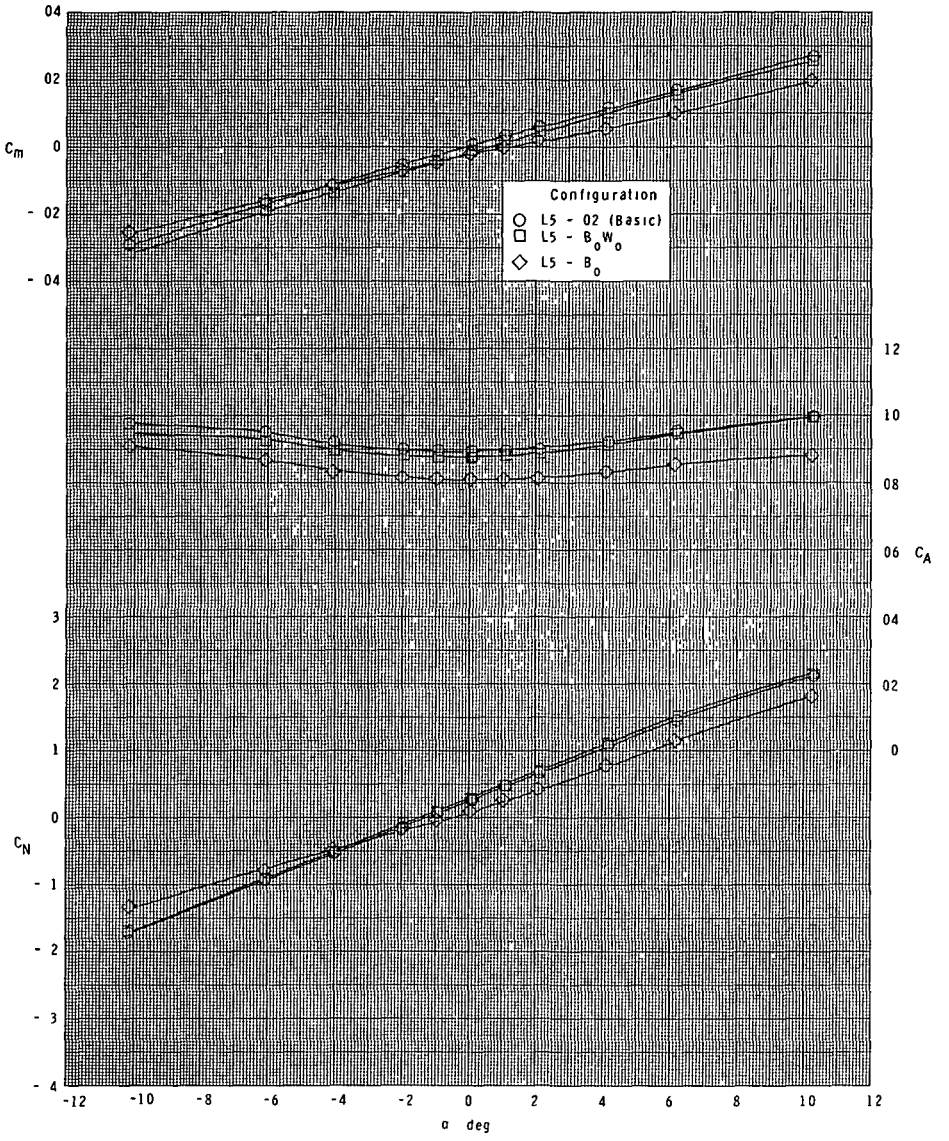

(d) M = 4.60.

Figure 5.- Continued.

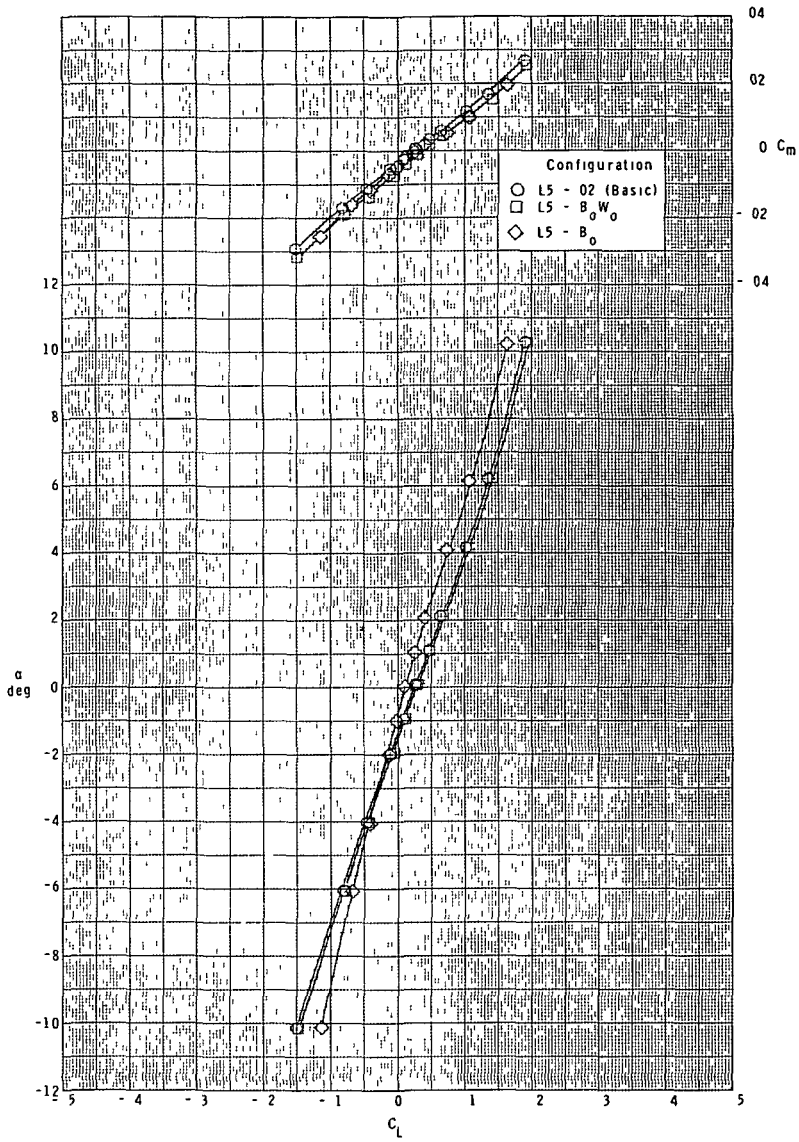

(d) Continued.

Figure 5.- Continued.

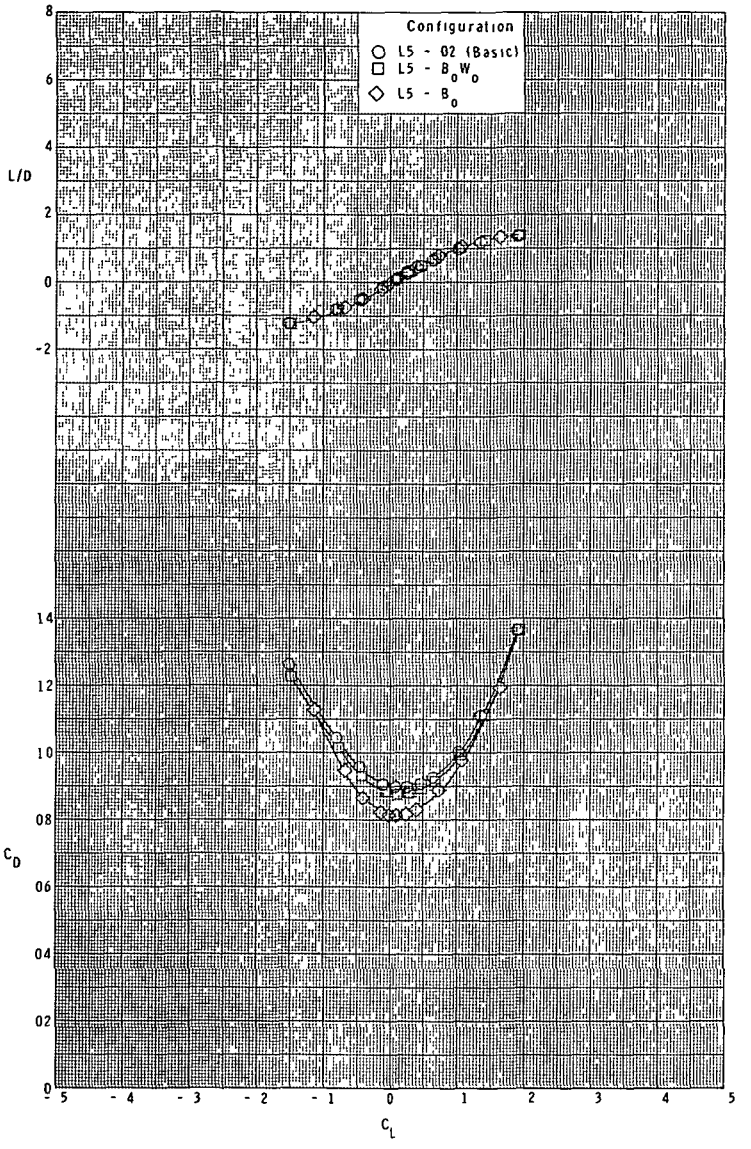

(d) Concluded.

Figure 5.- Concluded.

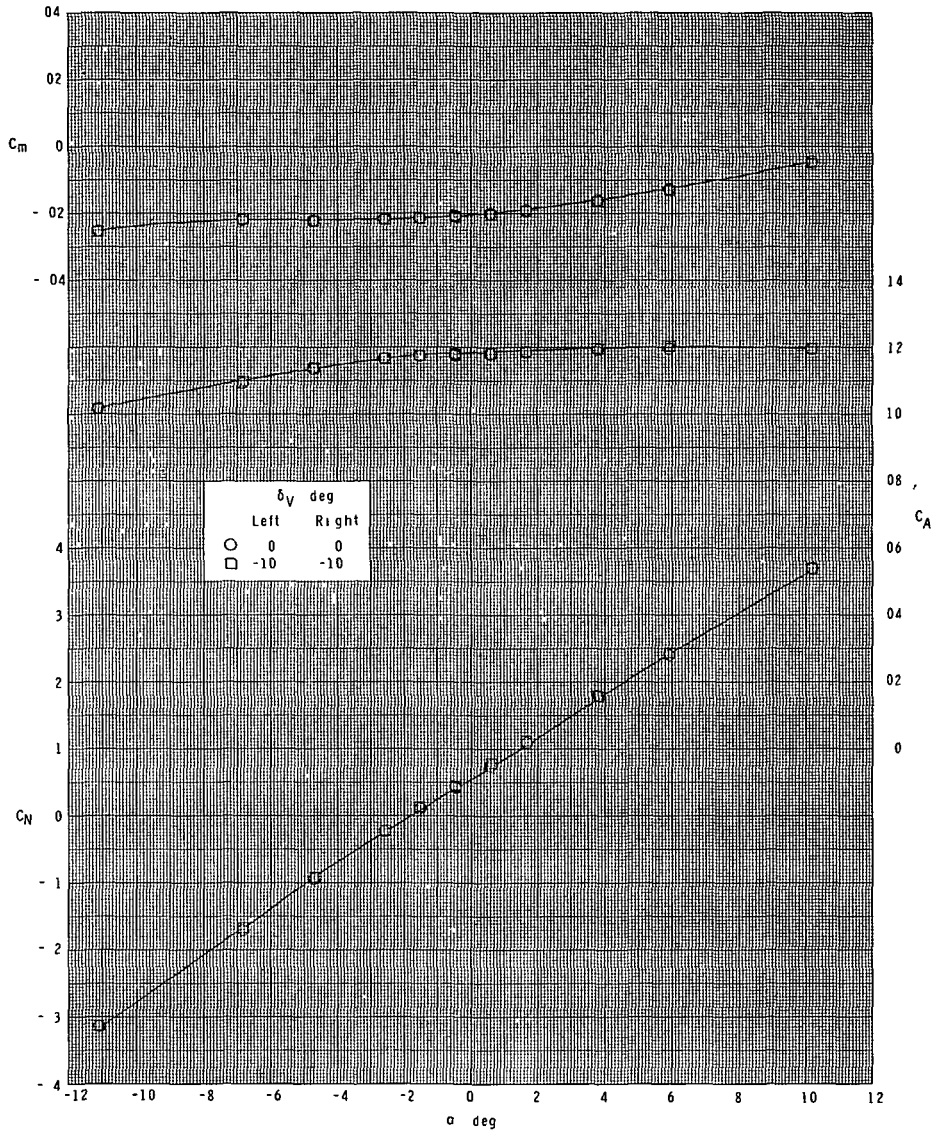

(a) M = 2.30.

Figure 6.- Effect of booster vertical-fin rudder deflection on longitudinal characteristics. Ascent configuration.

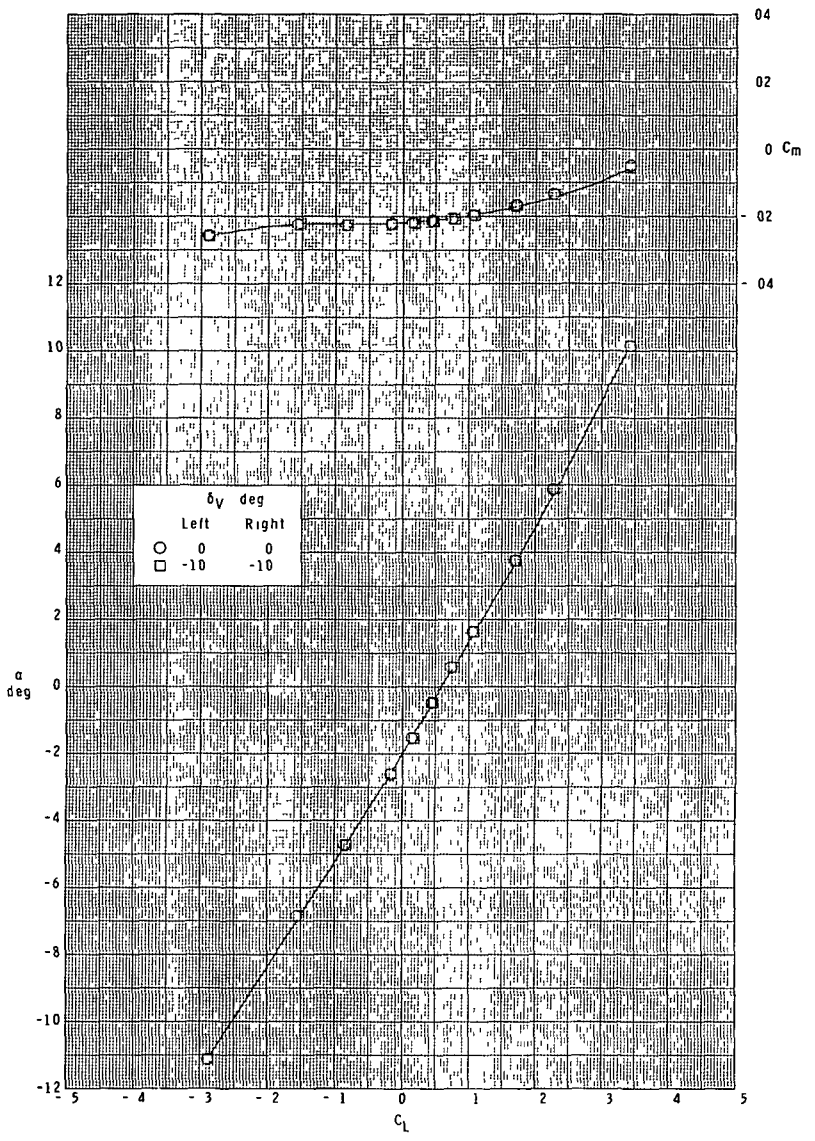

(a) Continued.

Figure 6.- Continued.

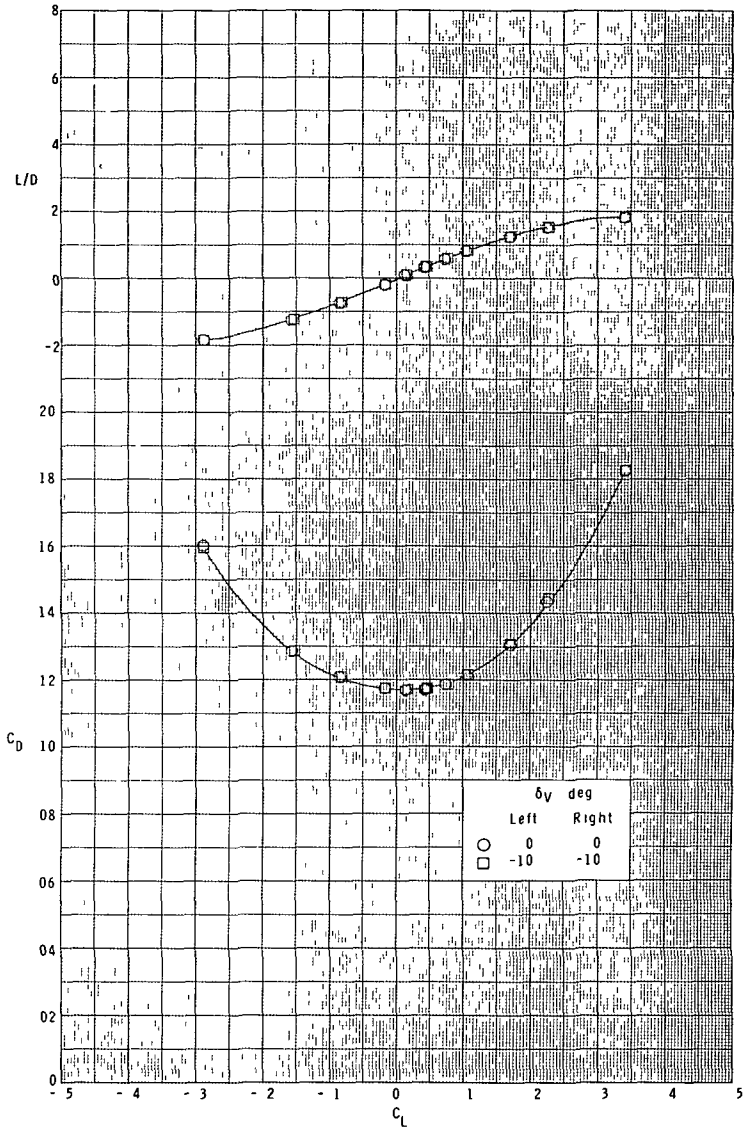

(a) Concluded.

Figure 6.- Continued.

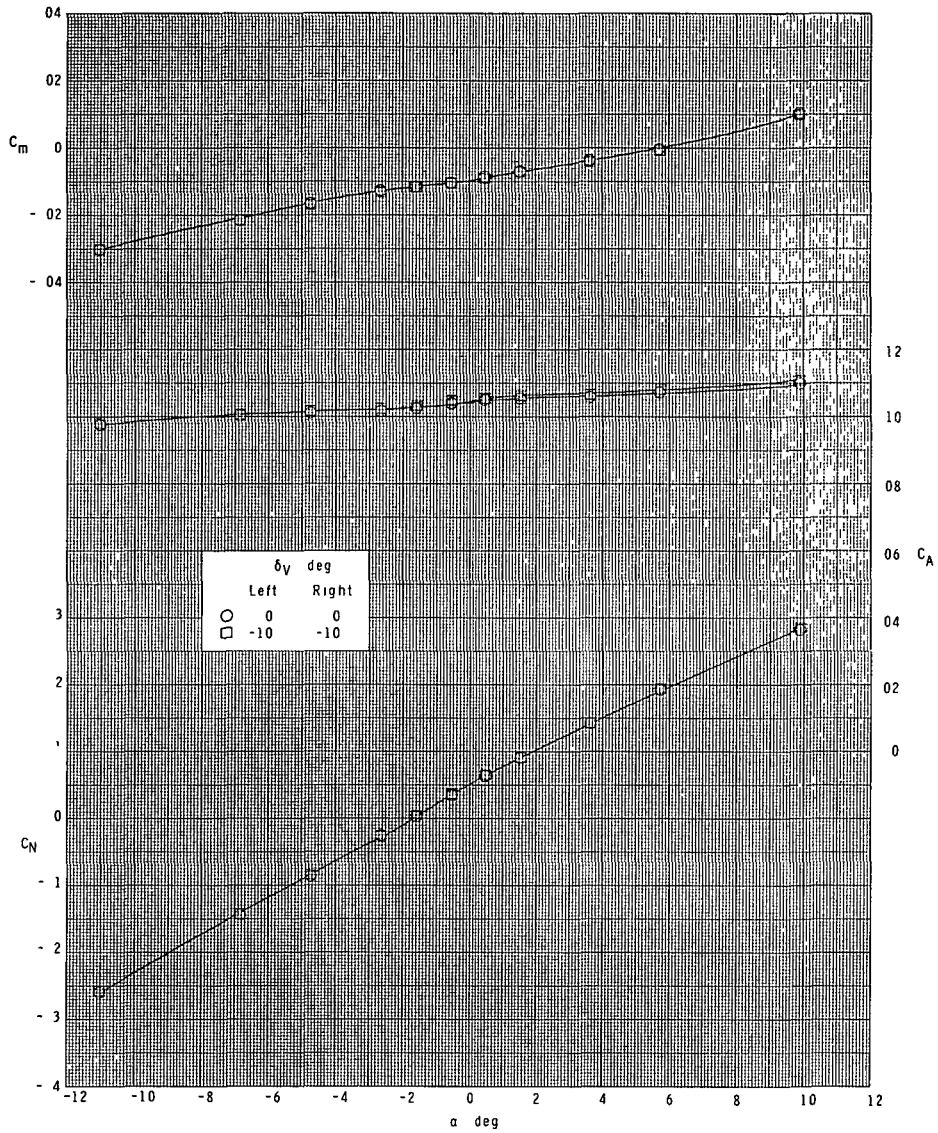

(b) M = 2.96.

Figure 6.- Continued.

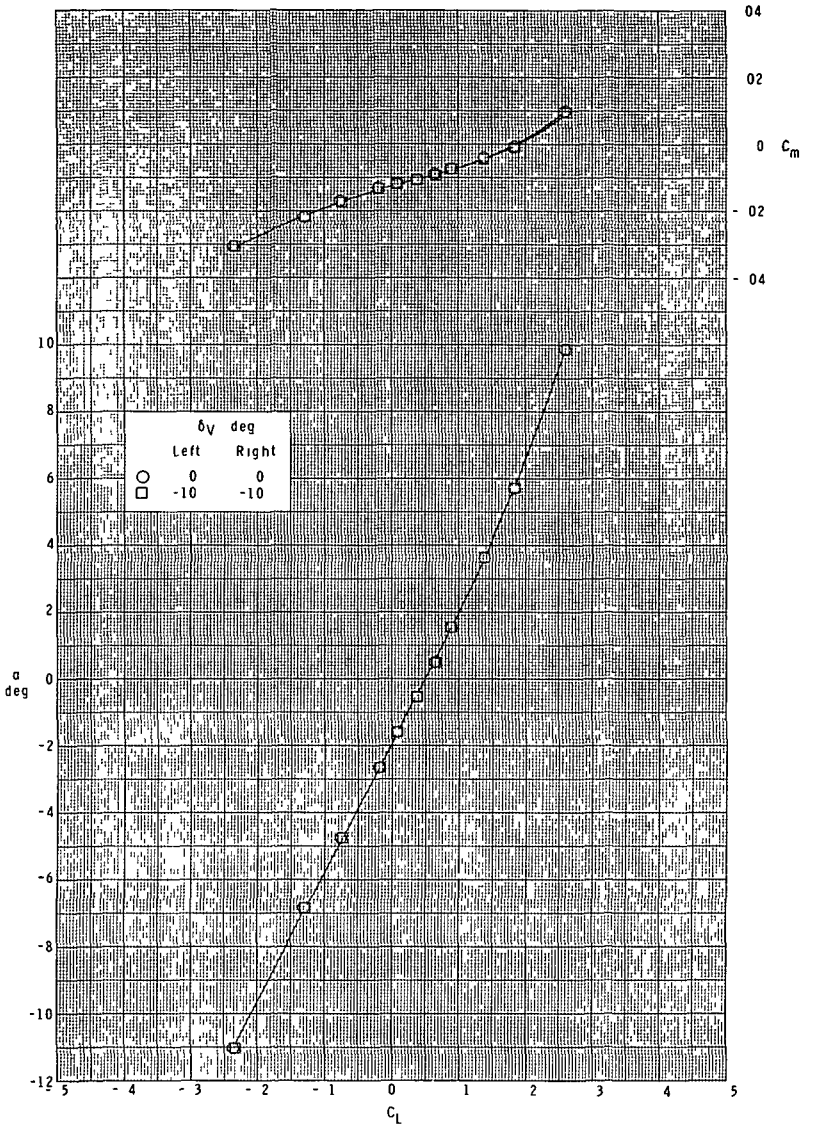

(b) Continued.

Figure 6.- Continued.

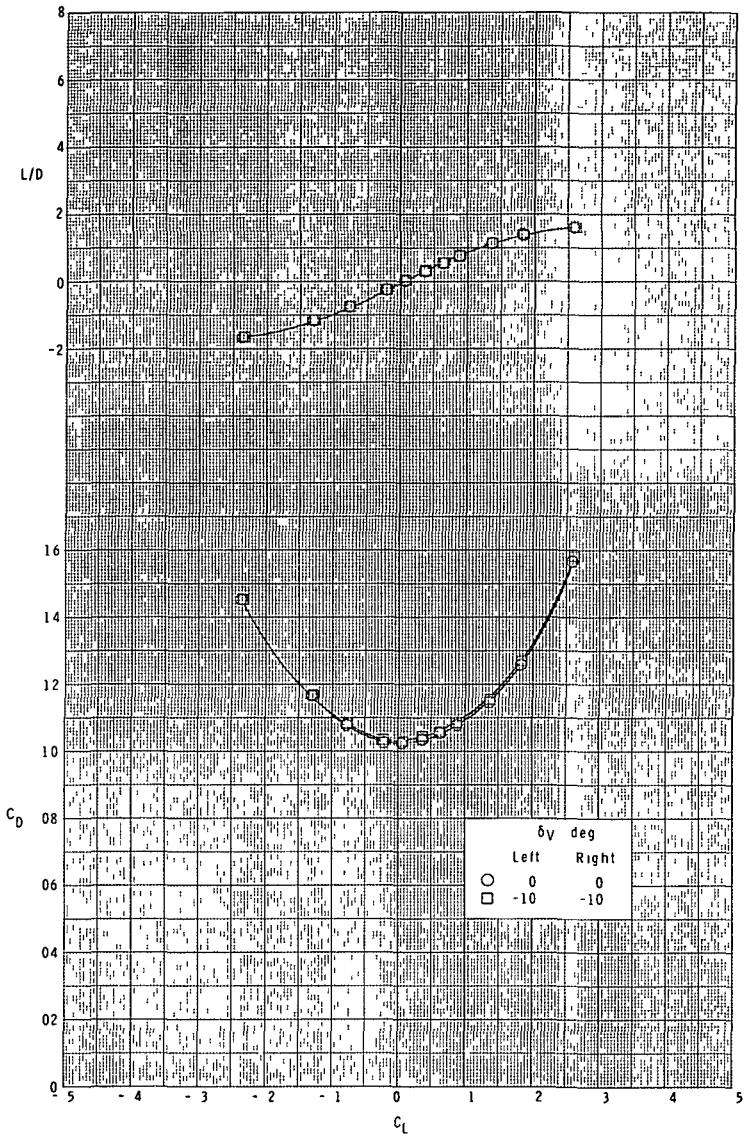

(b) Concluded.

Figure 6.- Continued

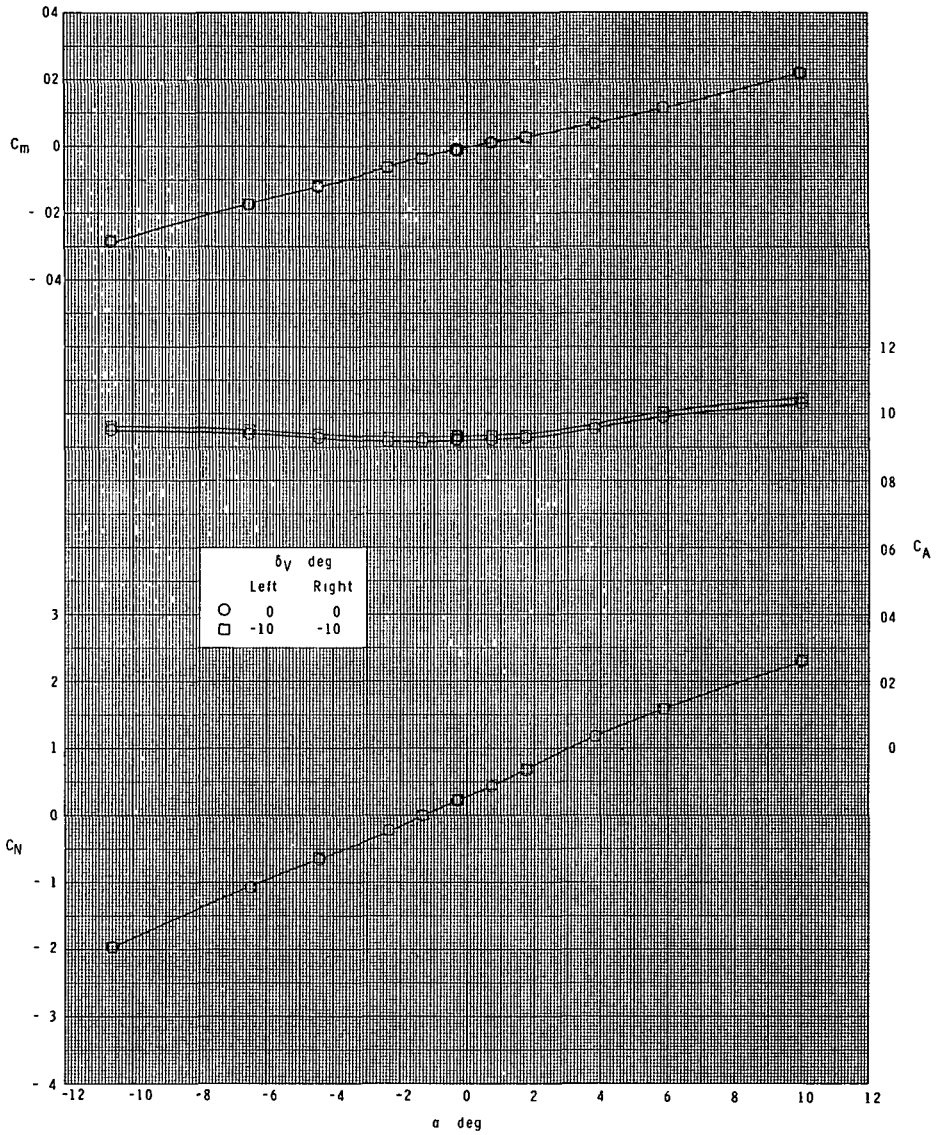

(c) M = 3.95.

Figure 6.- Continued.

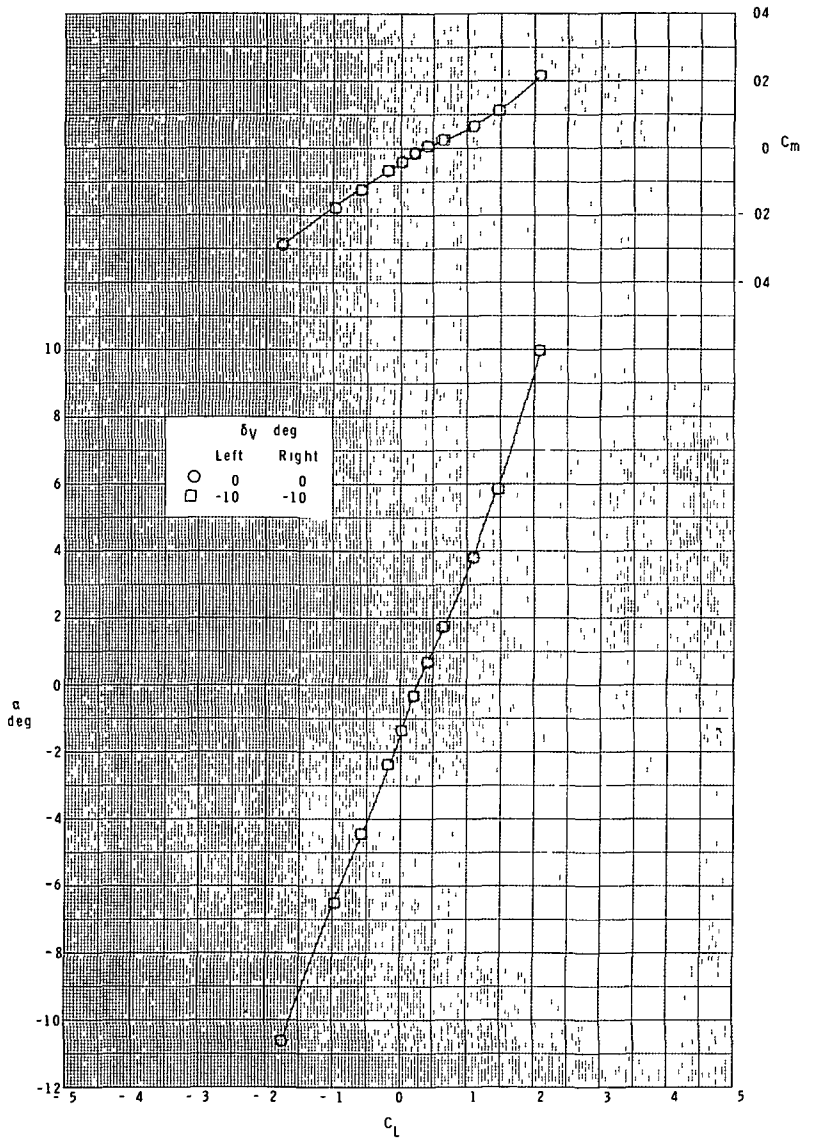

(c) Continued.

Figure 6.- Continued.

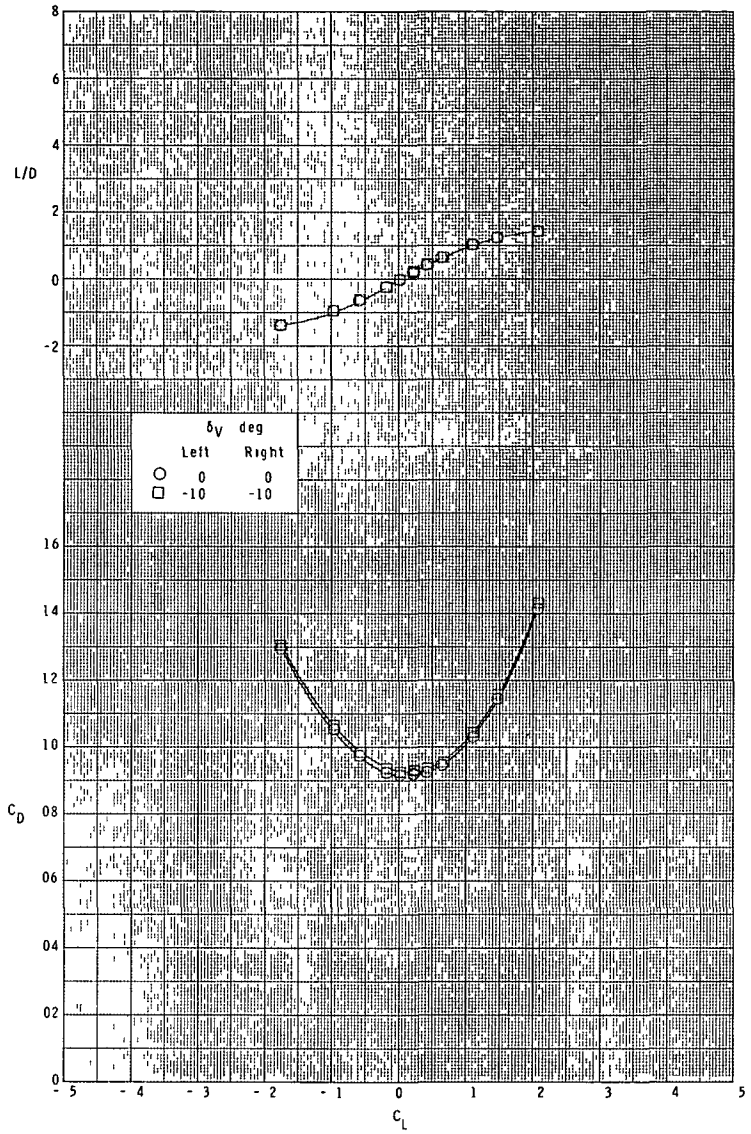

(c) Concluded.

Figure 6.- Continued.

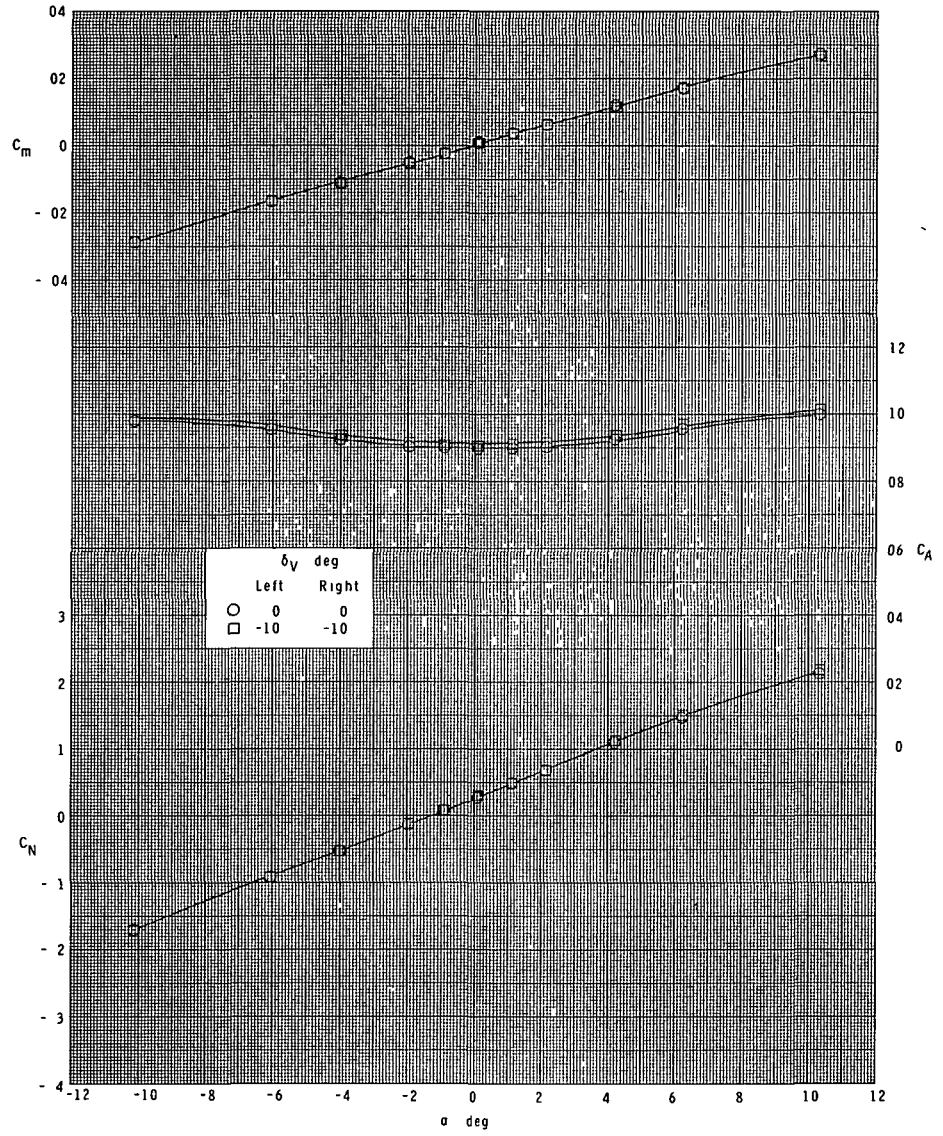

(d) M = 4.60.

Figure 6.- Continued.

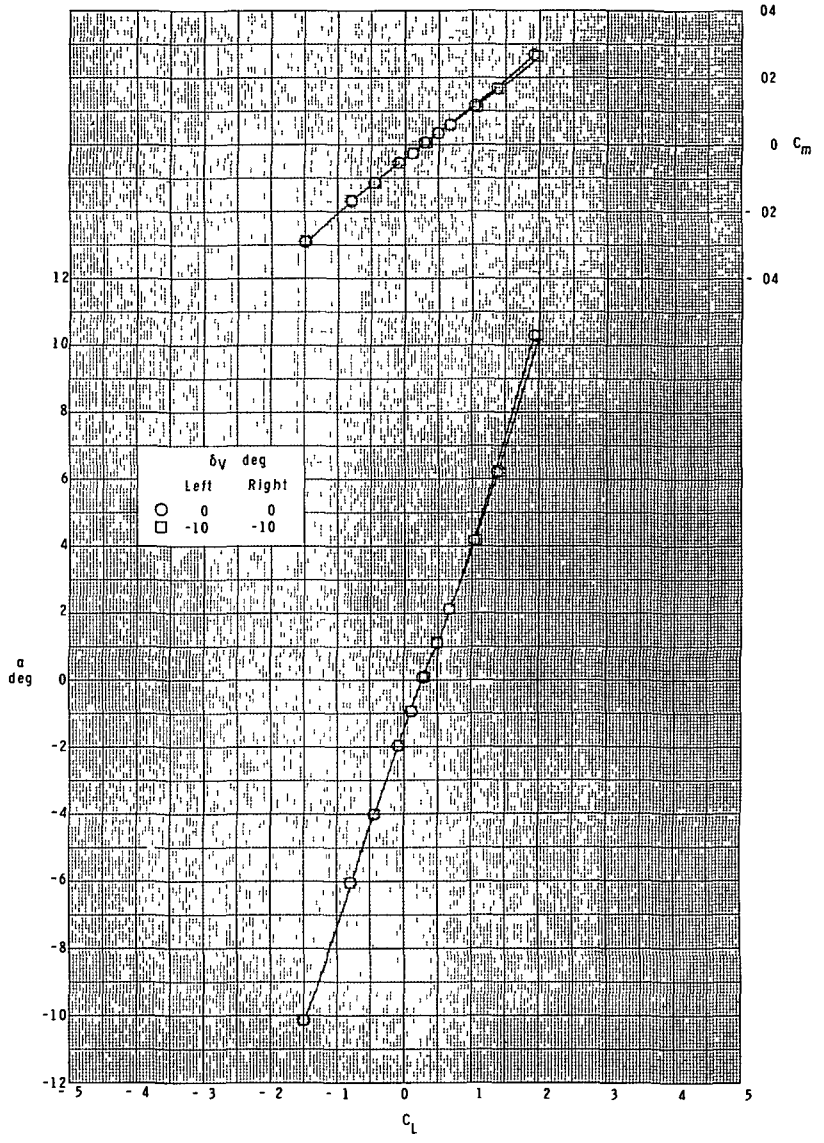

(d) Continued.

Figure 6.- Continued.

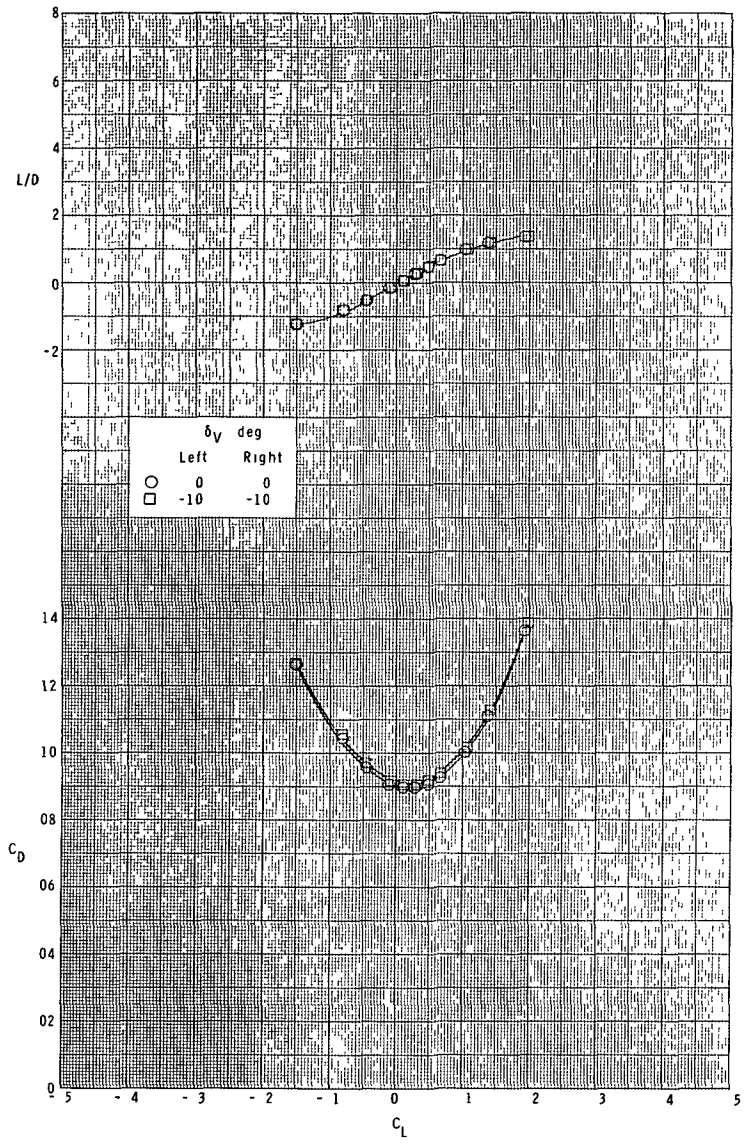

(d) Concluded.

Figure 6.- Concluded.

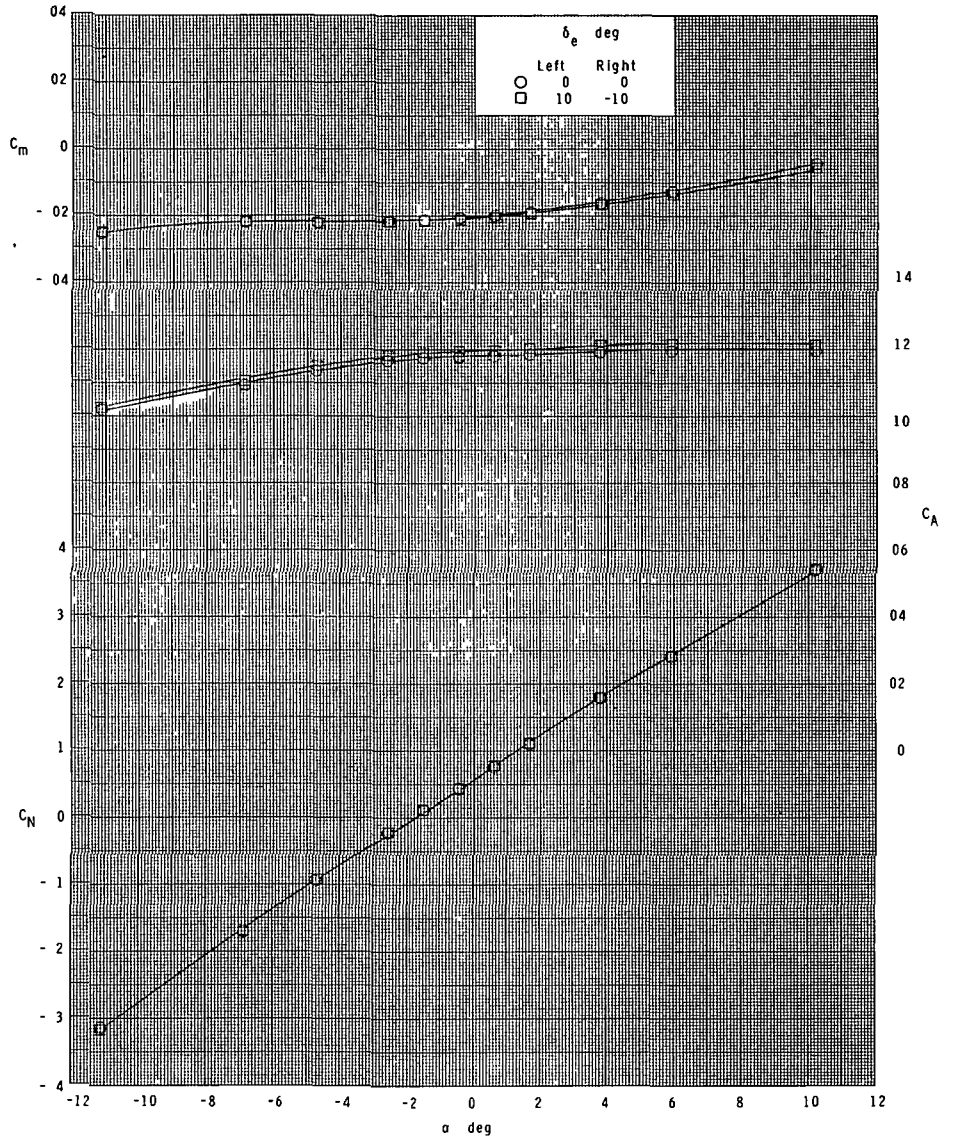

(a) M = 2.30.

Figure 7.- Effect of booster-elevon deflection-in-roll on longitudinal characteristics. Ascent configuration.

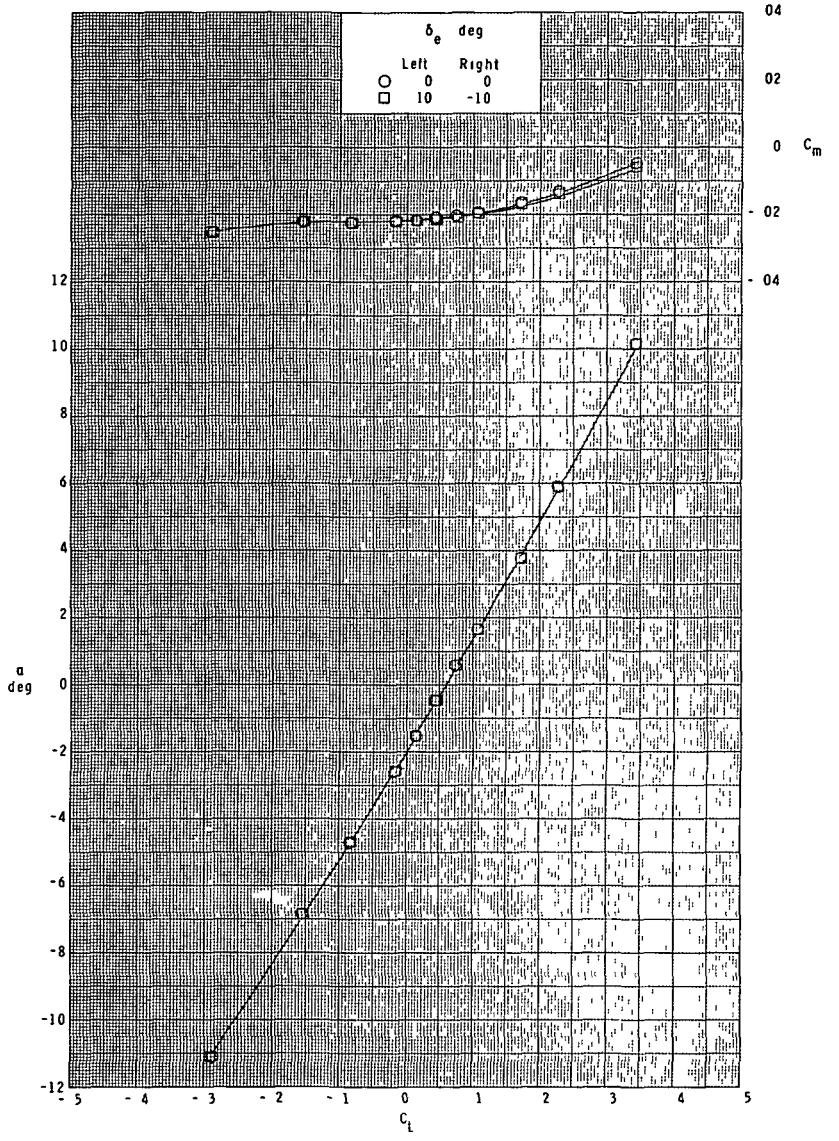

(a) Continued.

Figure 7.- Continued.

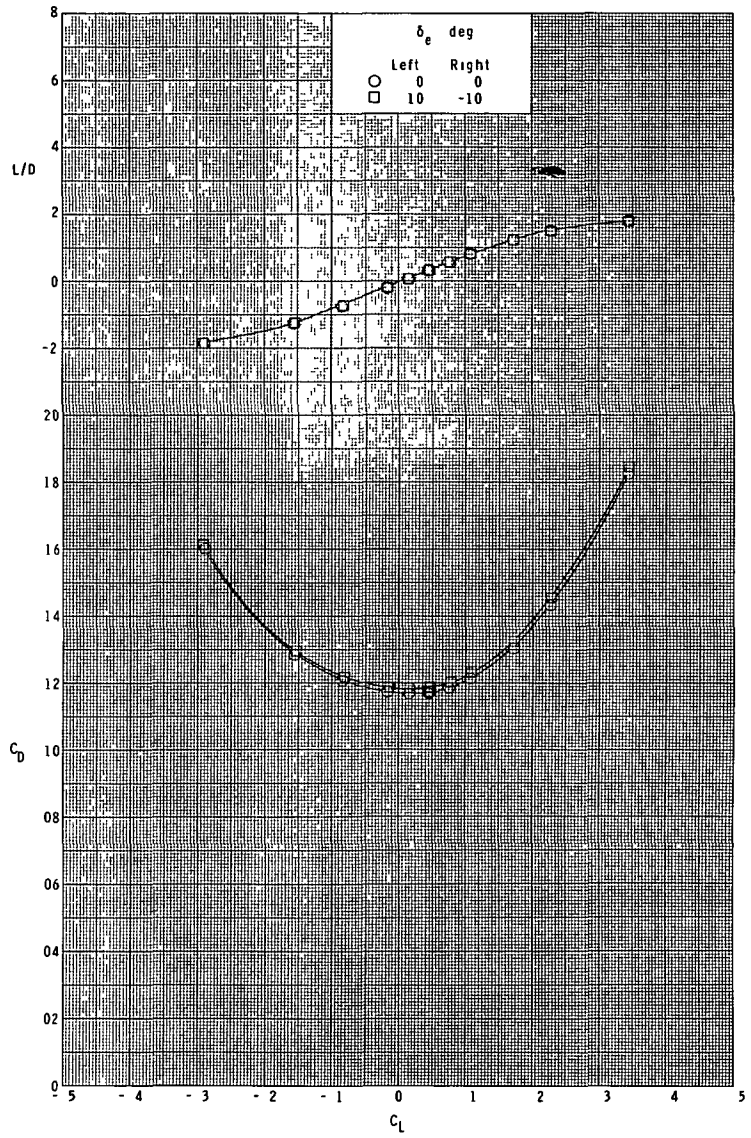

(a) Concluded.

Figure 7.- Continued.

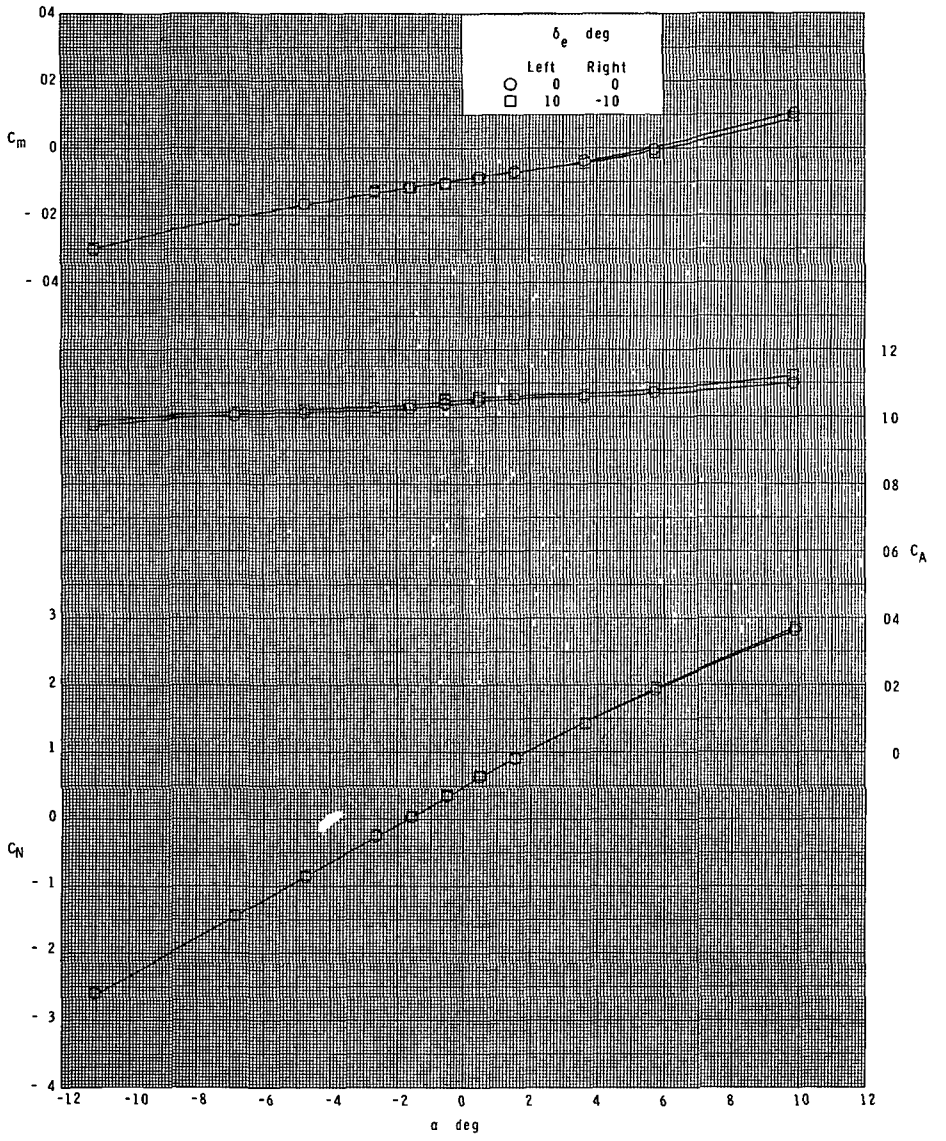

(b) M = 2.96.

Figure 7.- Continued.

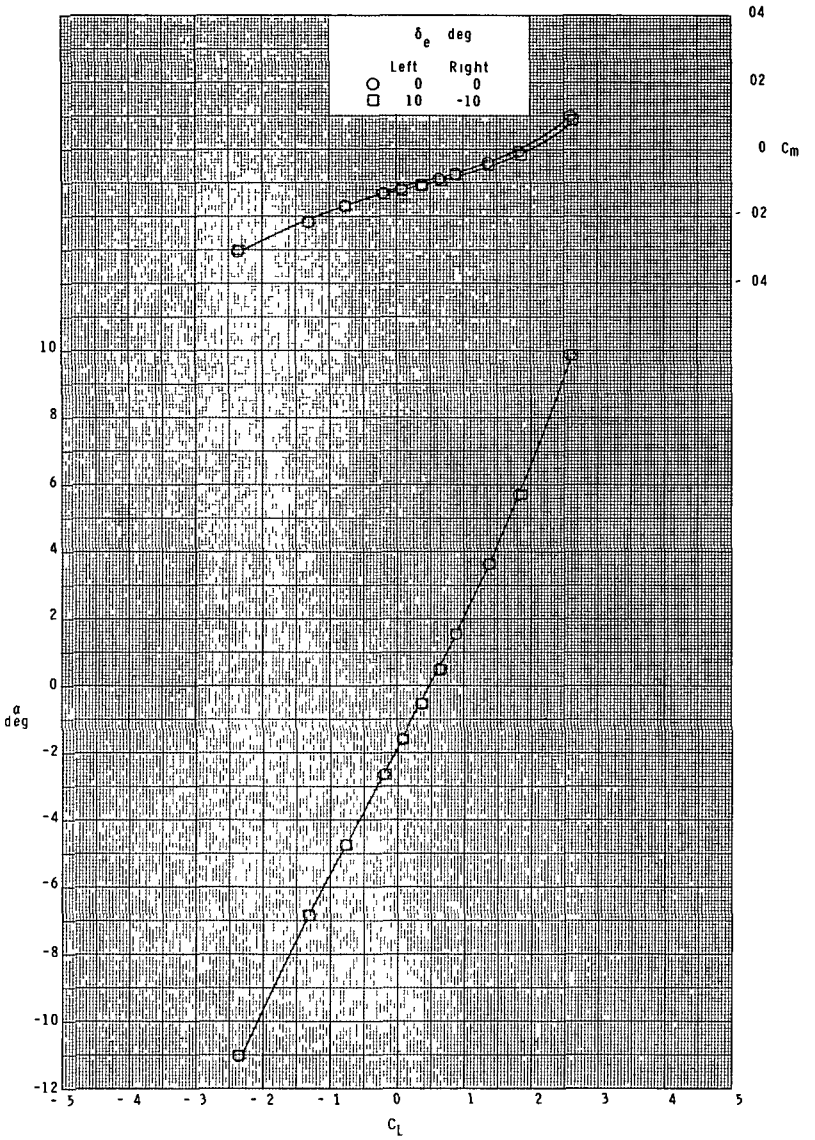

(b) Continued.

Figure 7.- Continued.

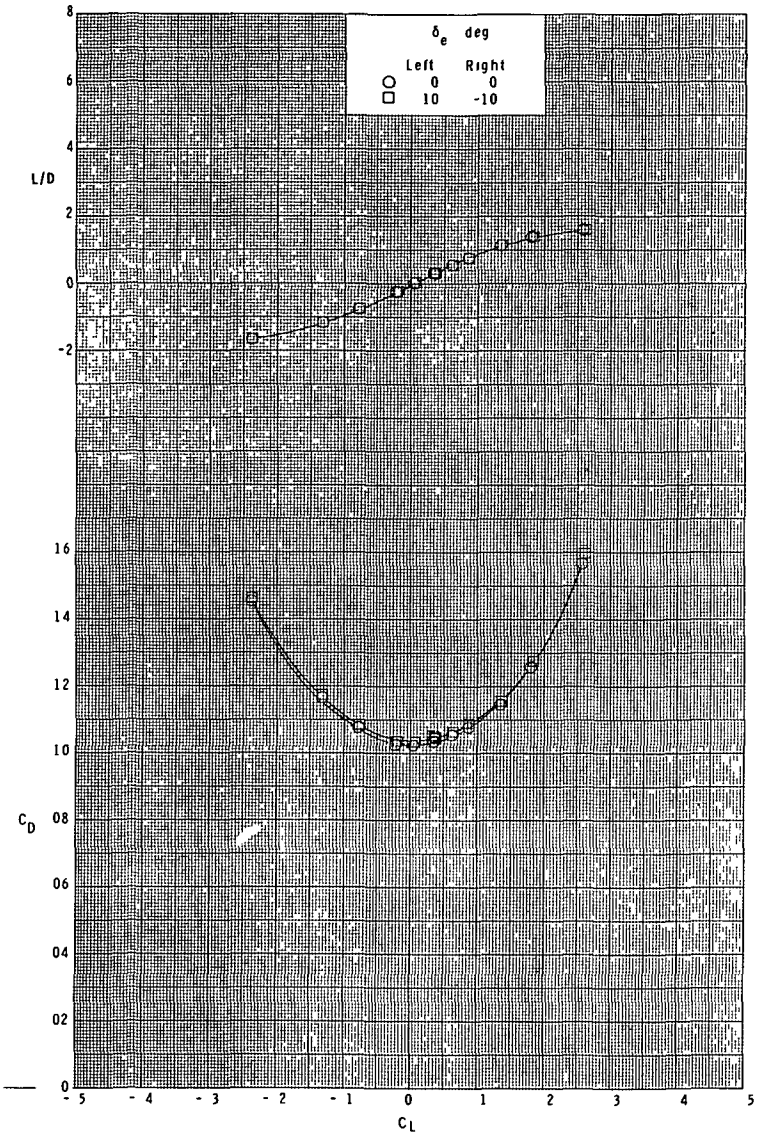

(b) Concluded.

Figure 7.- Continued.

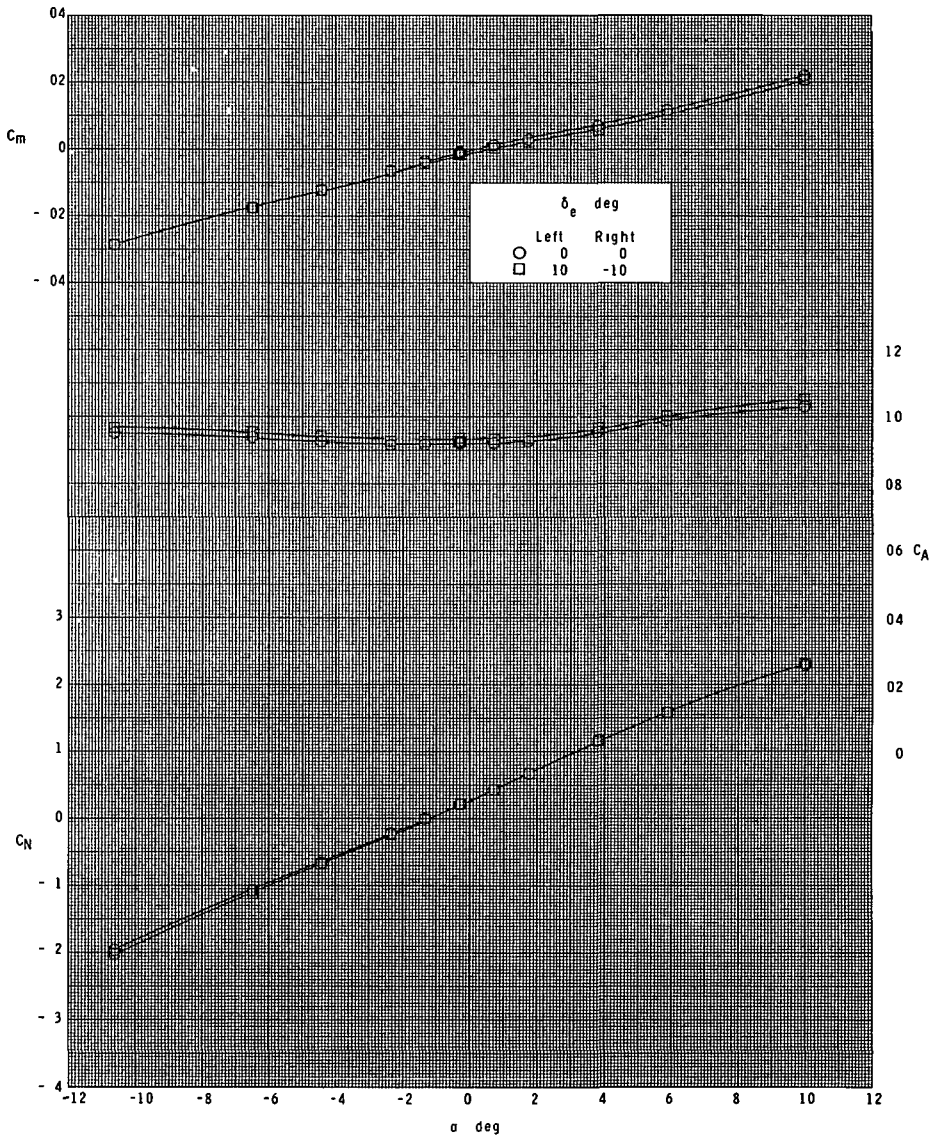

(c) M = 3.95.

Figure 7.- Continued.

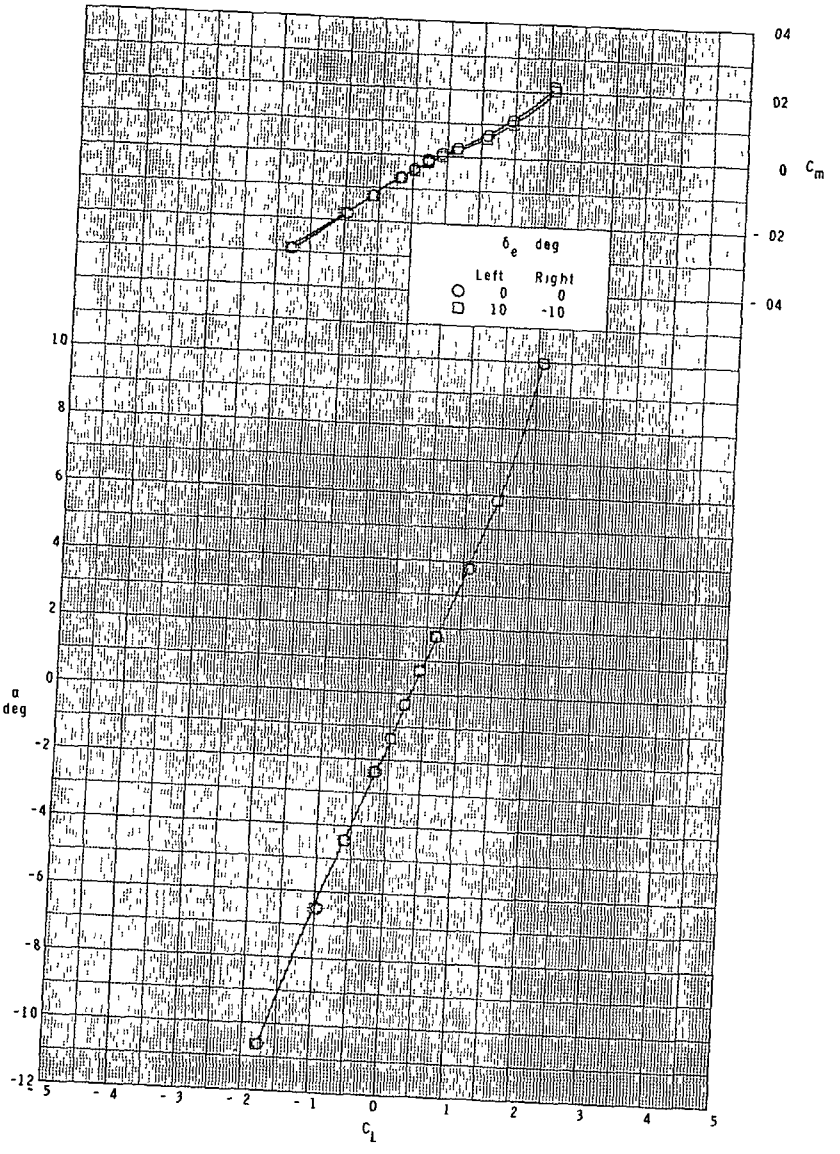

(c) Continued.

Figure 7.- Continued.

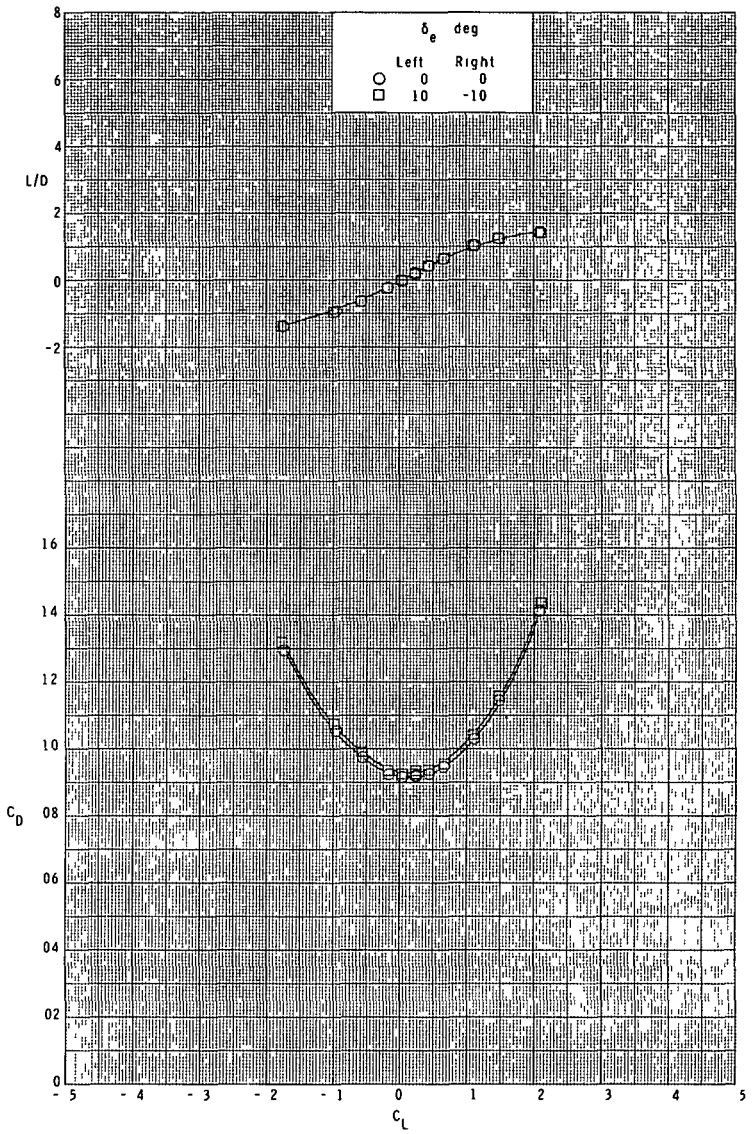

(c) Concluded.

Figure 7.- Continued.

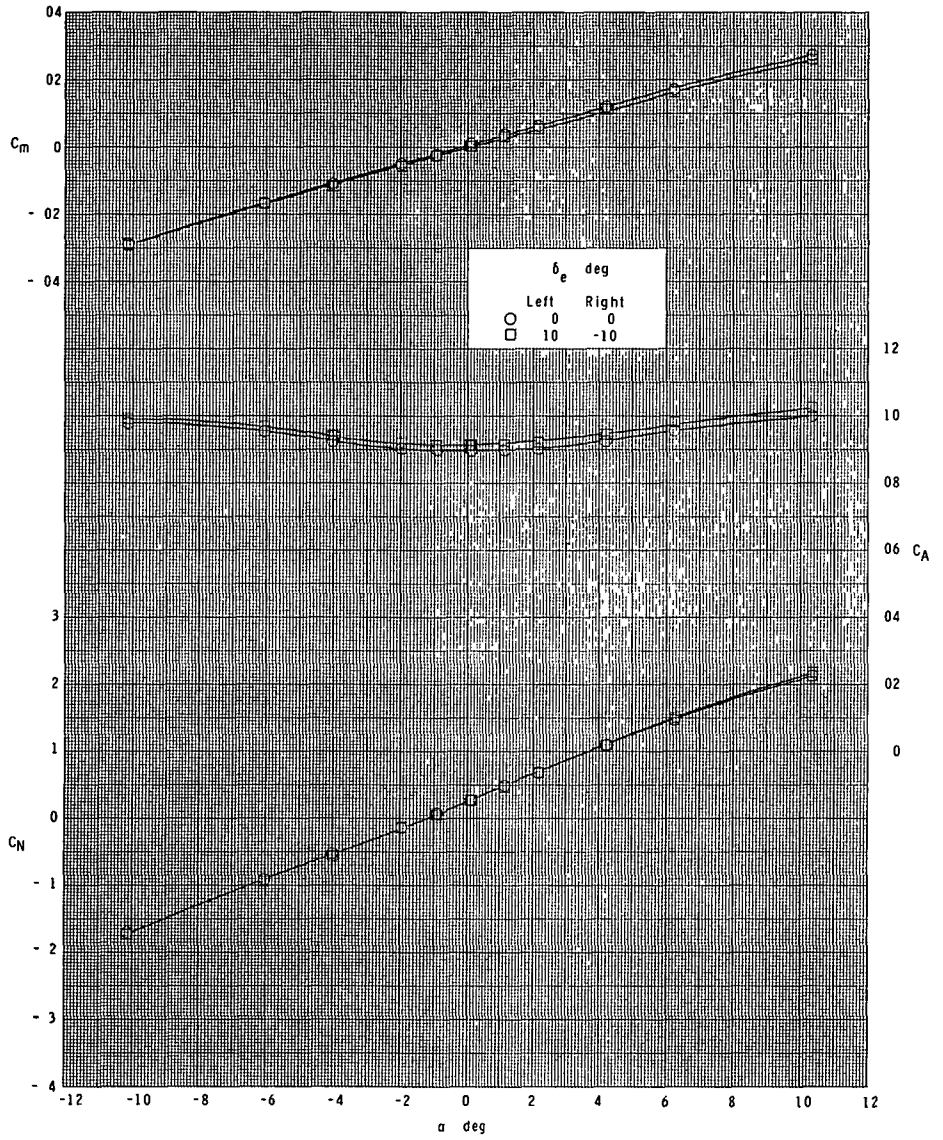

(d) M = 4.60.

Figure 7.- Continued.

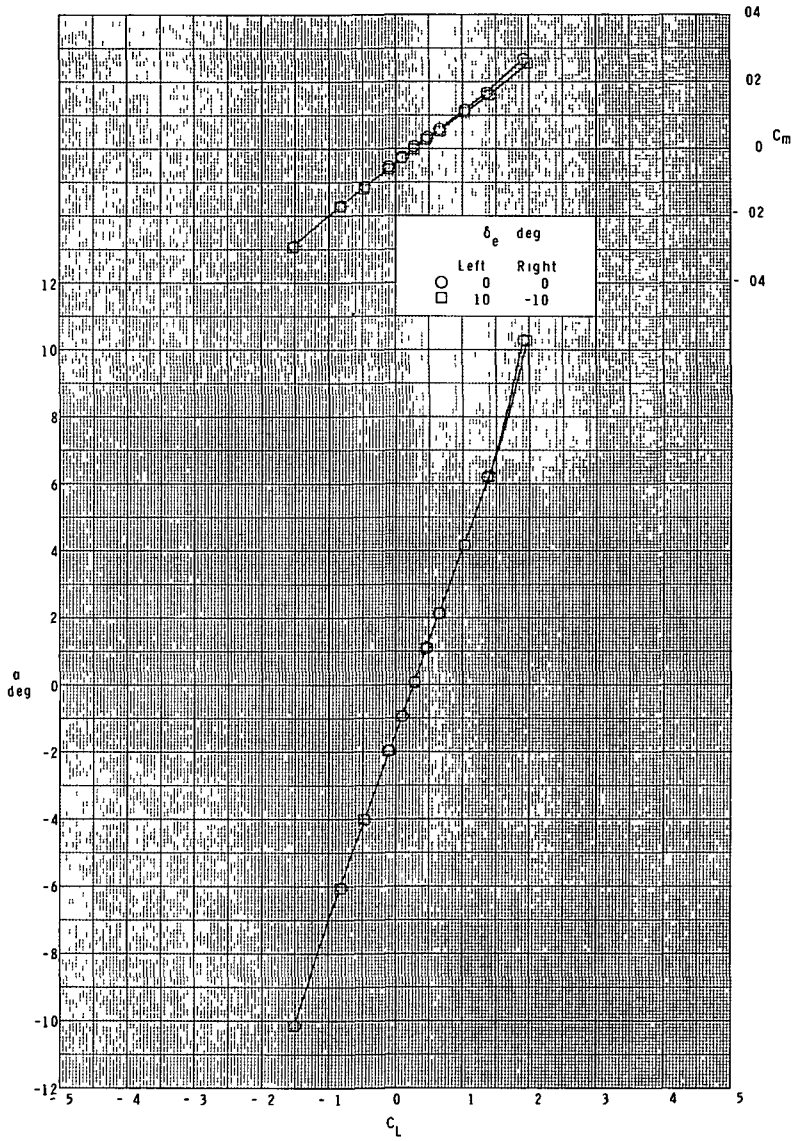

(d) Continued.

Figure 7.- Continued.

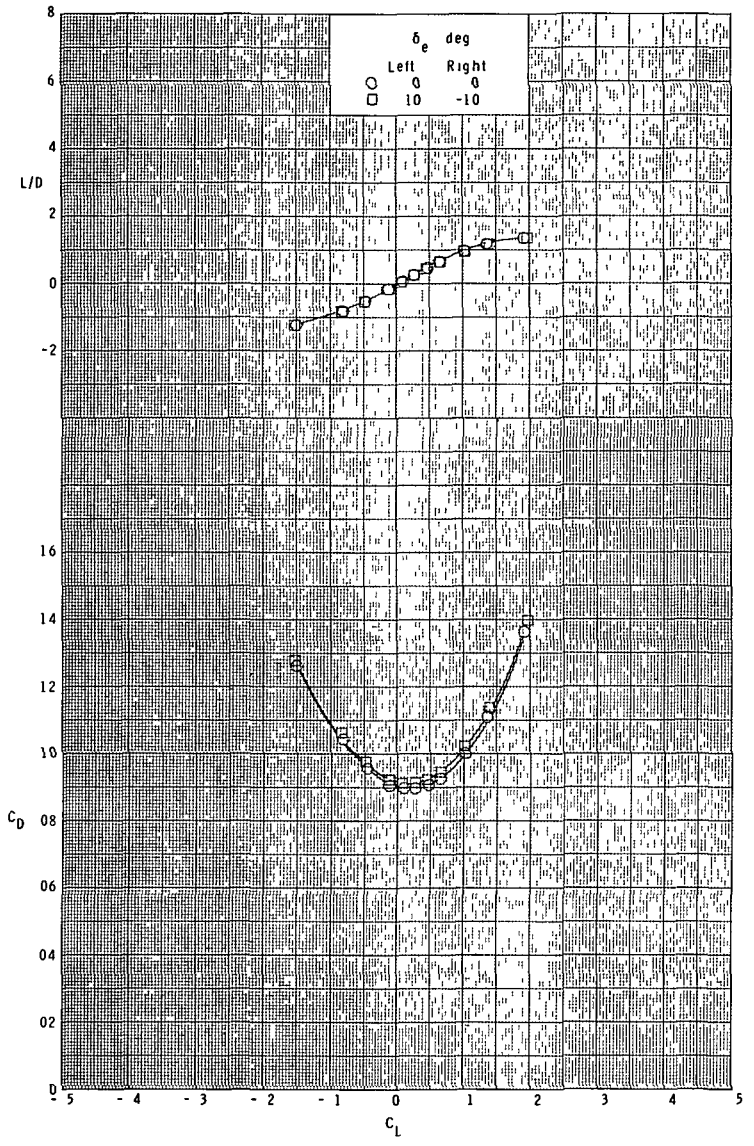

(d) Concluded.

Figure 7.- Concluded.

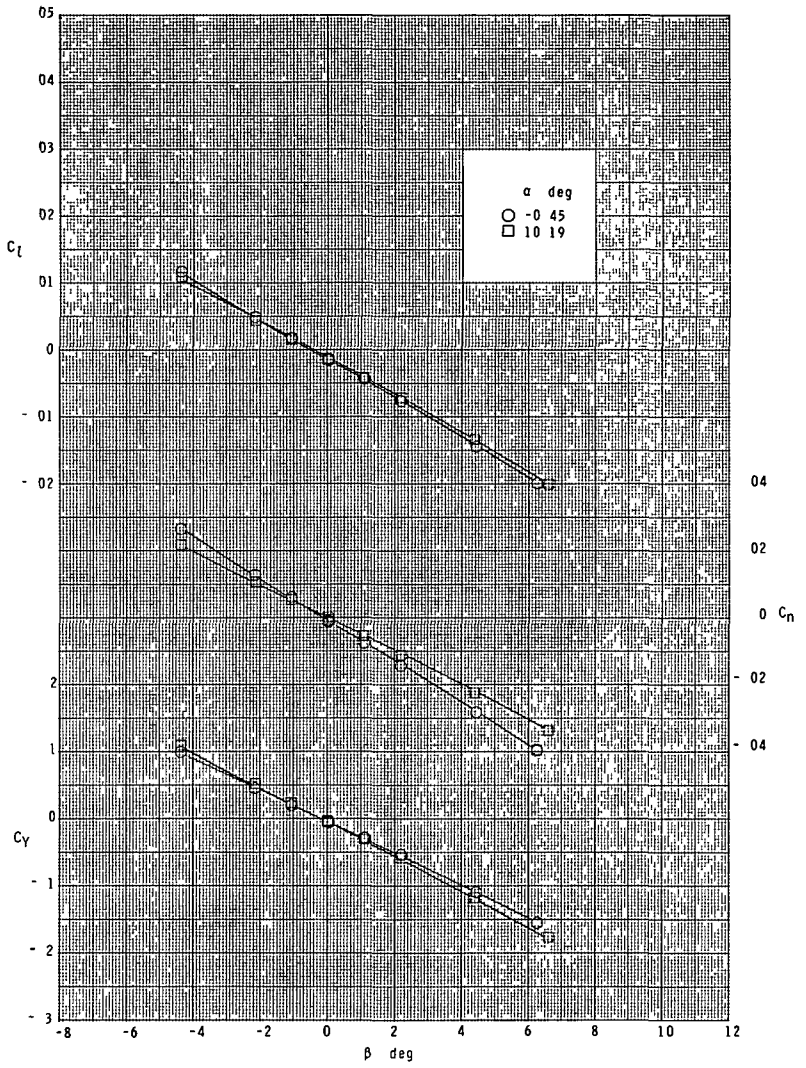

(a) M = 2.30.

Figure 8.- Lateral characteristics in sideslip. Ascent configuration.

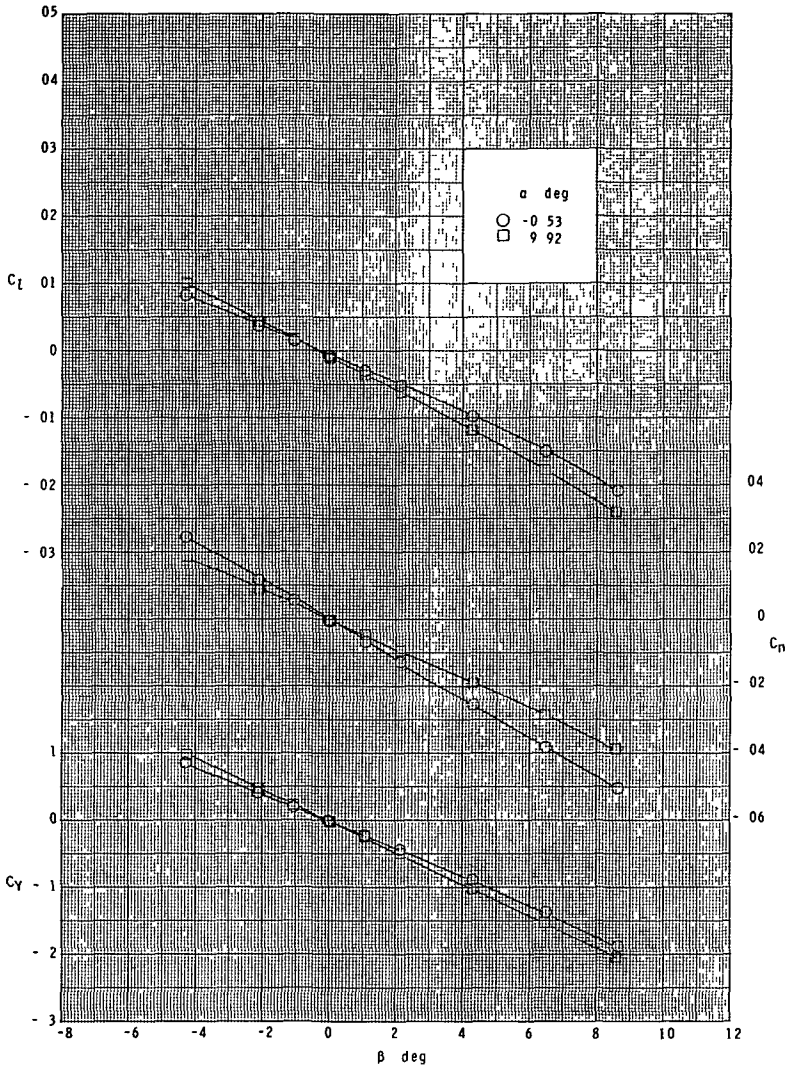

(b) M = 2.96.

Figure 8.- Continued.

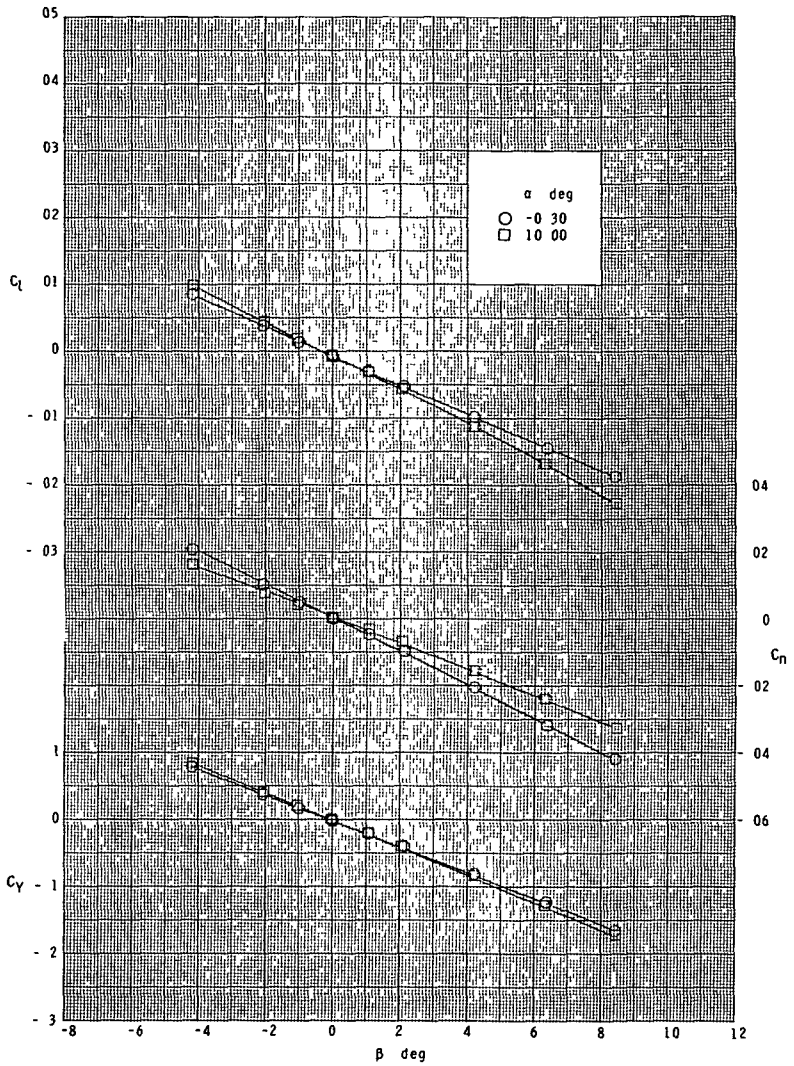

(c) M = 3.95.

Figure 8.- Continued.

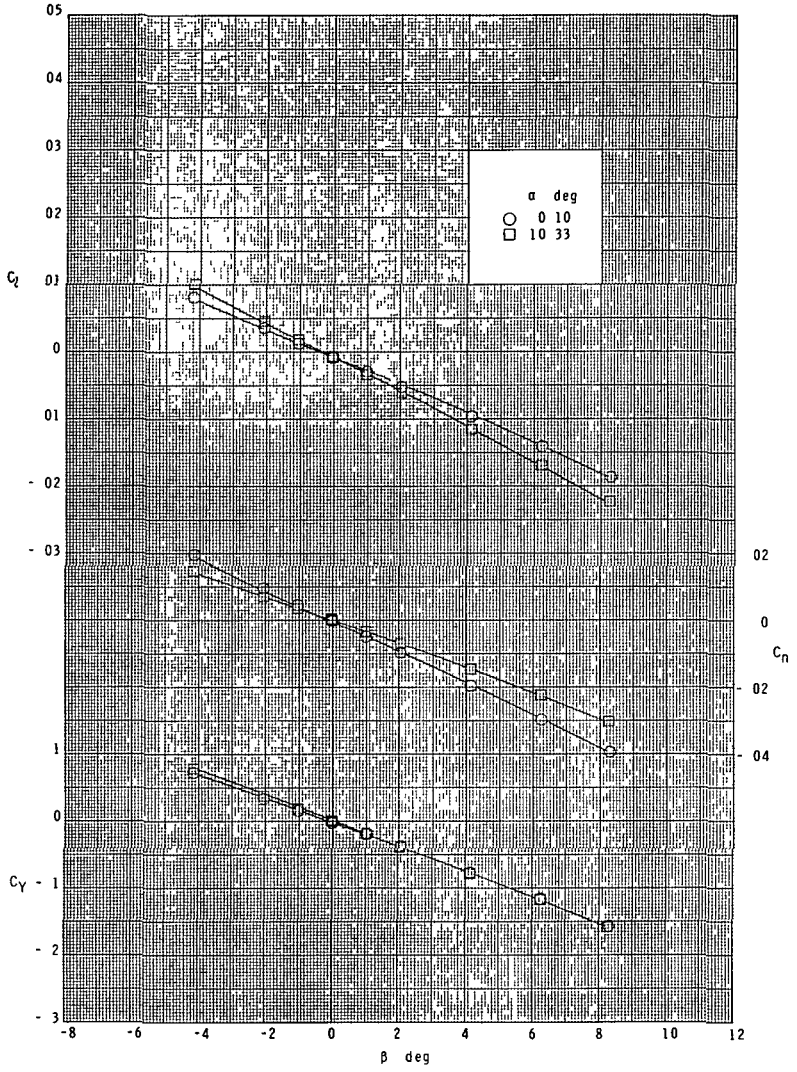

(d) M = 4.60.

Figure 8.- Concluded.

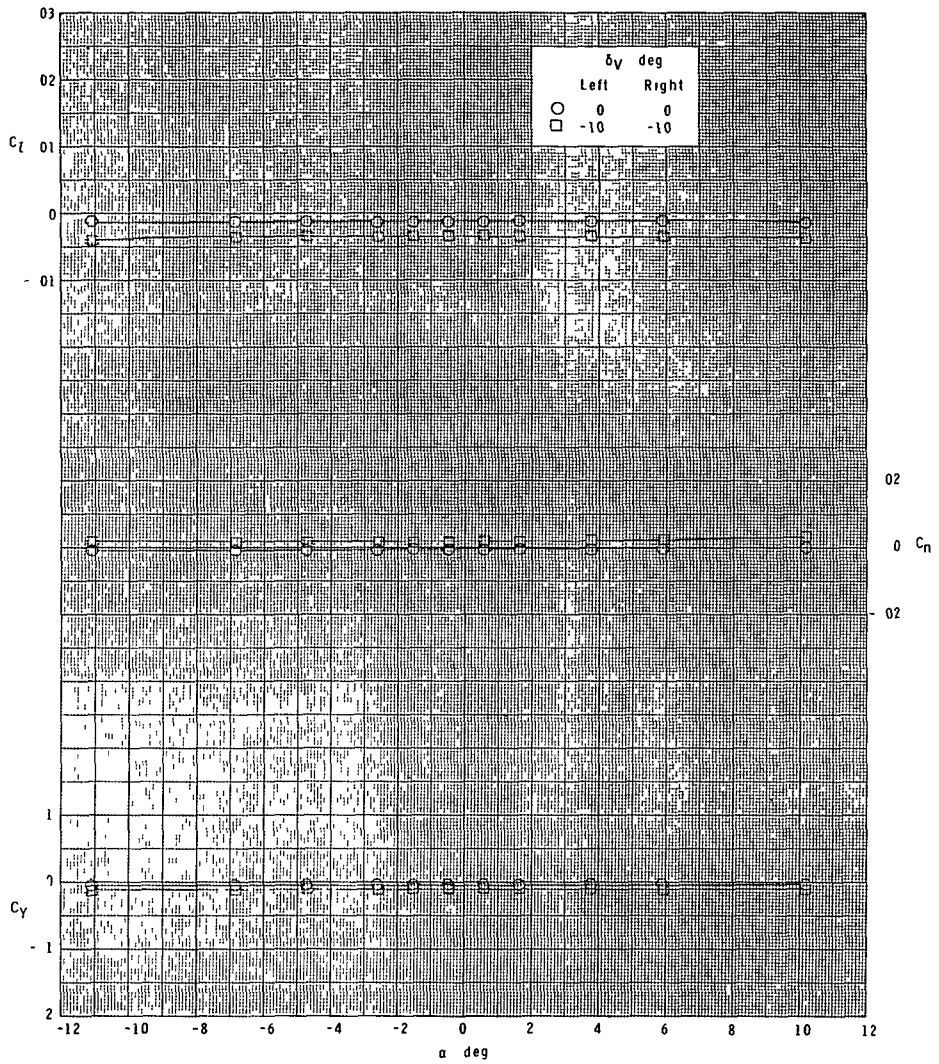

(a) M = 2.30.

Figure 9.- Booster vertical-fin rudder-control effectiveness. Ascent configuration.

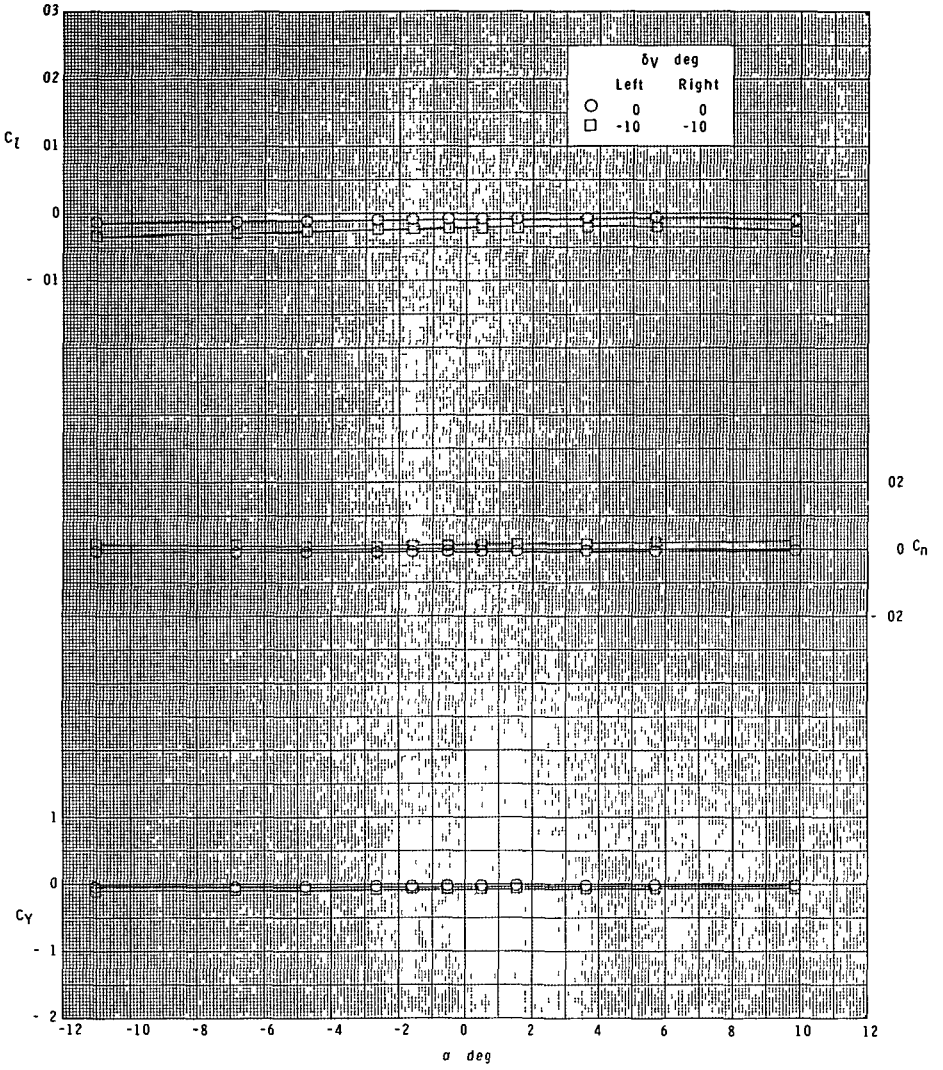

(b) M = 2.96.

Figure 9.- Continued.

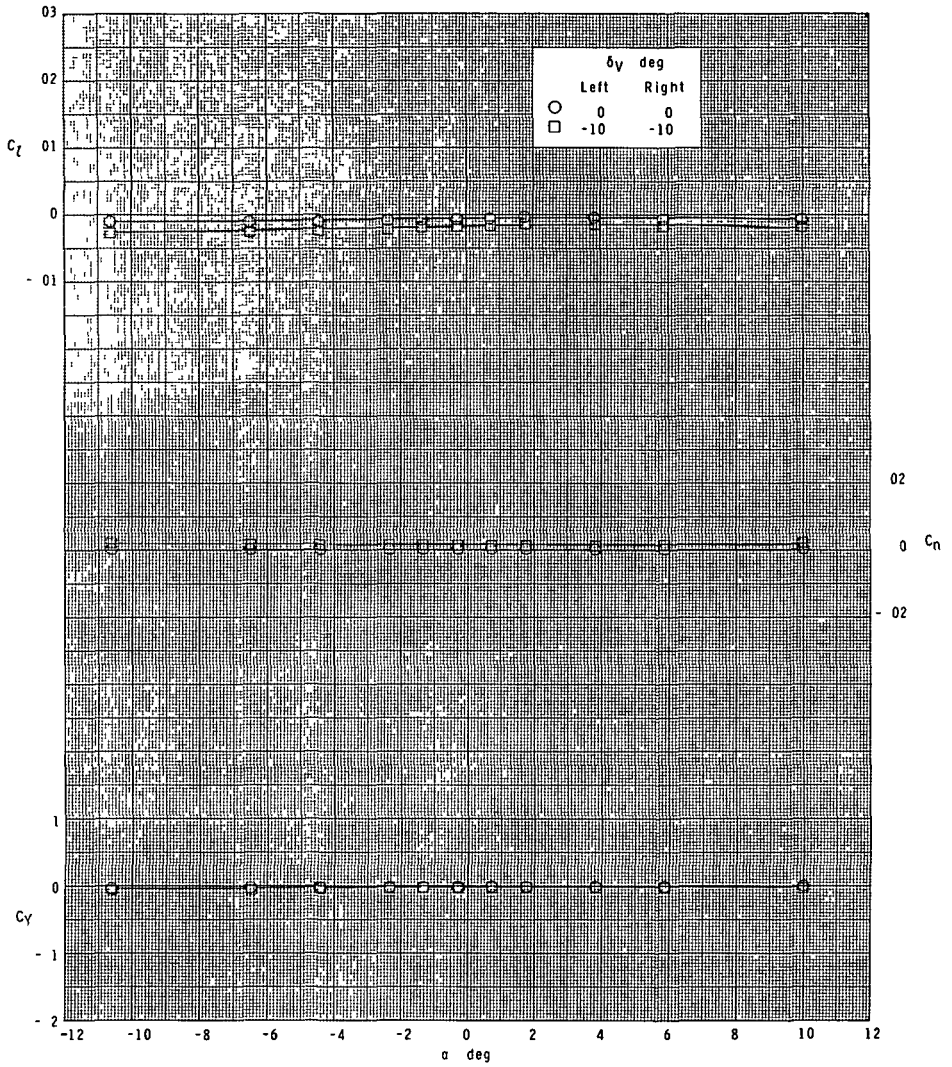

(c) M = 3.95.

Figure 9.- Continued.

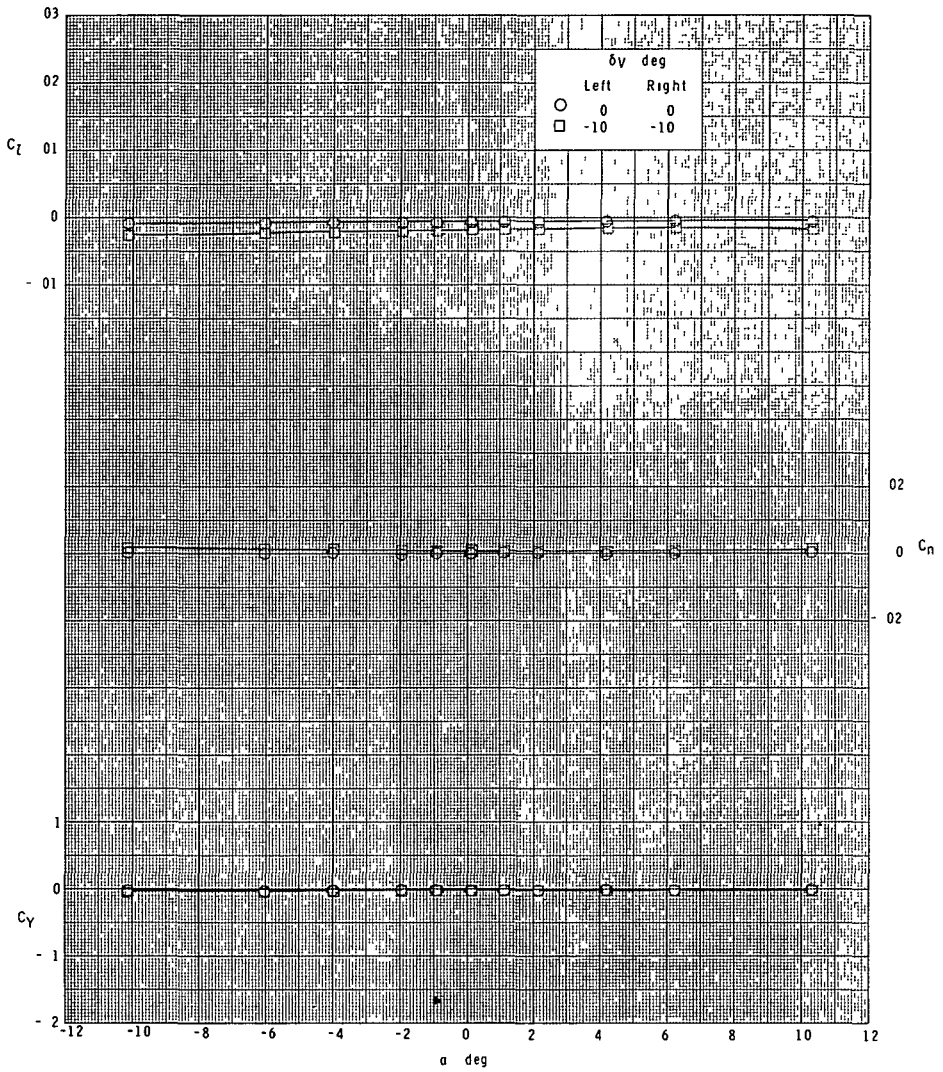

(d) M = 4.60.

Figure 9.- Concluded.

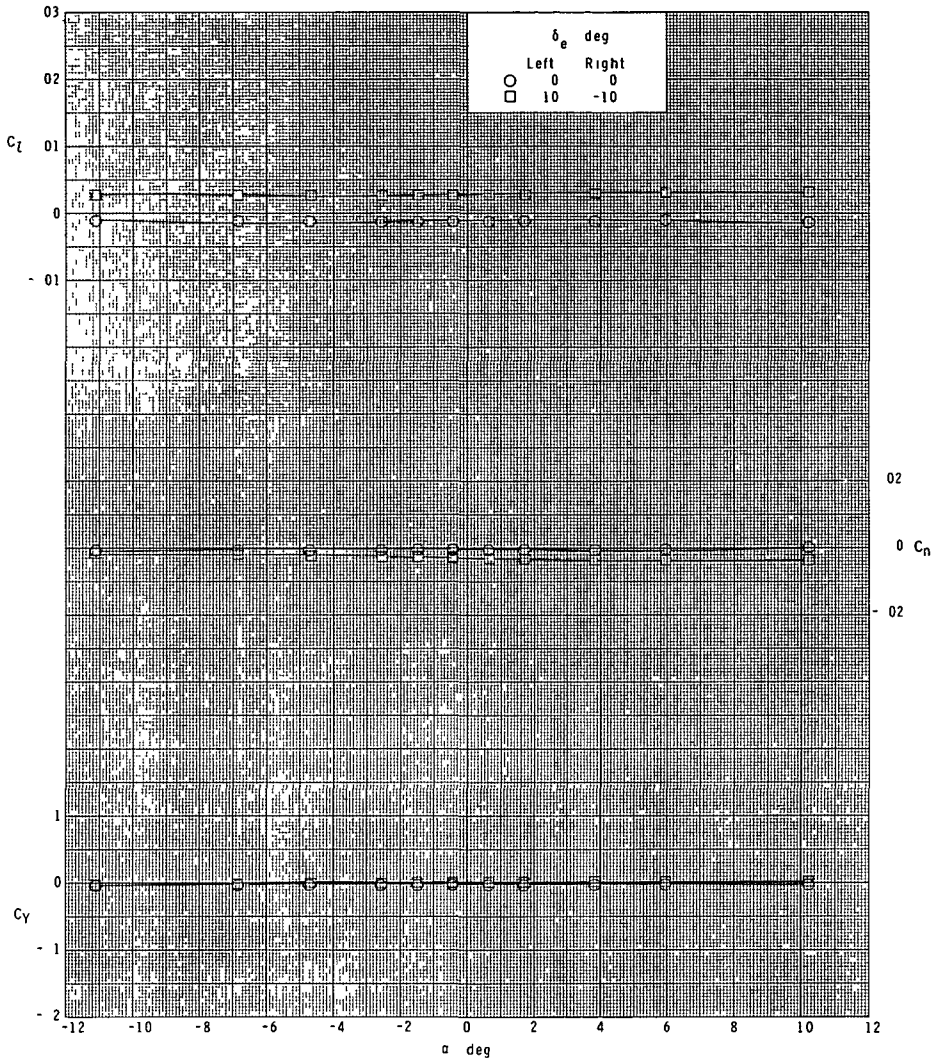

(a) M = 2 30.

Figure 10.- Booster-elevon roll-control effectiveness. Ascent configuration.

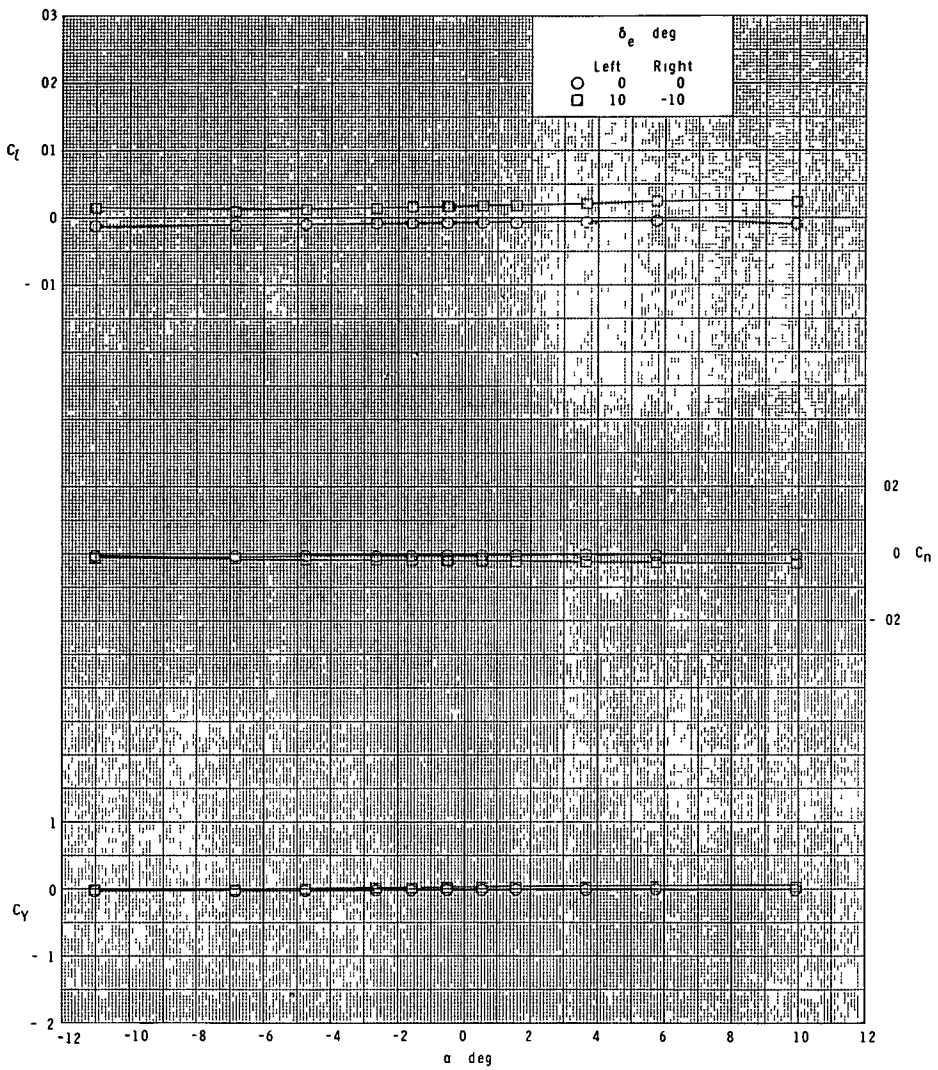

(b) M = 2.96.

Figure 10.- Continued.

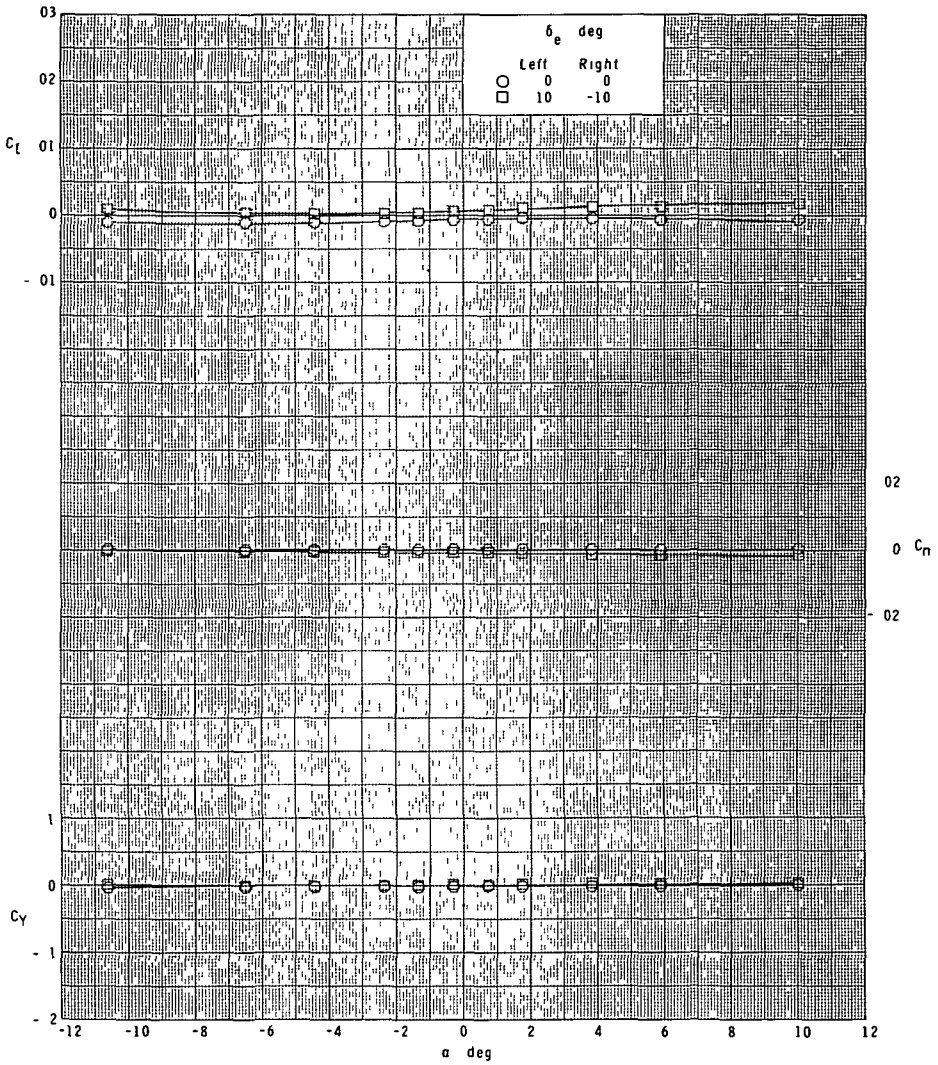

(c) M = 3.95.

Figure 10.- Continued.

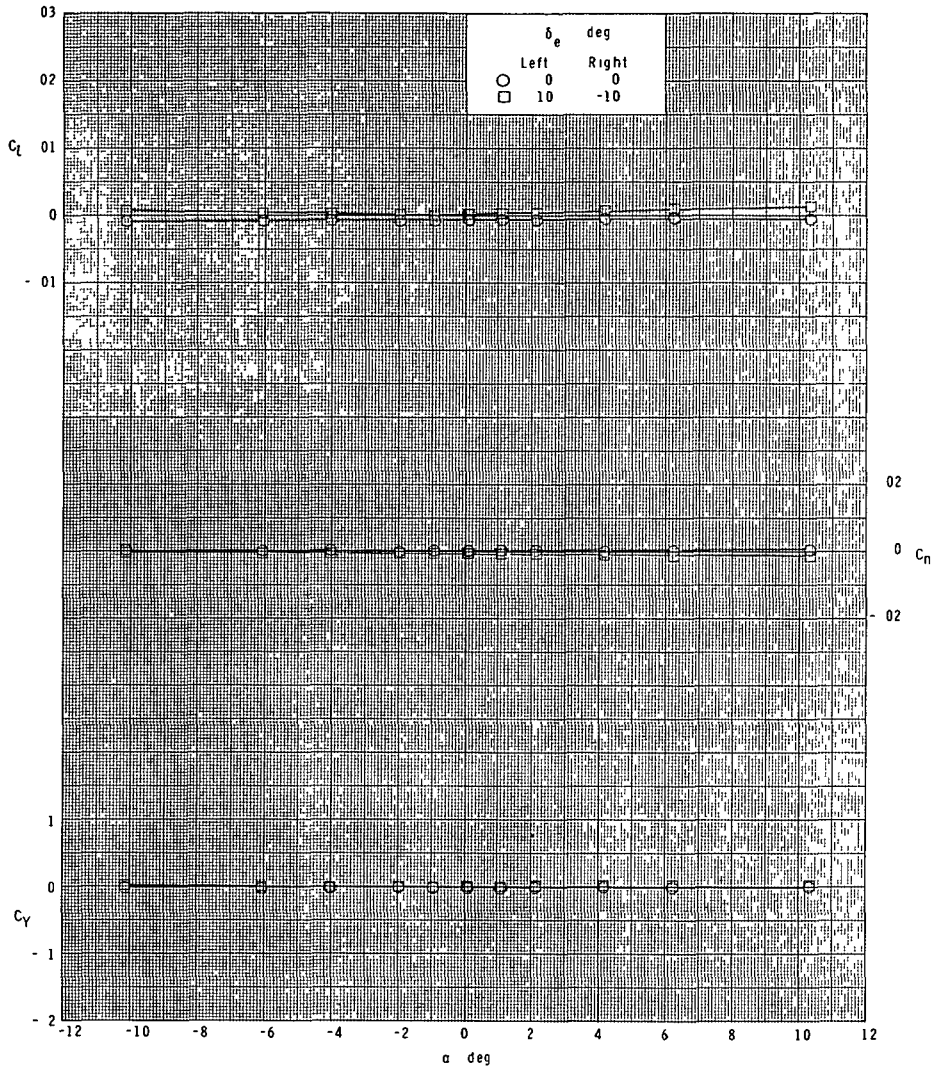

(d) M = 4.60.

Figure 10.- Concluded.

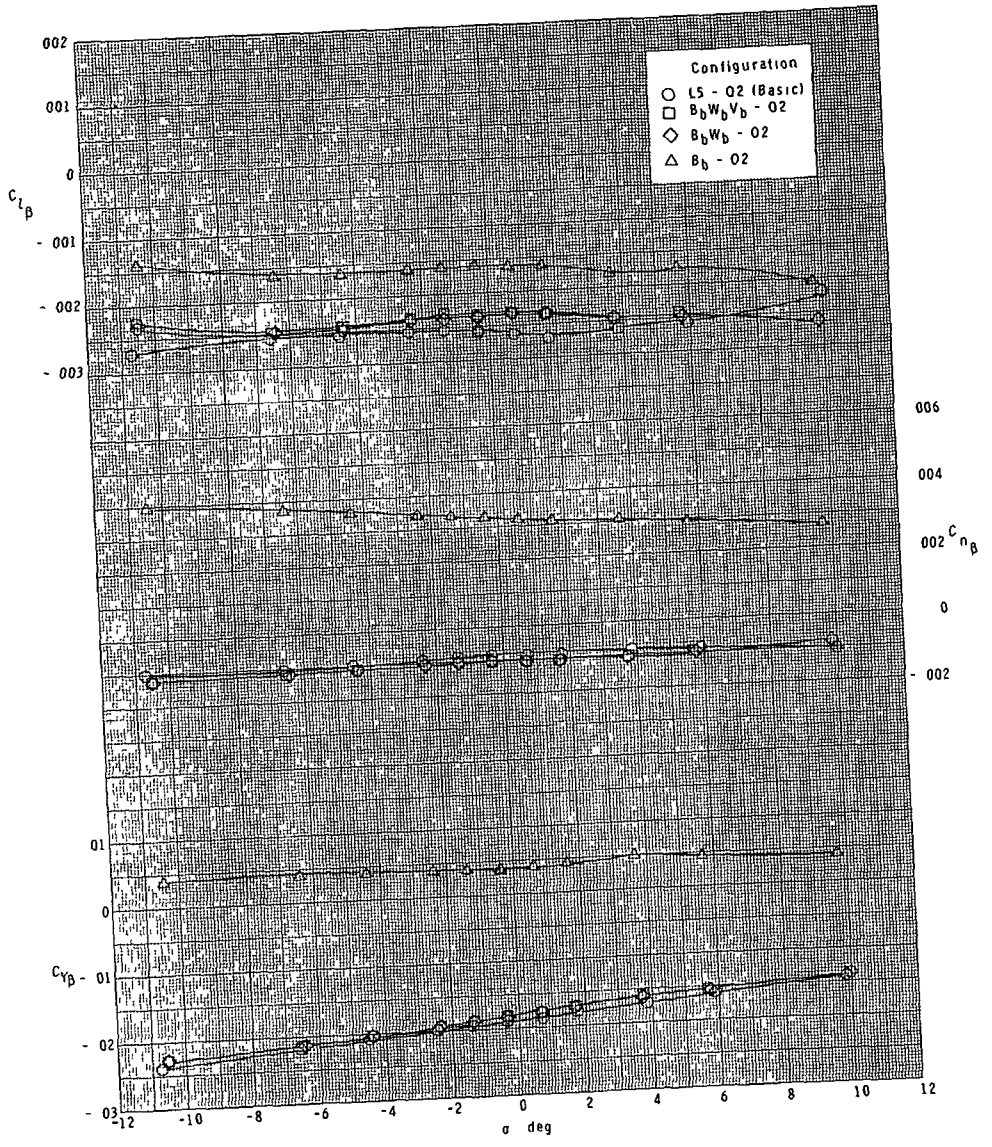

(a) M = 2.30.

Figure 11.- Lateral-stability parameters. Ascent configuration.

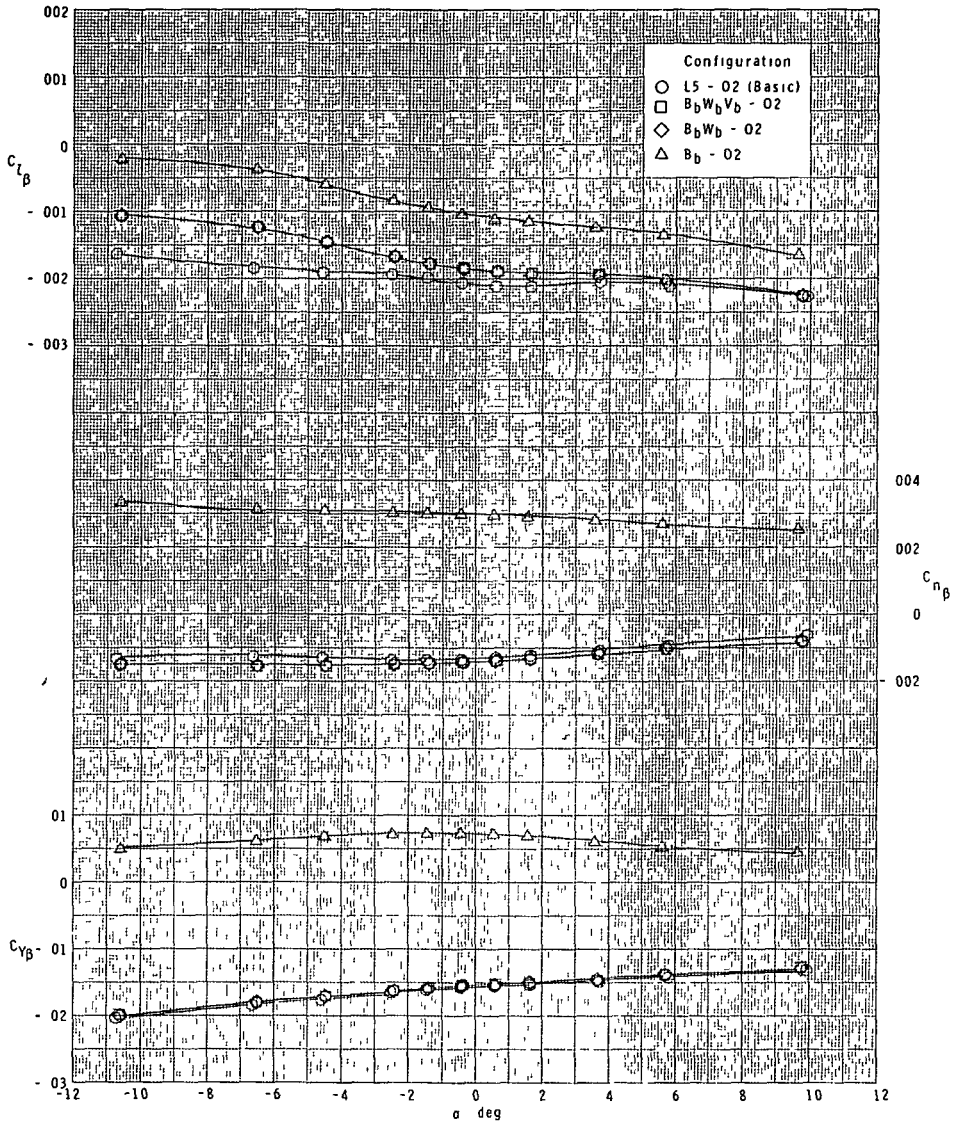

(b) M = 2.96.

Figure 11.- Continued.

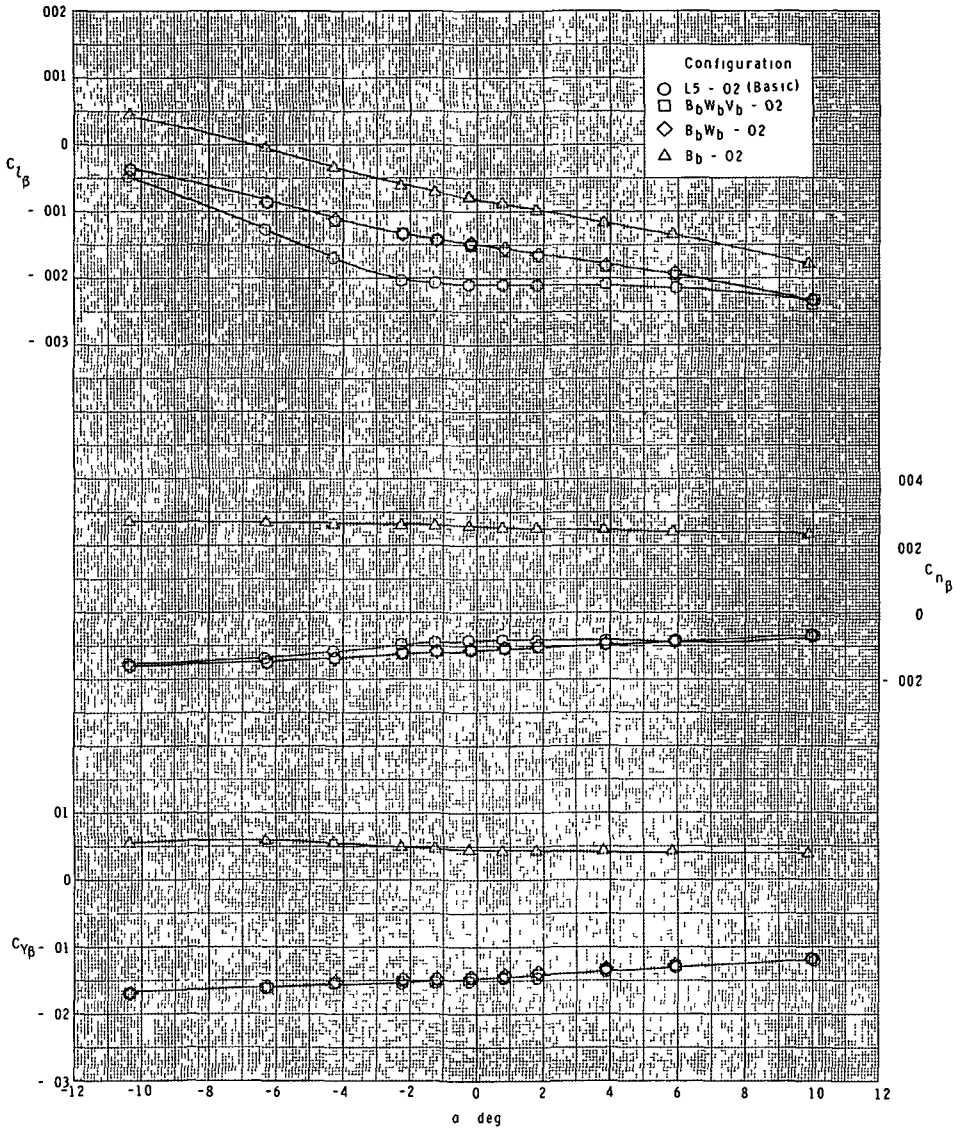

(c) M = 3.95.

Figure 11.- Continued.

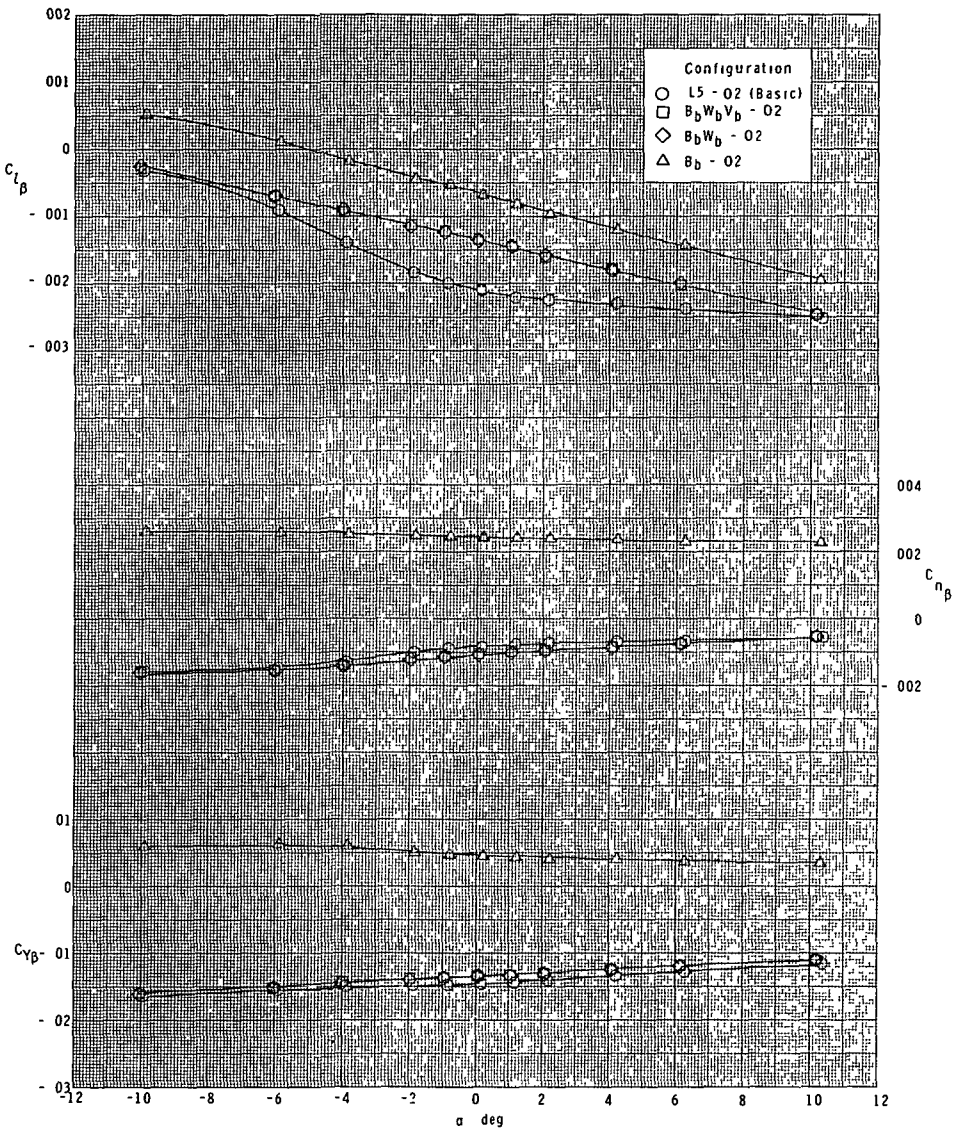

(d) M = 4.60.

Figure 11.- Concluded.

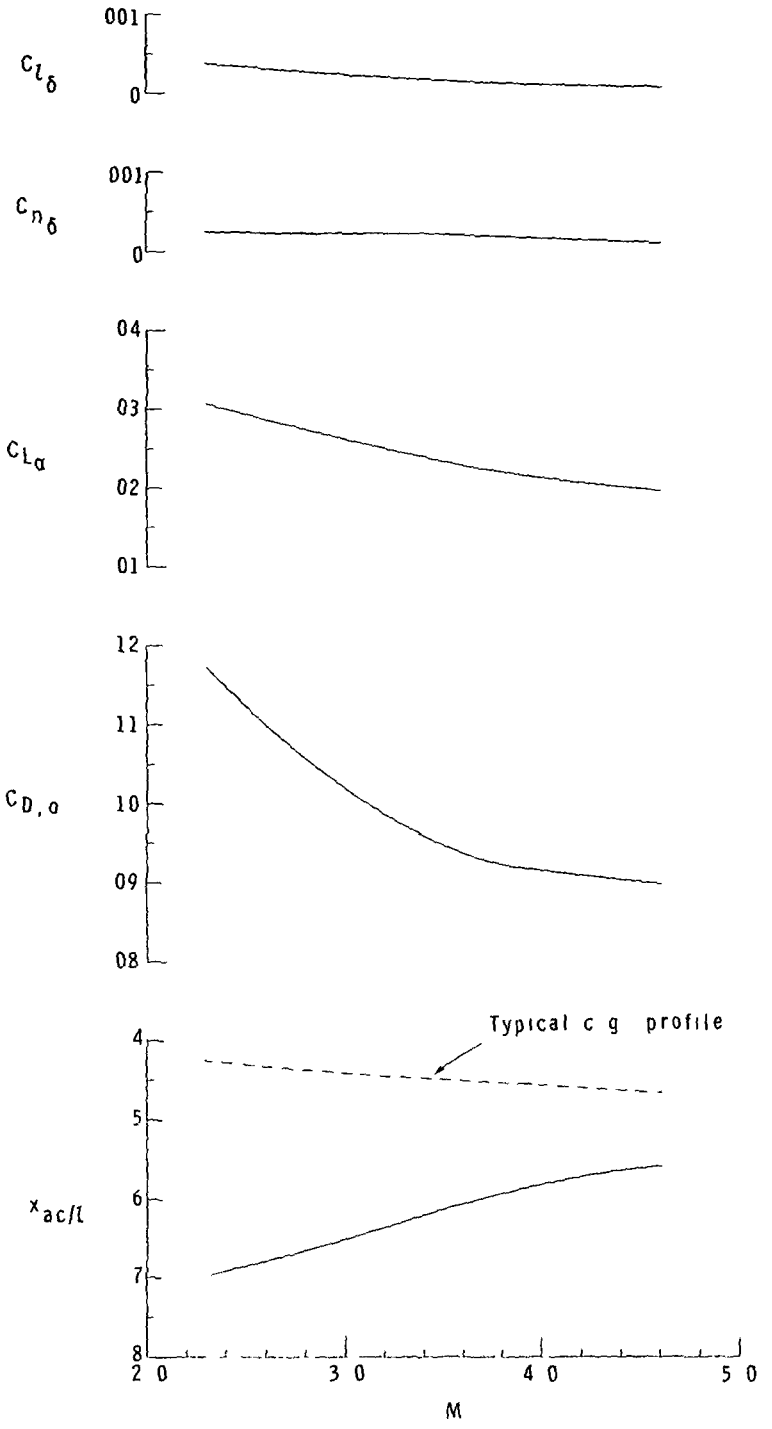

Figure 12.- Summary of characteristics.
Ascent configuration.

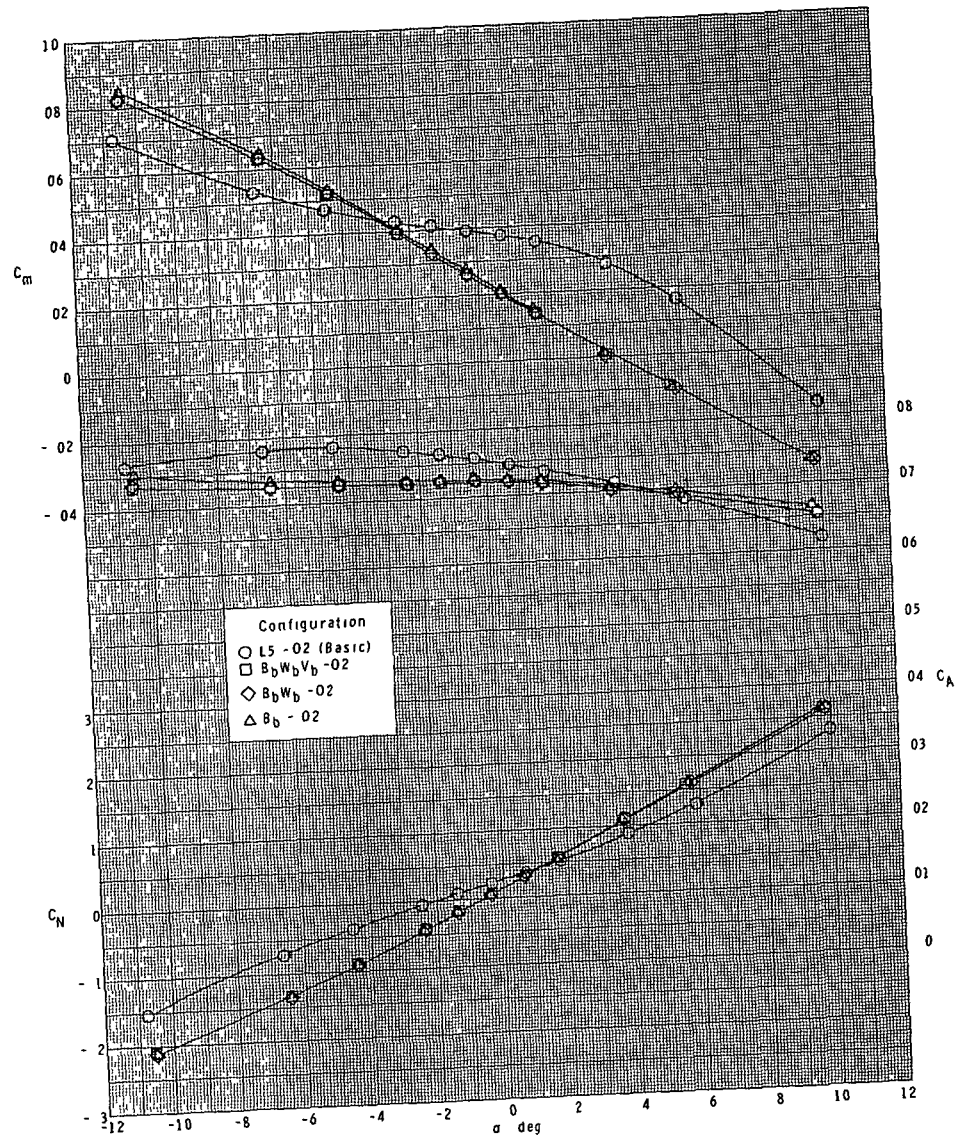

(a) M = 2.30.

Figure 13.- Effect of booster components on longitudinal characteristics of orbiter. Ascent configuration.

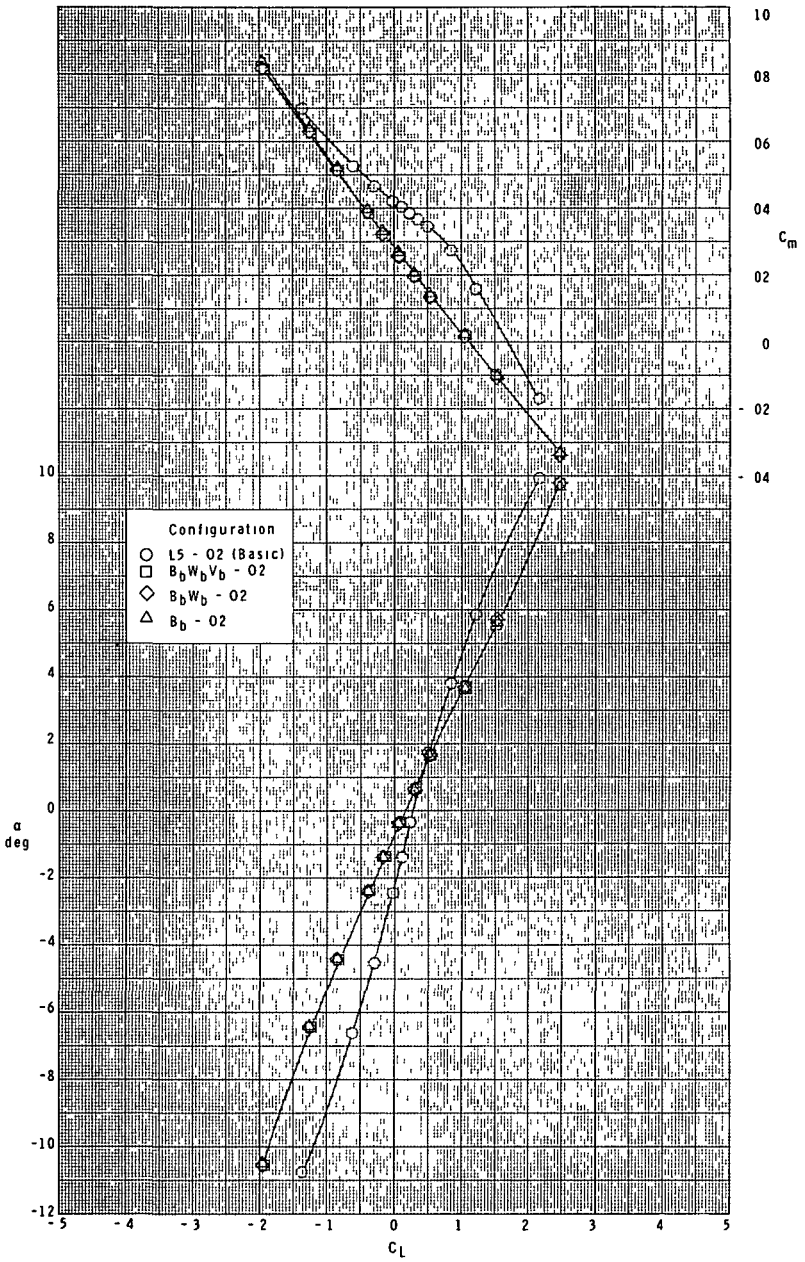

(a) Continued.

Figure 13.- Continued.

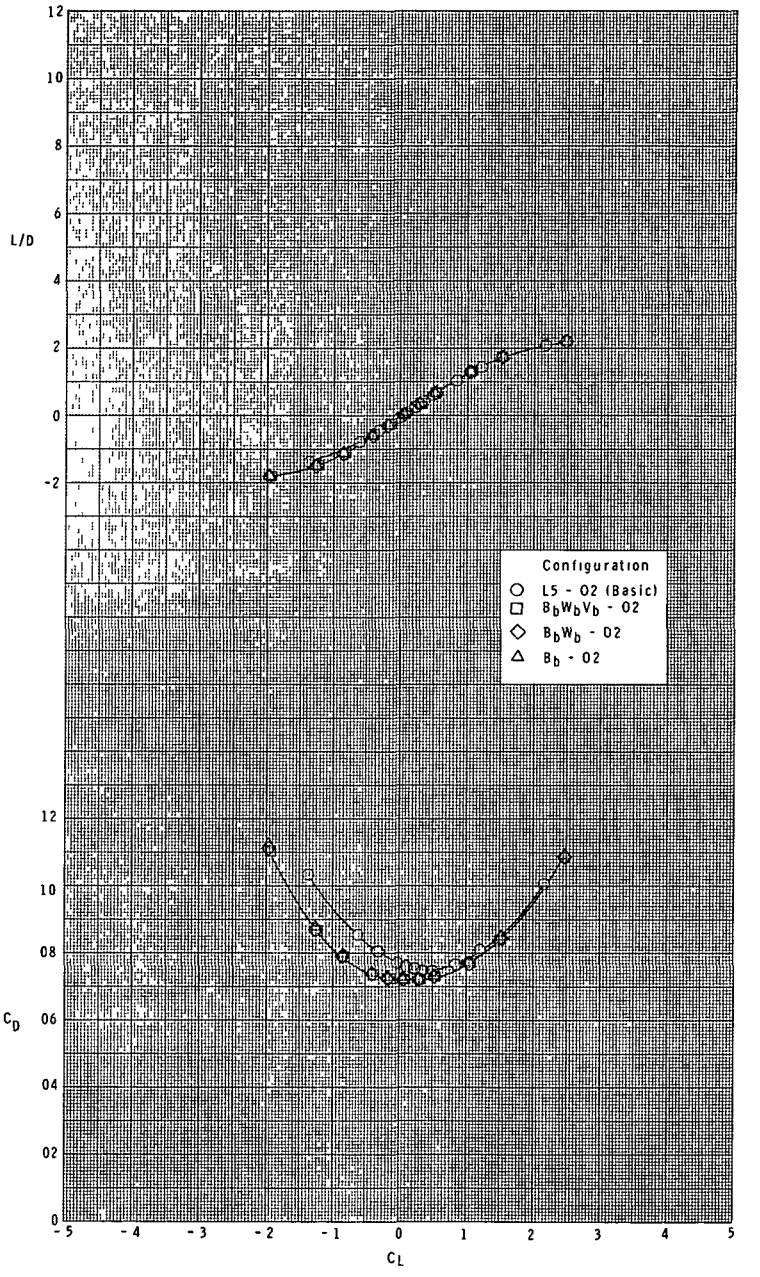

(a) Concluded.

Figure 13.- Continued.

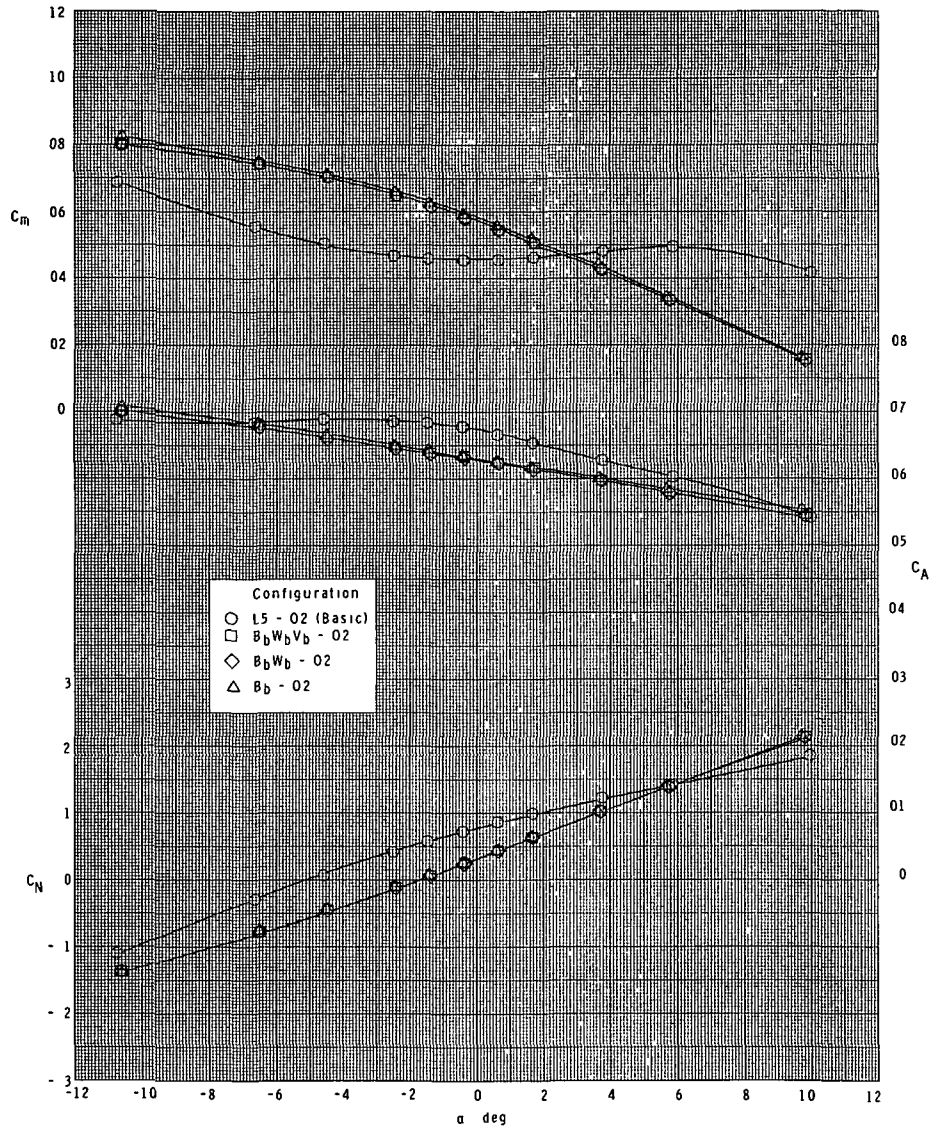

(b) M = 2.96.

Figure 13.- Continued.

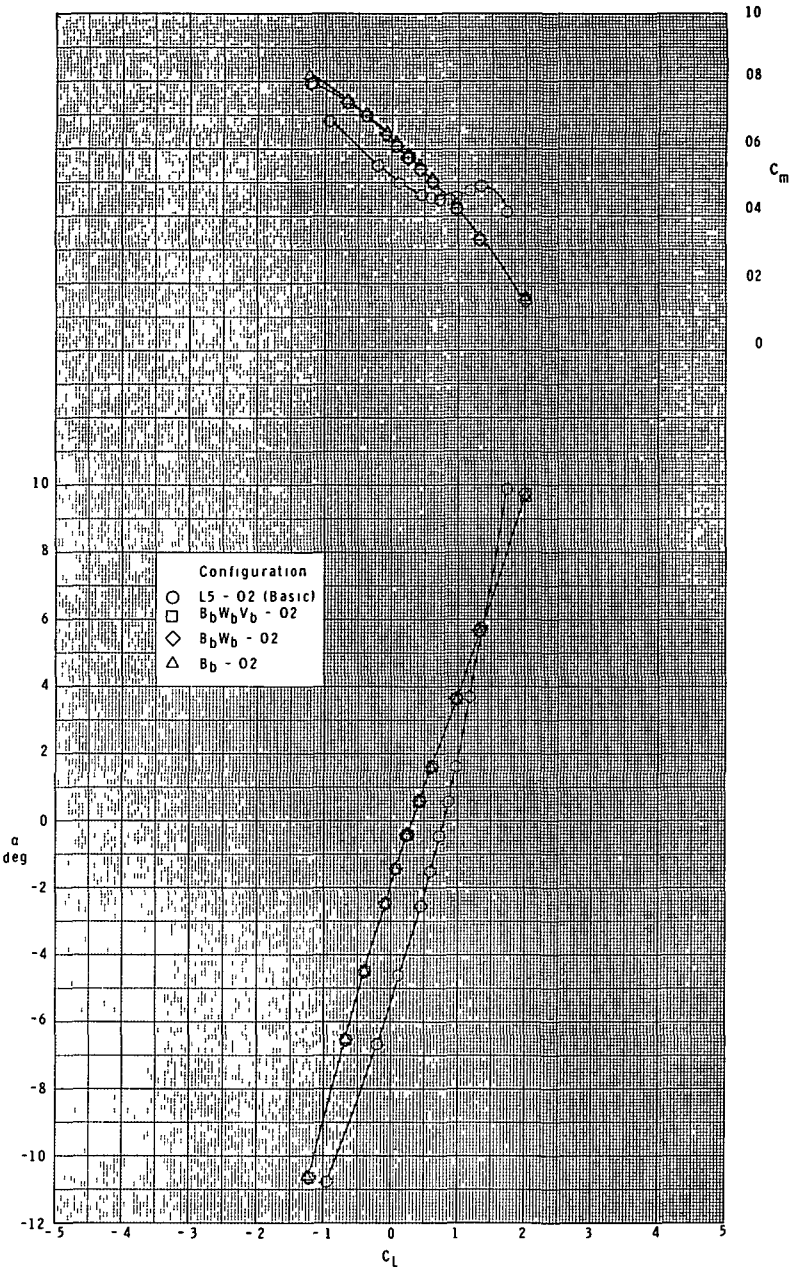

(b) Continued.

Figure 13.- Continued.

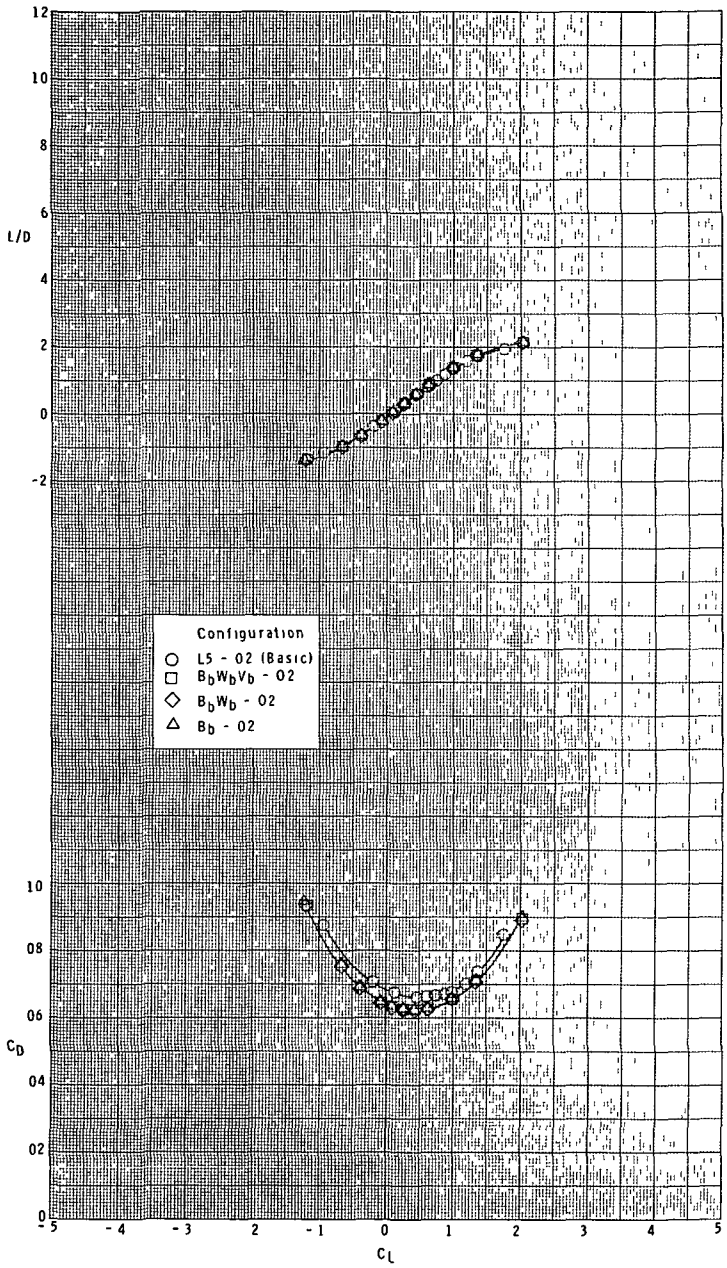

(b) Concluded.

Figure 13.- Continued.

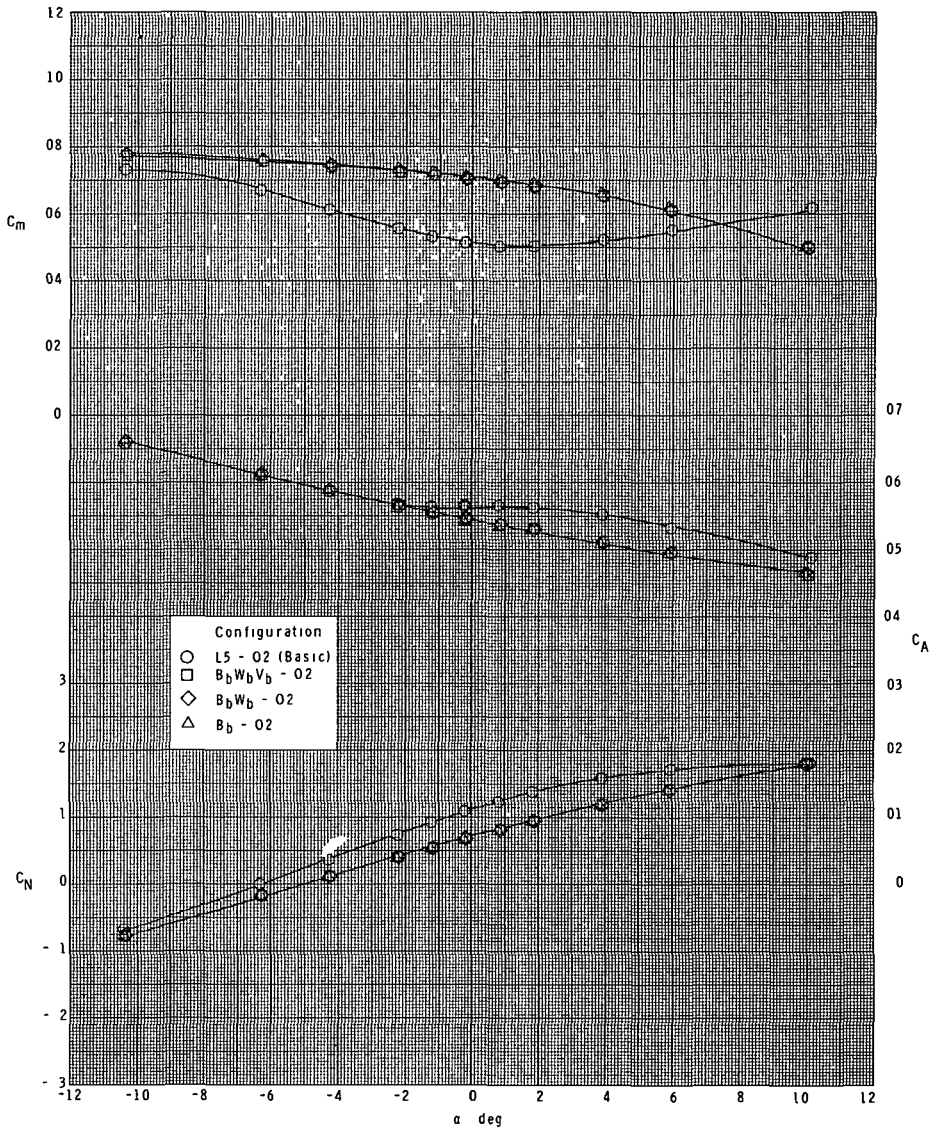

(c) M = 3.95.

Figure 13.- Continued.

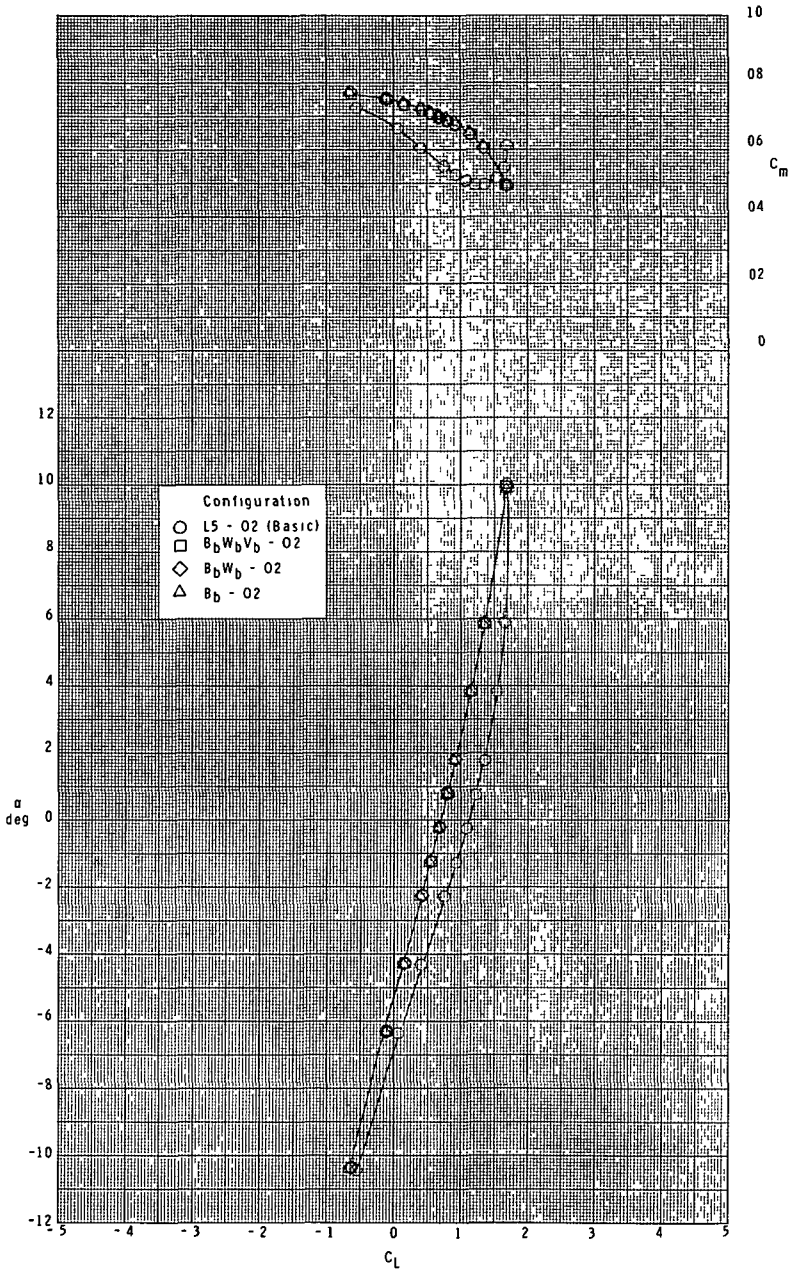

(c) Continued.

Figure 13.- Continued.

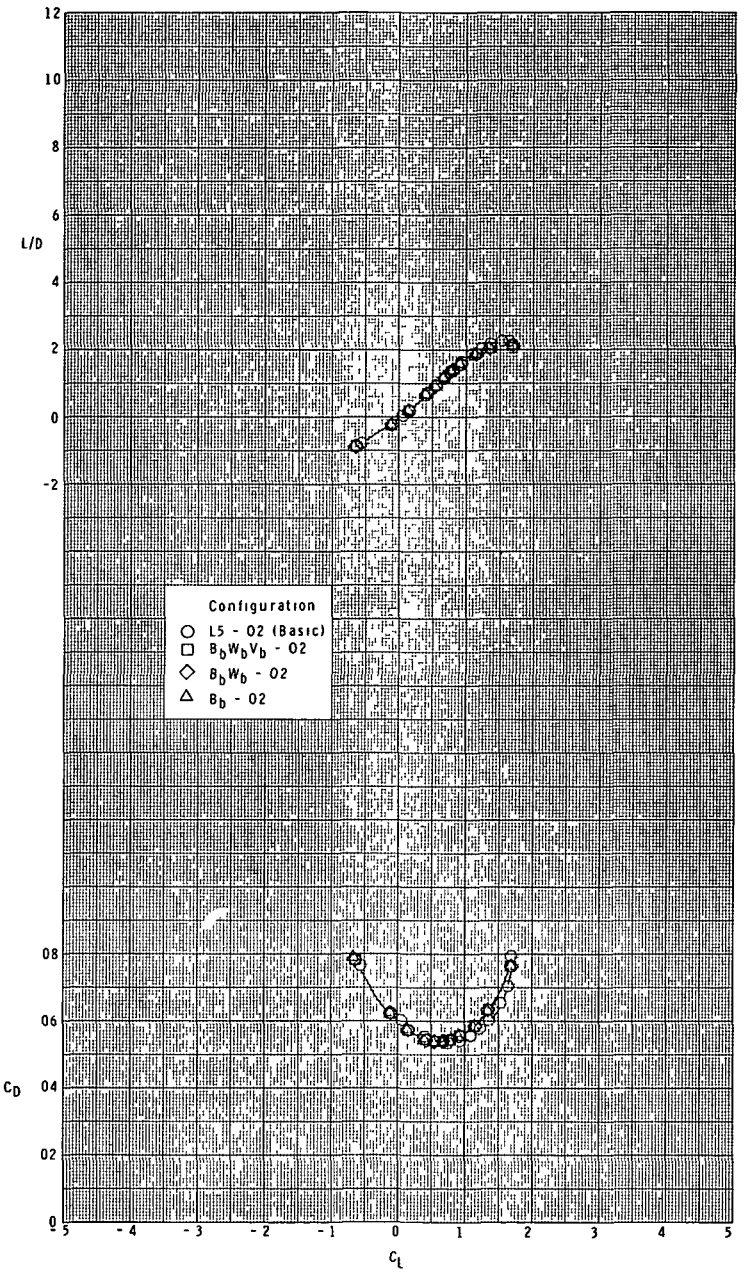

(c) Concluded.

Figure 13.- Continued.

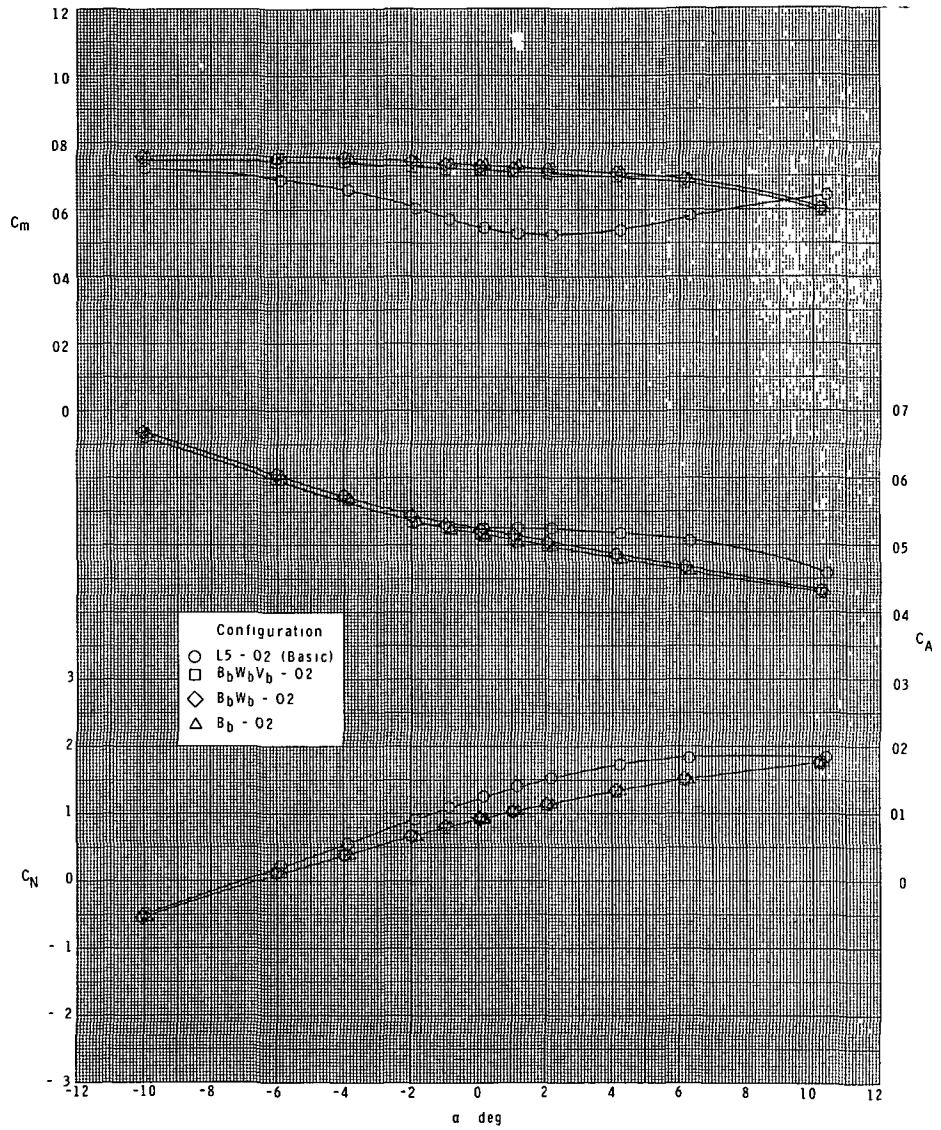

(d) M = 4.60.

Figure 13.- Continued.

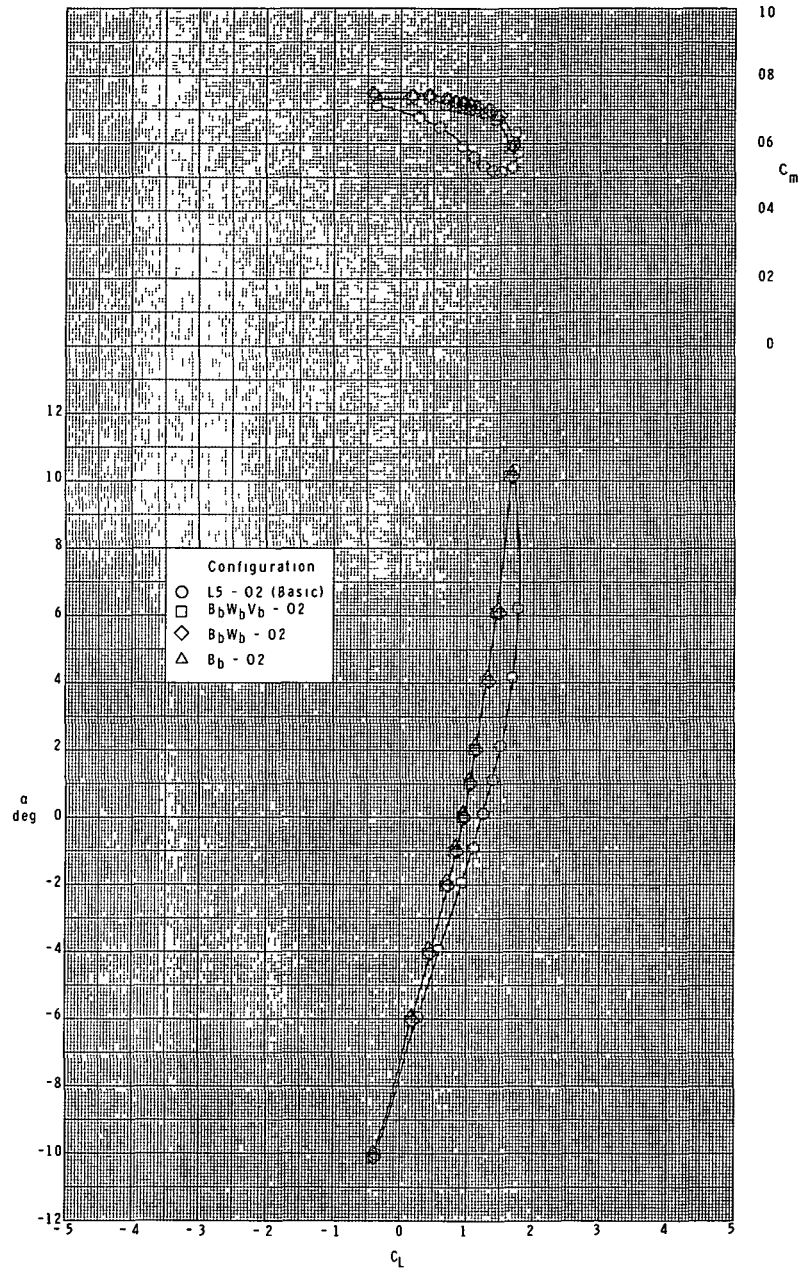

(d) Continued.

Figure 13.- Continued.

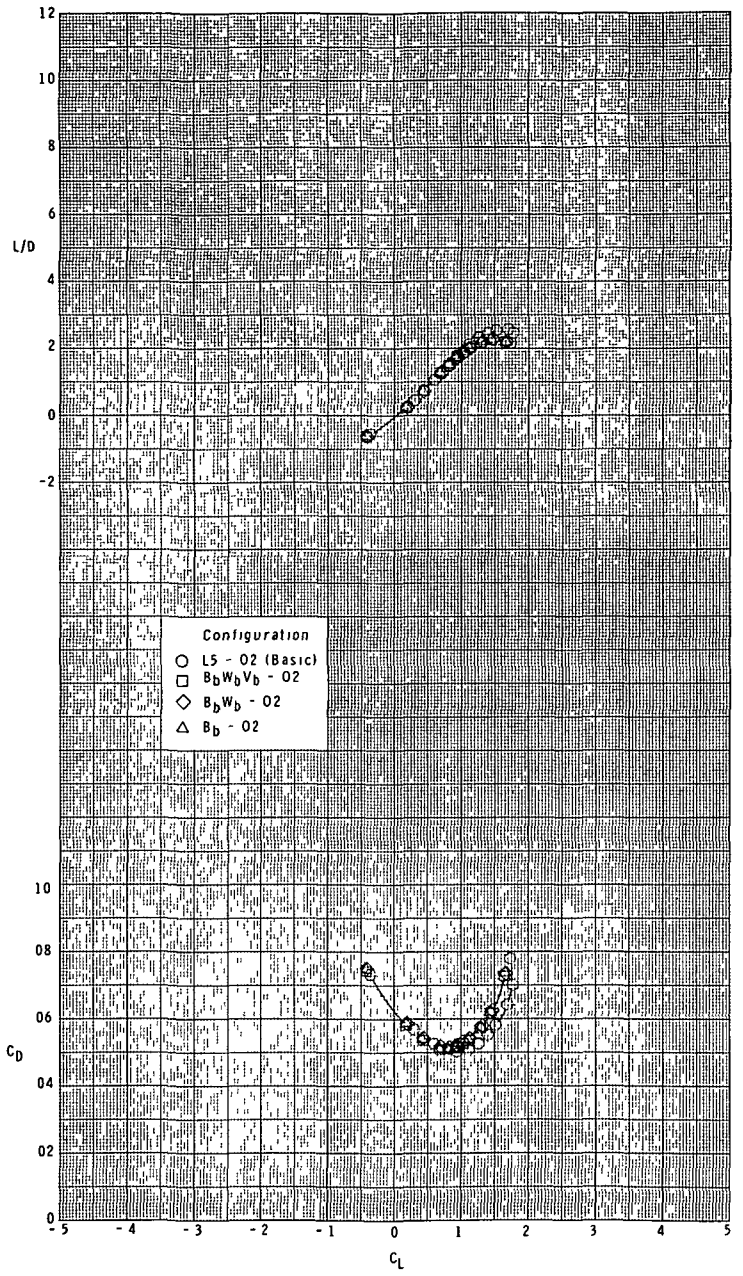

(d) Concluded.

Figure 13.- Concluded.

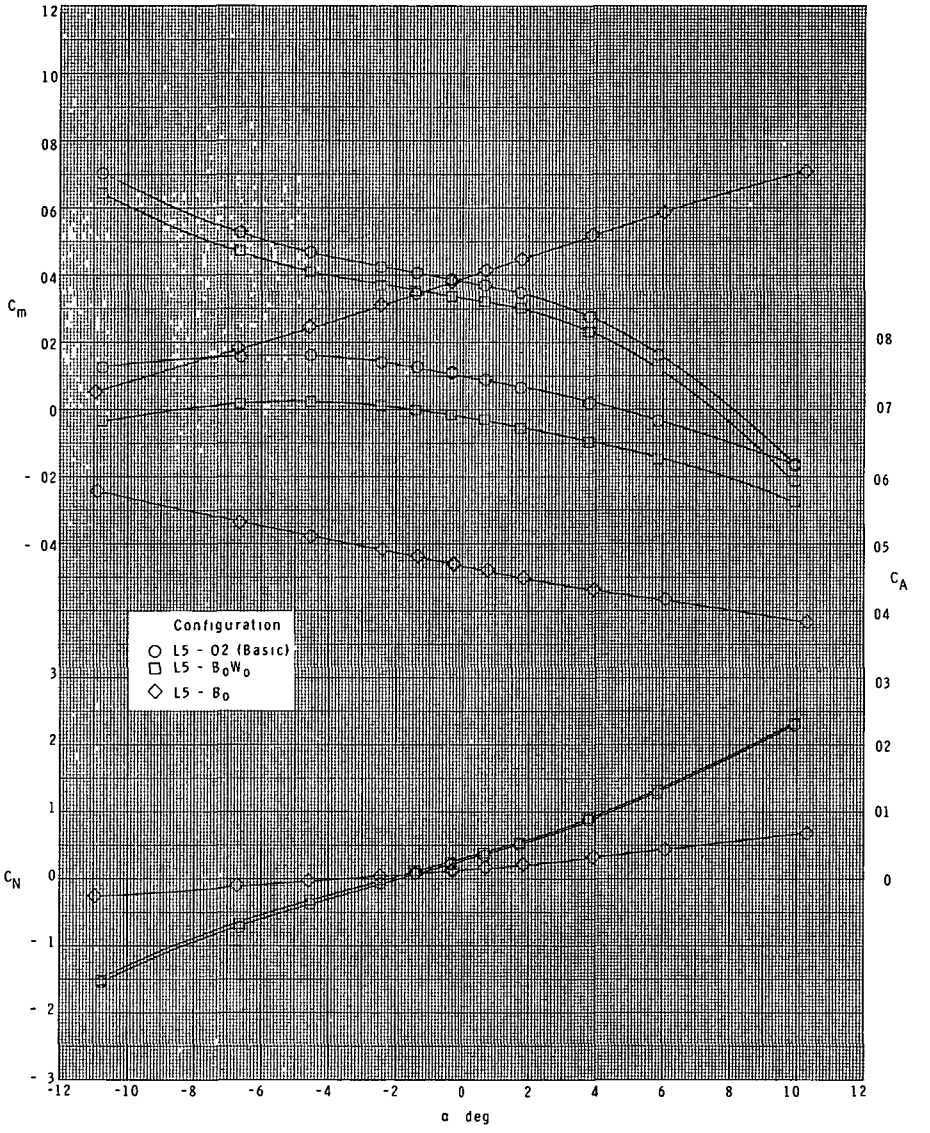

(a) M = 2.30.

Figure 14.- Effect of orbiter components on longitudinal characteristics of orbiter. Ascent configuration.

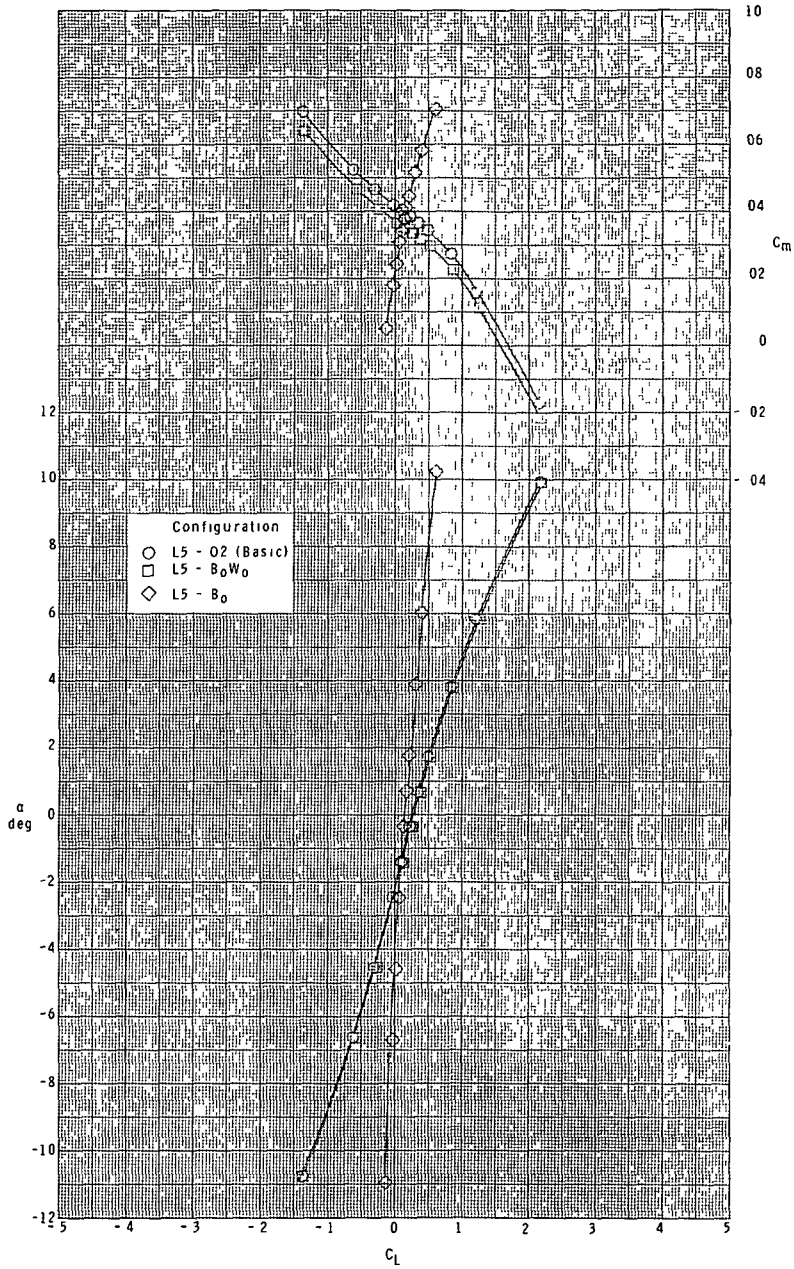

(a) Continued.

Figure 14.- Continued.

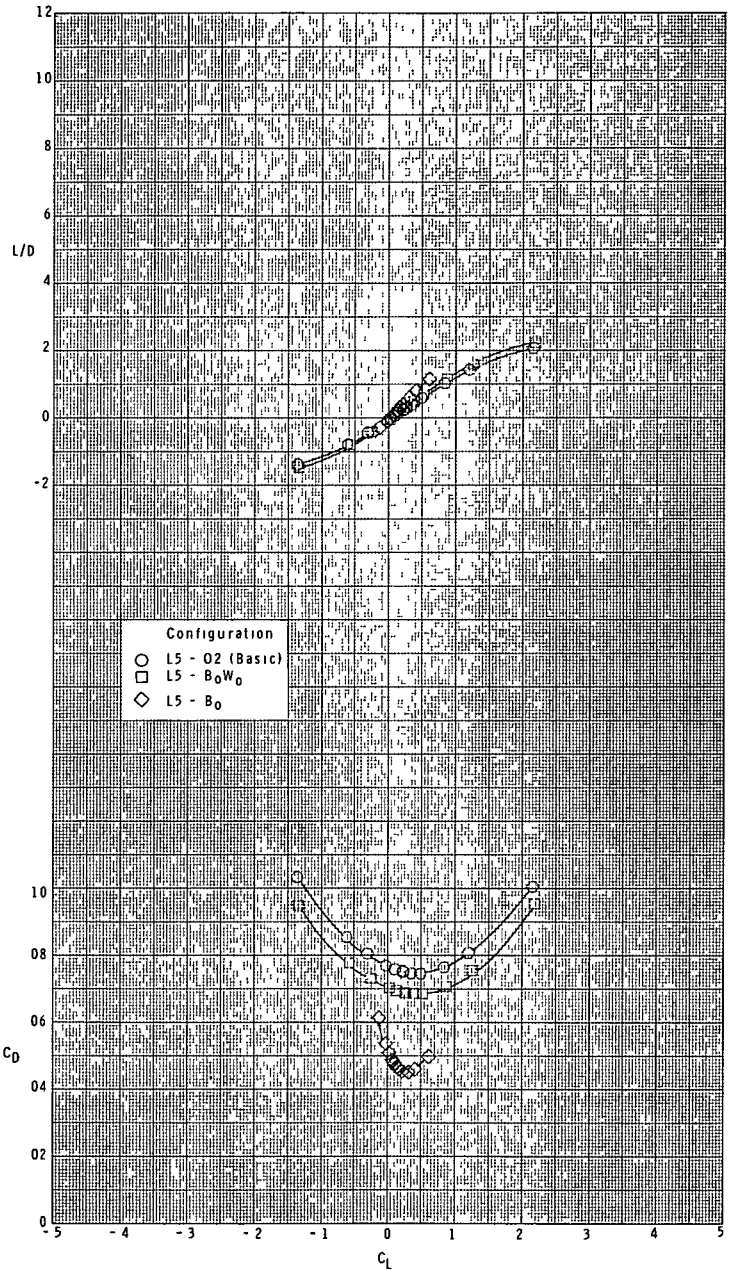

(a) Concluded.

Figure 14.- Continued.

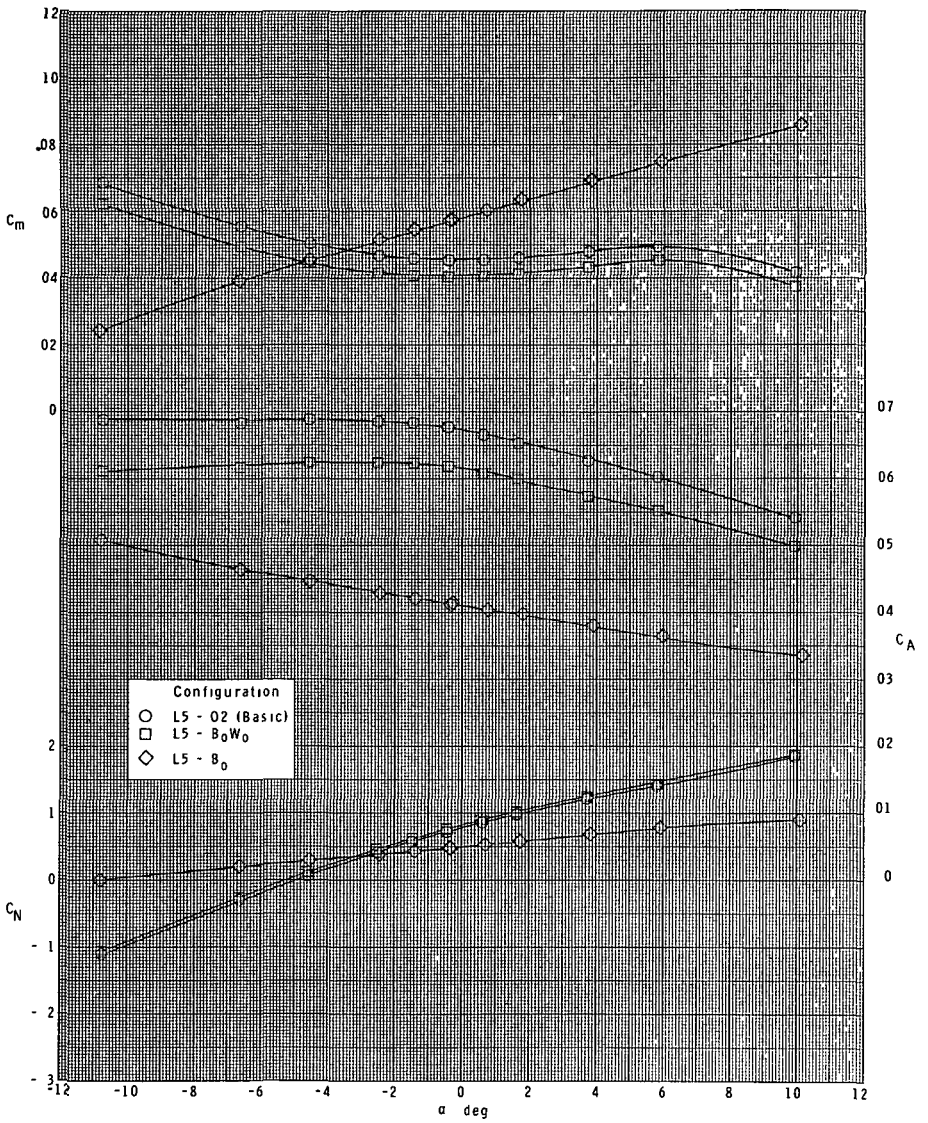

(b) M = 2.96.

Figure 14.- Continued.

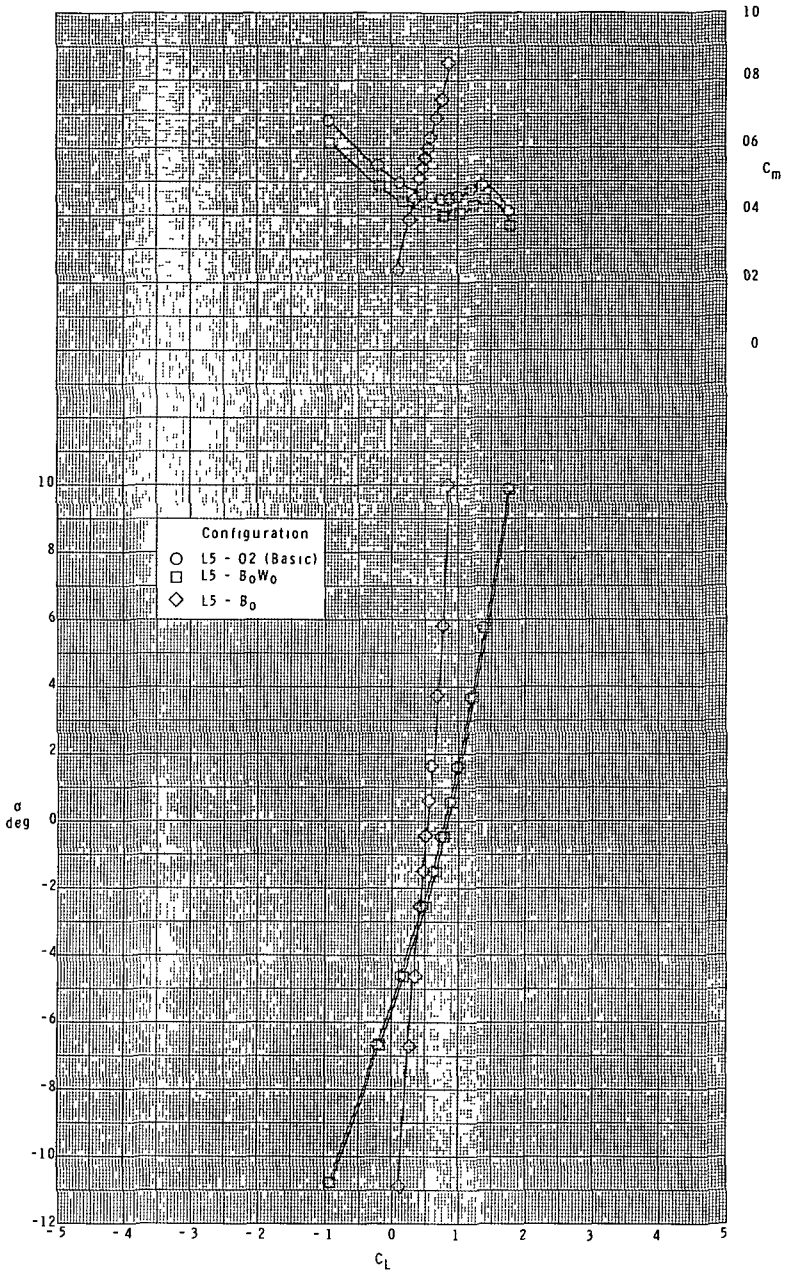

(b) Continued.

Figure 14.- Continued.

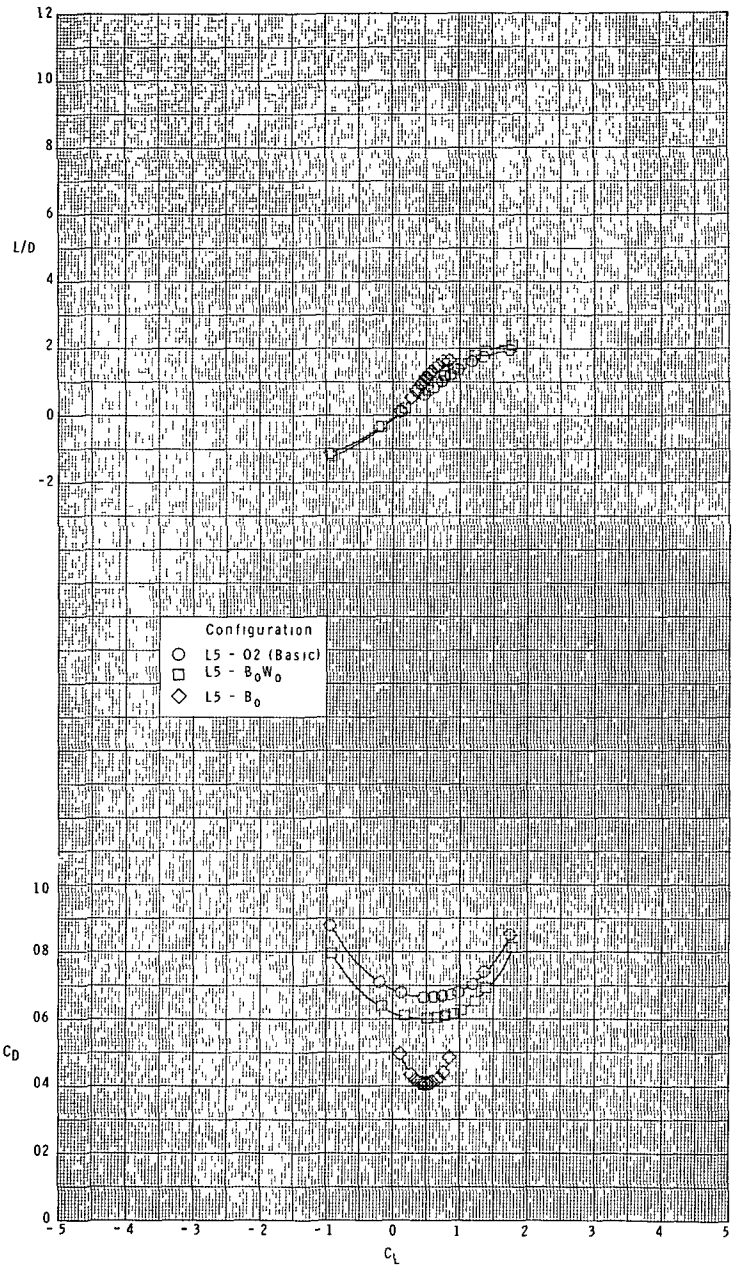

(b) Concluded.

Figure 14.- Continued.

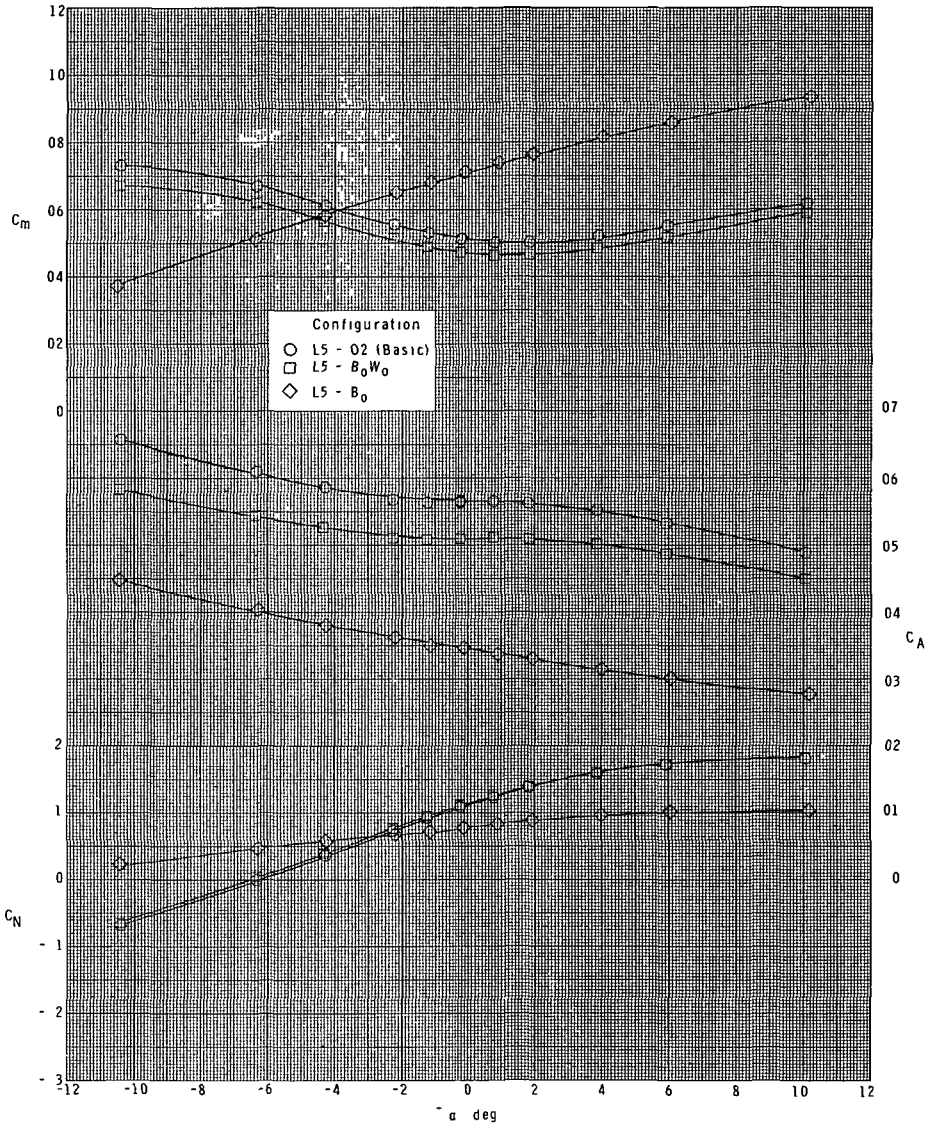

(c) M = 3.95.

Figure 14.- Continued.

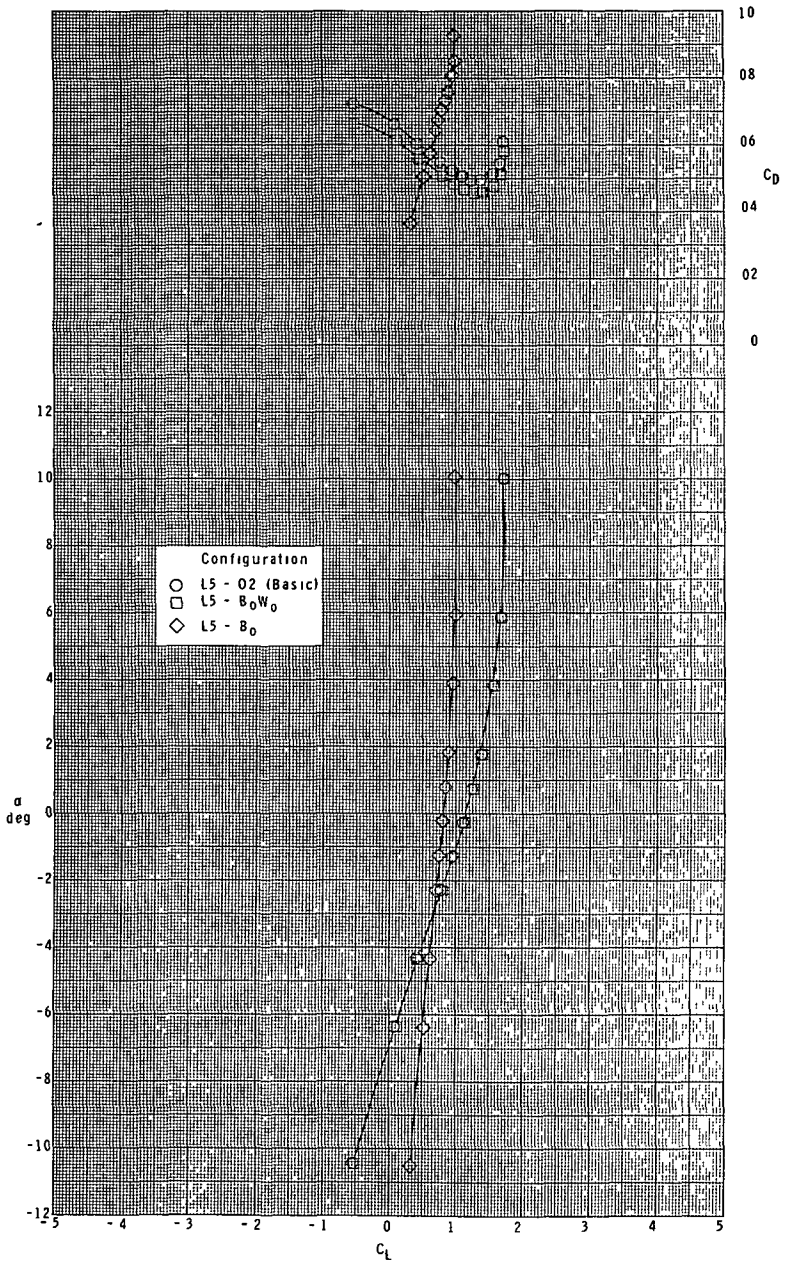

(c) Continued.

Figure 14.- Continued.

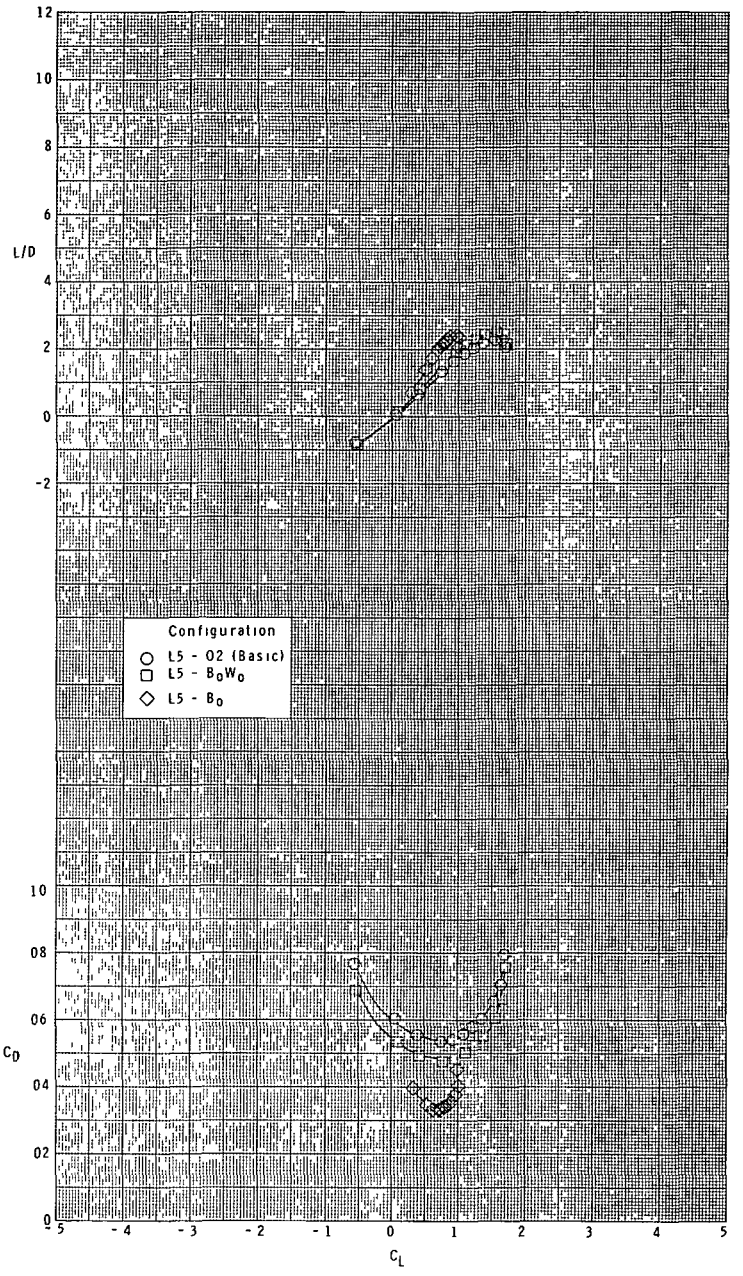

(c) Concluded.

Figure 14.- Continued.

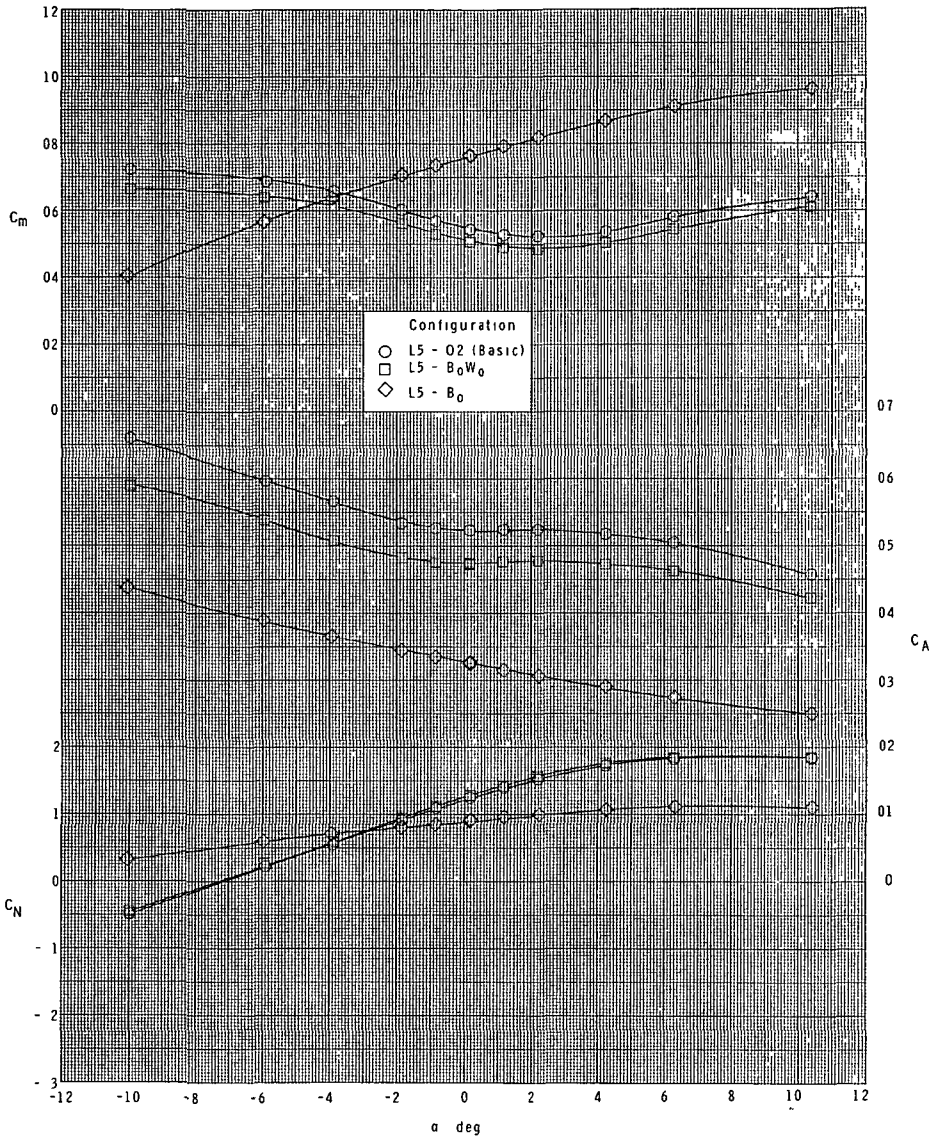

(d) M = 4.60.

Figure 14.- Continued.

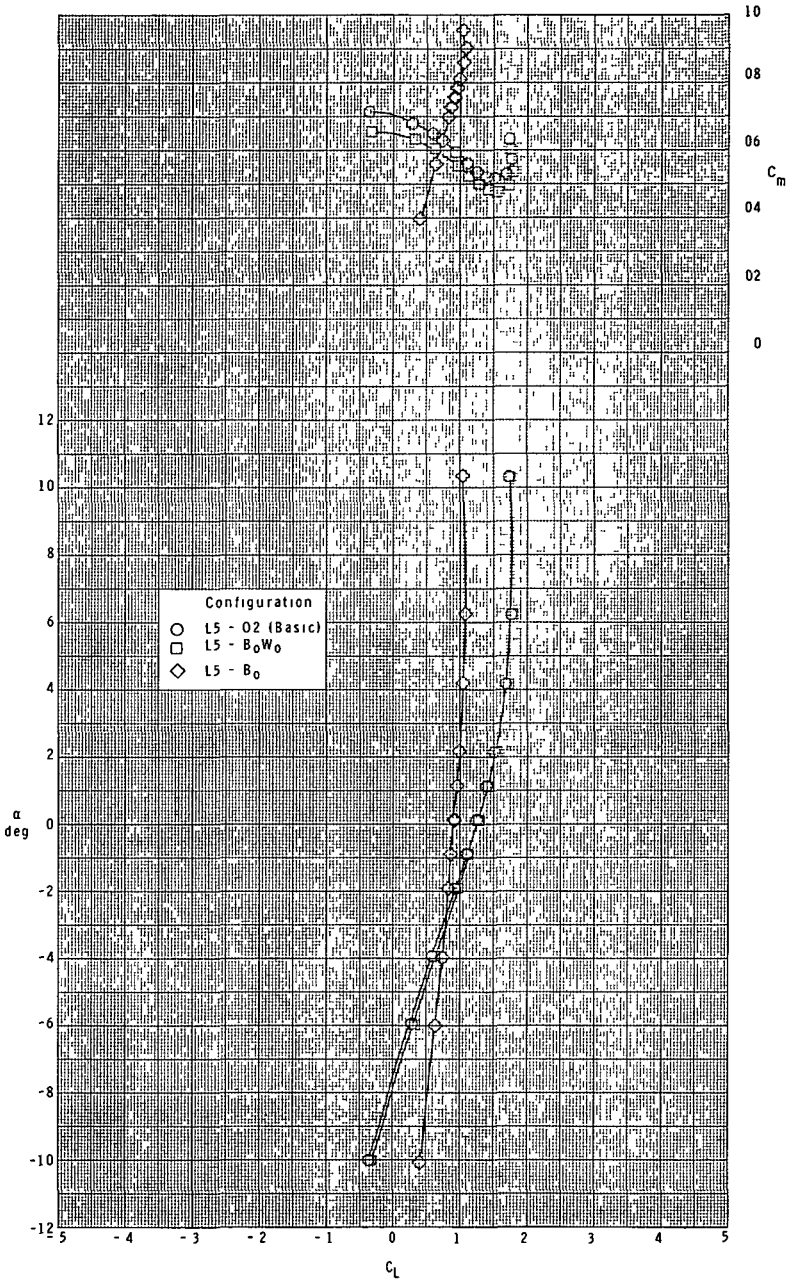

(d) Continued.

Figure 14.- Continued.

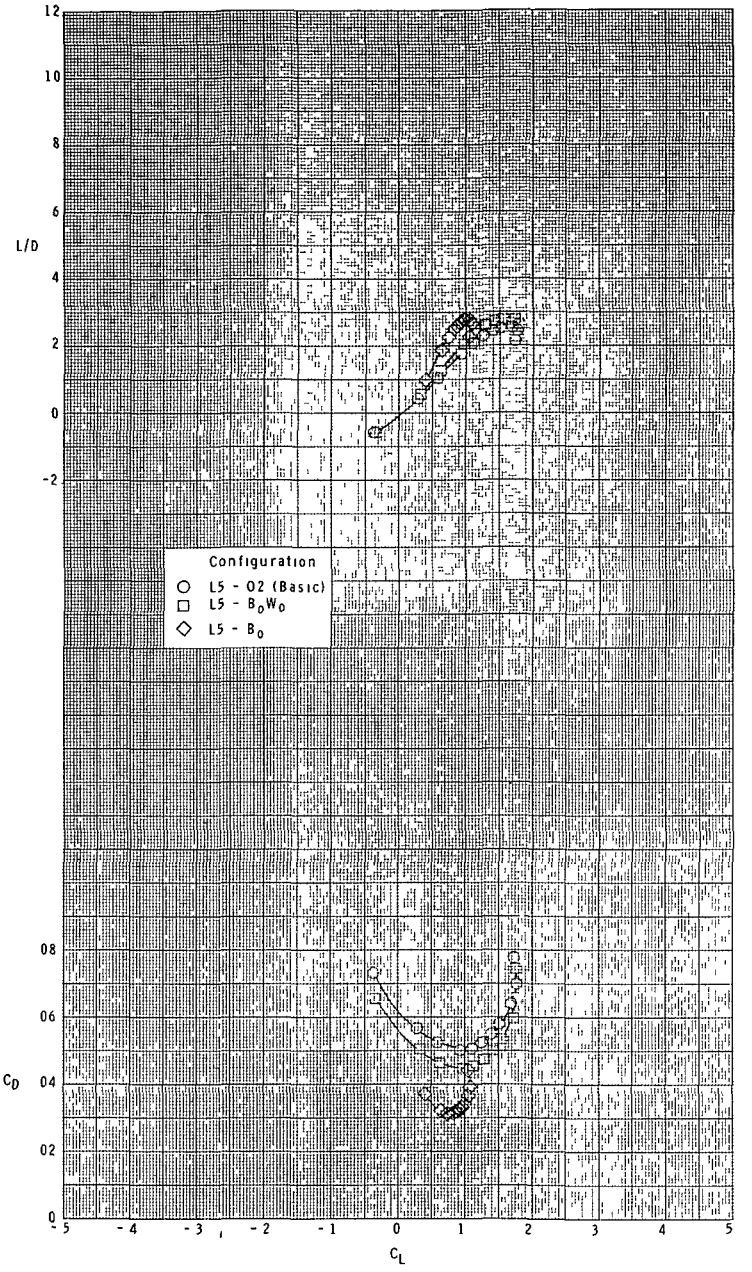

(d) Concluded.

Figure 14.- Concluded.

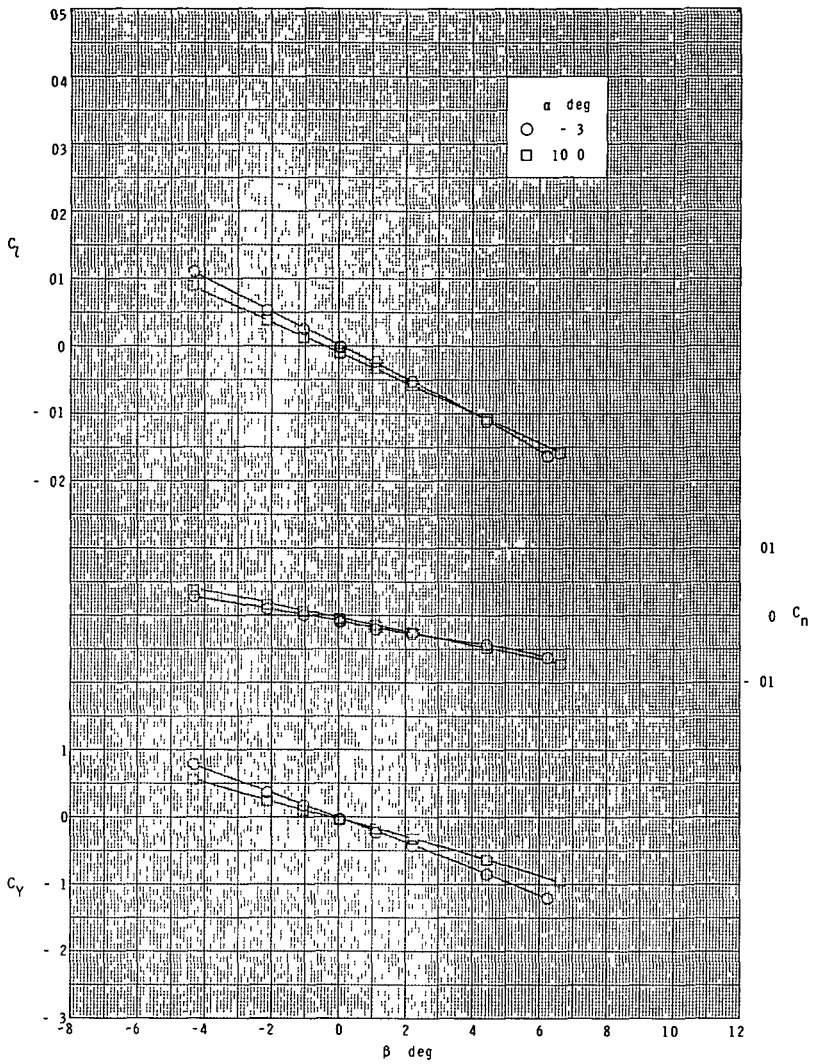

(a) M = 2.30.

Figure 15.- Lateral characteristics of orbiter in sideslip. Ascent configuration.

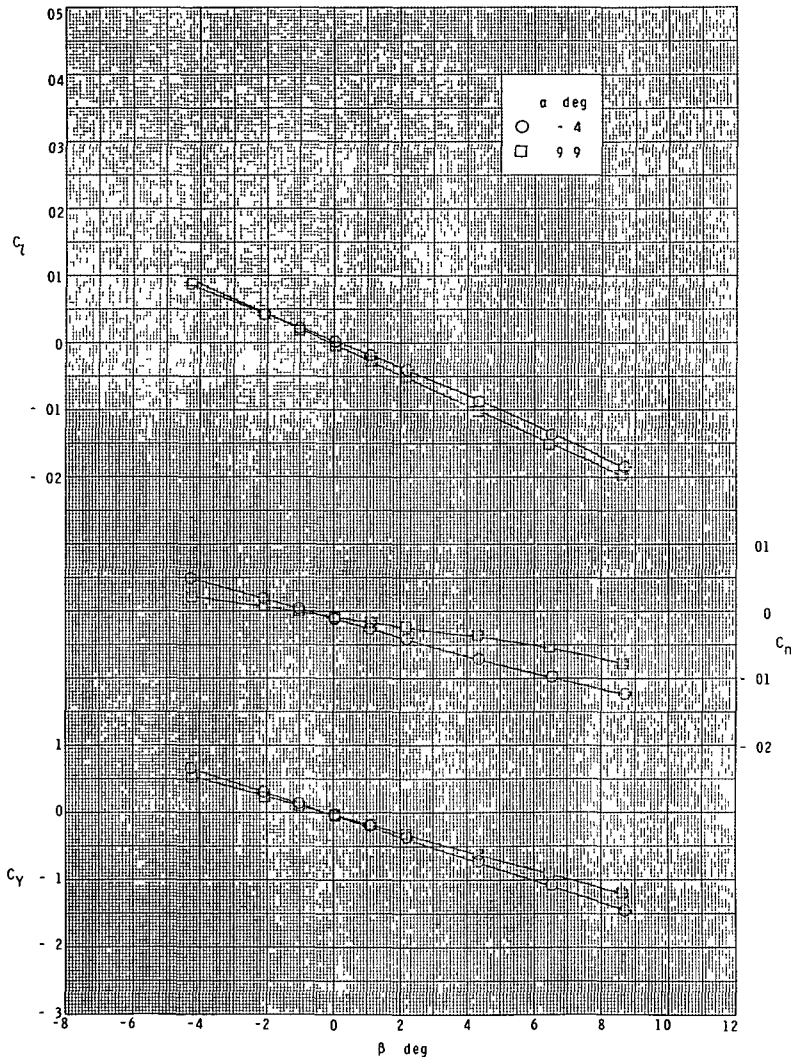

(b) M = 2.96.

Figure 15.- Continued.

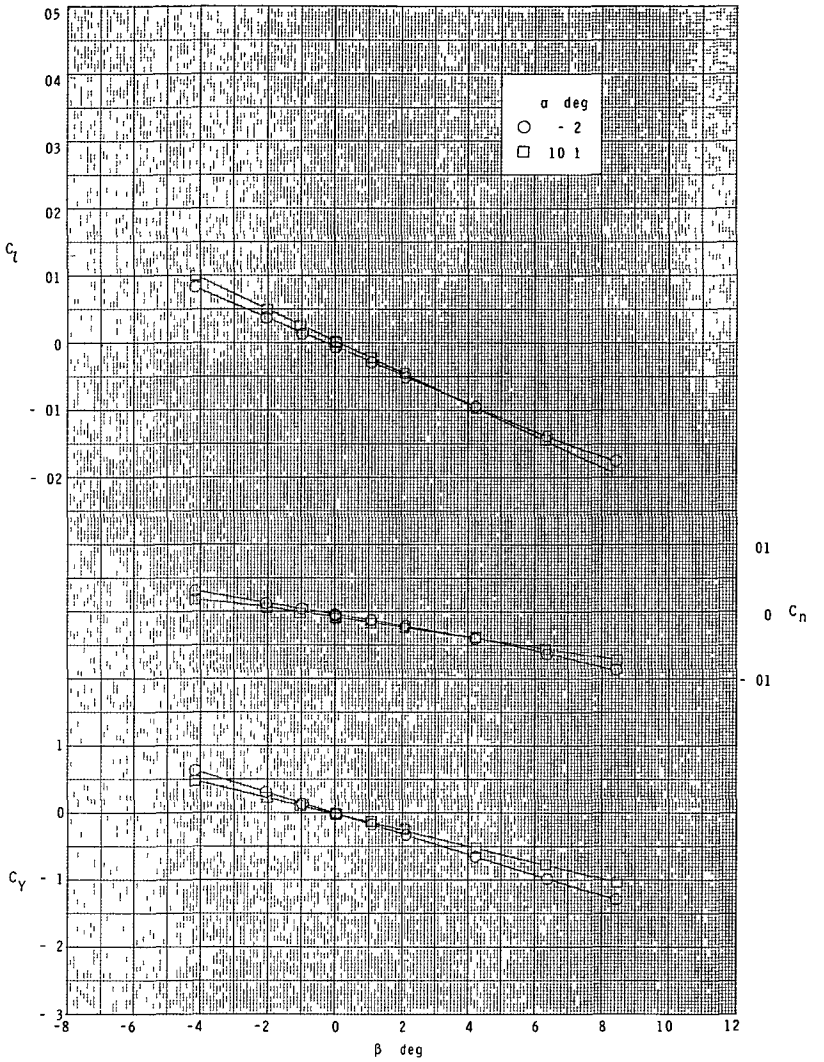

(c) M = 3.95.

Figure 15.- Continued.

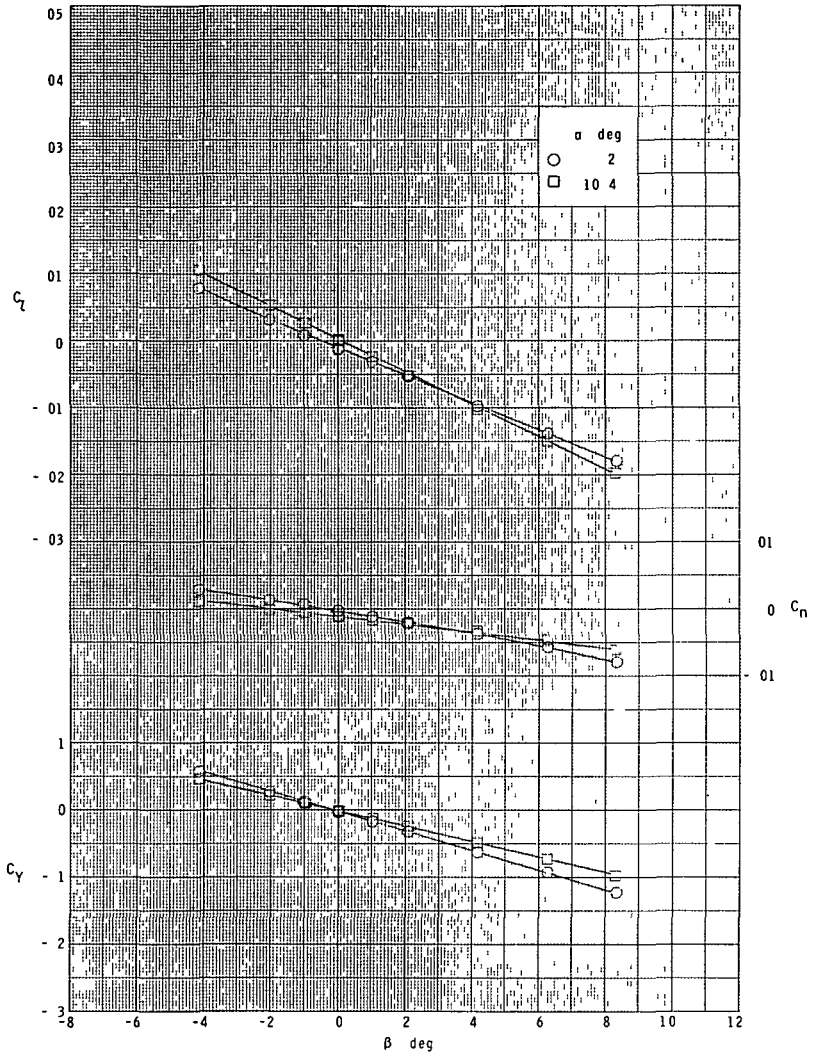

(d) M = 4.60.

Figure 15.- Concluded.

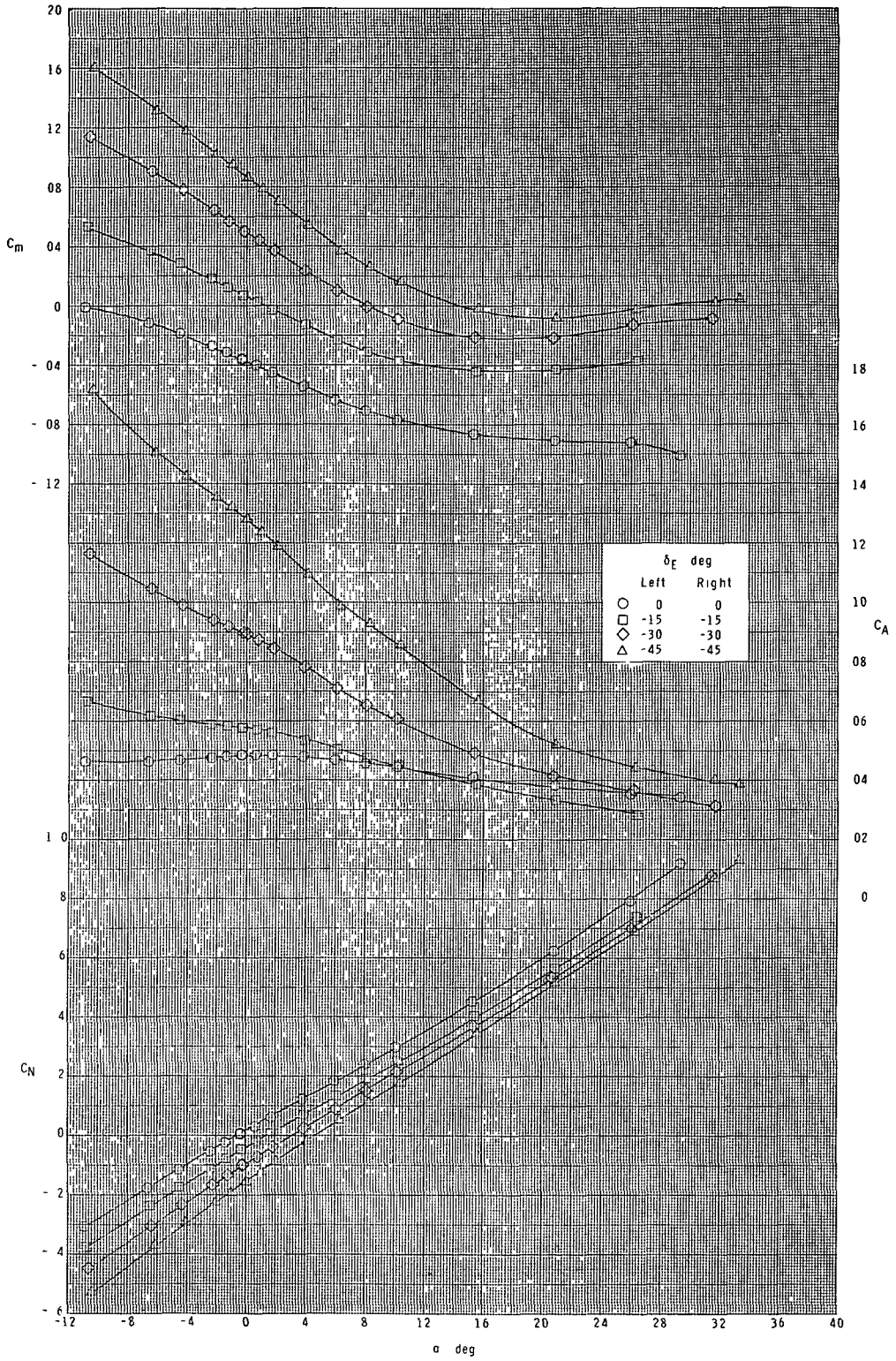

(a) M = 2.30.

Figure 16.- Elevon pitch-control effectiveness. Orbiter configuration.

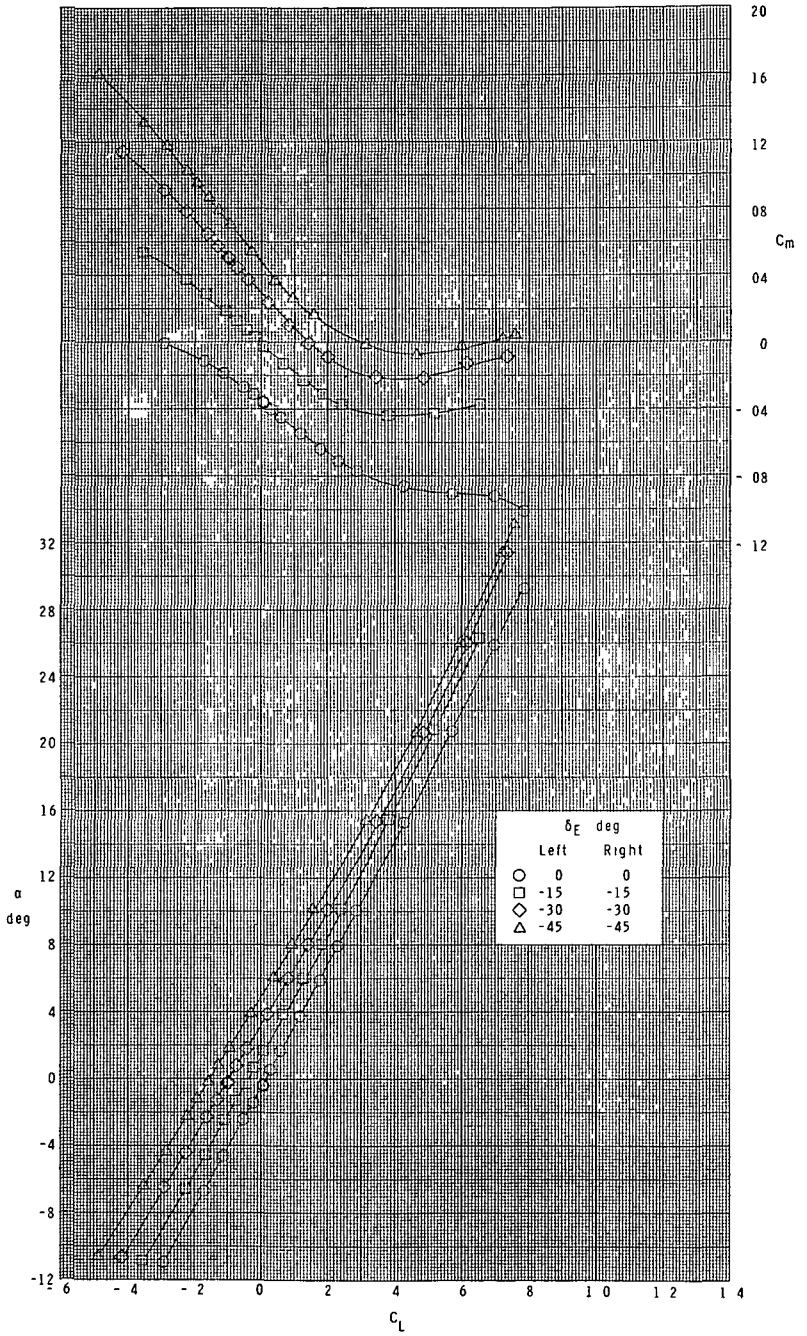

(a) Continued.

Figure 16.- Continued.

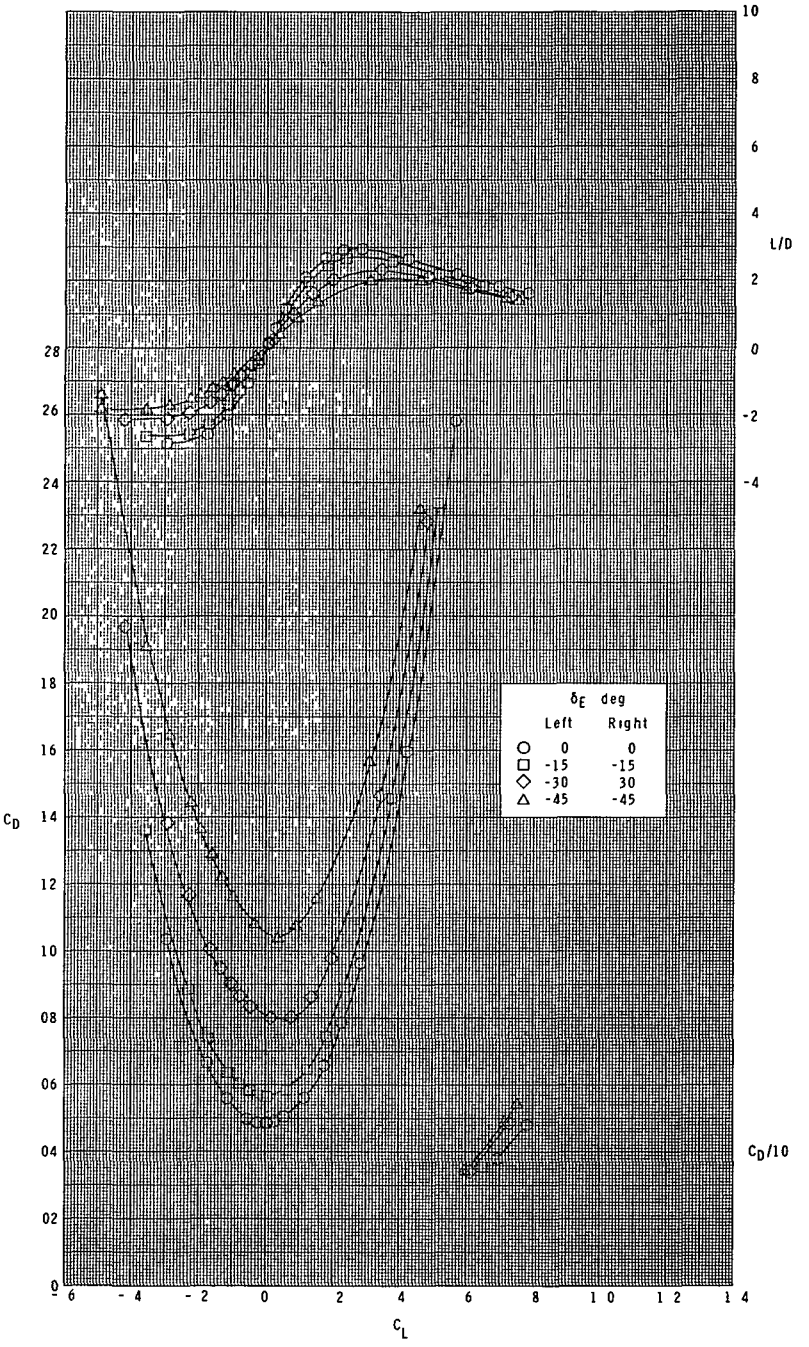

(a) Concluded.

Figure 16.- Continued.

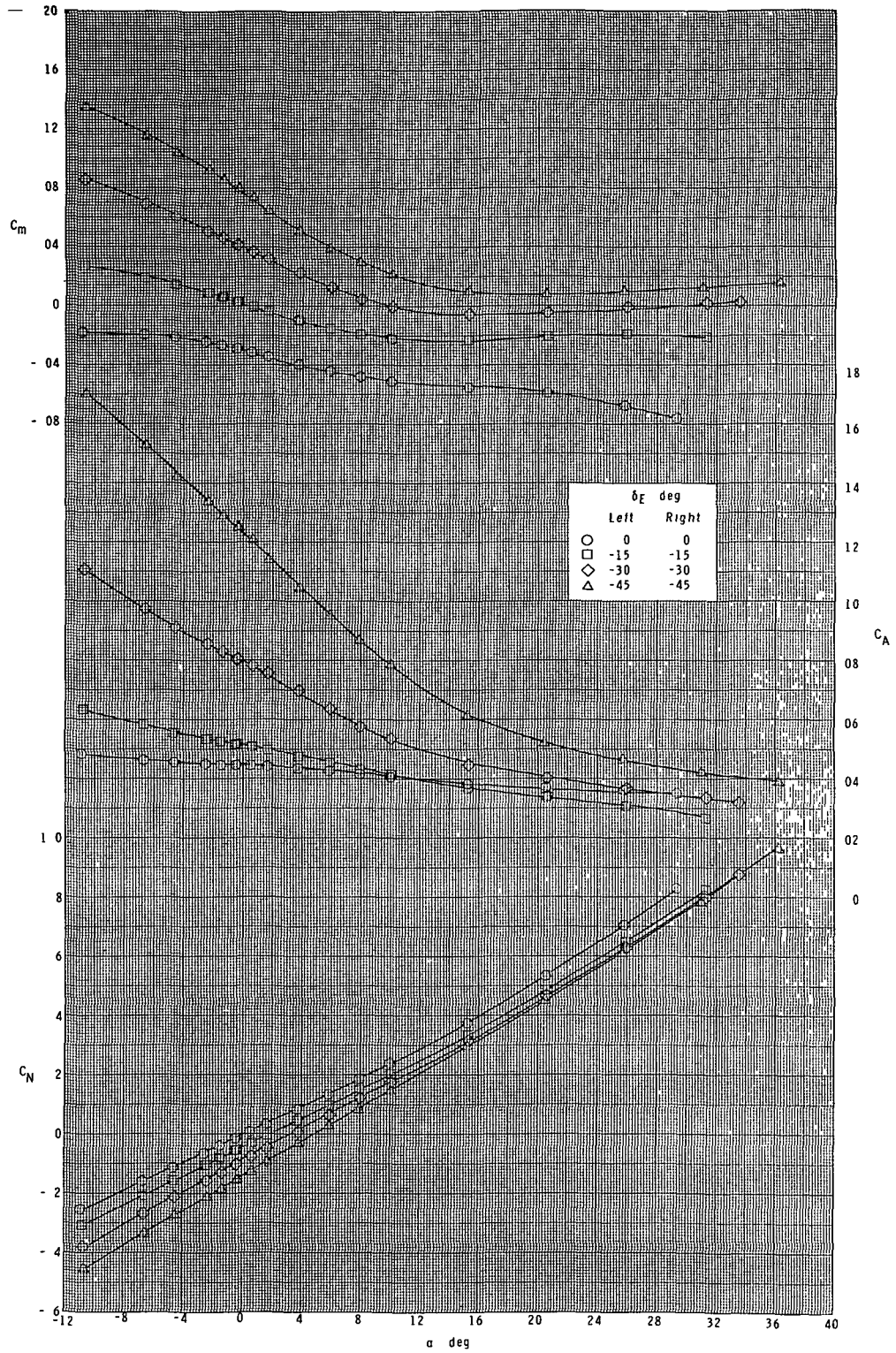

(b) M = 2.96.

Figure 16.- Continued.

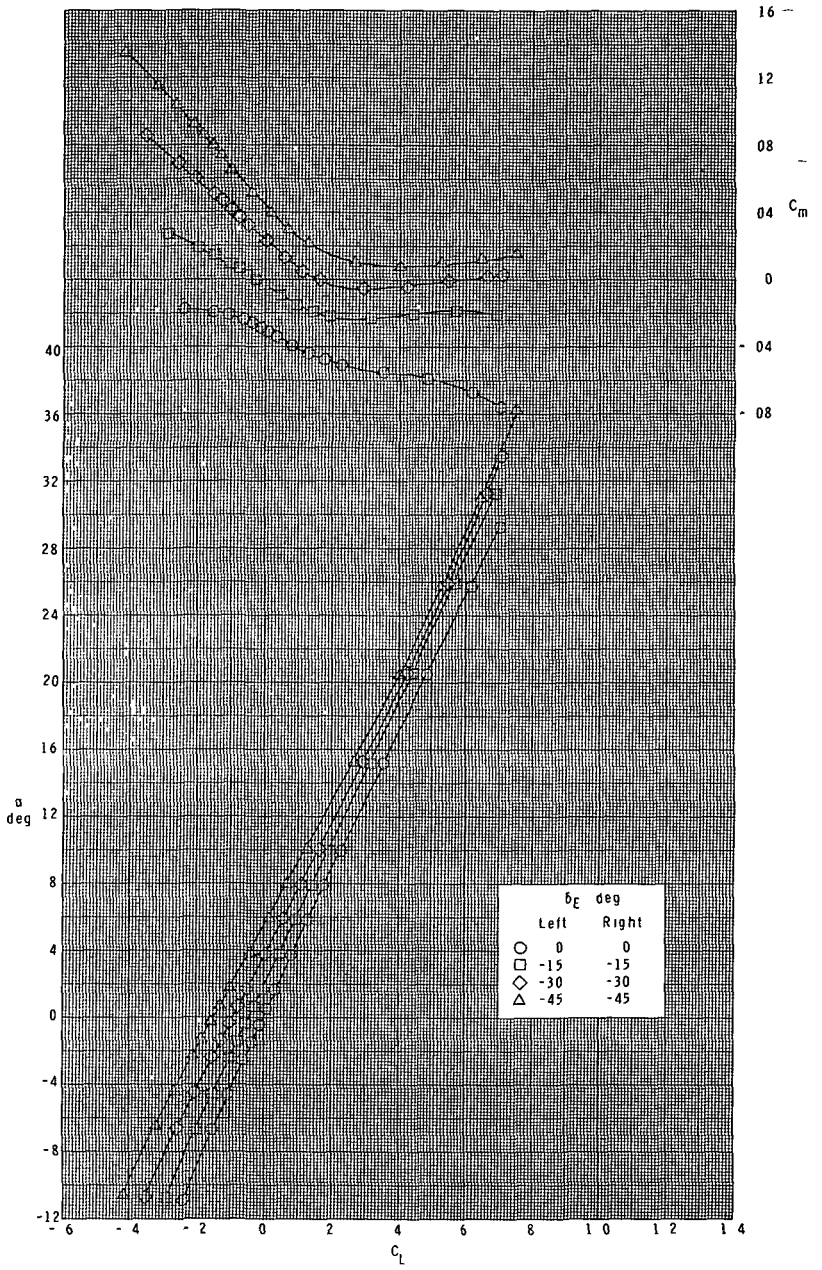

(b) Continued.

Figure 16.- Continued.

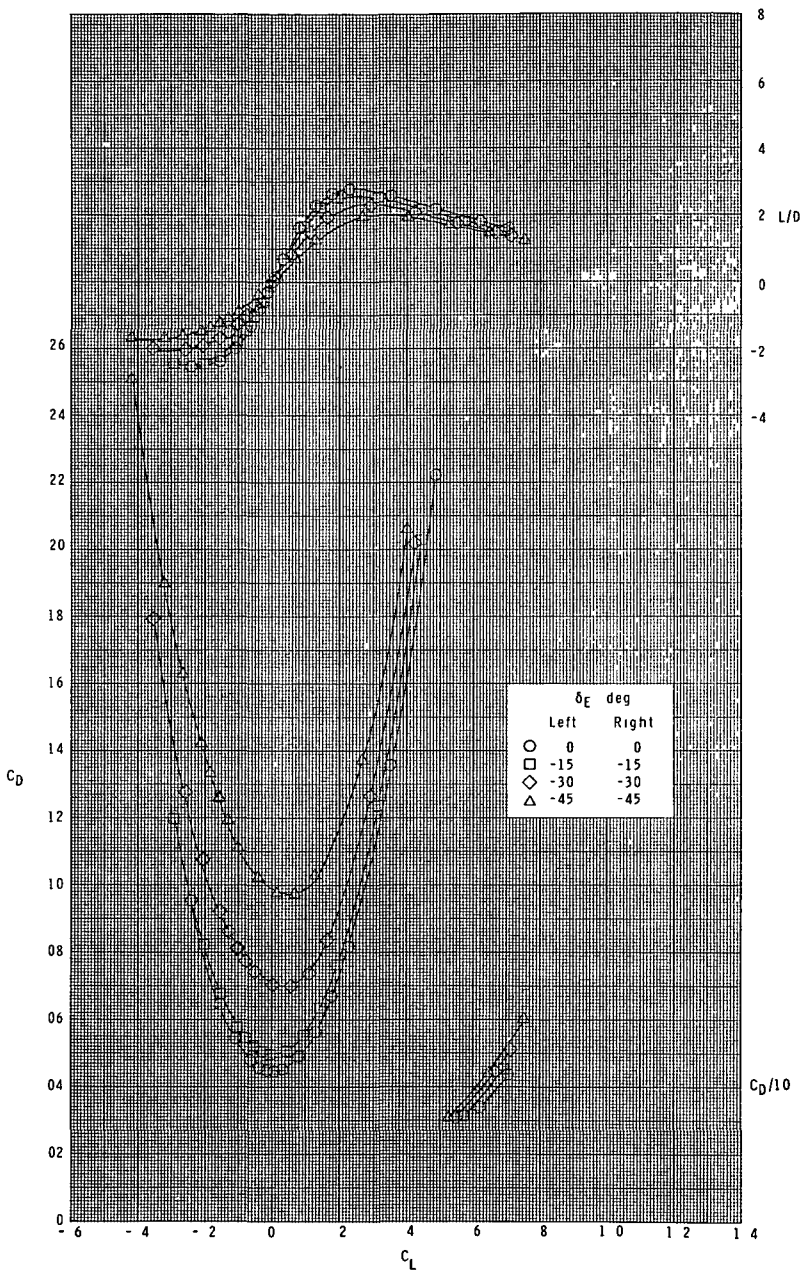

(b) Concluded.

Figure 16.- Continued.

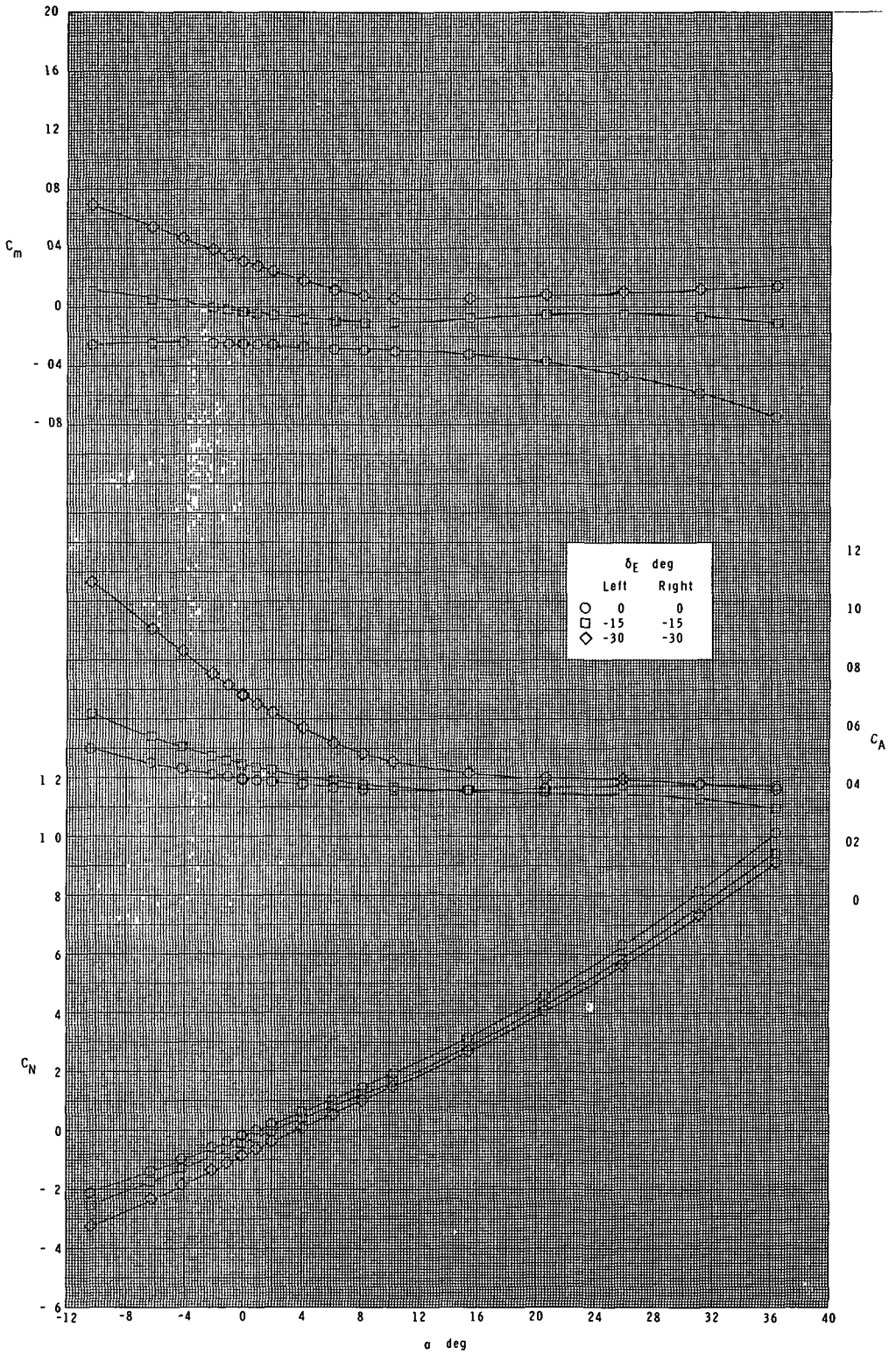

(c) M = 3.95.

Figure 16.- Continued.

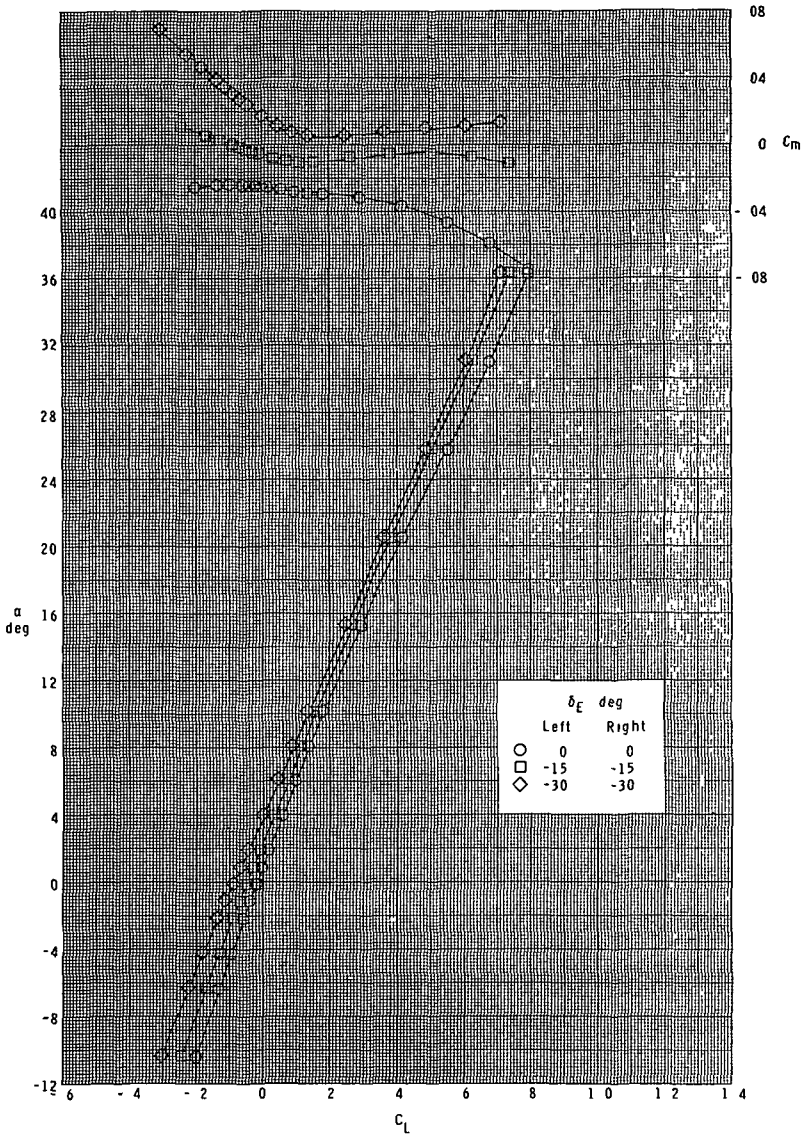

(c) Continued.

Figure 16.- Continued.

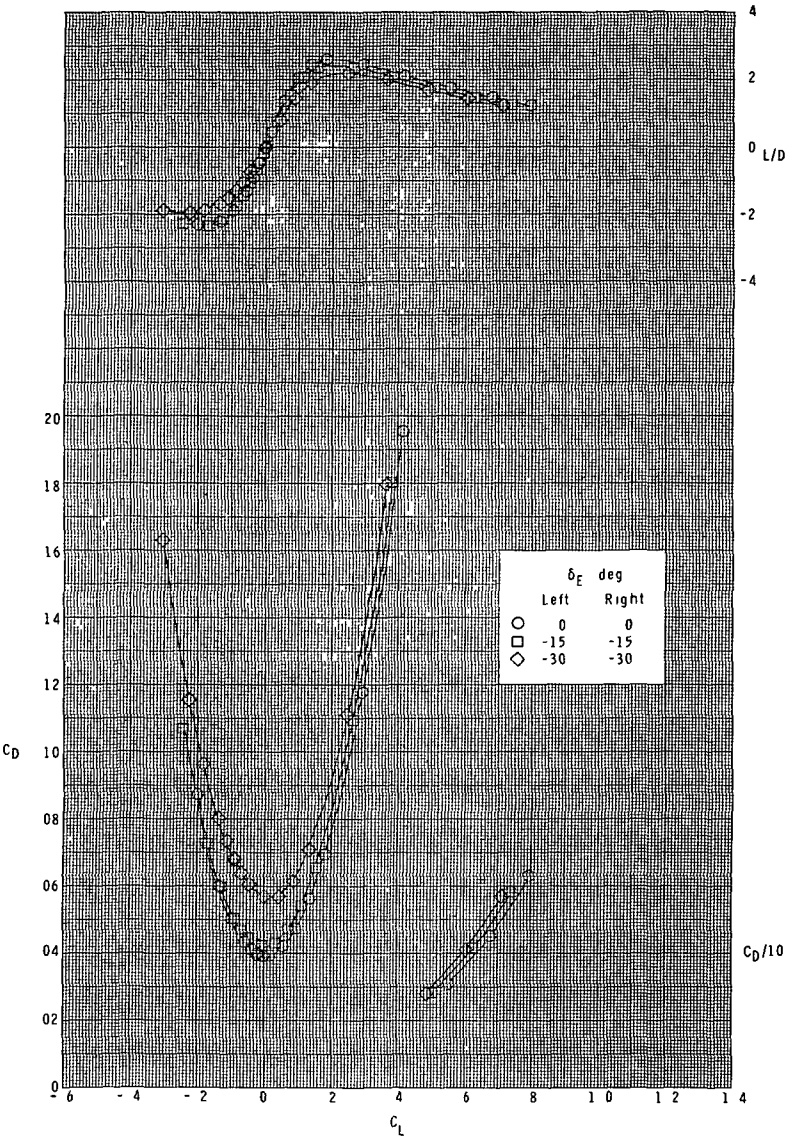

(c) Concluded.

Figure 16.- Continued.

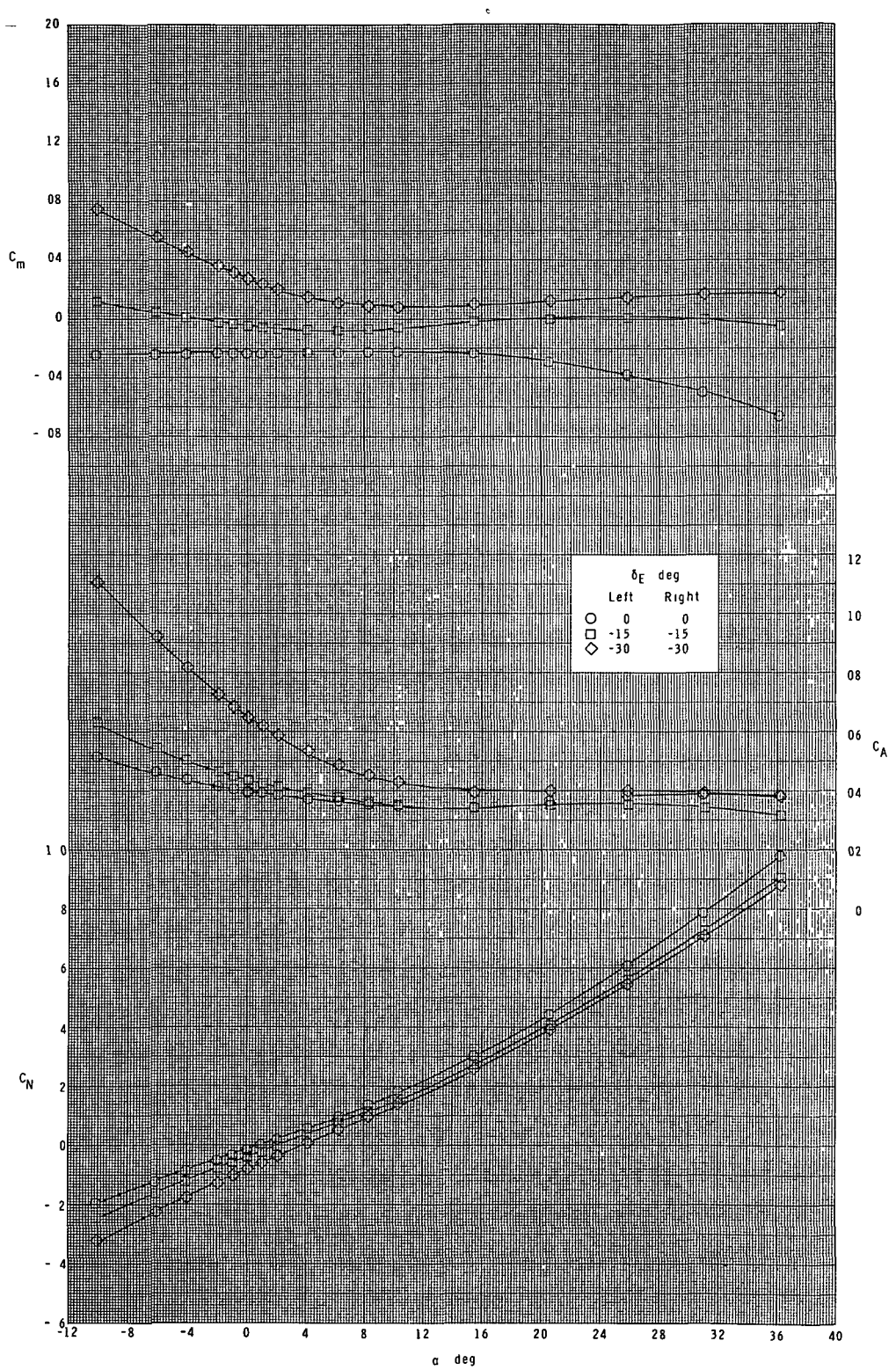

(d) M = 4.63.

Figure 16.- Continued.

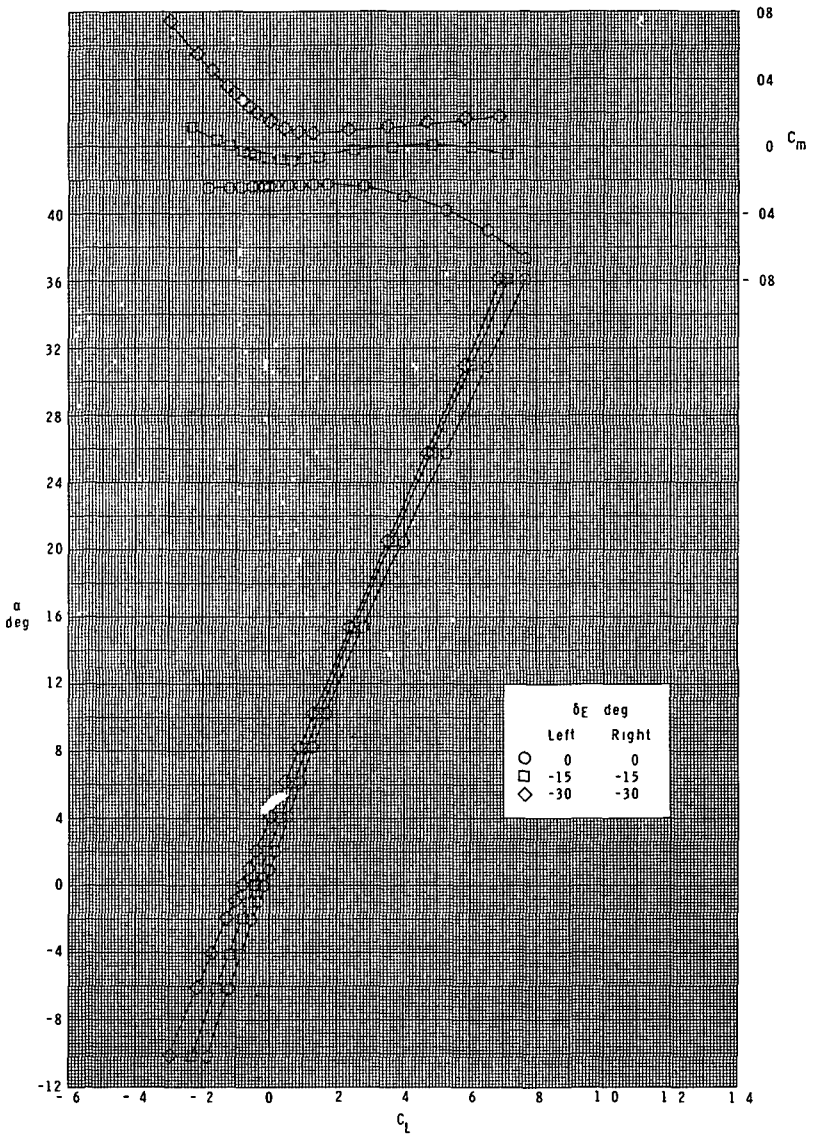

(d) Continued.

Figure 16.- Continued.

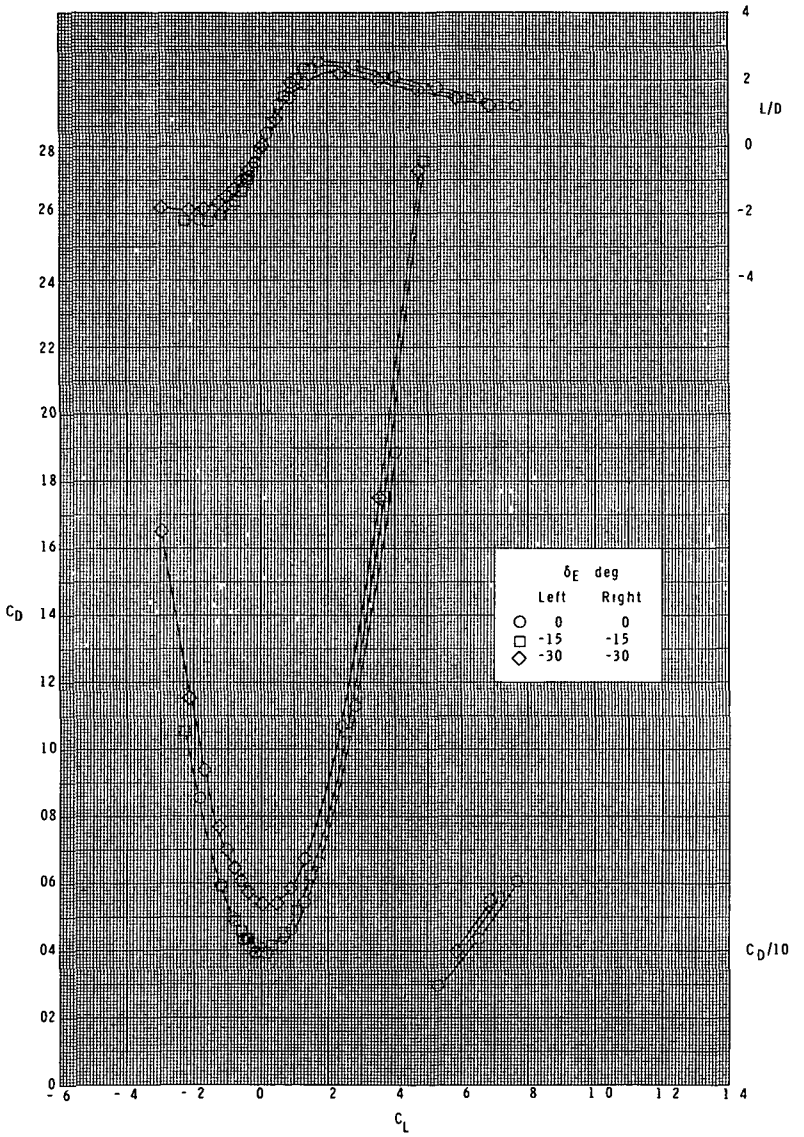

(d) Concluded.

Figure 16.- Concluded.

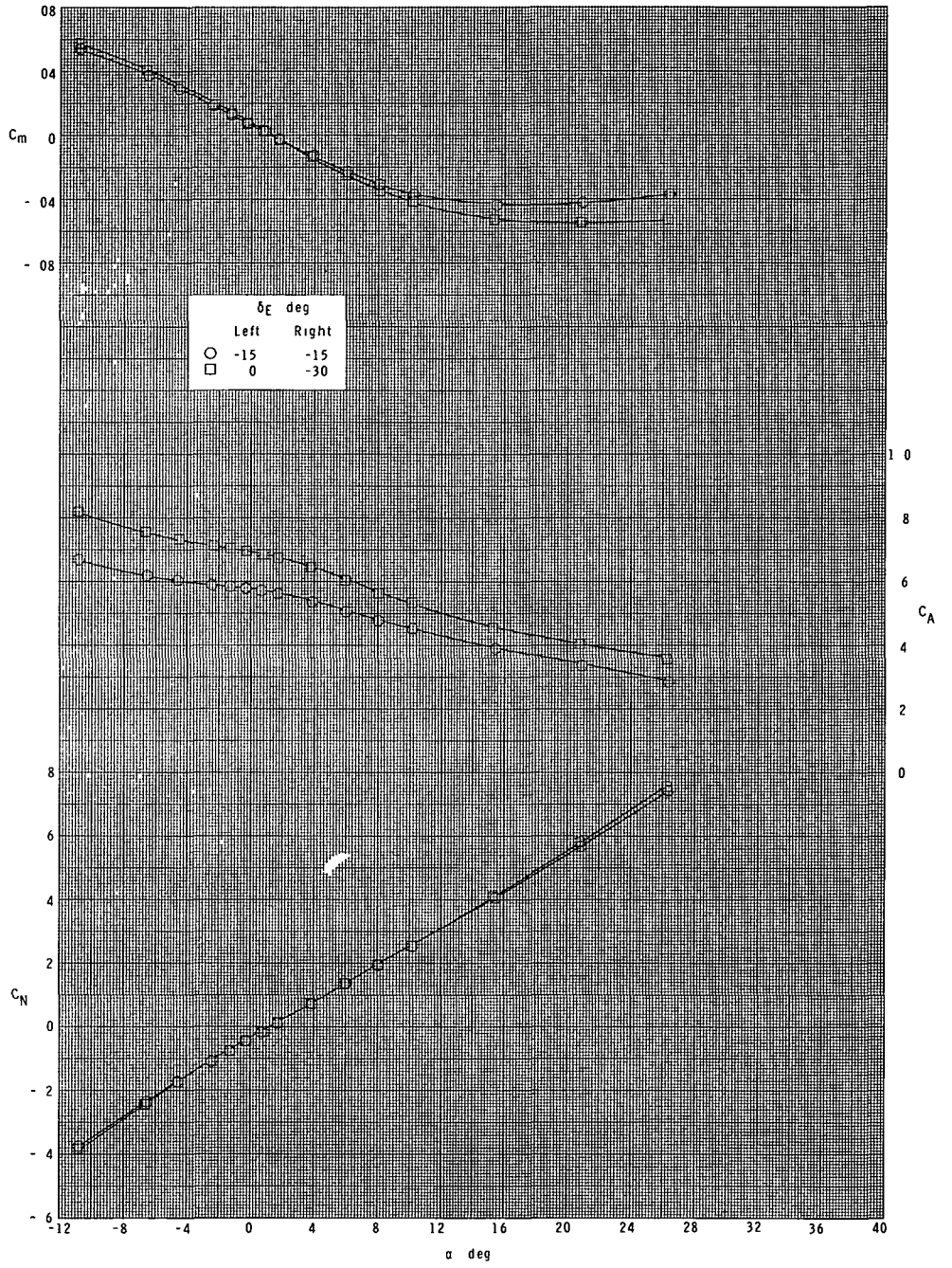

(a) M = 2.30.

Figure 17.- Effect of elevon deflection-in-roll on longitudinal characteristics. Orbiter configuration.

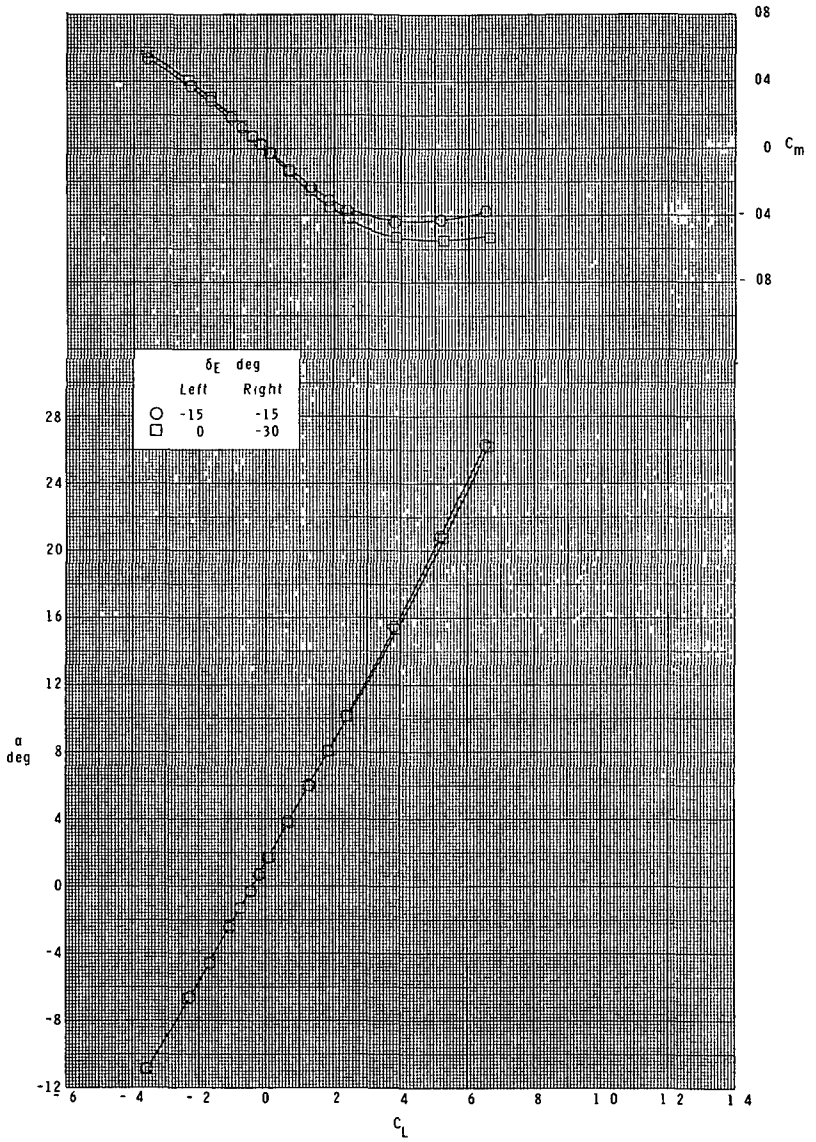

(a) Continued.

Figure 17.- Continued.

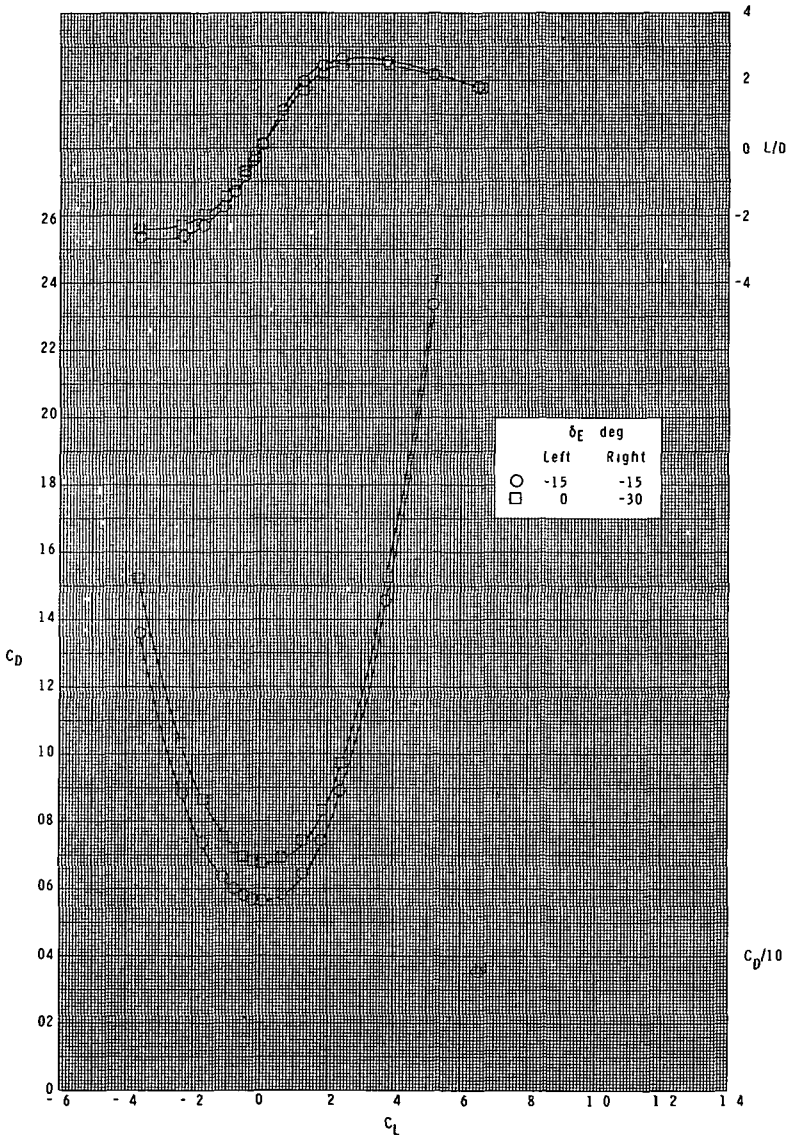

(a) Concluded.

Figure 17.- Continued.

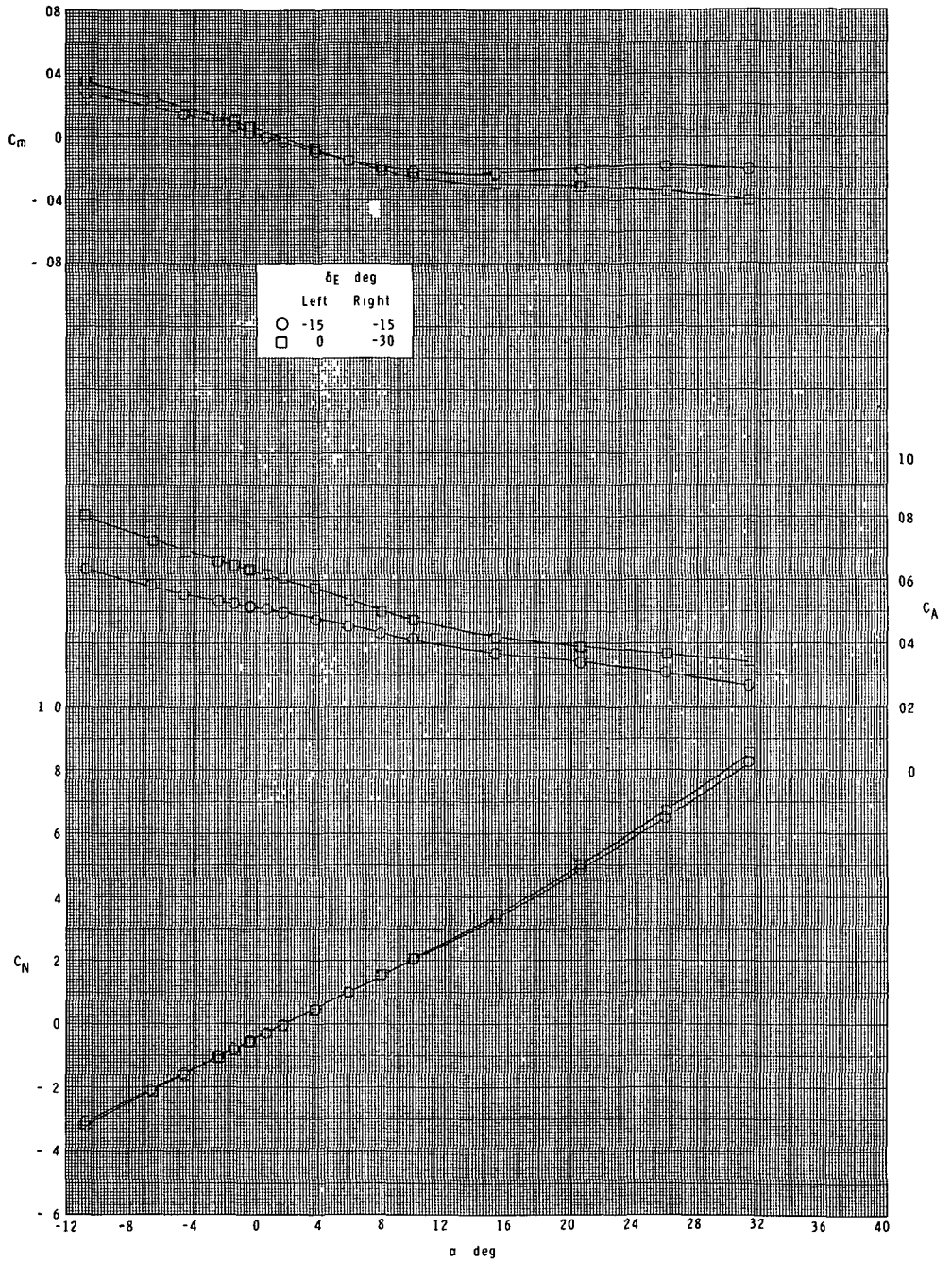

(b) M = 2.96.

Figure 17.- Continued.

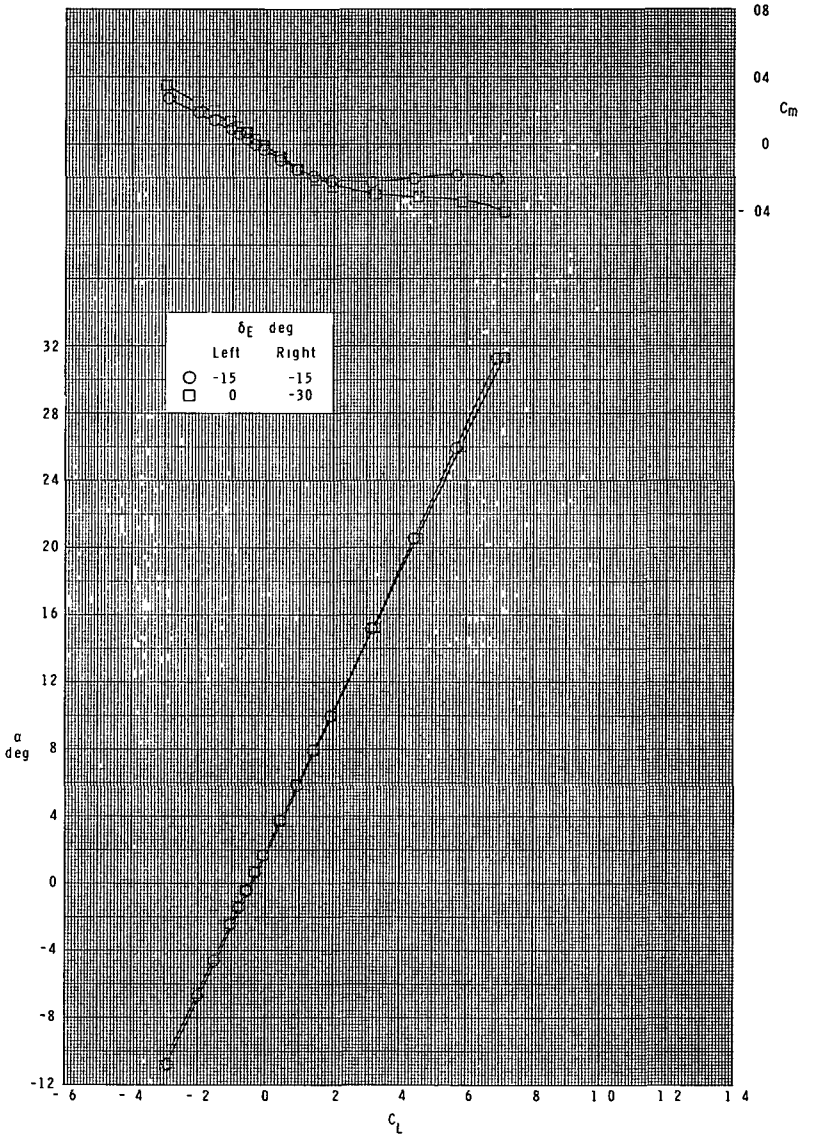

(b) Continued.

Figure 17.- Continued.

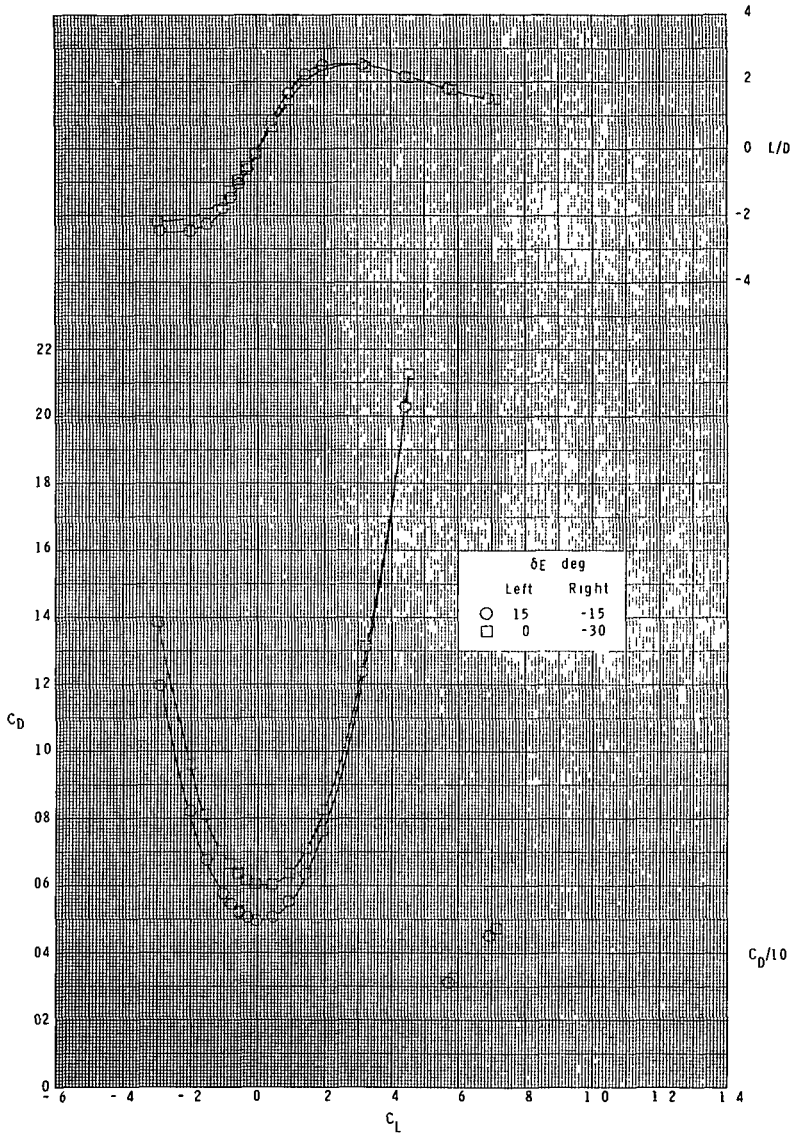

(b) Concluded.

Figure 17.- Continued.

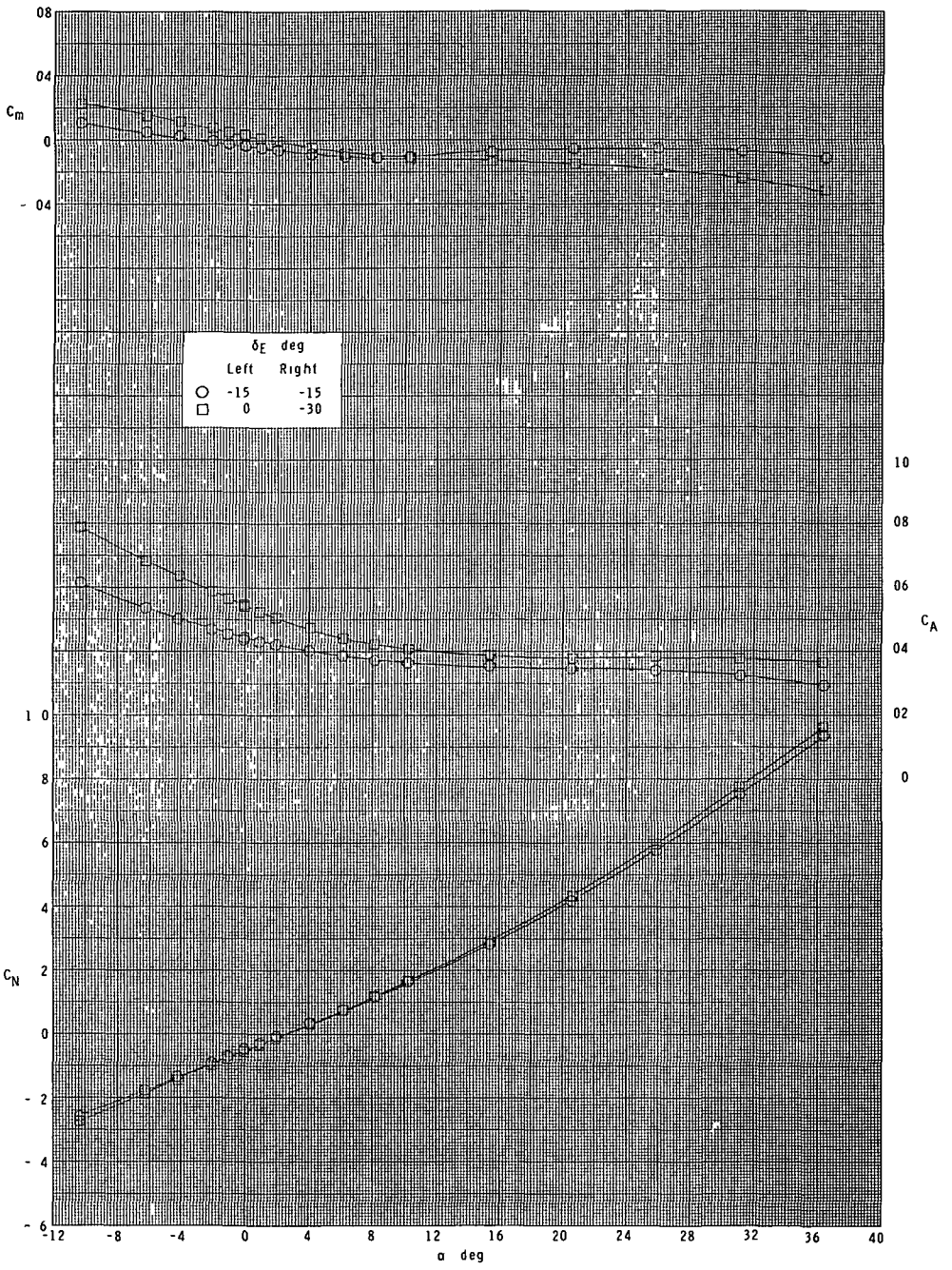

(c) M = 3.95.

Figure 17.- Continued.

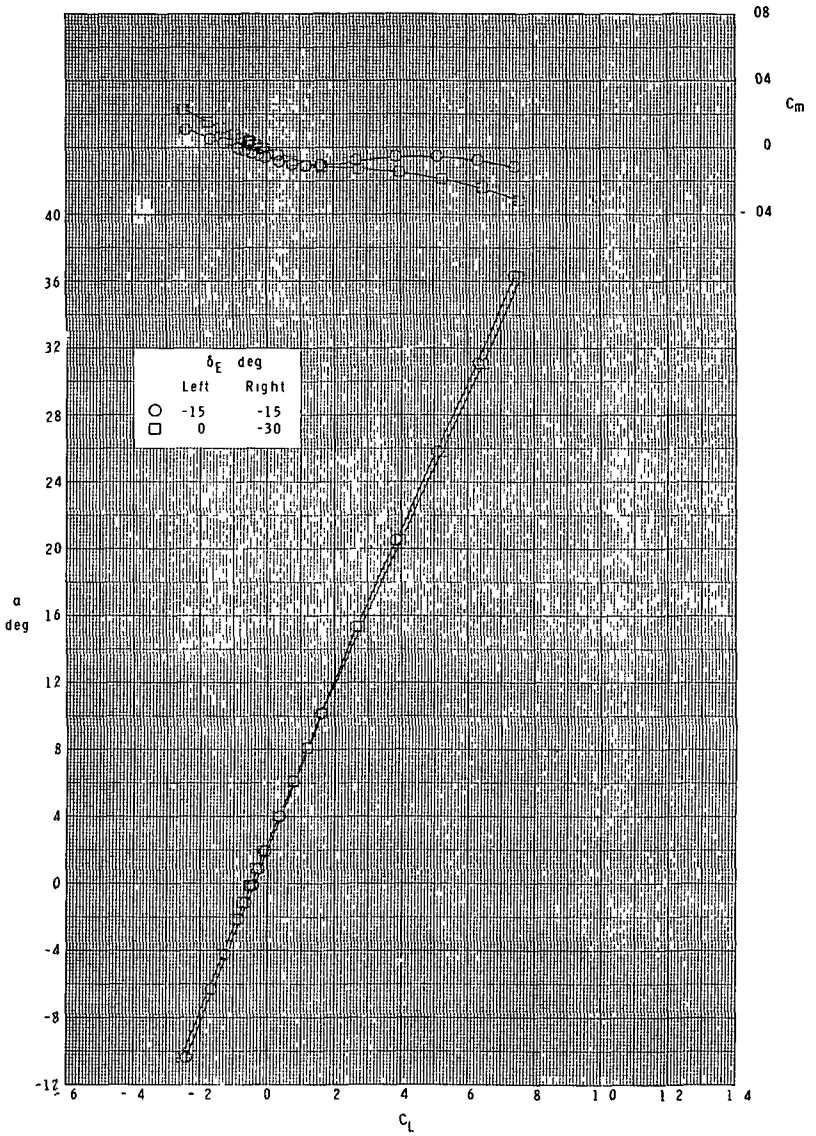

(c) Continued.

Figure 17.- Continued.

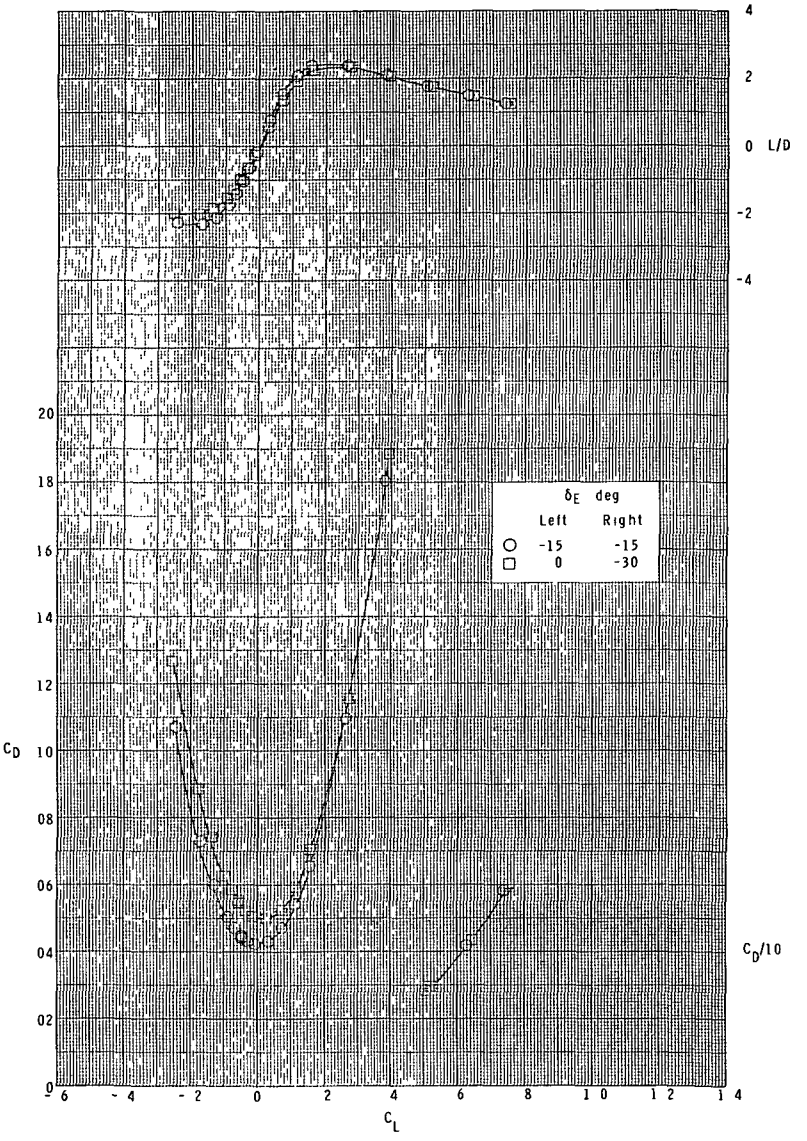

(c) Concluded.

Figure 17.- Continued.

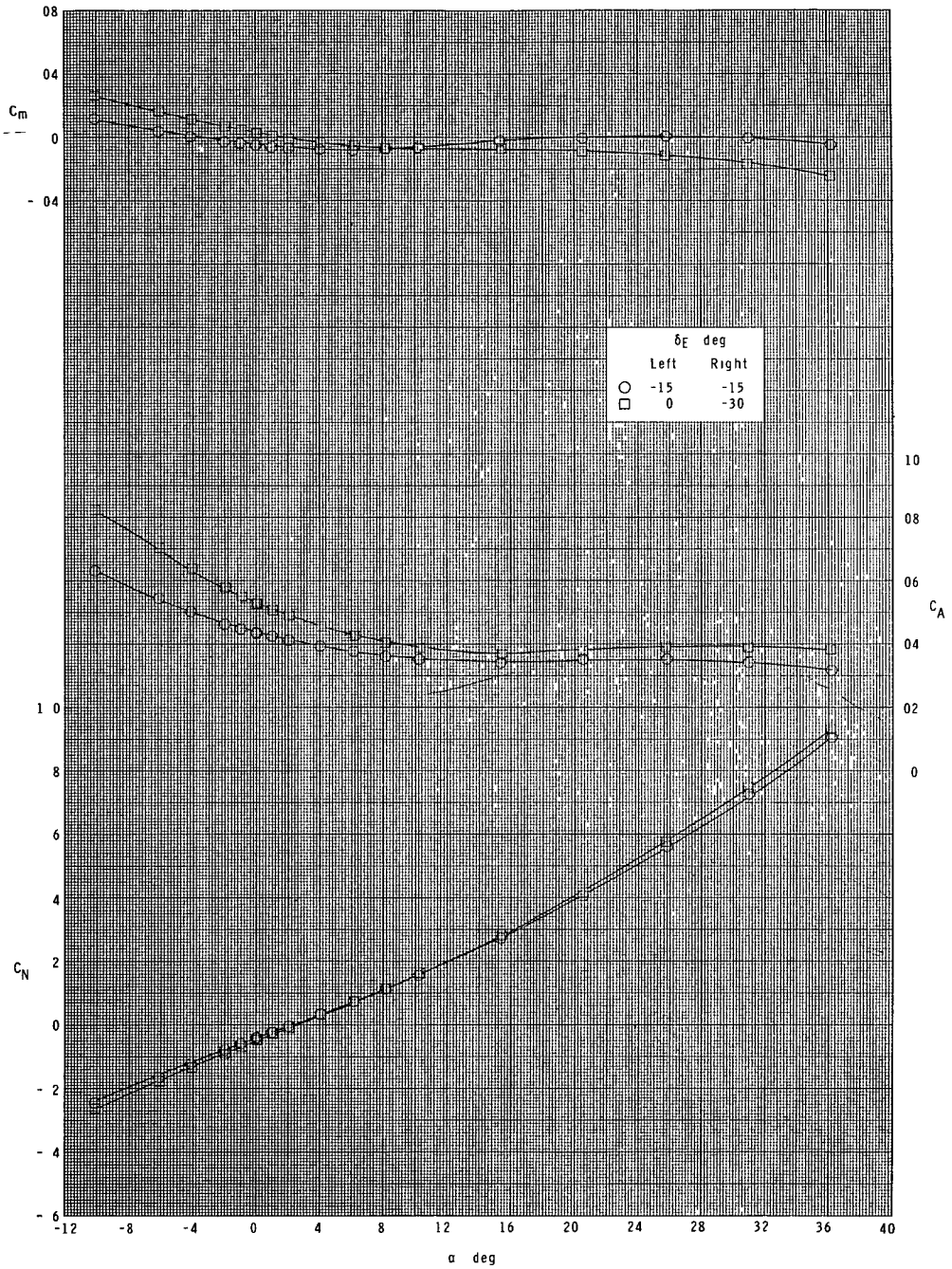

(d) M = 4.60.

Figure 17.- Continued.

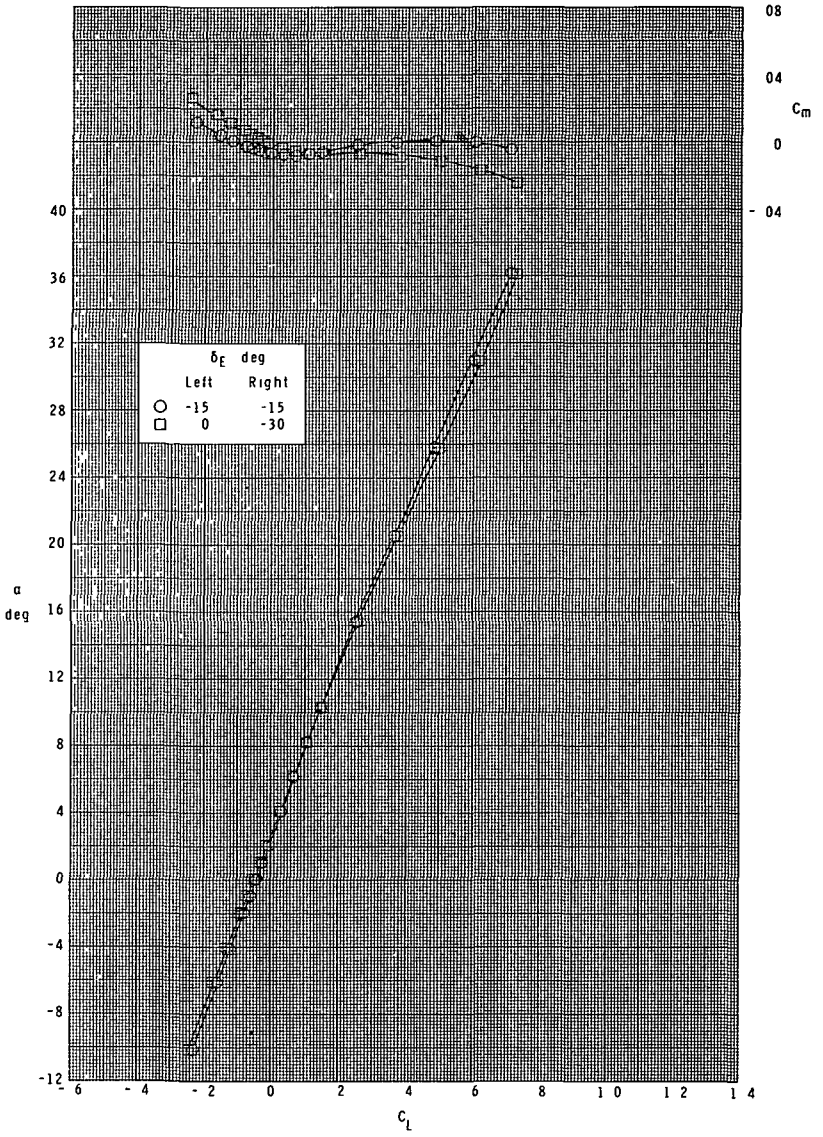

(d) Continued.

Figure 17.- Continued.

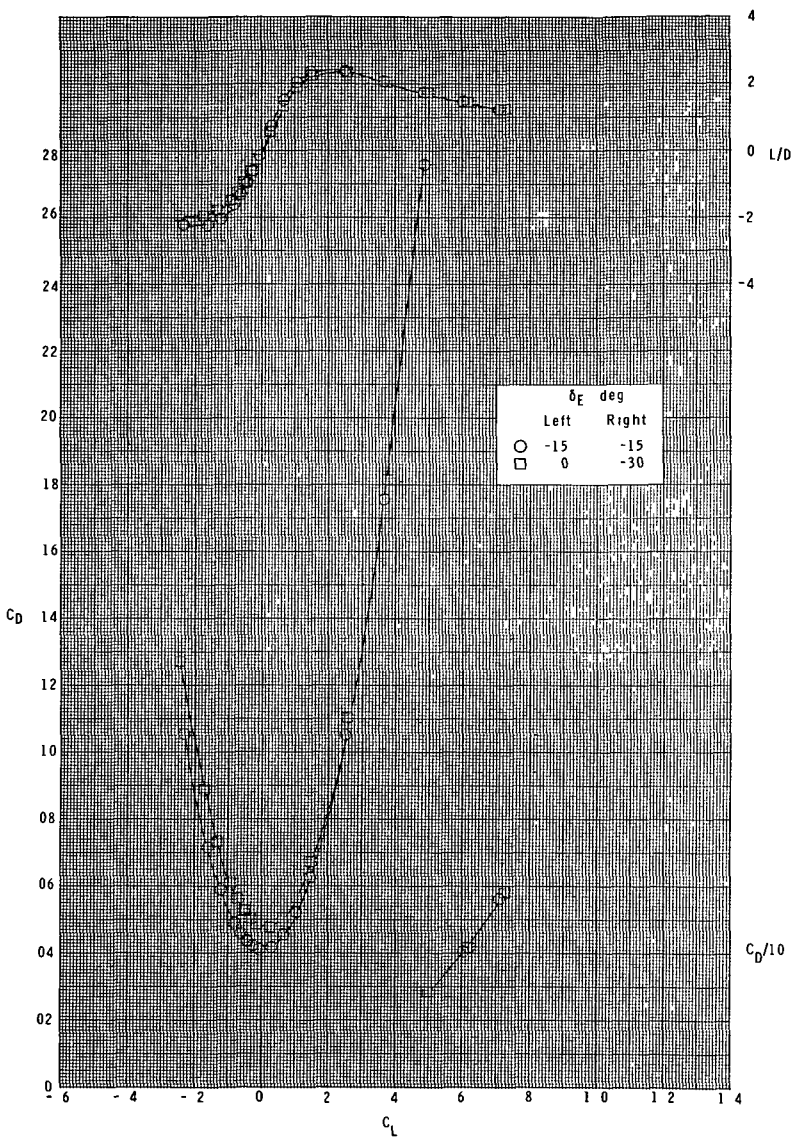

(d) Concluded.

Figure 17.- Concluded.

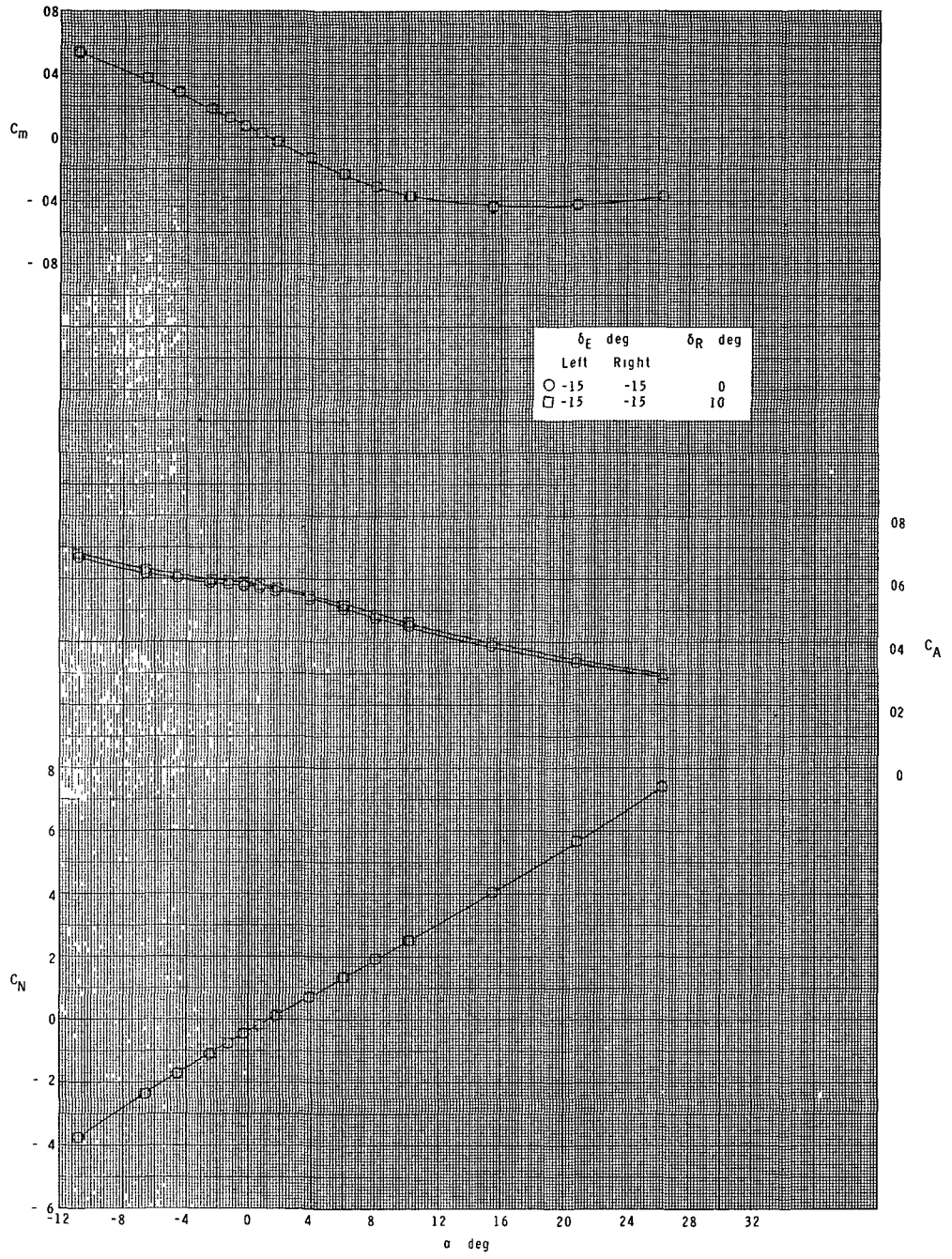

(a) M = 2.30.

Figure 18.- Effect of vertical-tail rudder deflection on longitudinal characteristics. Orbiter configuration.

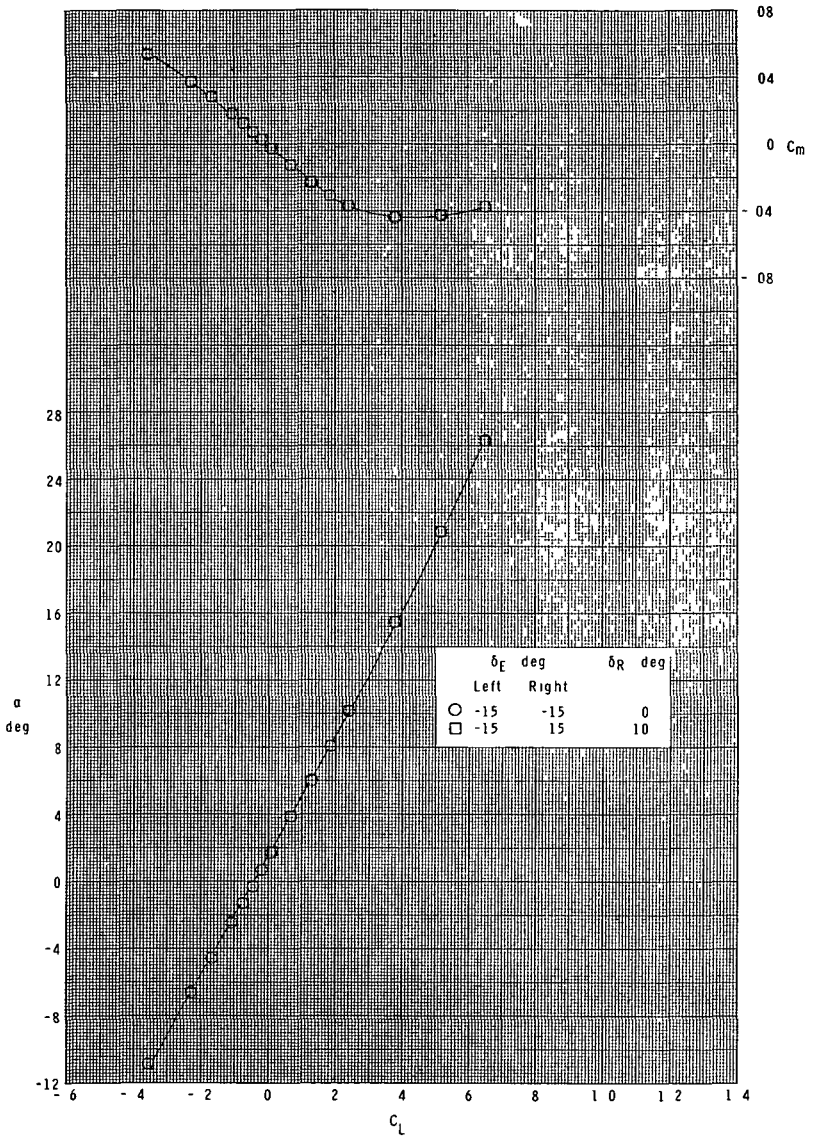

(a) Continued.

Figure 18.- Continued.

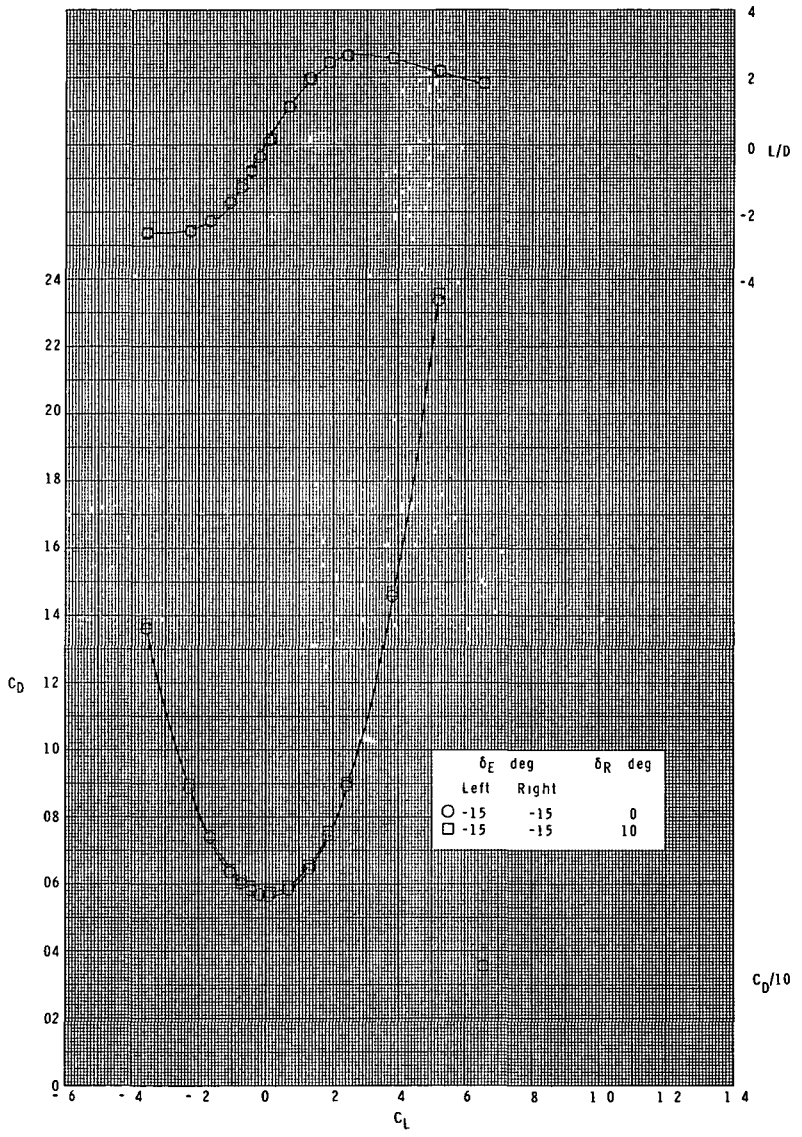

(a) Concluded.

Figure 18.- Continued.

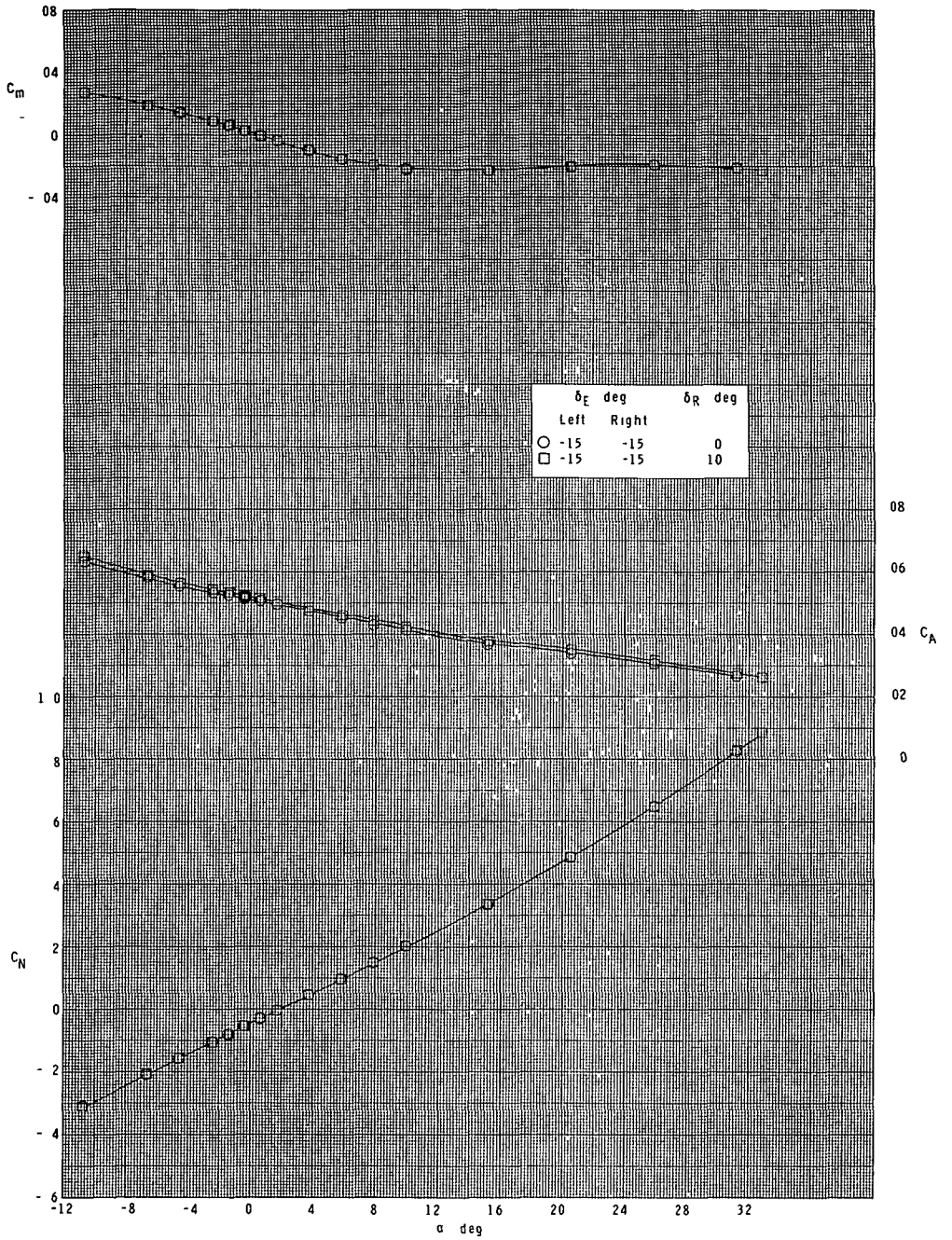

(b) M = 2.96.

Figure 18.- Continued.

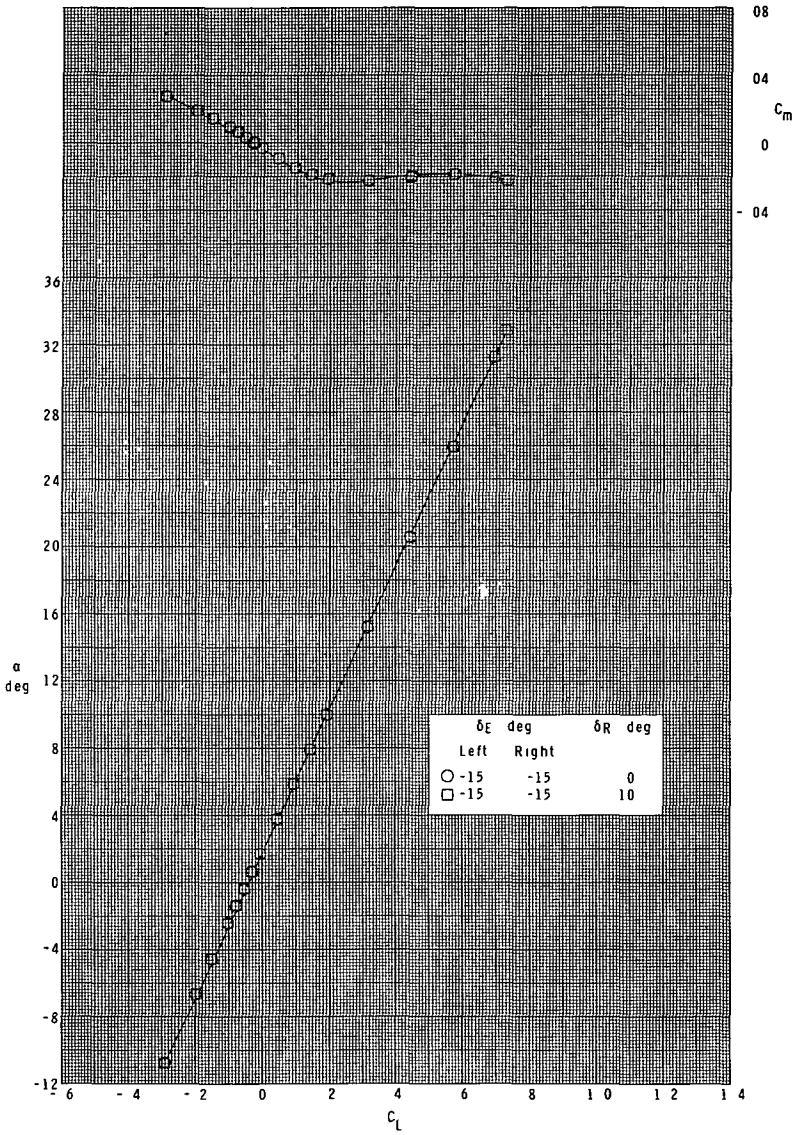

(b) Continued.

Figure 18.- Continued.

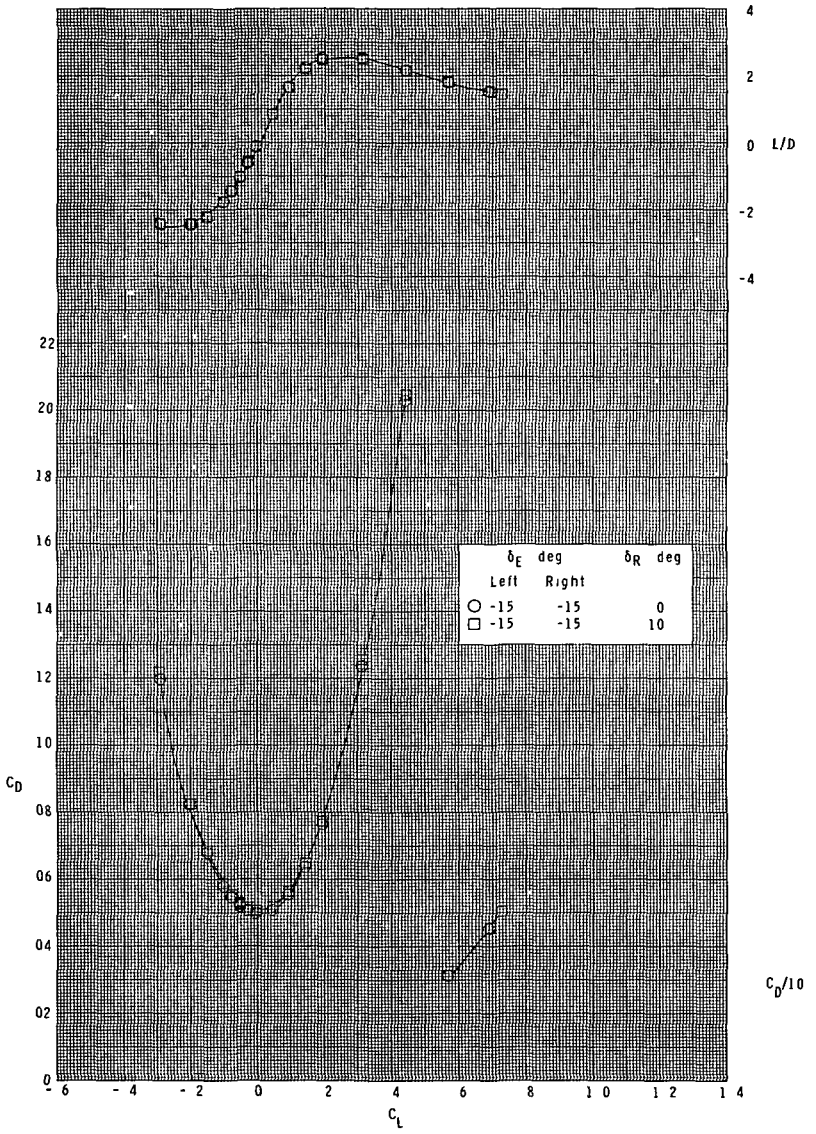

(b) Concluded.

Figure 18.- Continued.

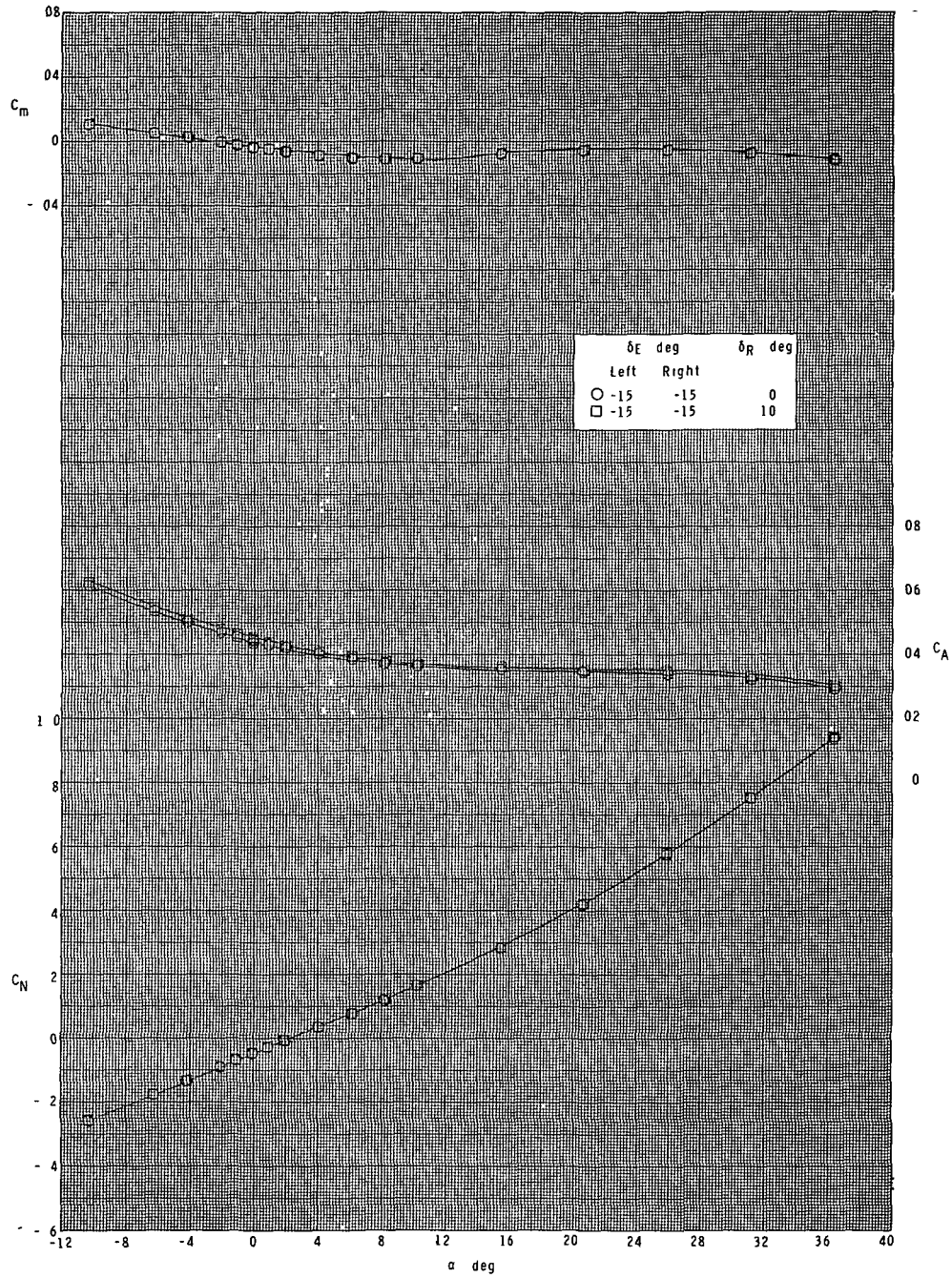

(c) M = 3.95.

Figure 18.- Continued.

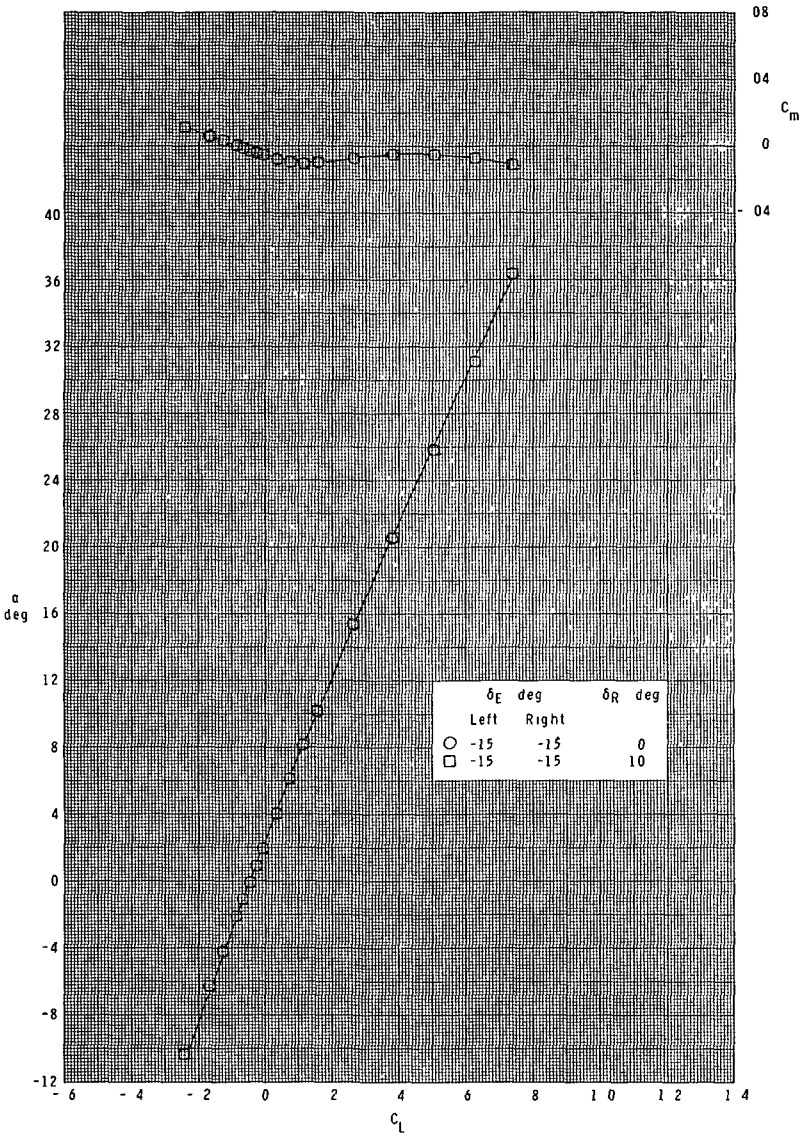

(c) Continued.

Figure 18.- Continued.

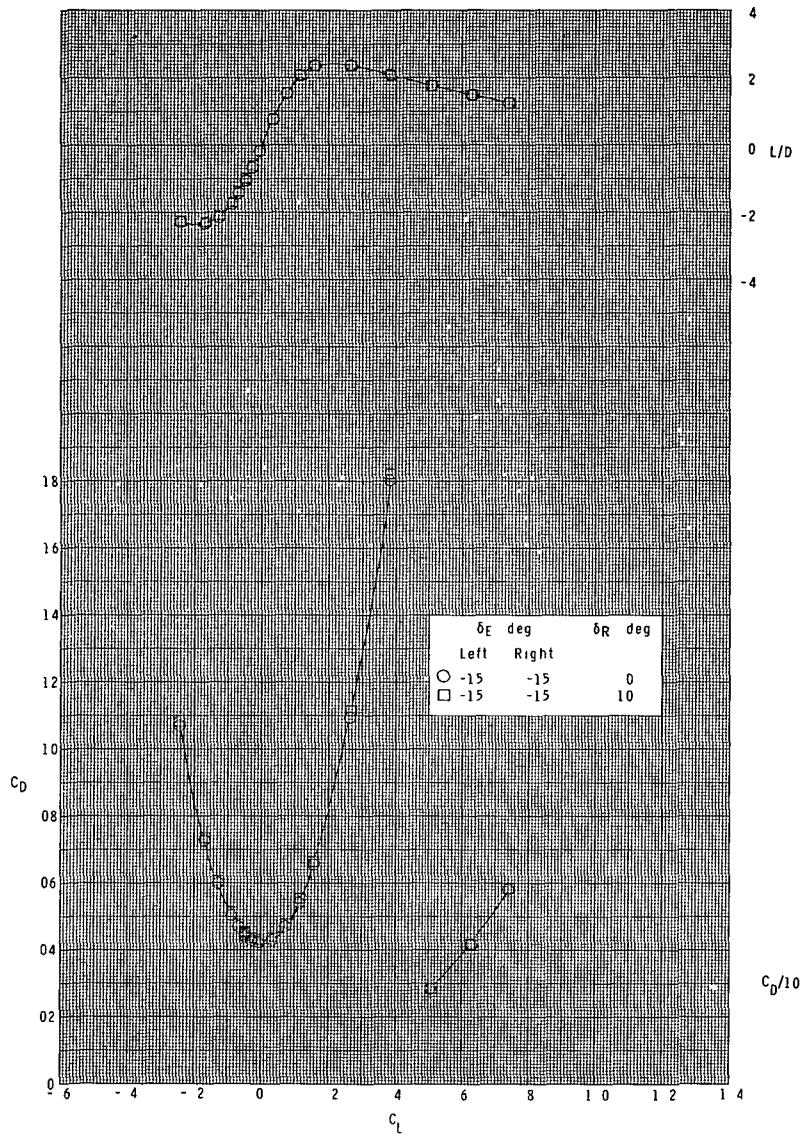

(c) Concluded.

Figure 18.- Continued.

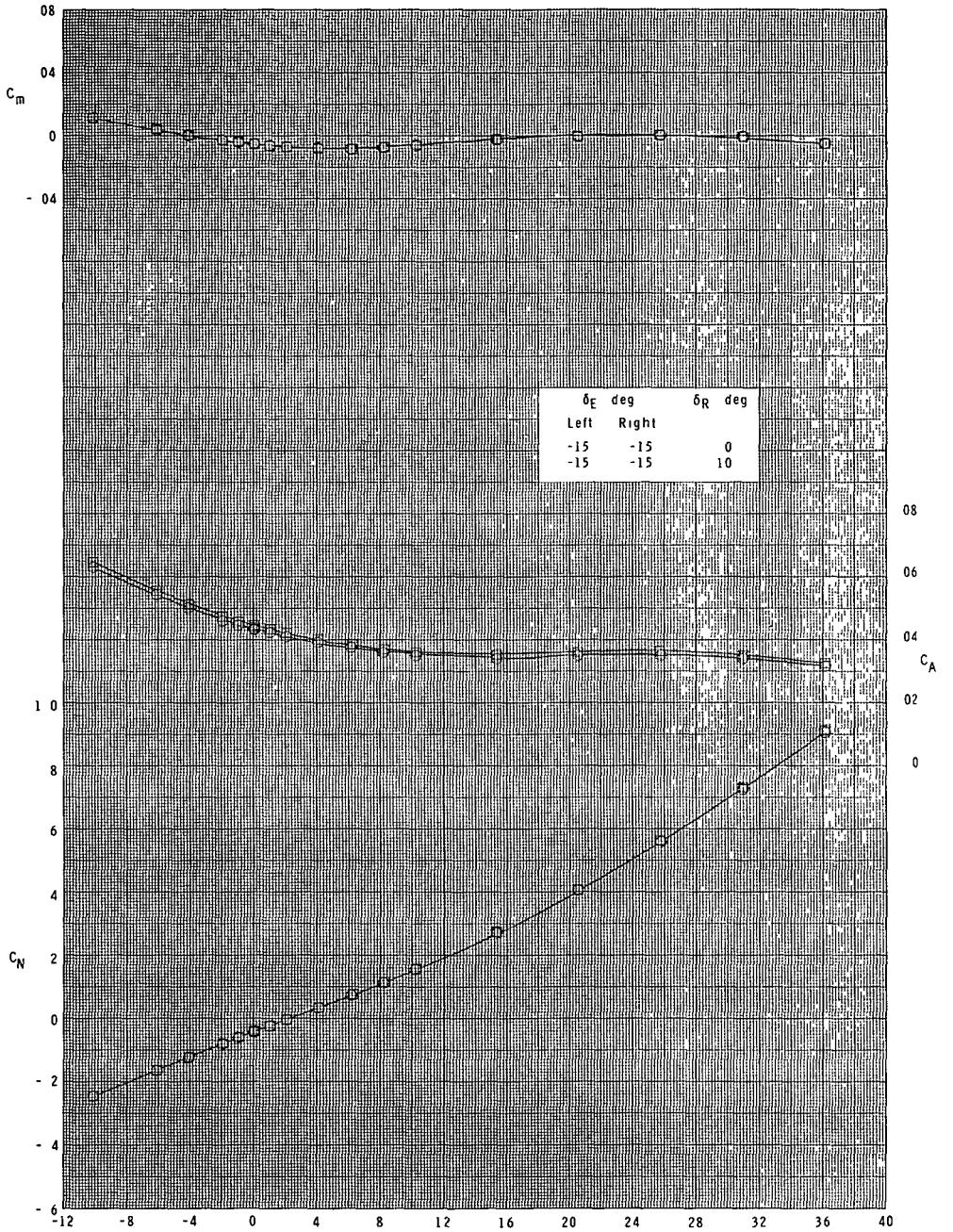

(d) M = 4.60.

Figure 18.- Continued.

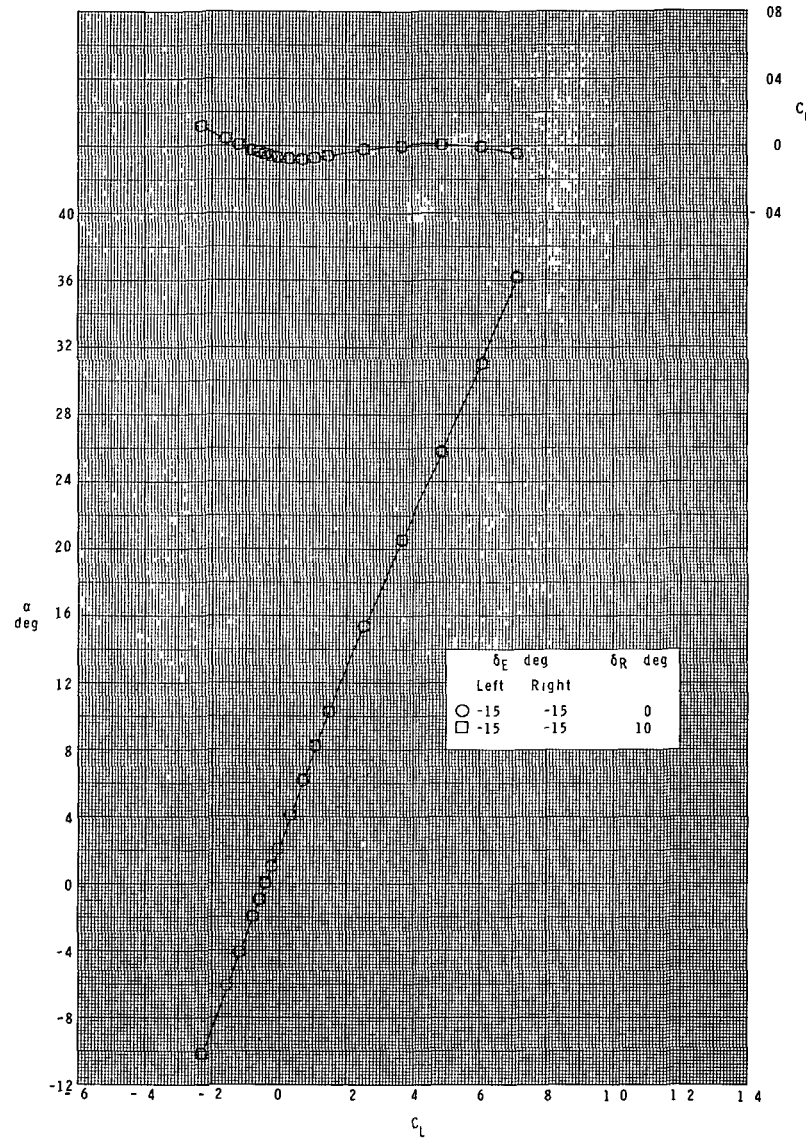

(d) Continued.

Figure 18.- Continued.

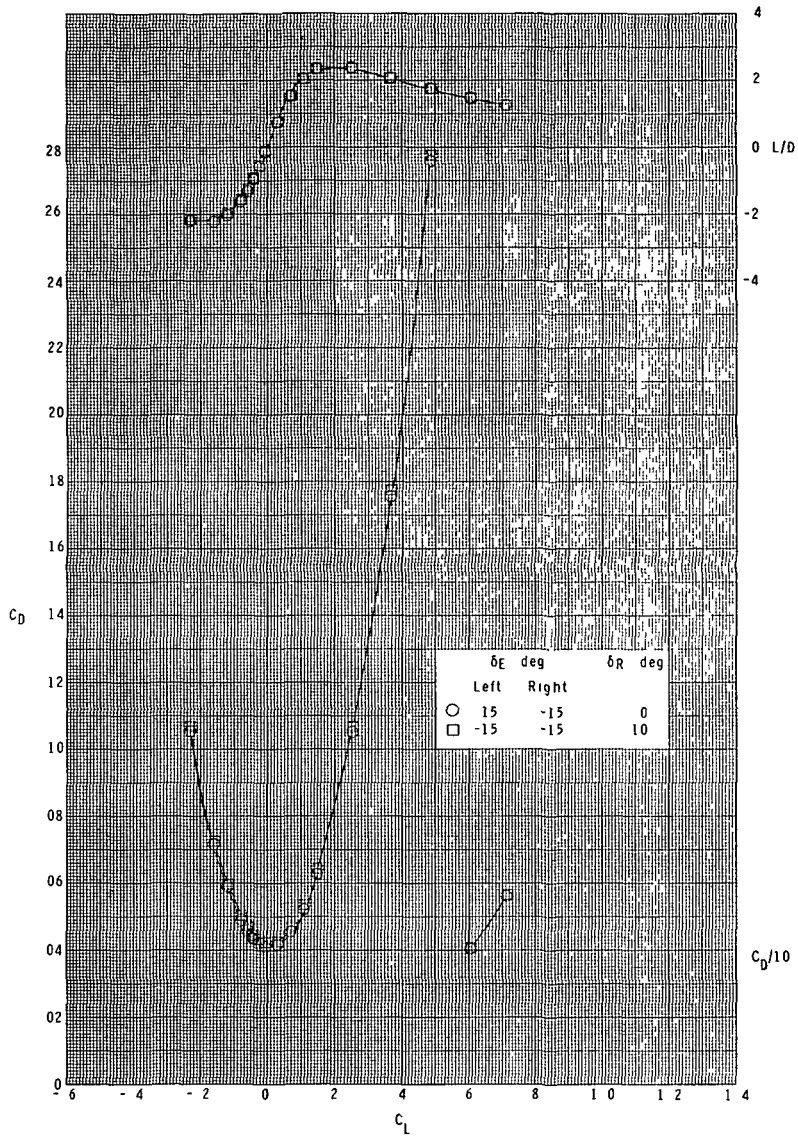

(d) Concluded.

Figure 18.- Concluded.

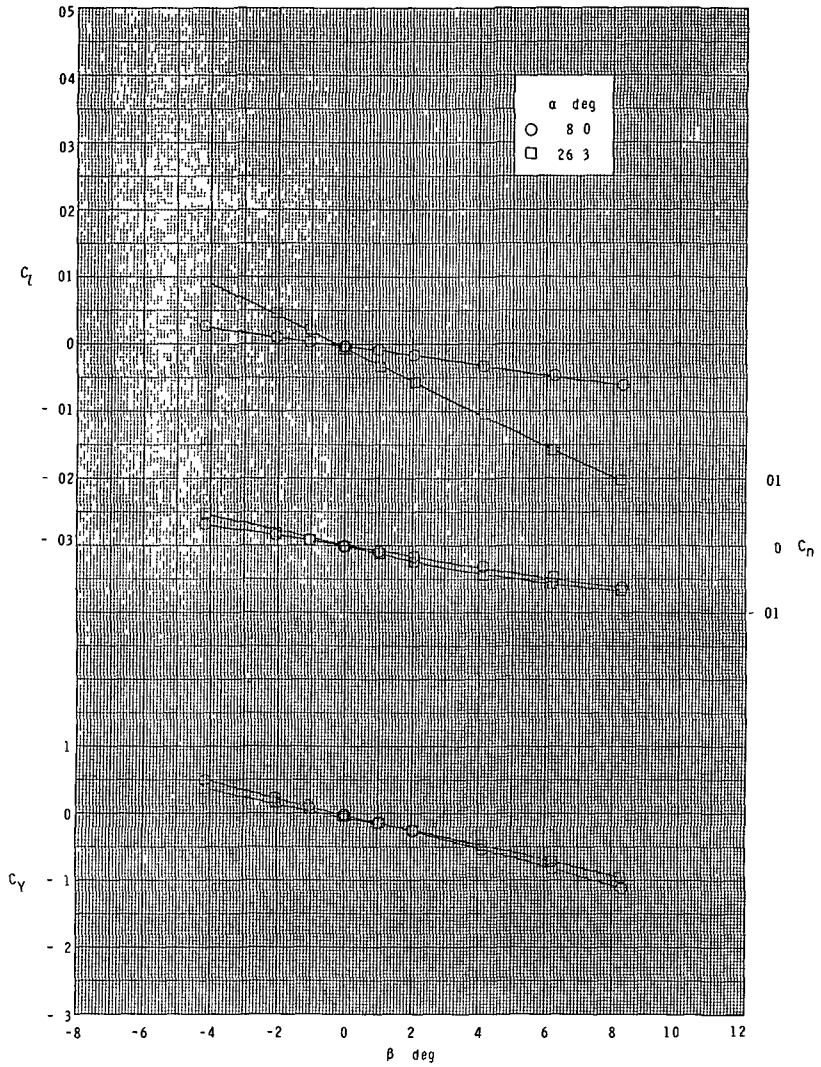

(a) M = 2.30.

Figure 19.- Lateral characteristics in sideslip. Orbiter configuration.

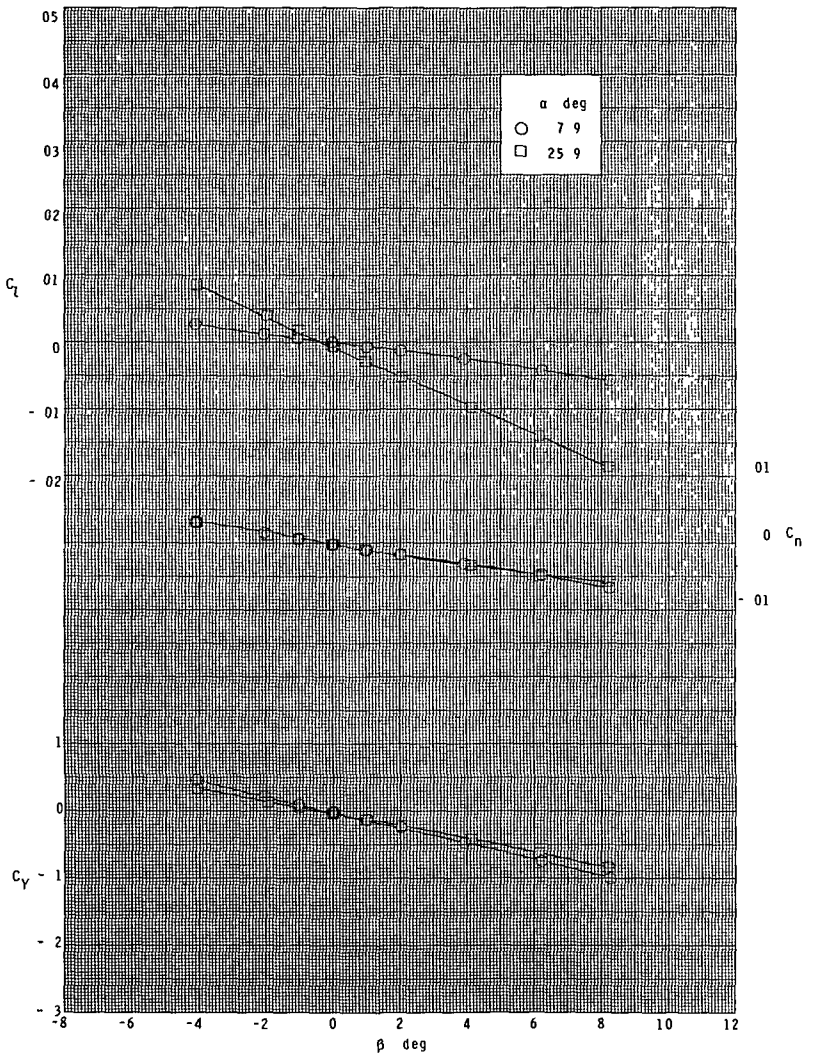

(b) M = 2.96.

Figure 19.- Continued.

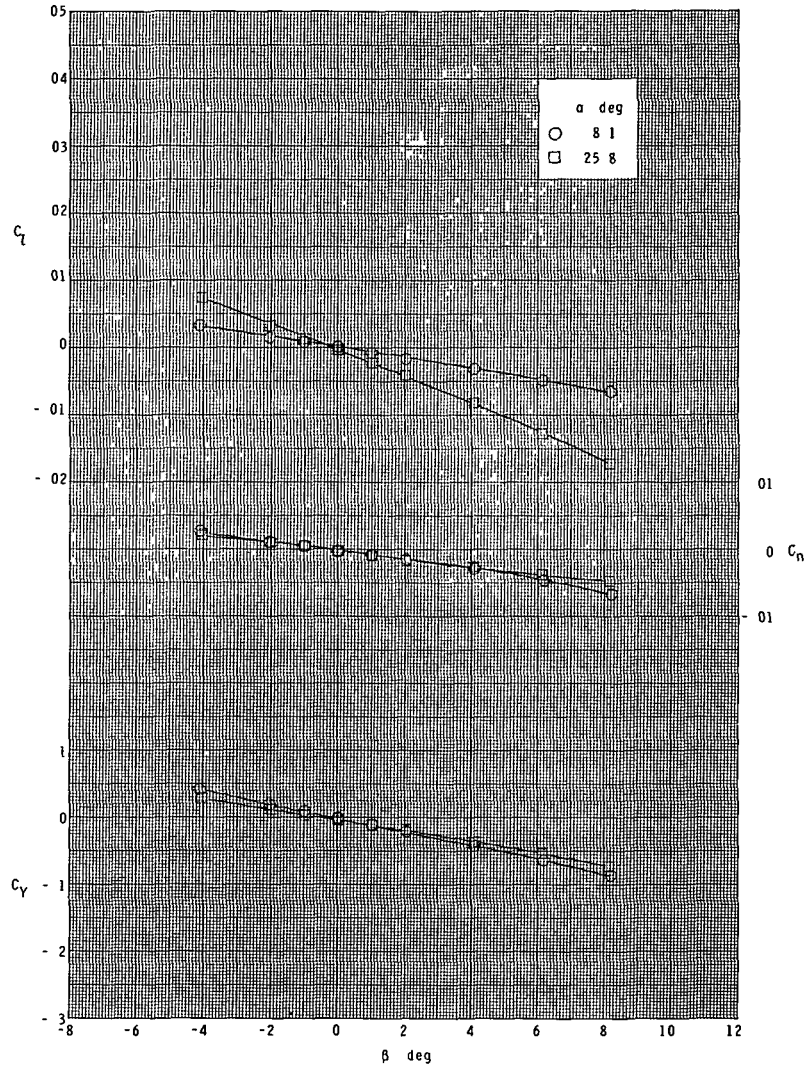

(c) M = 3.95.

Figure 19.- Continued.

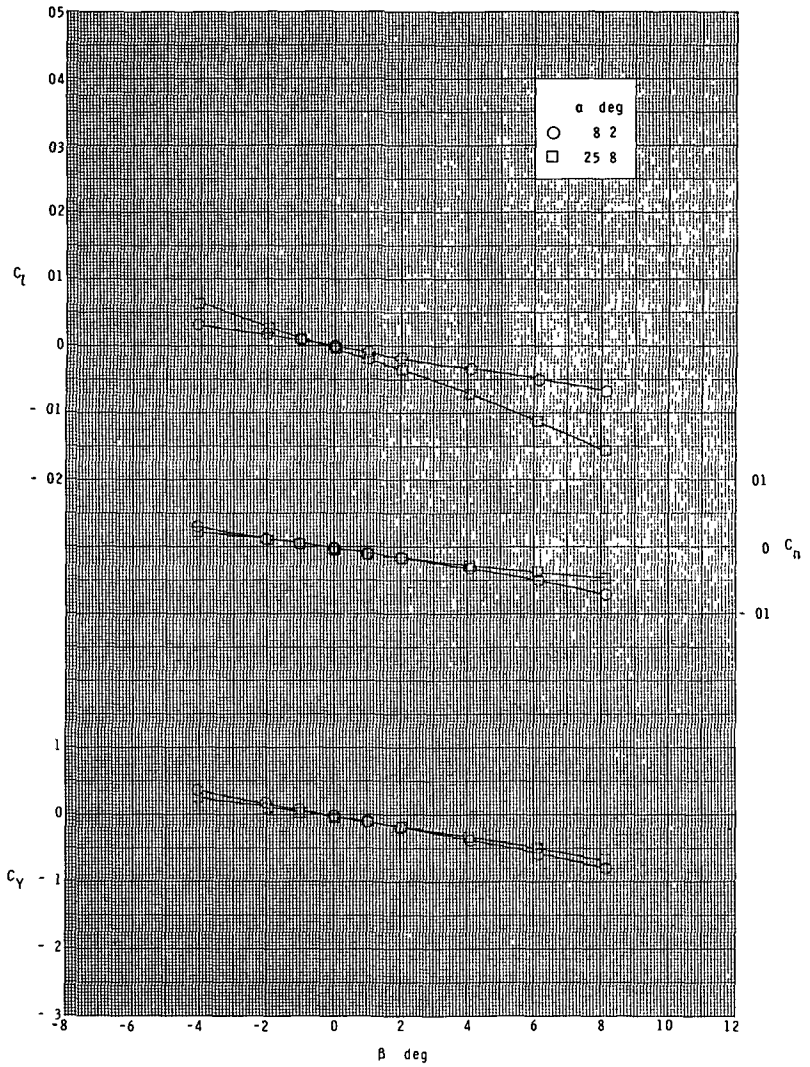

(d) M = 4.60.

Figure 19.- Concluded.

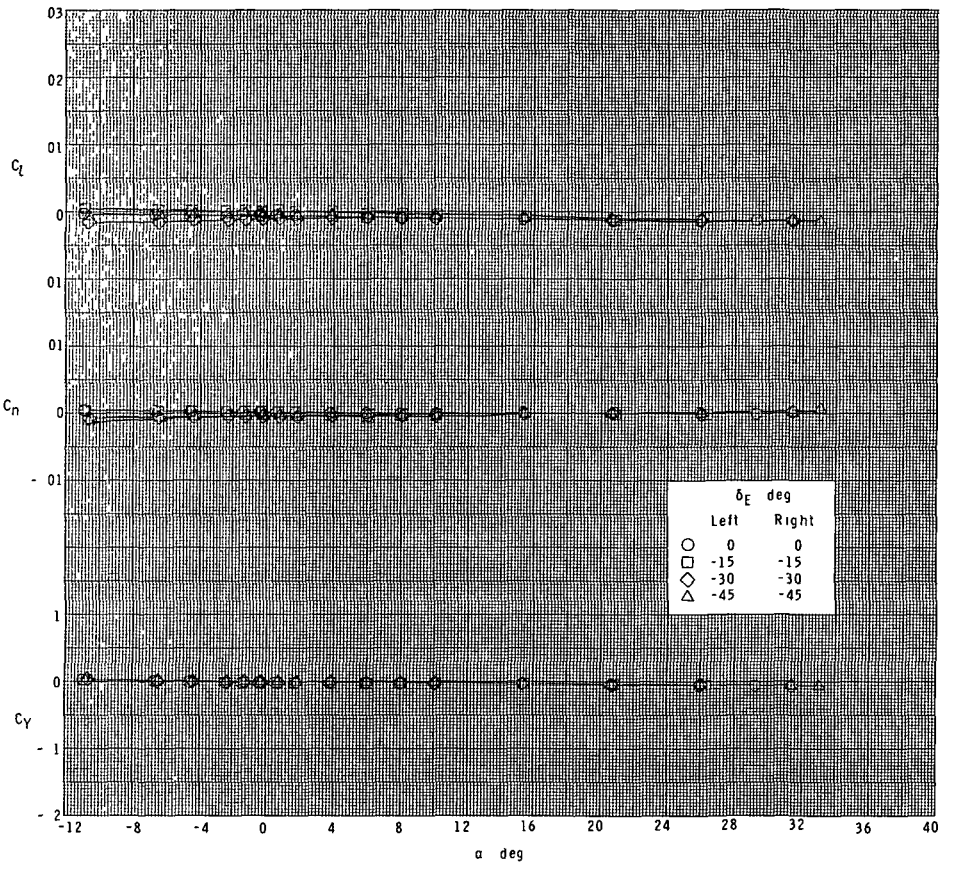

(a) M = 2.30.

Figure 20.- Effect of elevon deflection-in-pitch on lateral characteristics. Orbiter configuration.

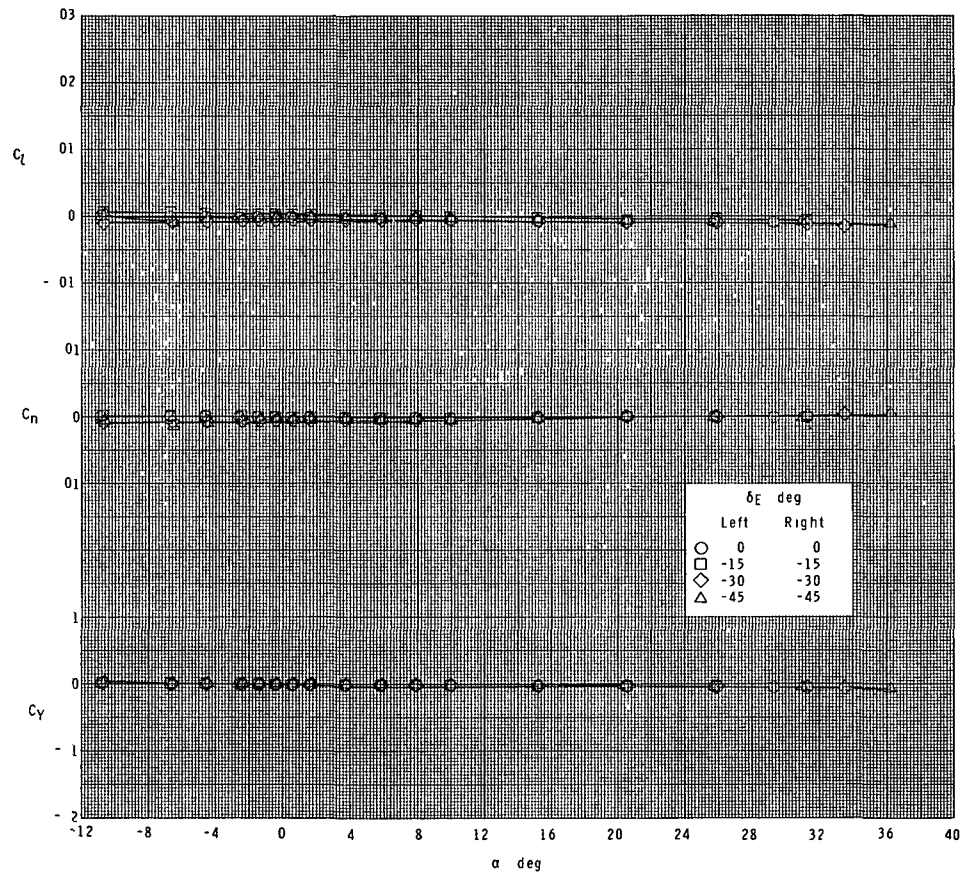

(b) M = 2.96.

Figure 20.- Continued.

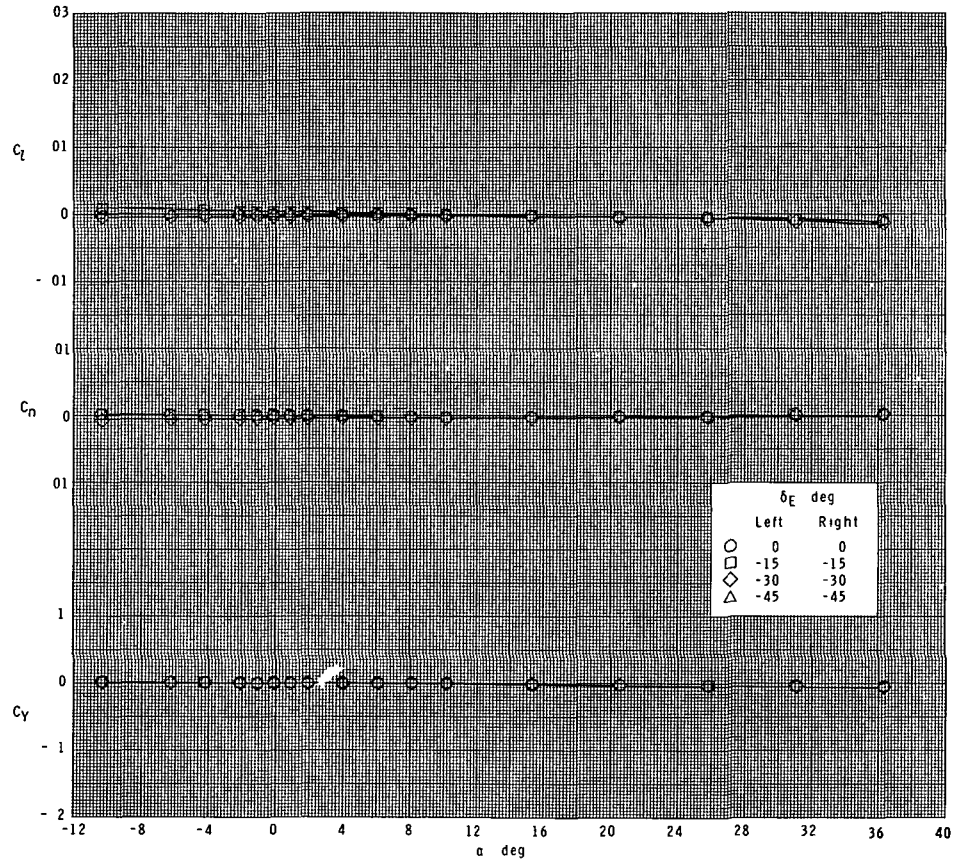

(c) M = 3.95.

Figure 20.- Continued.

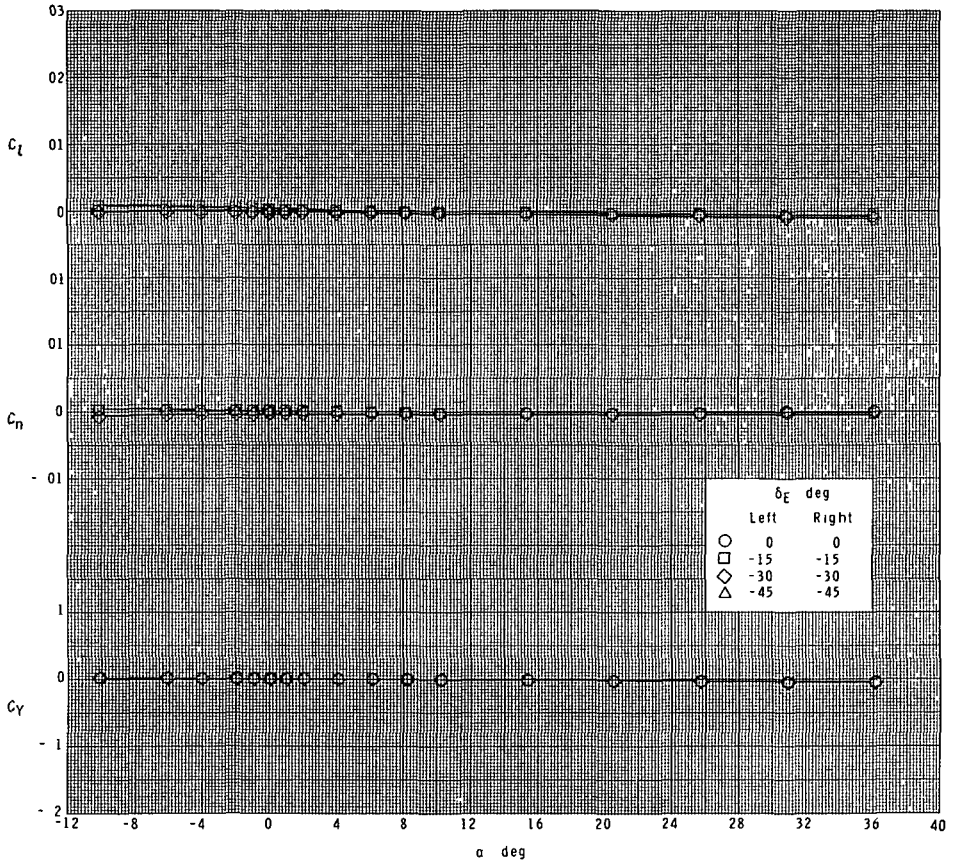

(d) M = 4.60.

Figure 20.- Concluded.

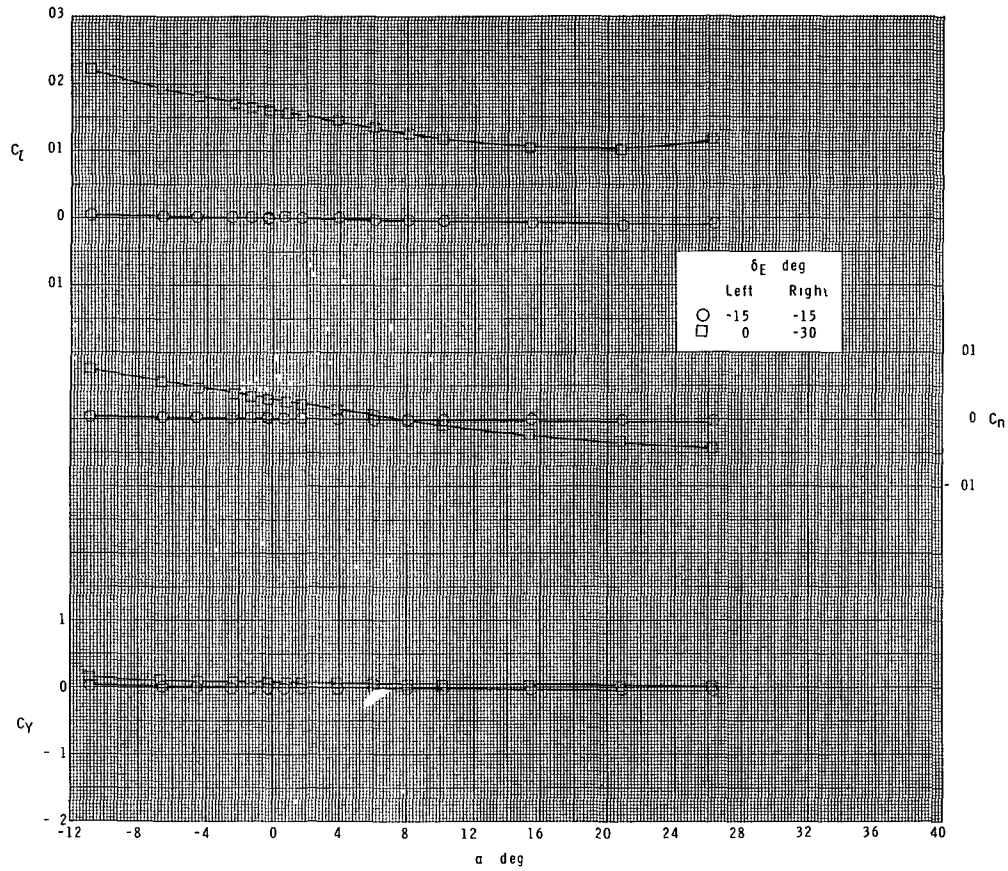

(a) M = 2.30.

Figure 21.- Elevon roll-control effectiveness. Orbiter configuration.

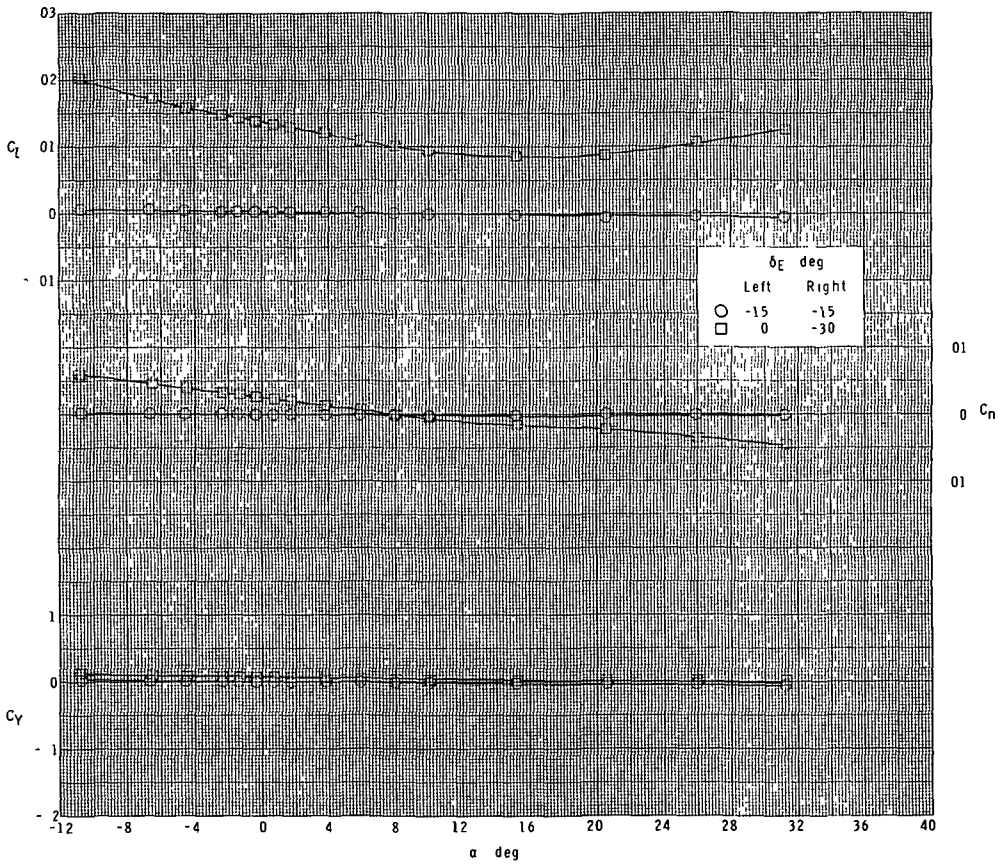

(b) M = 2.96.

Figure 21.- Continued.

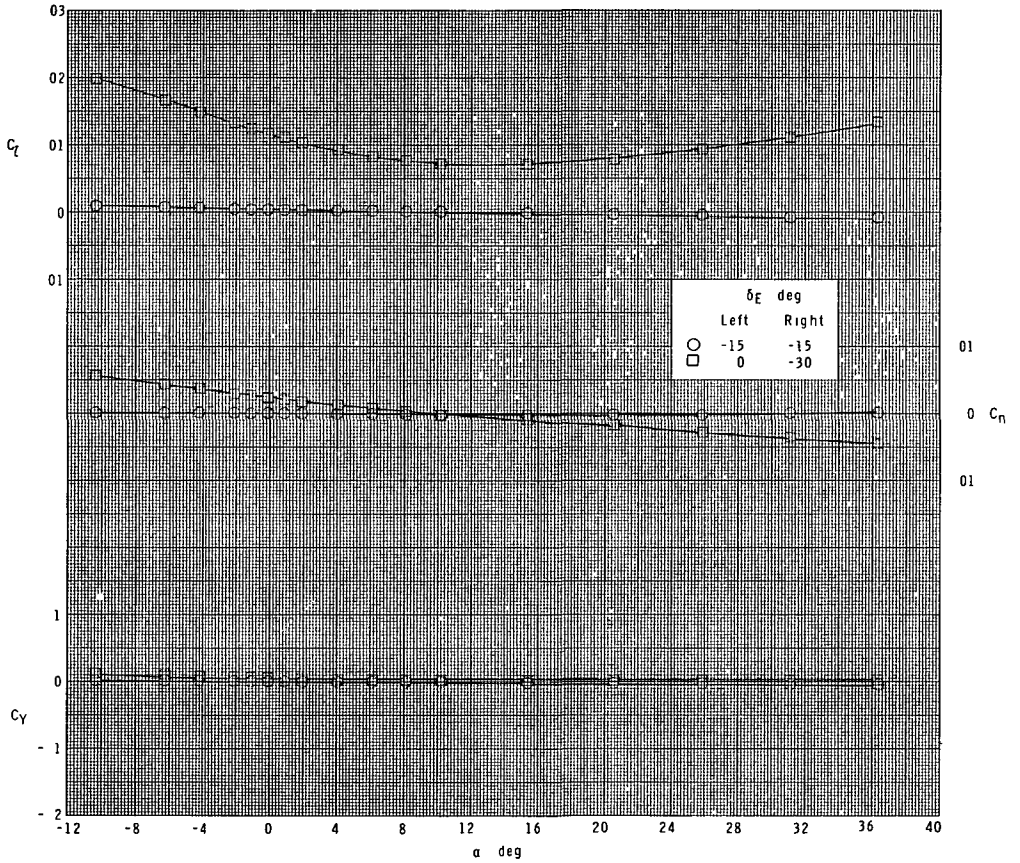

(c) M = 3.95.

Figure 21.- Continued.

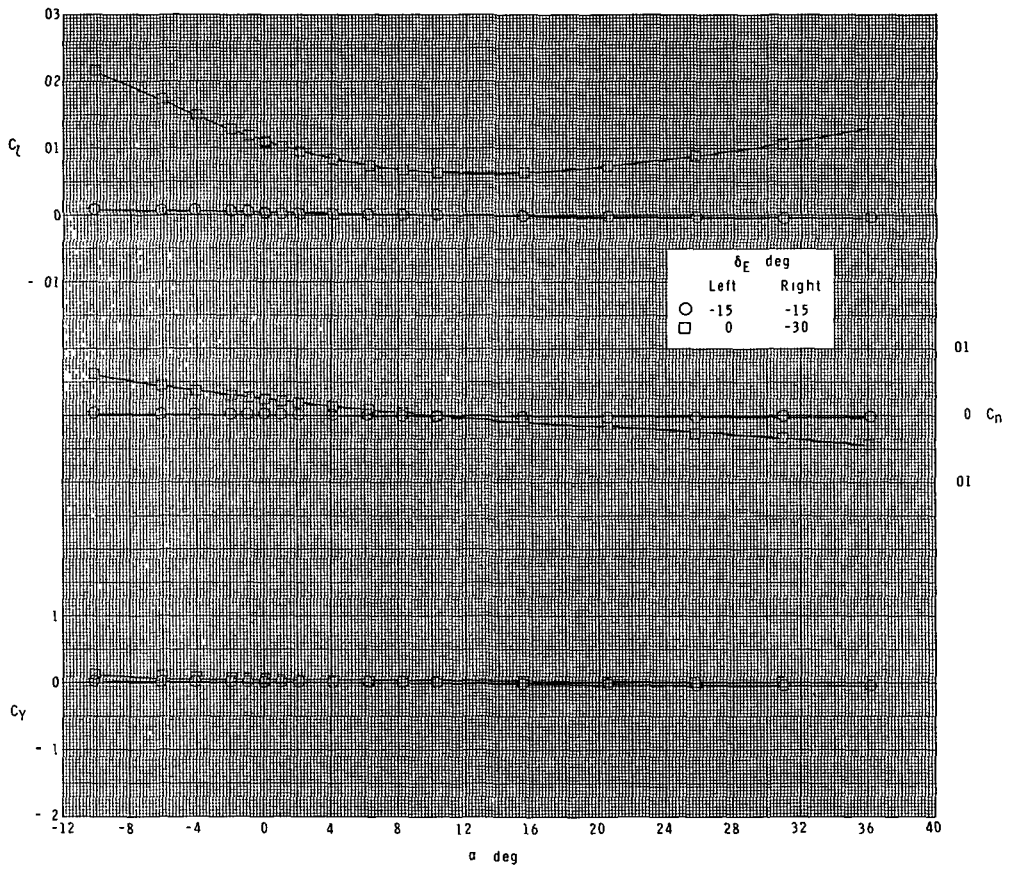

(d) M = 4.60.

Figure 21.- Concluded.

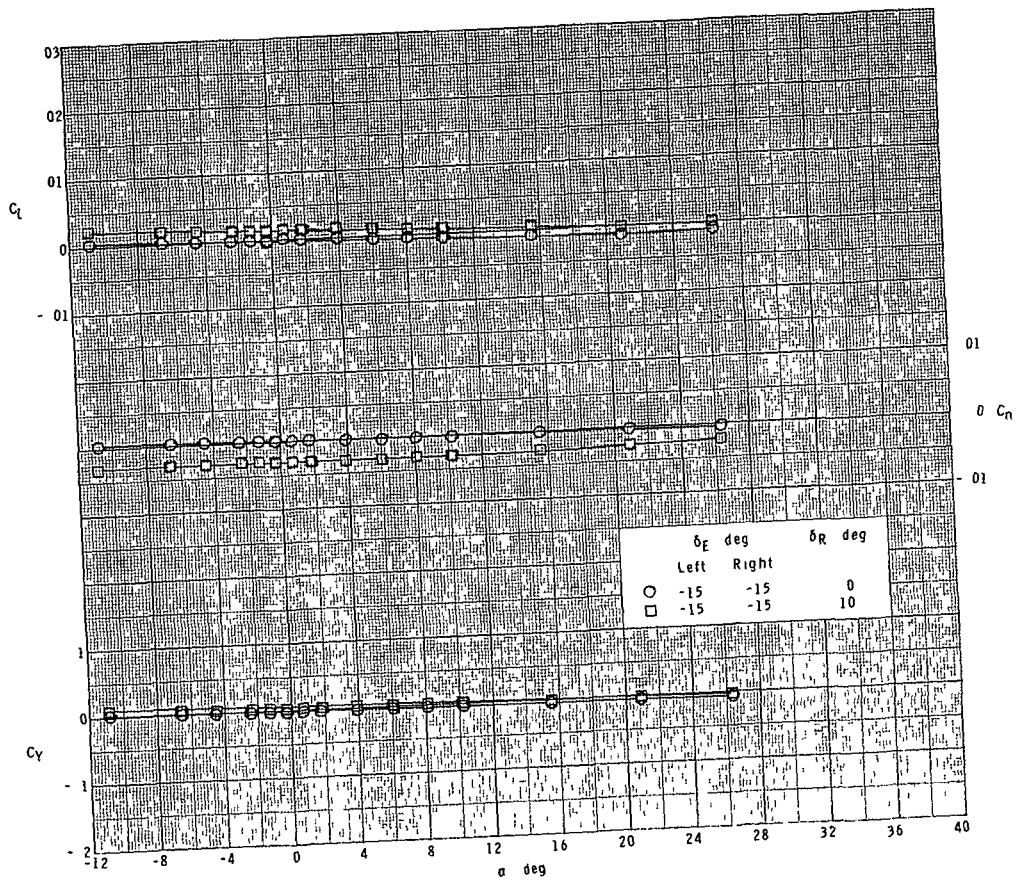

(a) M = 2.30.

Figure 22.- Effect of vertical-tail rudder deflection on lateral characteristics. Orbiter configuration.

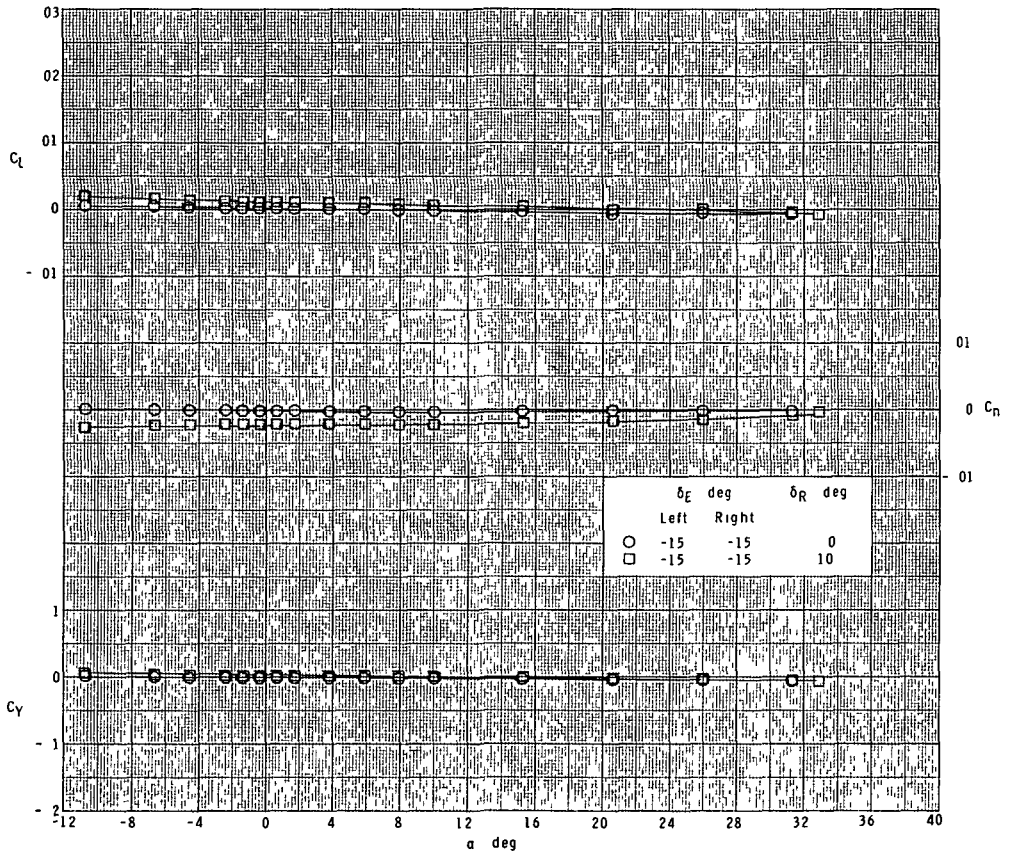

(b) M = 2.96.

Figure 22.- Continued.

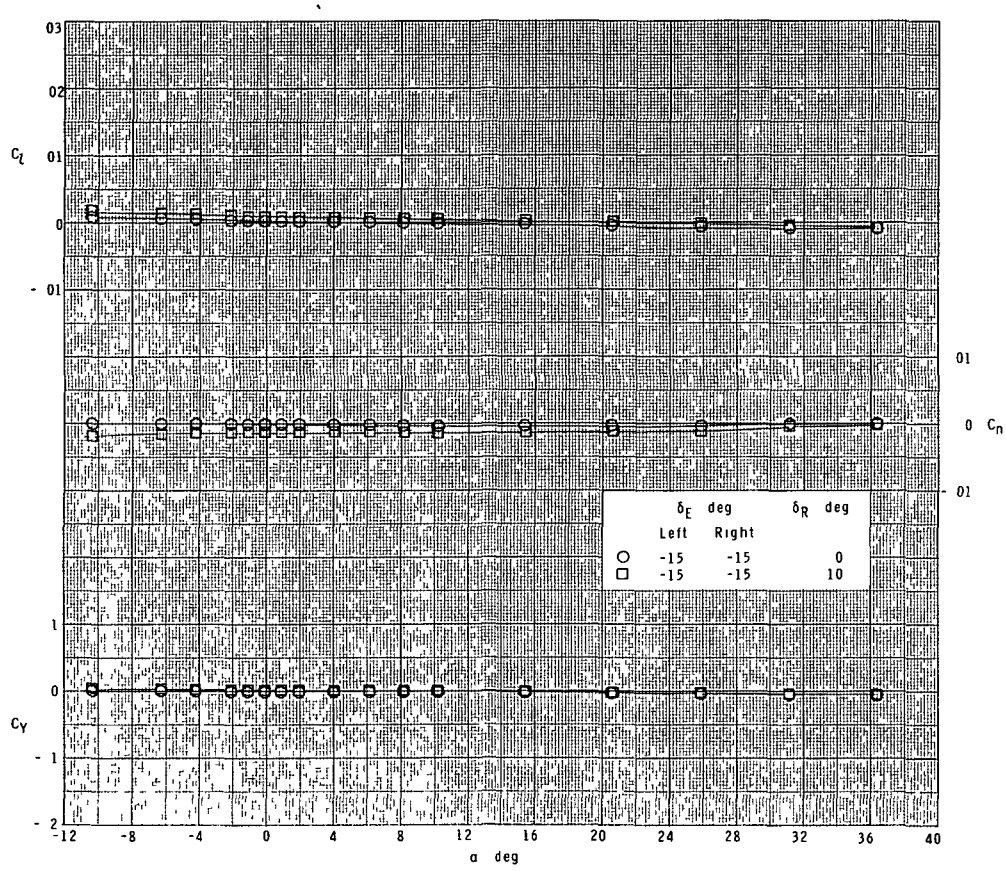

(c) M = 3.95.

Figure 22.- Continued.

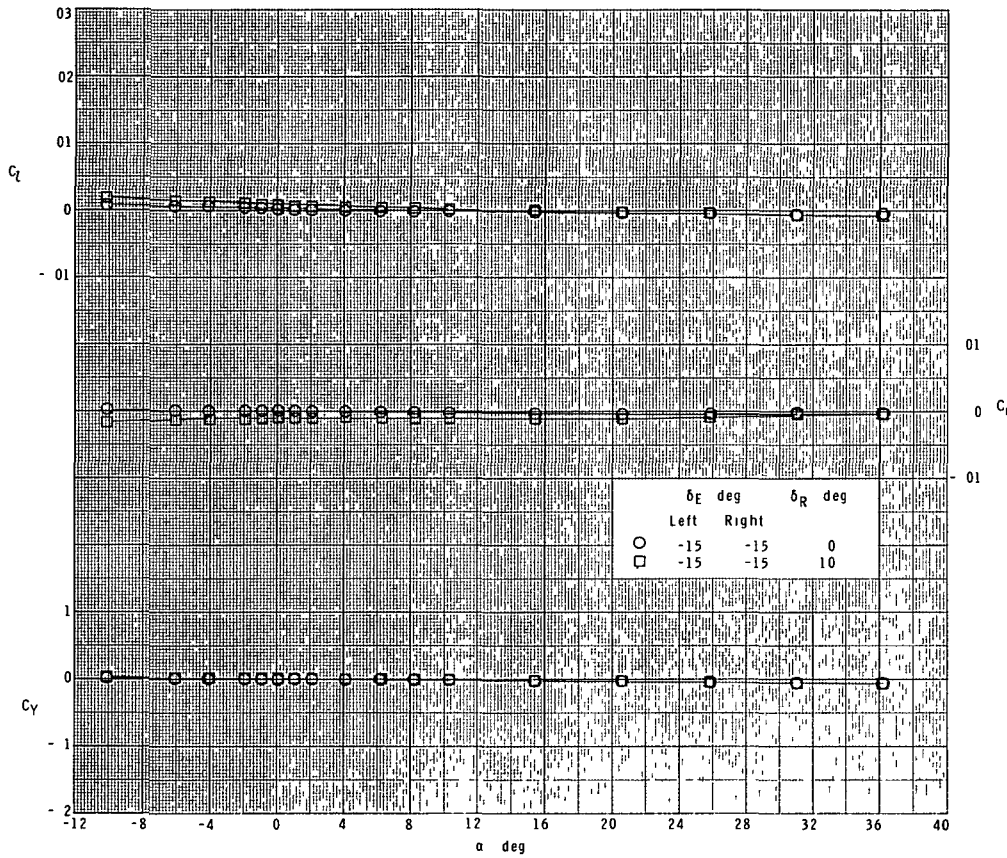

(d) M = 4.60.

Figure 22.- Concluded.

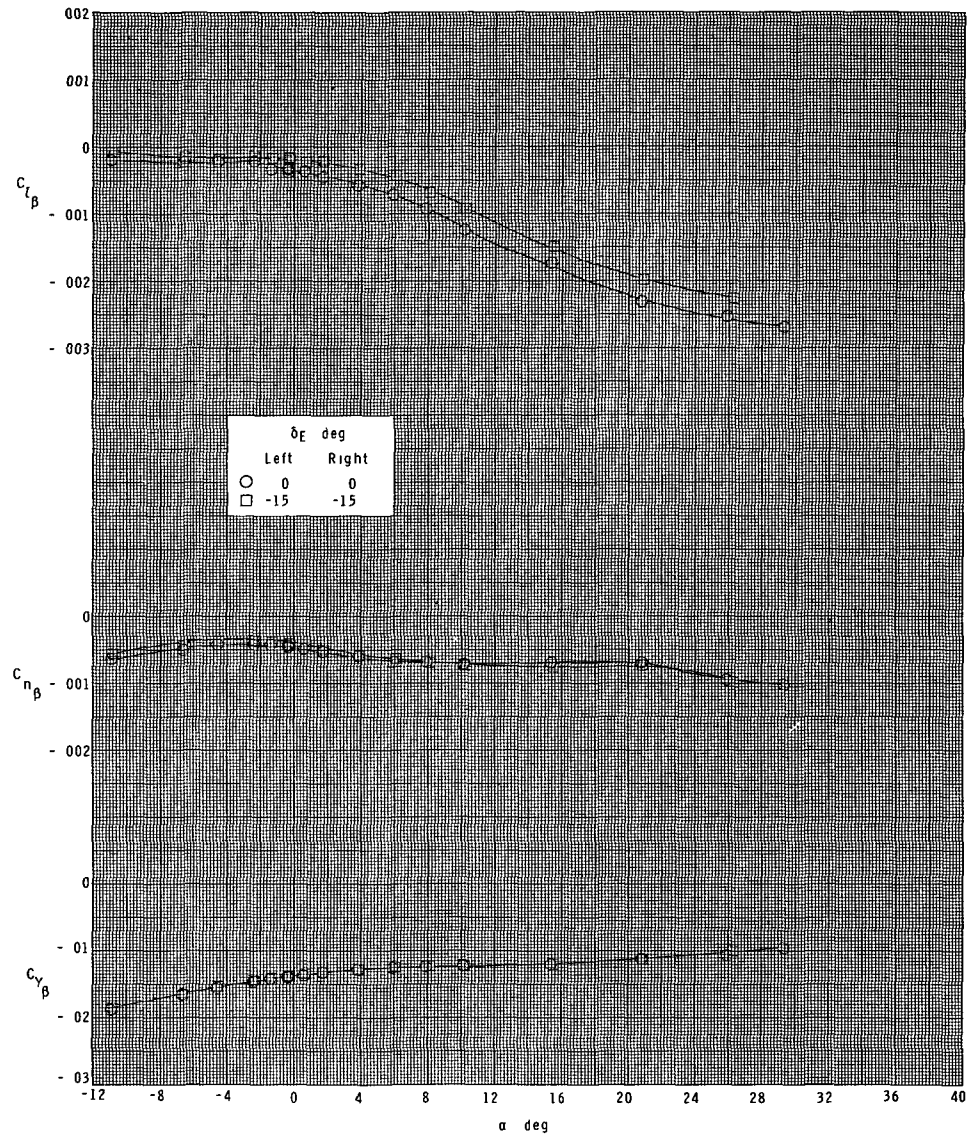

(a) M = 2.30.

Figure 23.- Lateral-stability parameters. Orbiter configuration.

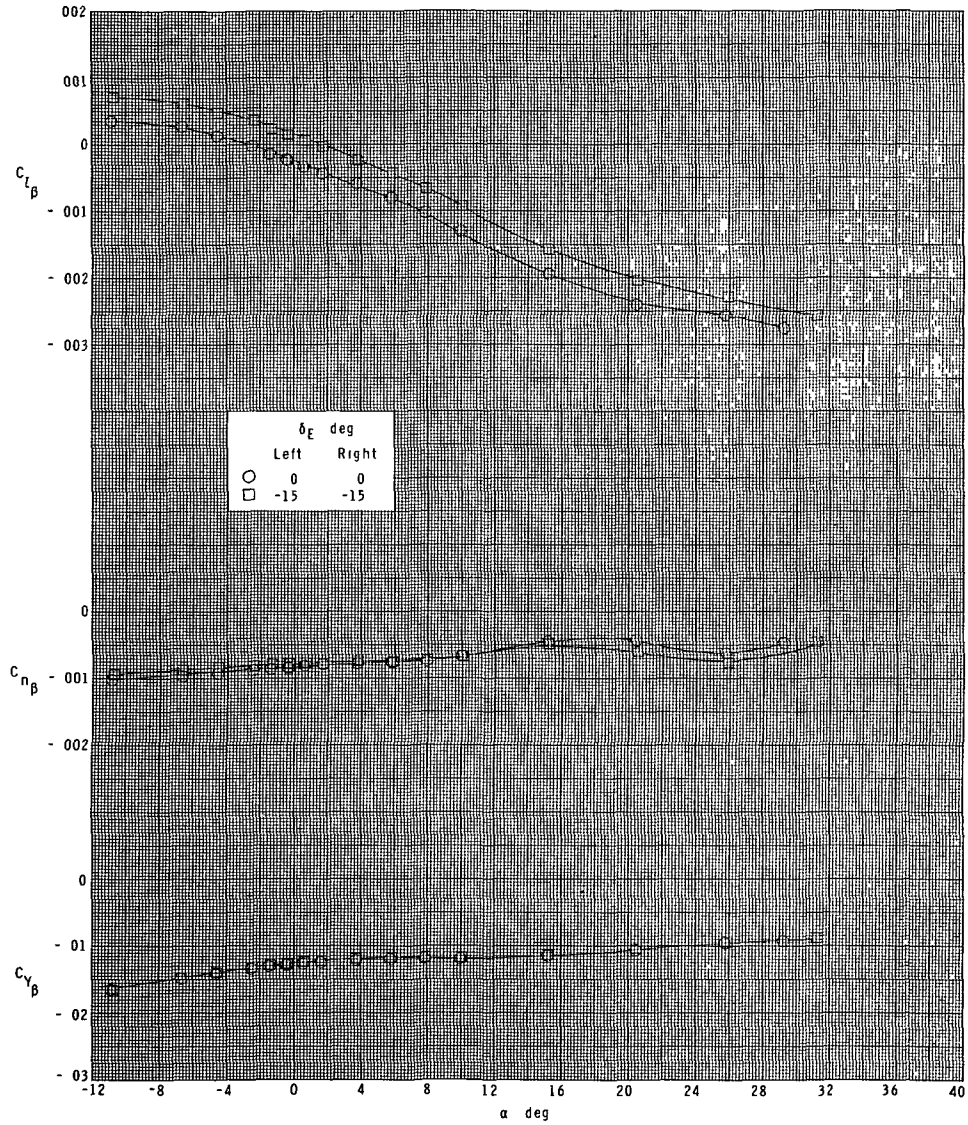

(b) M = 2.96.

Figure 23.- Continued.

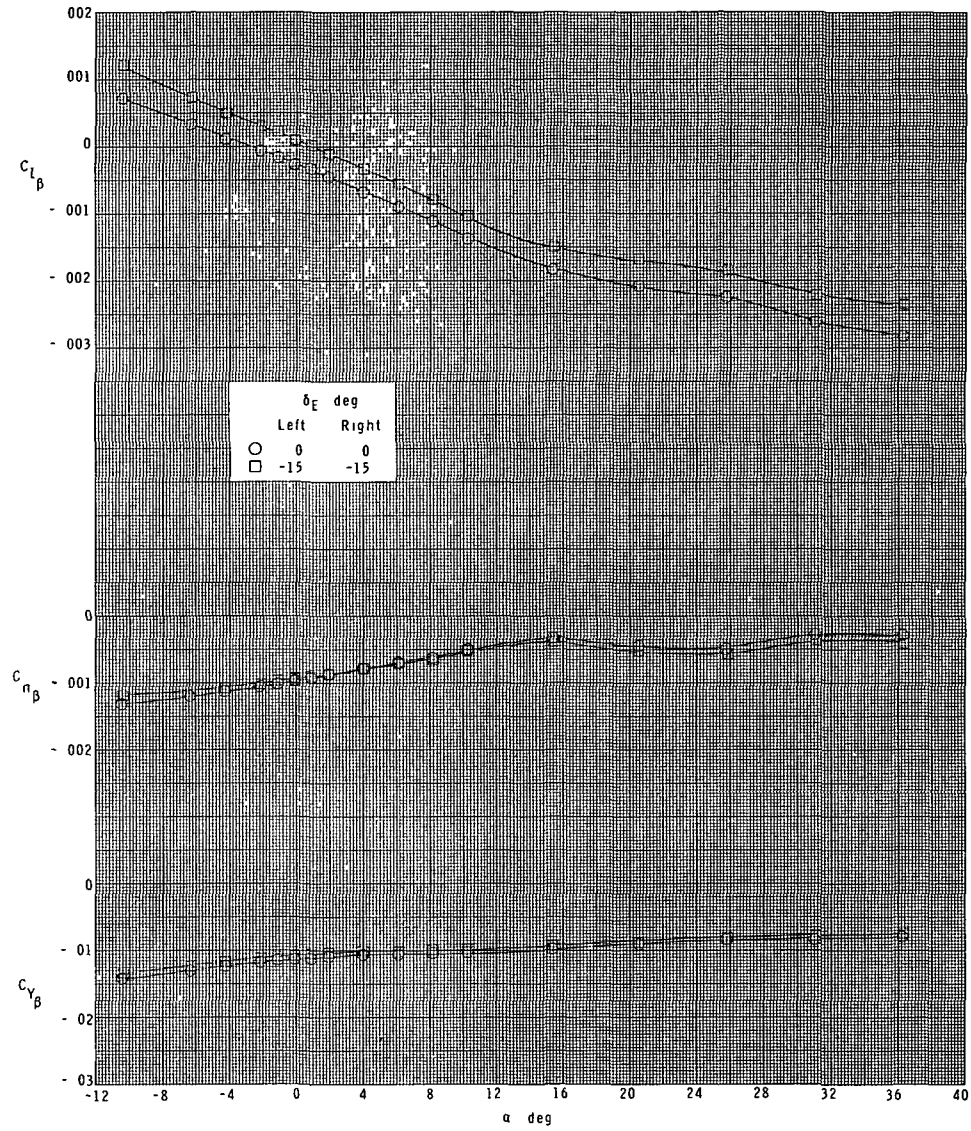

(c) M = 3.95.

Figure 23.- Continued.

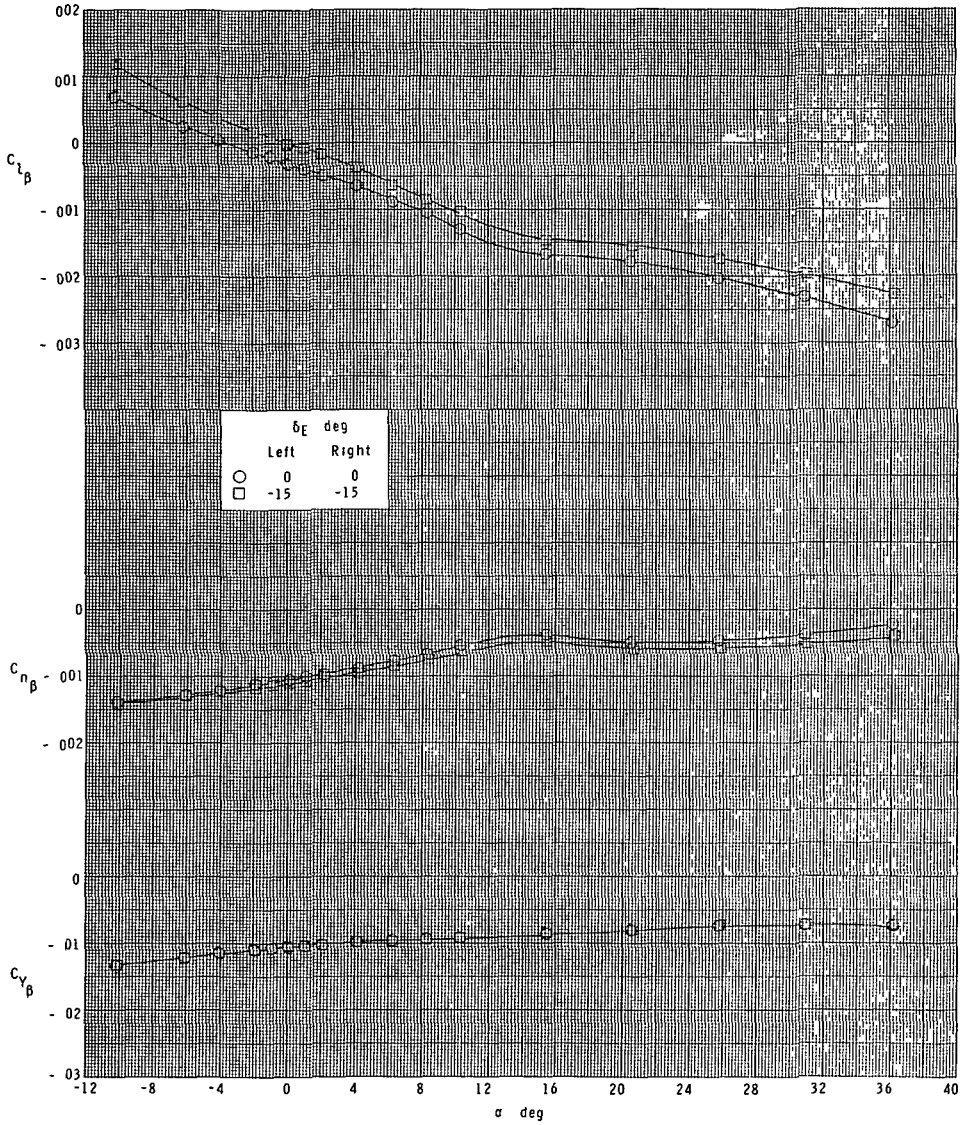

(d) M = 4.60.

Figure 23.- Concluded.

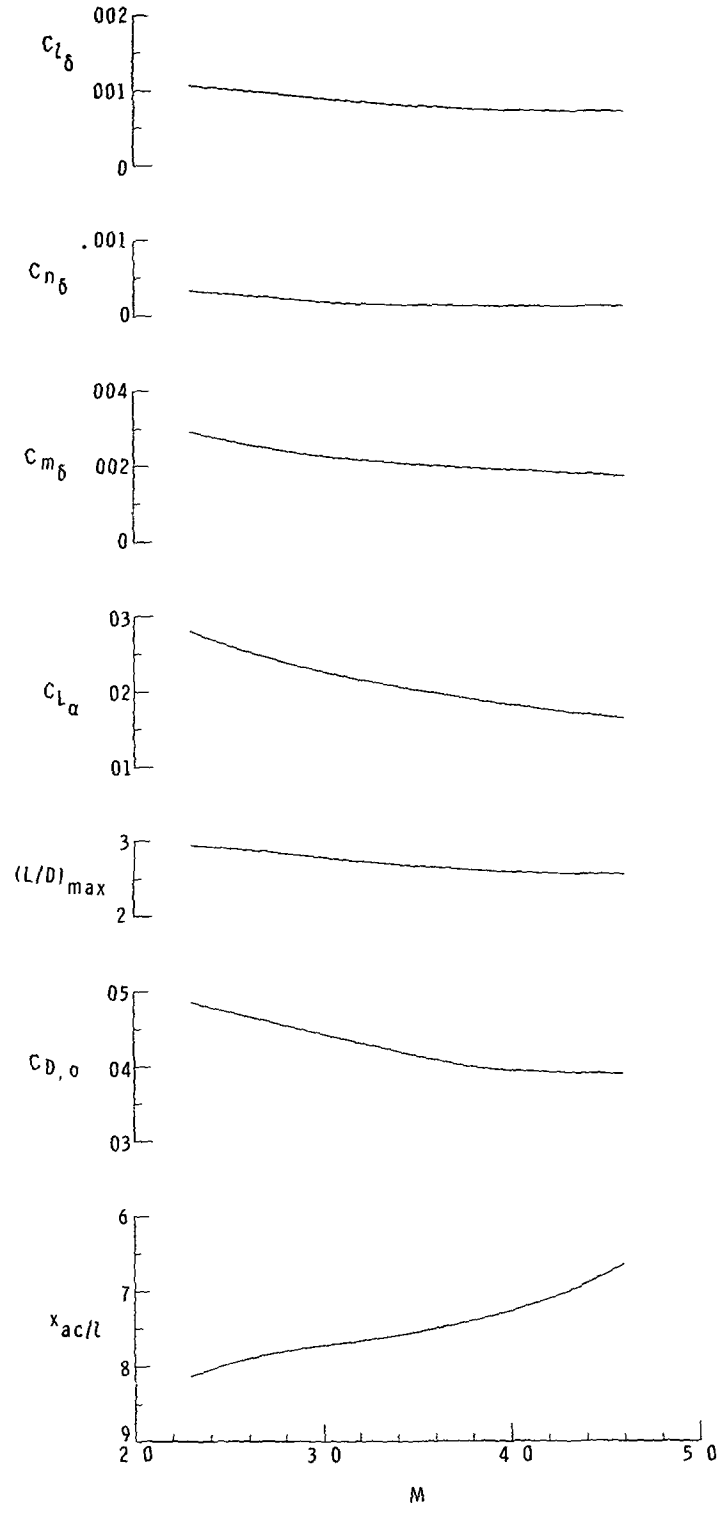

Figure 24.- Summary of characteristics. Orbiter configuration.

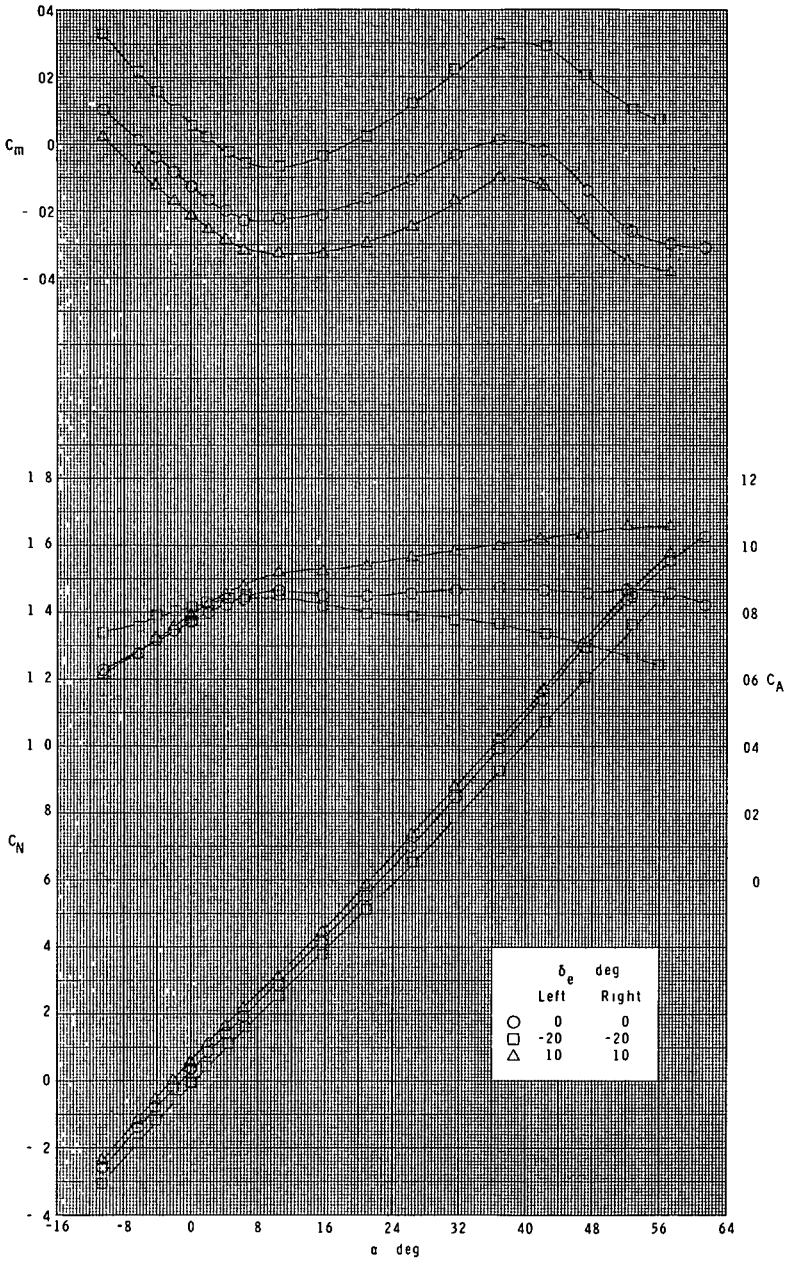

(a) M = 2.30.

Figure 25.- Elevon pitch-control effectiveness. Booster configuration.

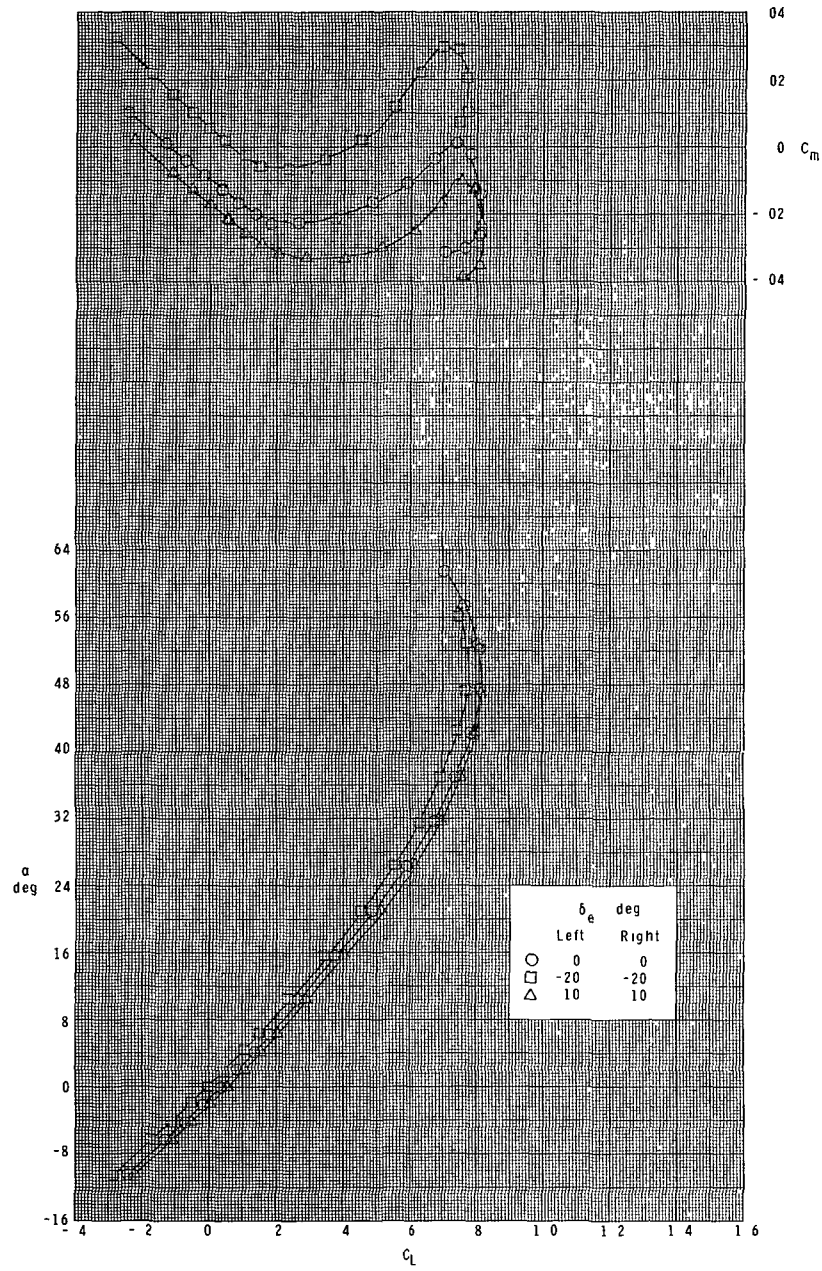

(a) Continued.

Figure 25.- Continued.

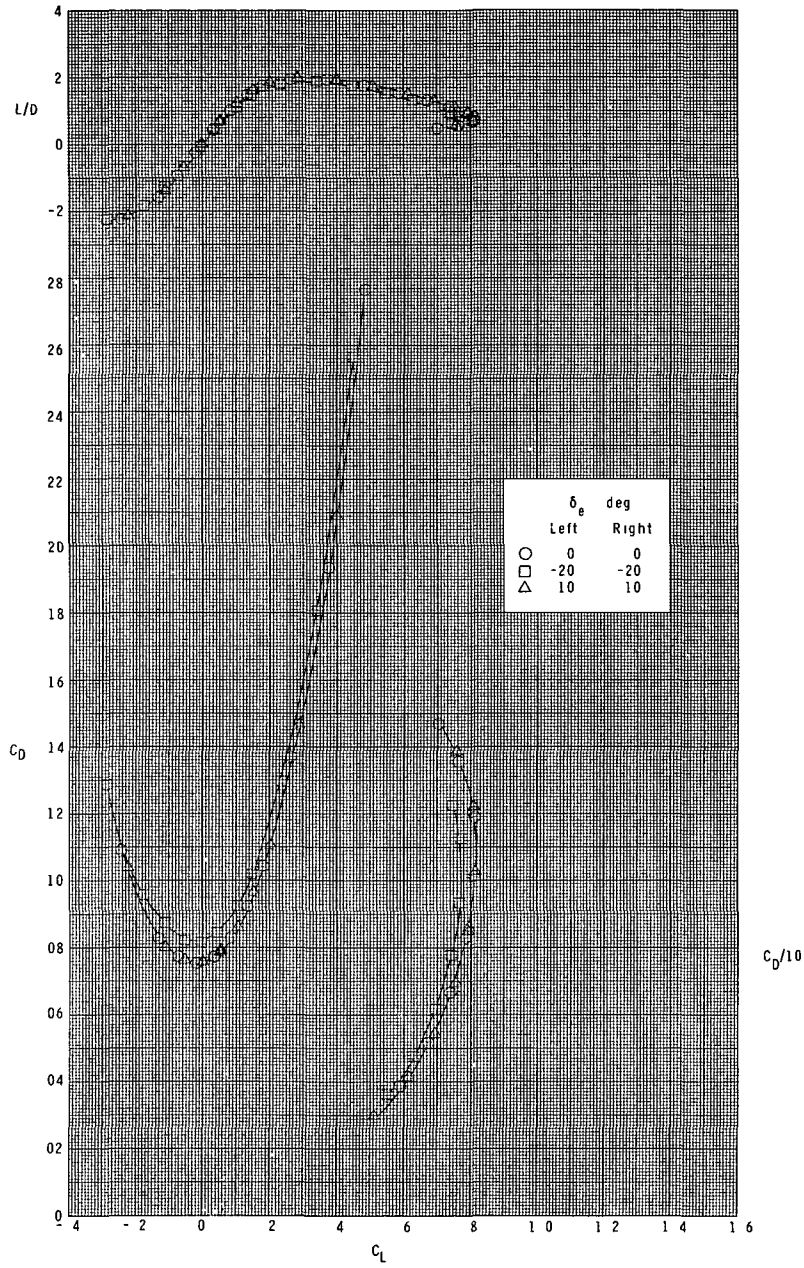

(a) Concluded.

Figure 25.- Continued.

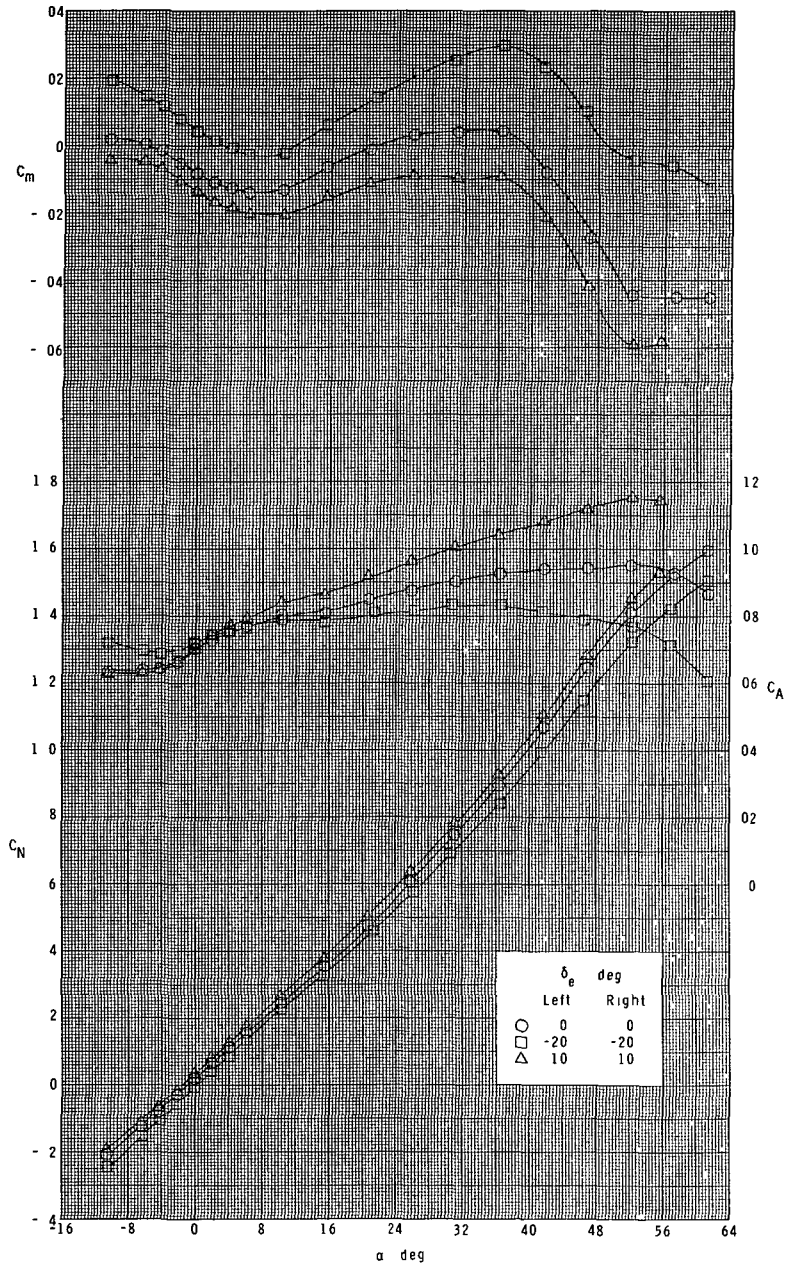

(b) M = 2.96.

Figure 25.- Continued.

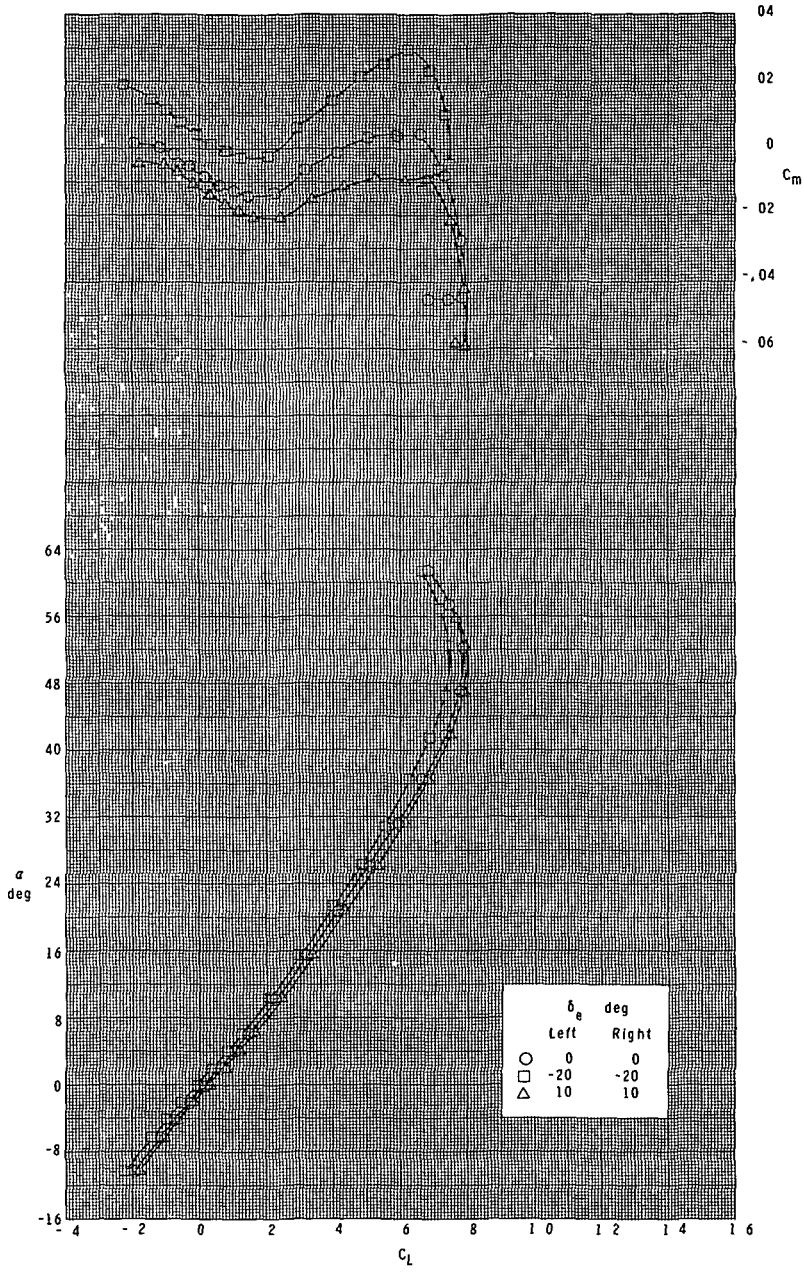

(b) Continued.

Figure 25.- Continued.

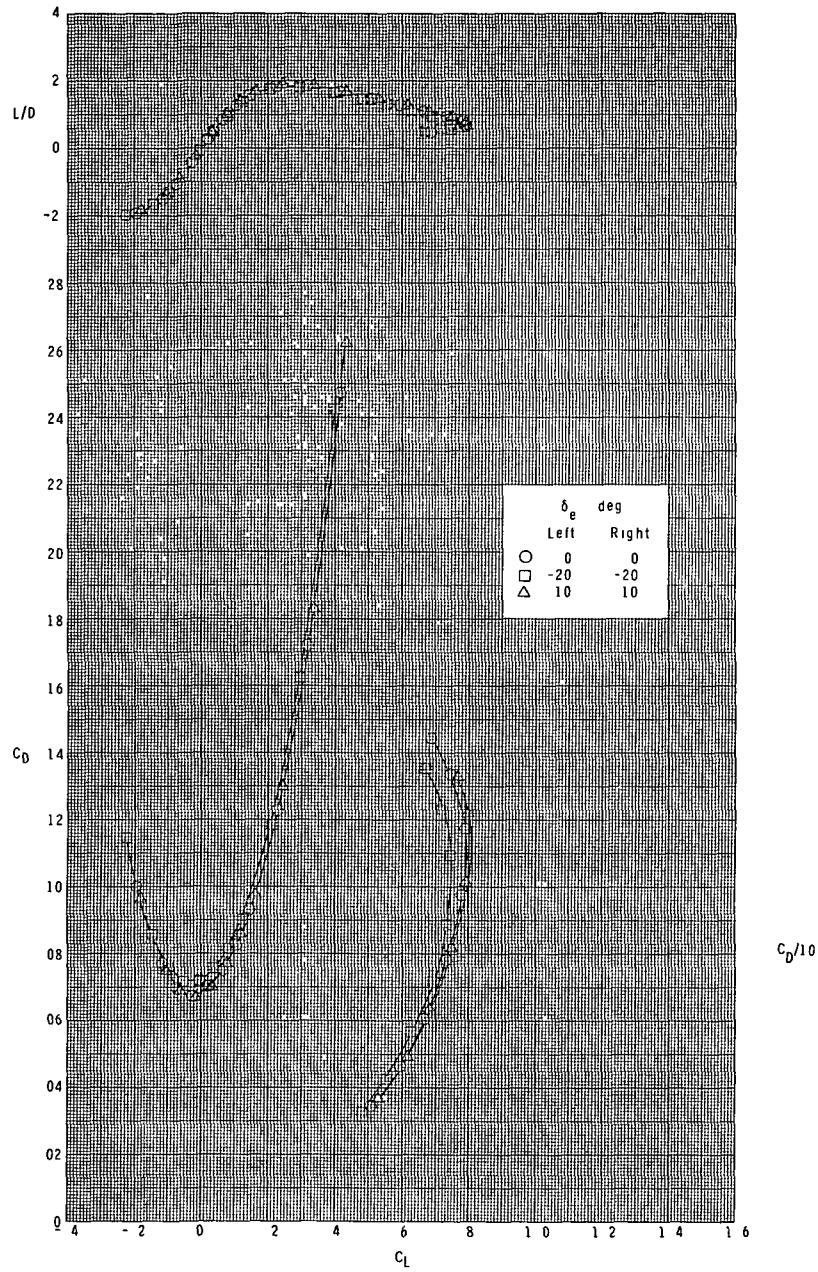

(b) Concluded.

Figure 25.- Continued.

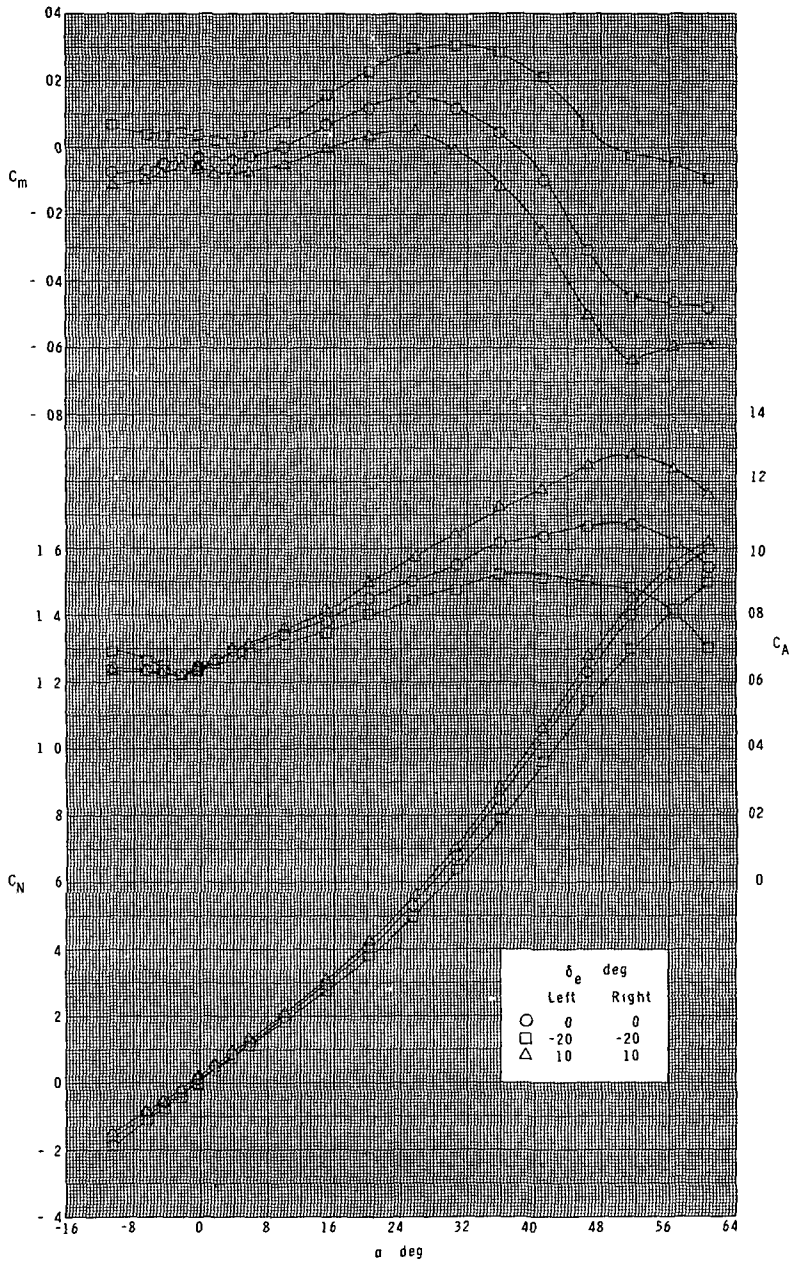

(c) M = 3.95.

Figure 25.- Continued.

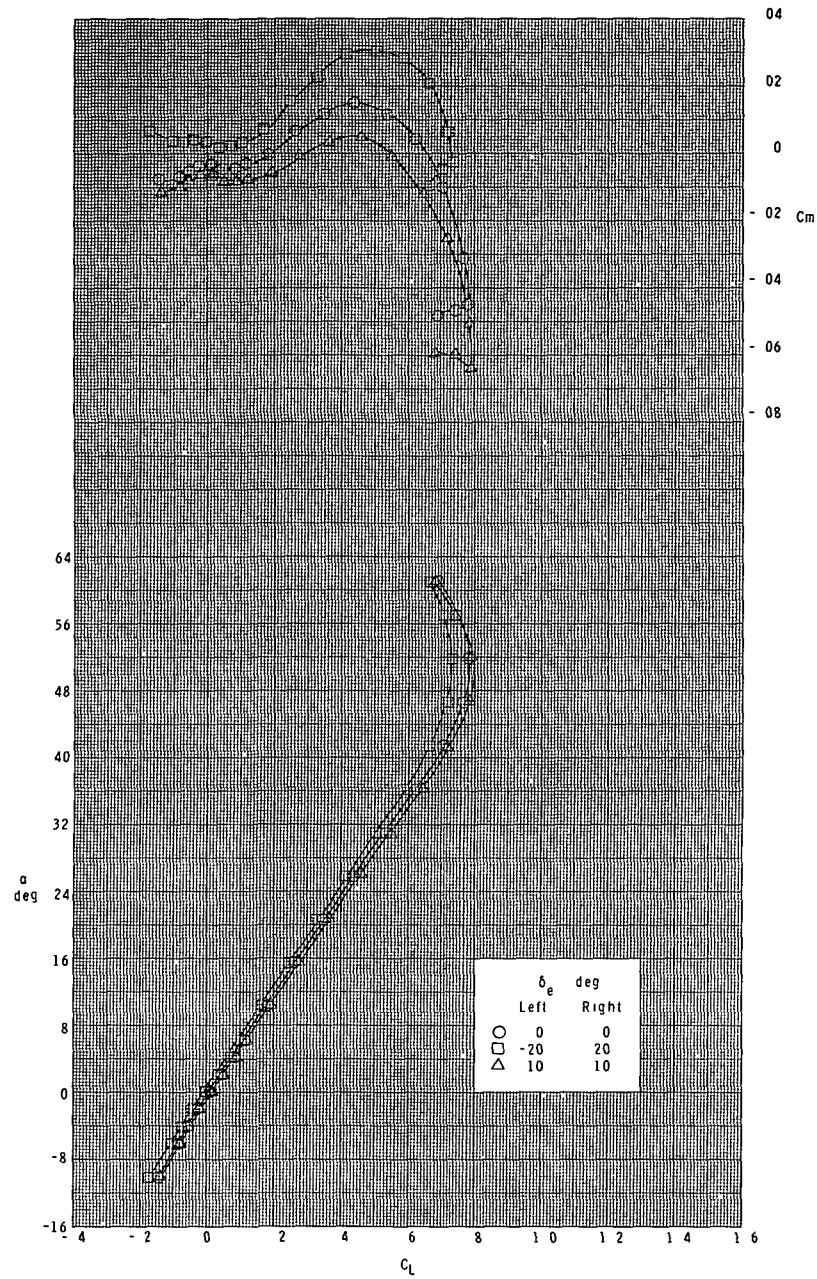

(c) Continued.

Figure 25.- Continued.

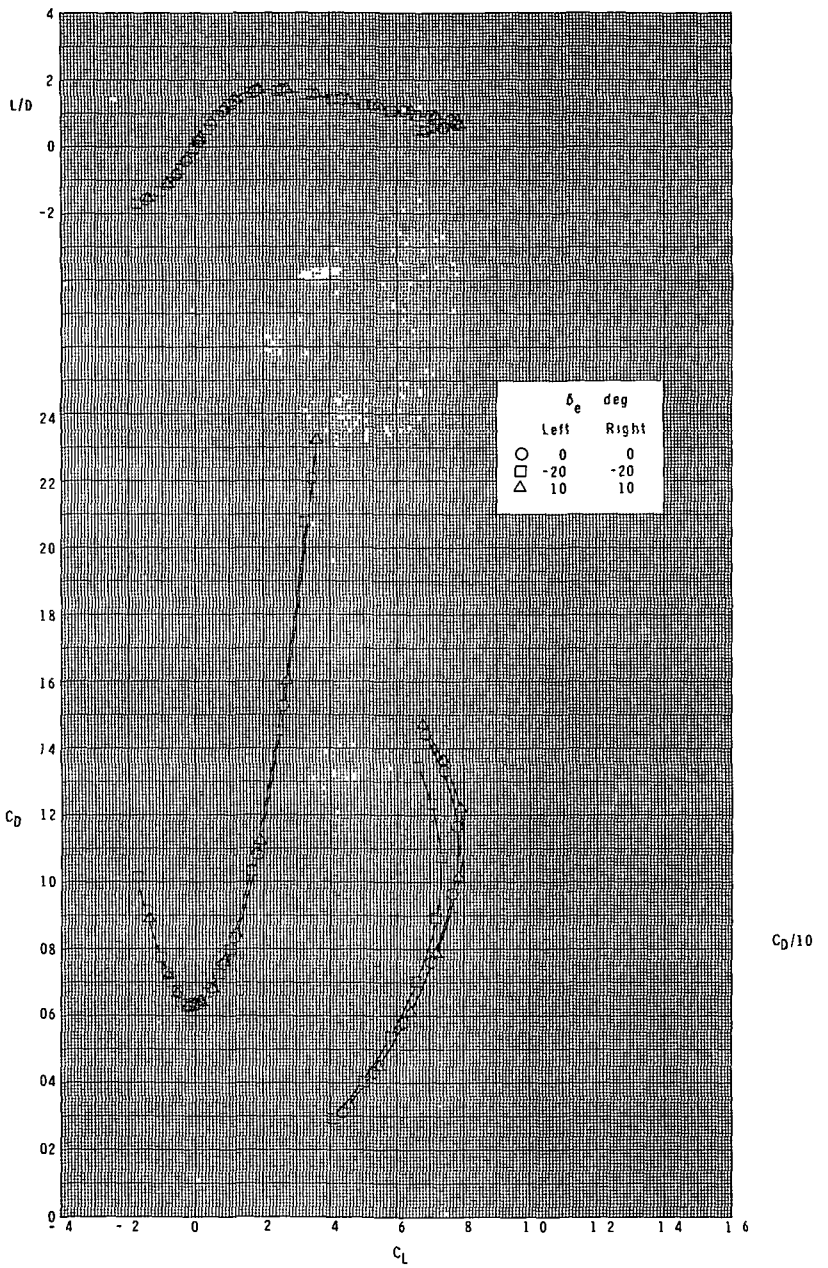

(c) Concluded.

Figure 25.- Continued.

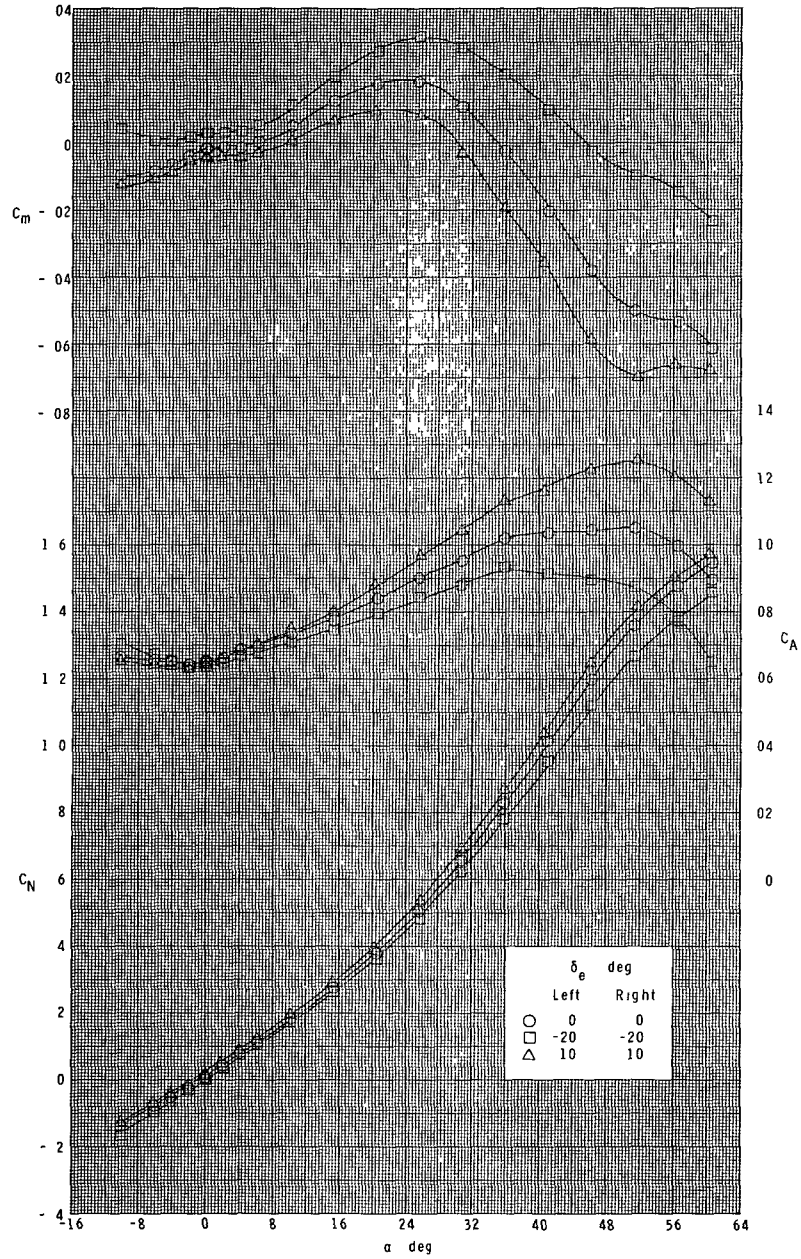

(d) M = 4.60.

Figure 25.- Continued.

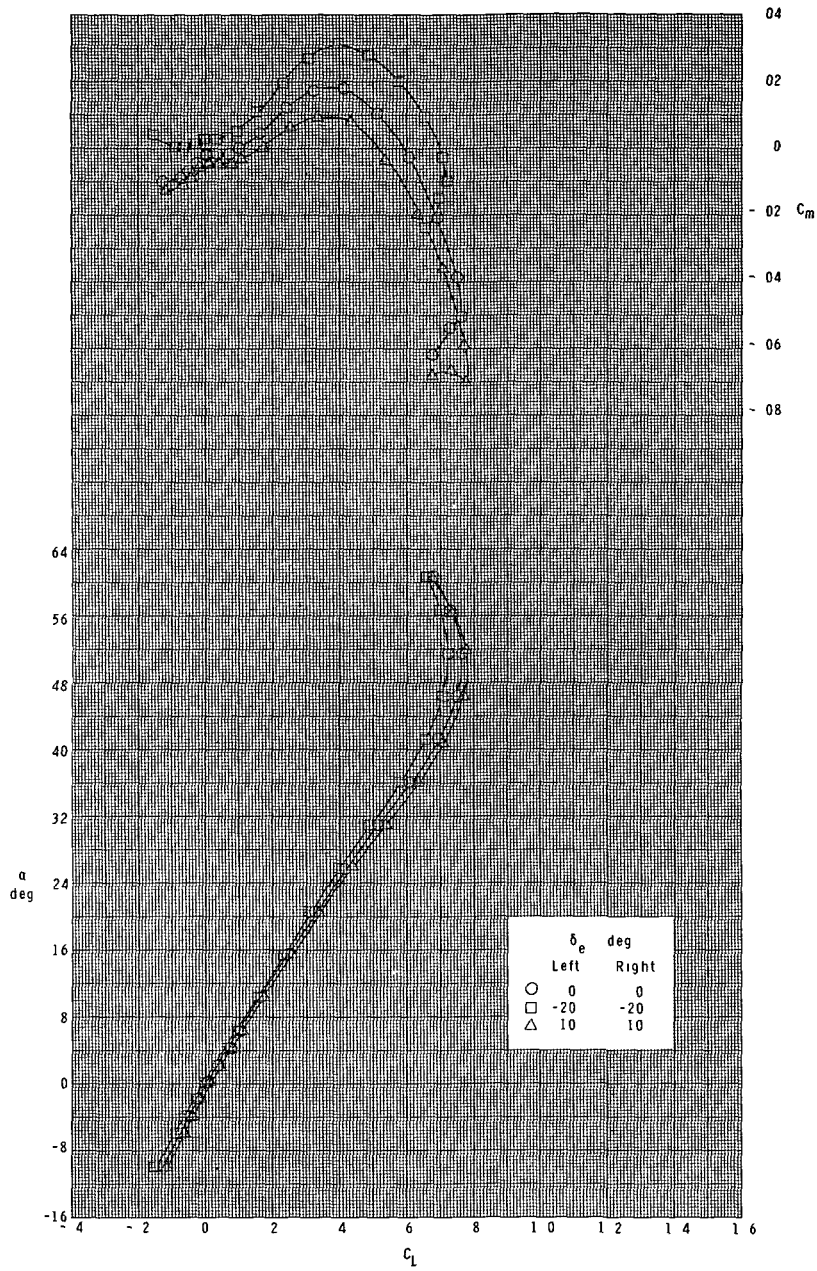

(d) Continued.

Figure 25.- Continued.

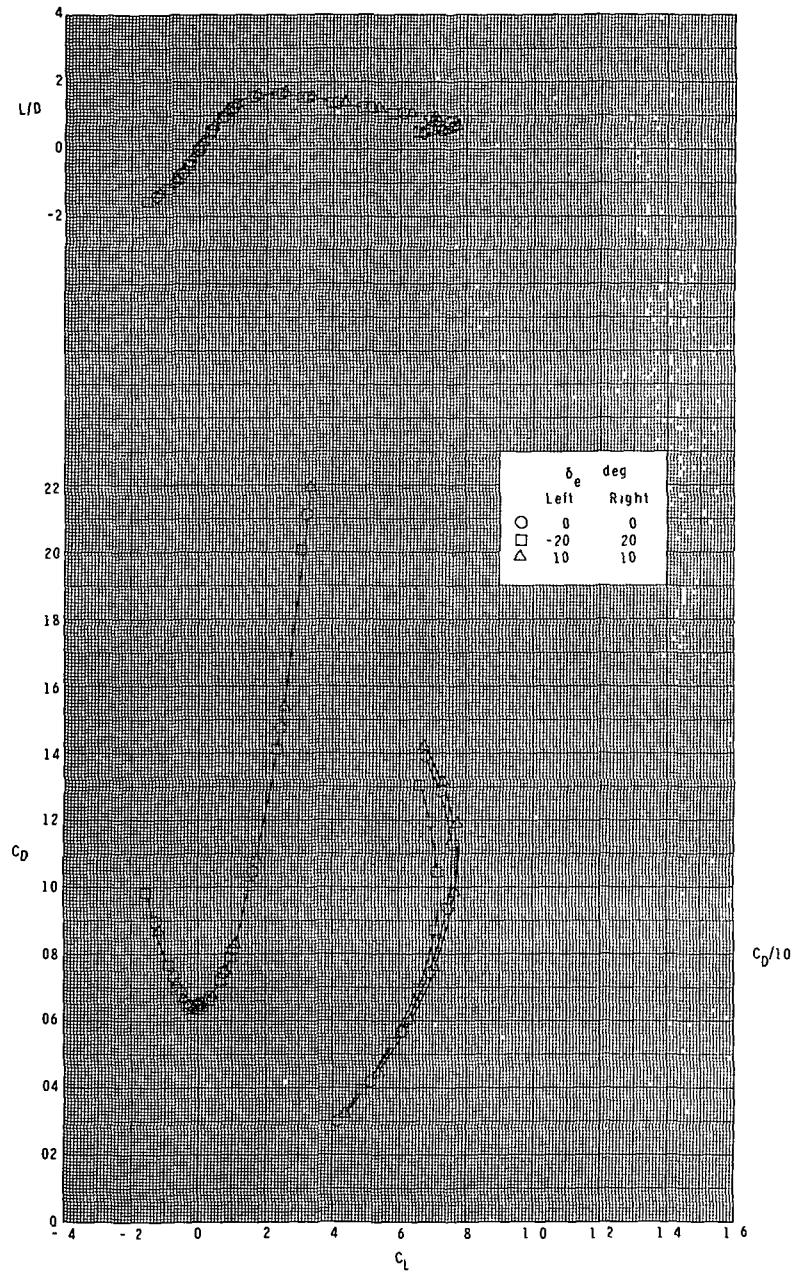

(d) Concluded.

Figure 25.- Concluded.

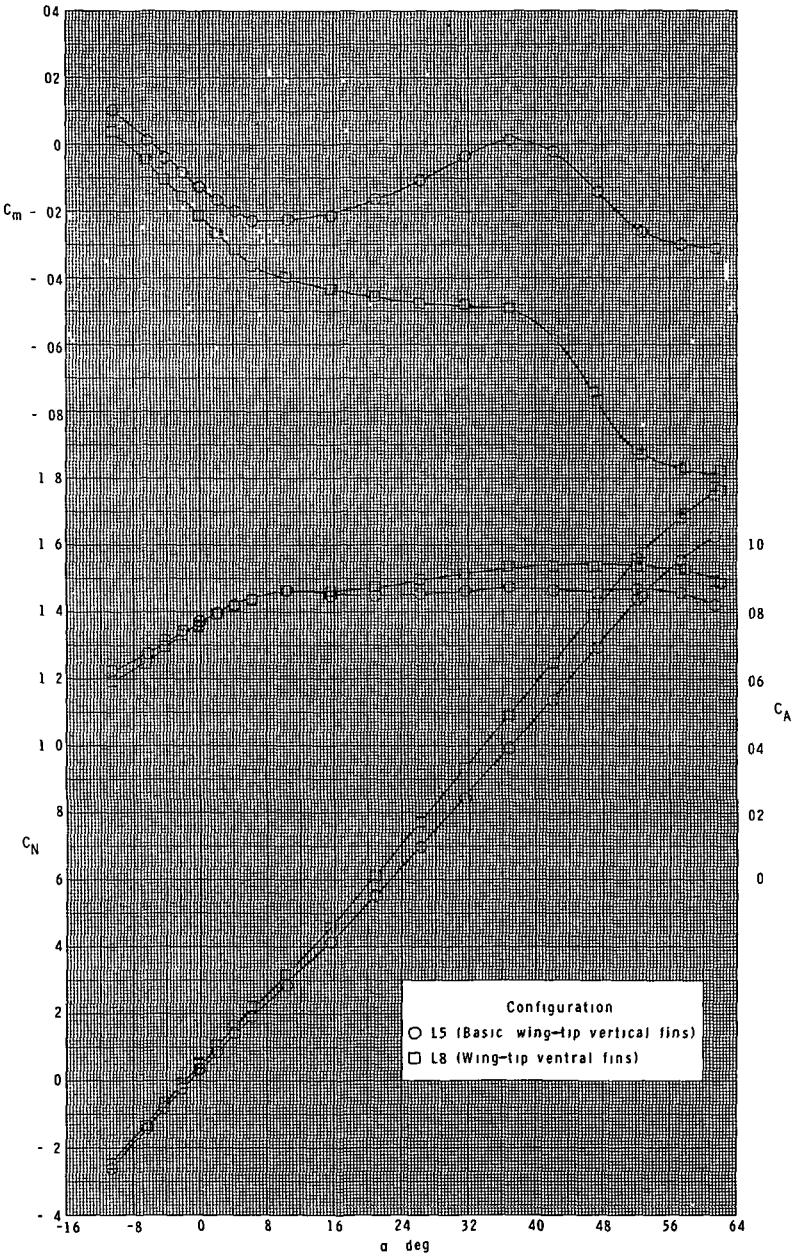

(a) M = 2.30.

Figure 26.- Effect of vertical location of wing-tip fins on longitudinal characteristics. Booster configuration.

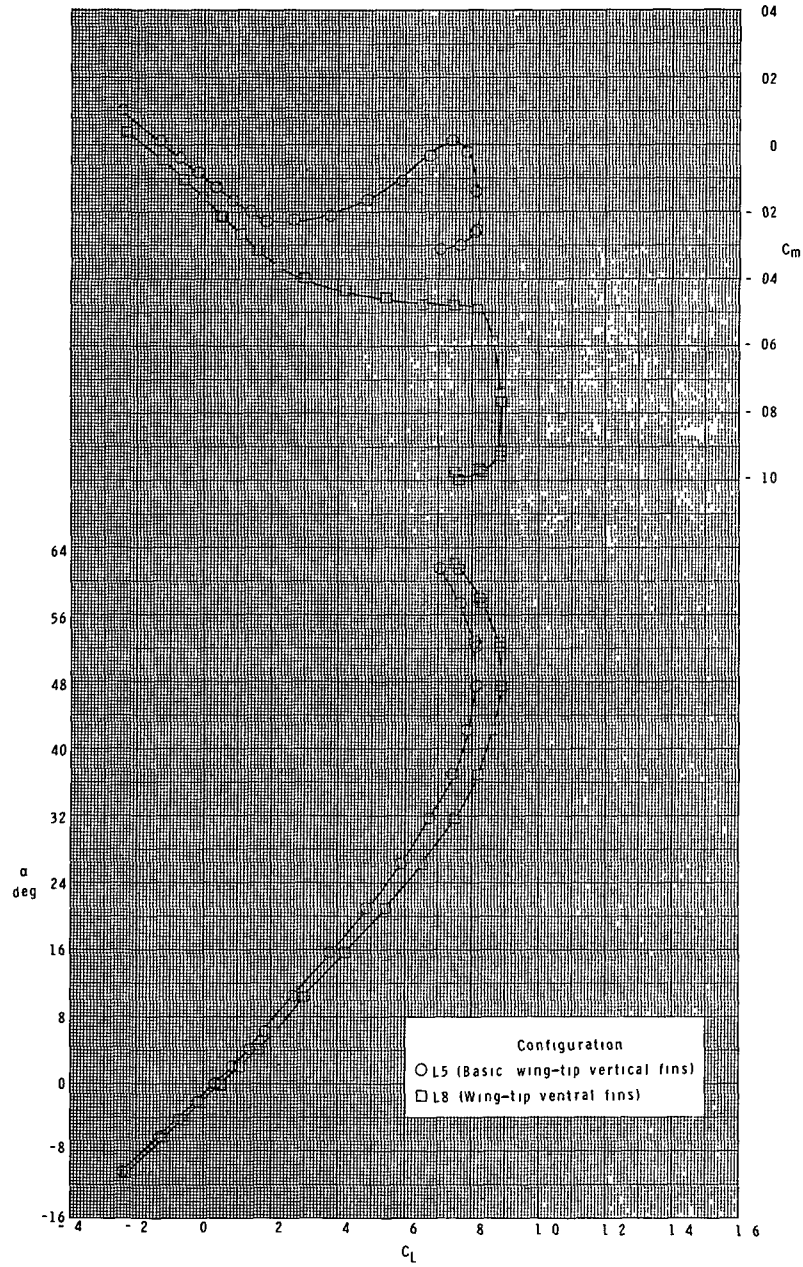

(a) Continued.

Figure 26.- Continued.

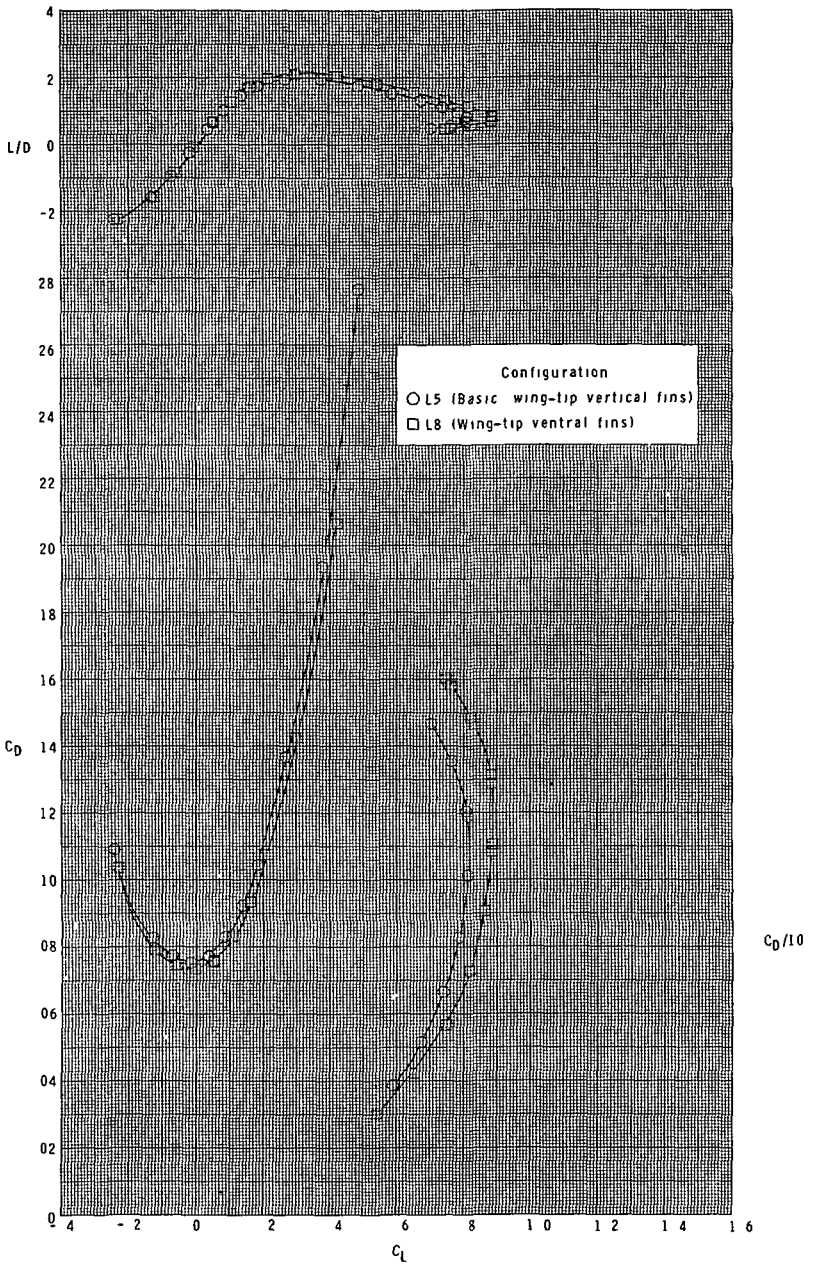

(a) Concluded.

Figure 26.- Continued.

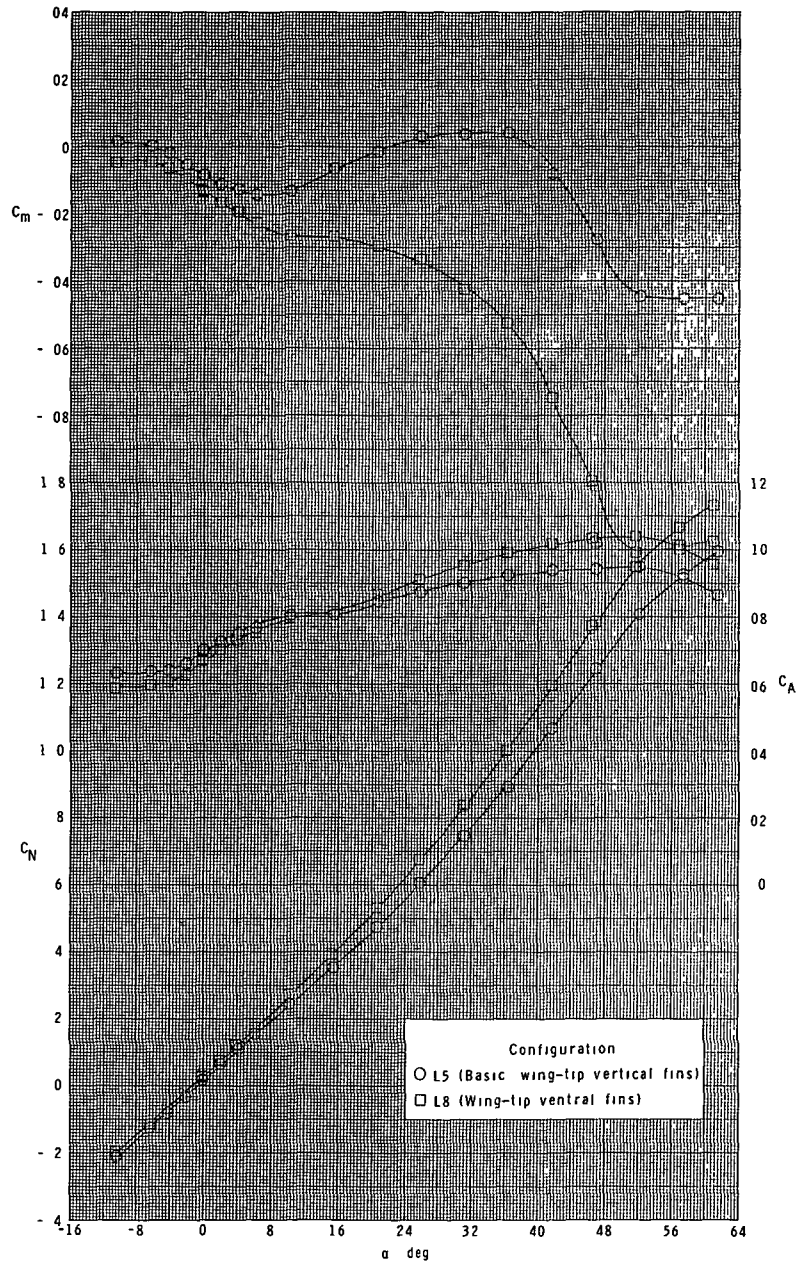

(b) M = 2.96.

Figure 26.- Continued.

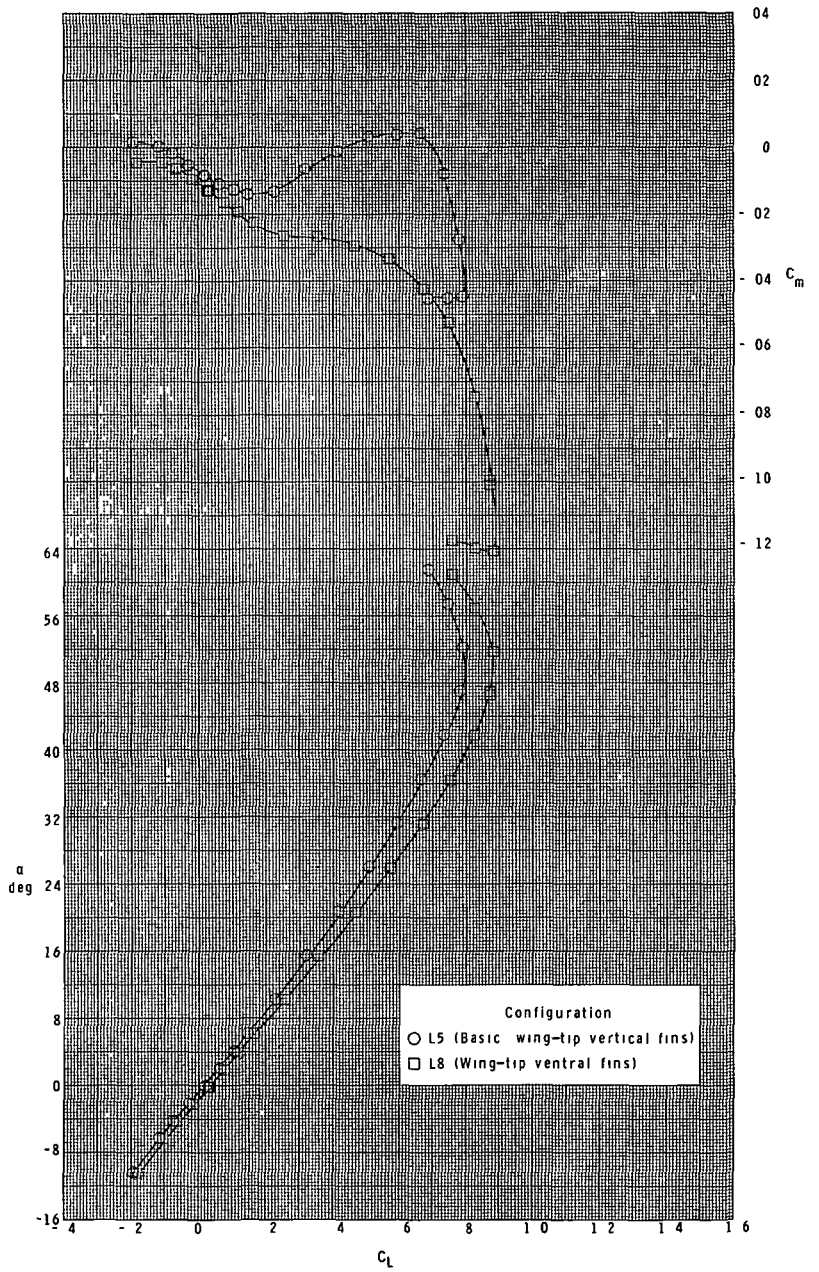

(b) Continued.

Figure 26.- Continued.

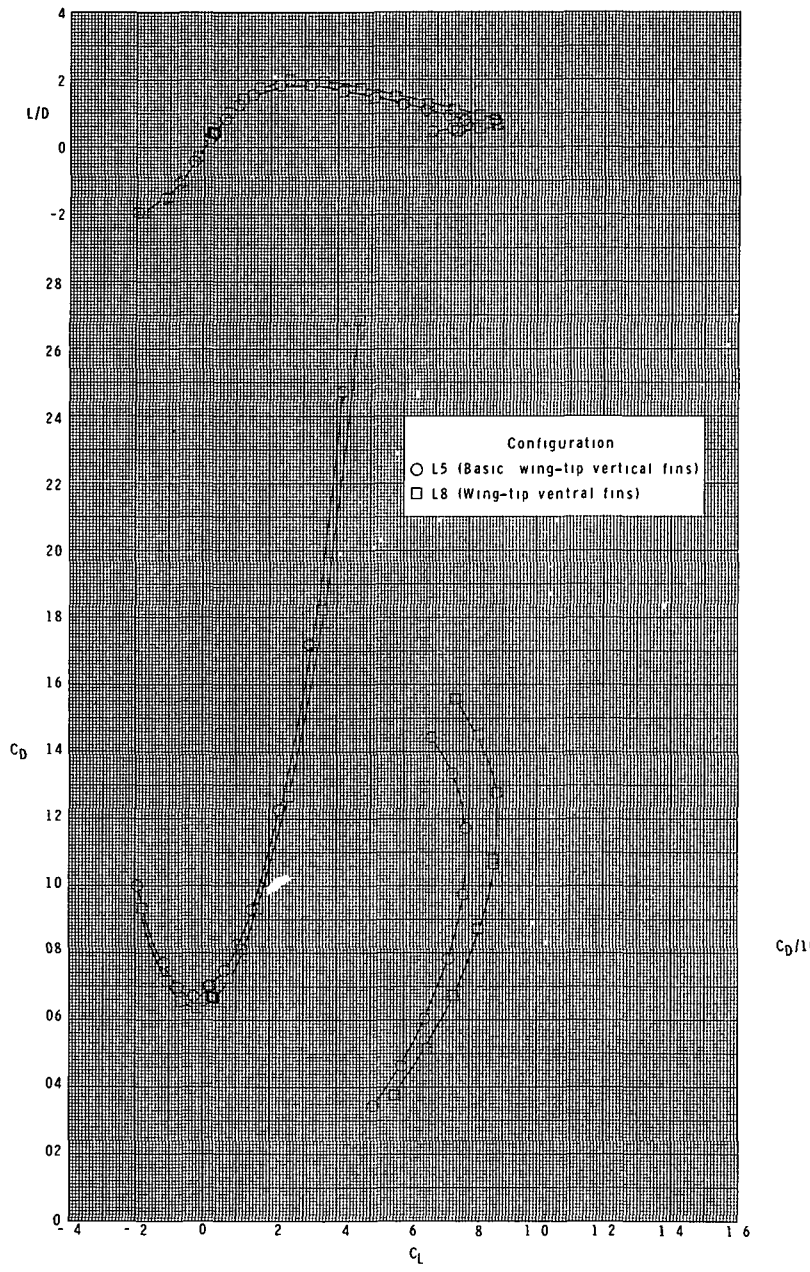

(b) Concluded.

Figure 26.- Continued.

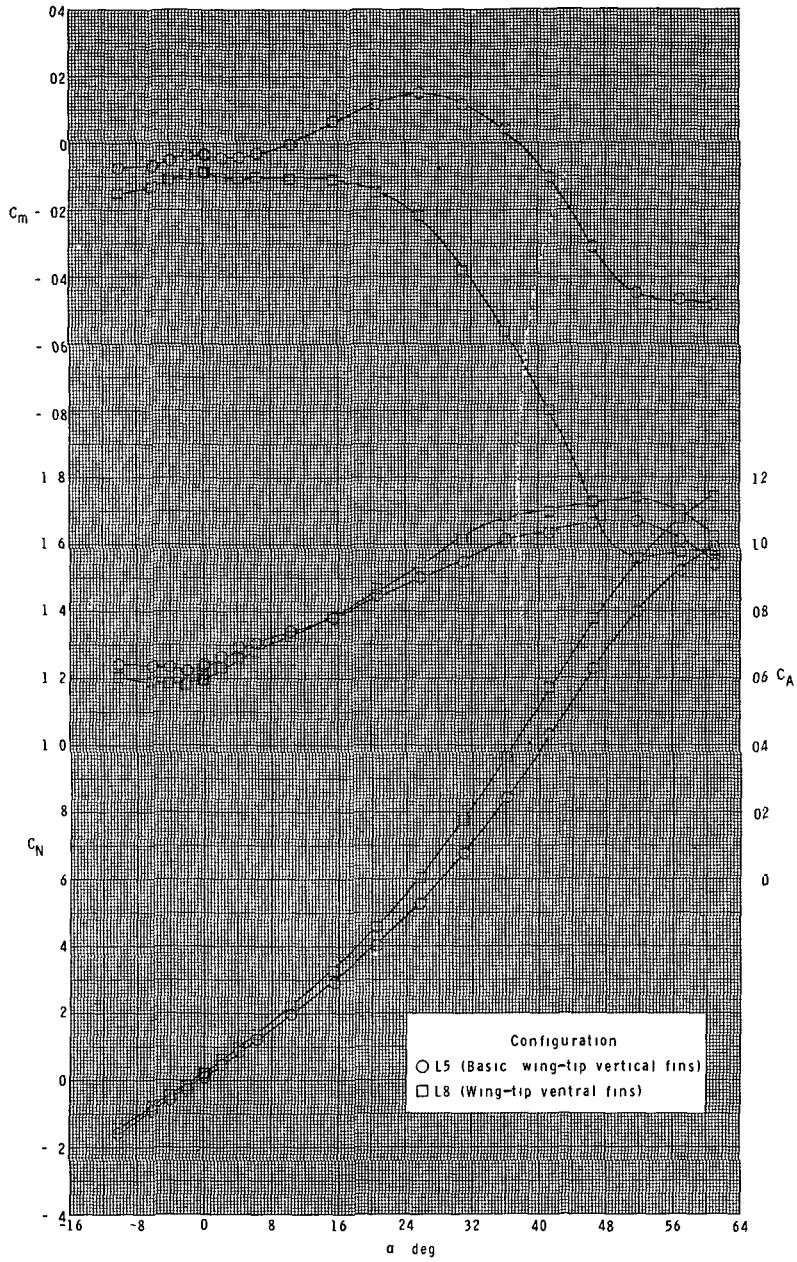

(c) M = 3.95.

Figure 26.- Continued.

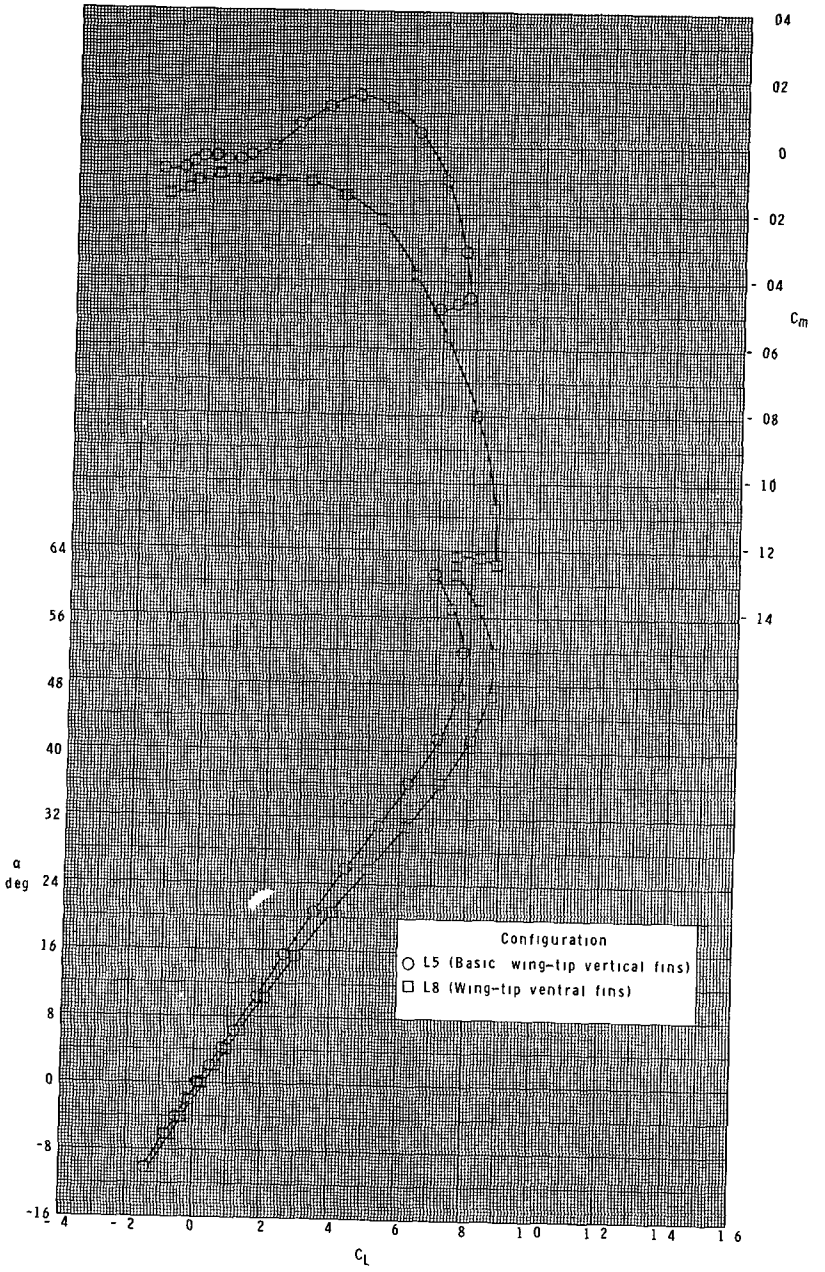

(c) Continued.

Figure 26.- Continued.

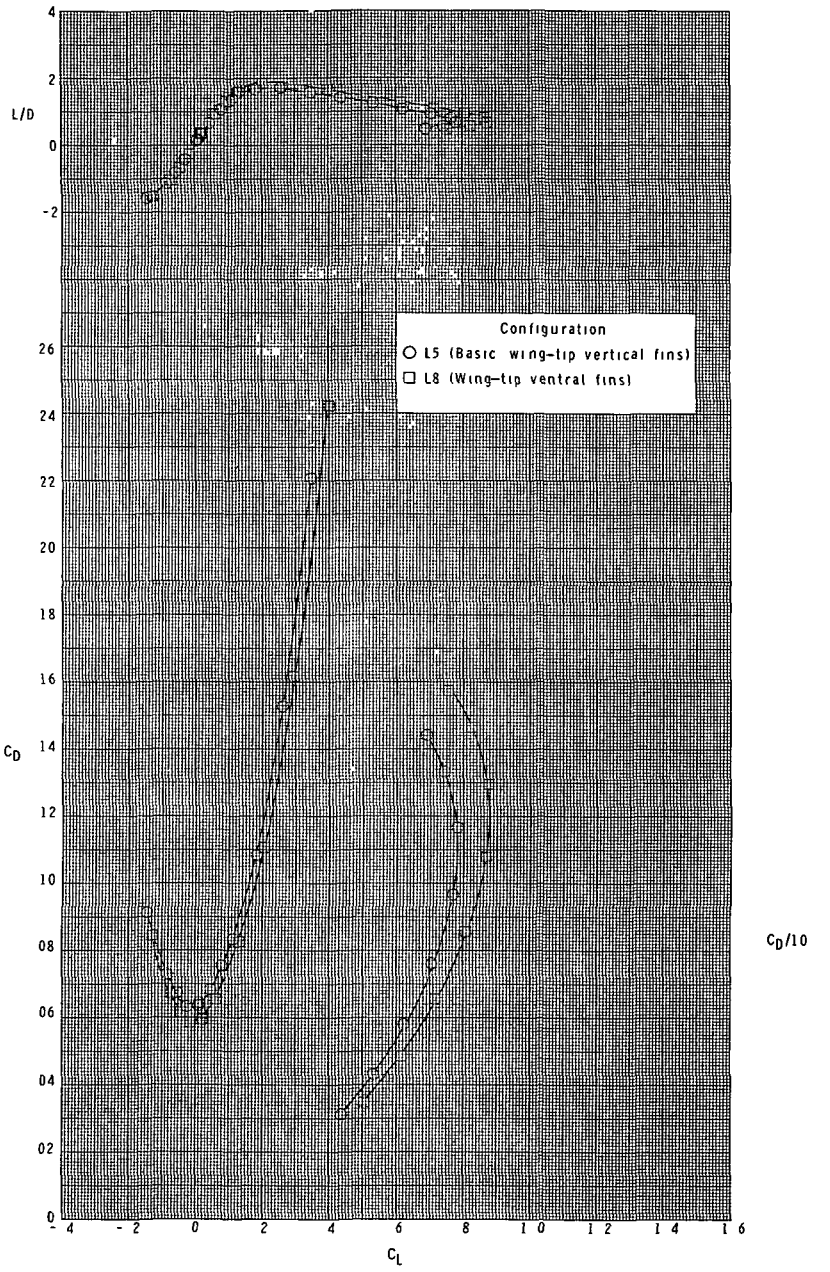

(c) Concluded.

Figure 26.- Continued.

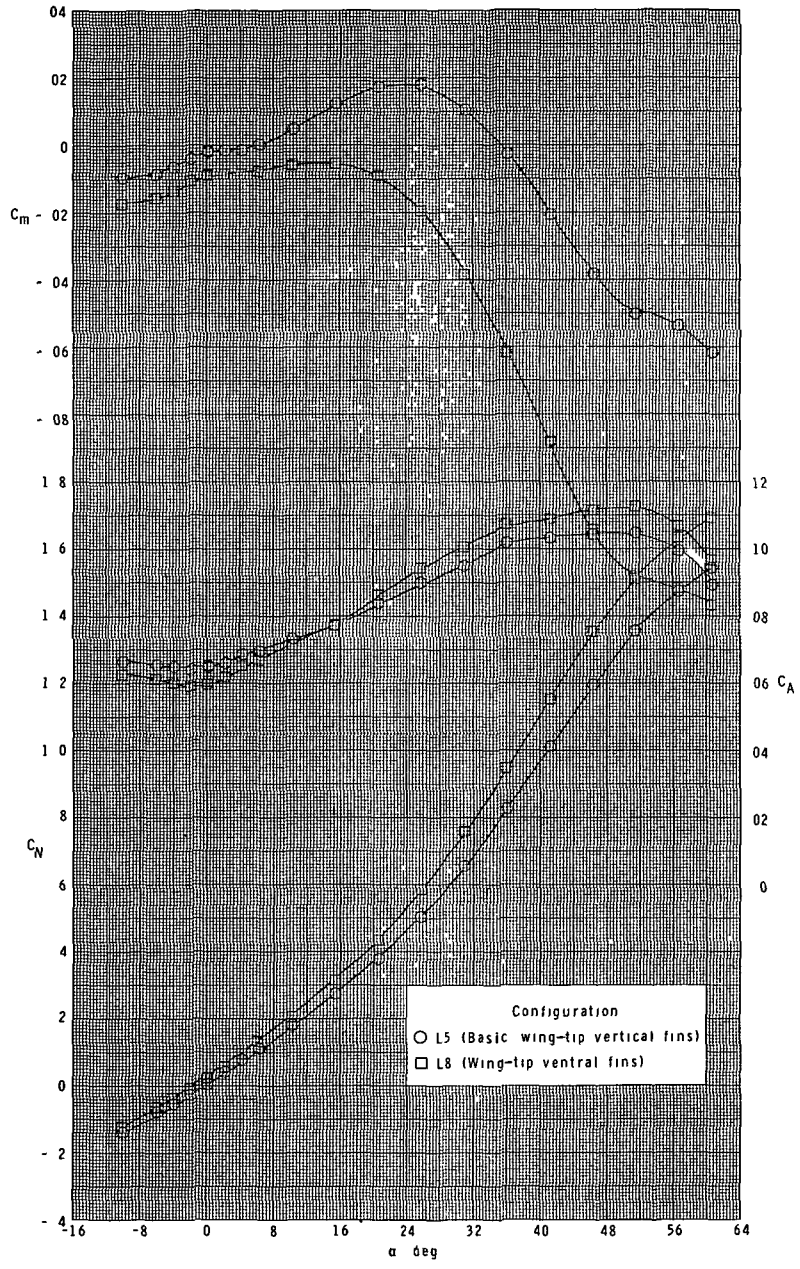

(d) M = 4.60.

Figure 26.- Continued.

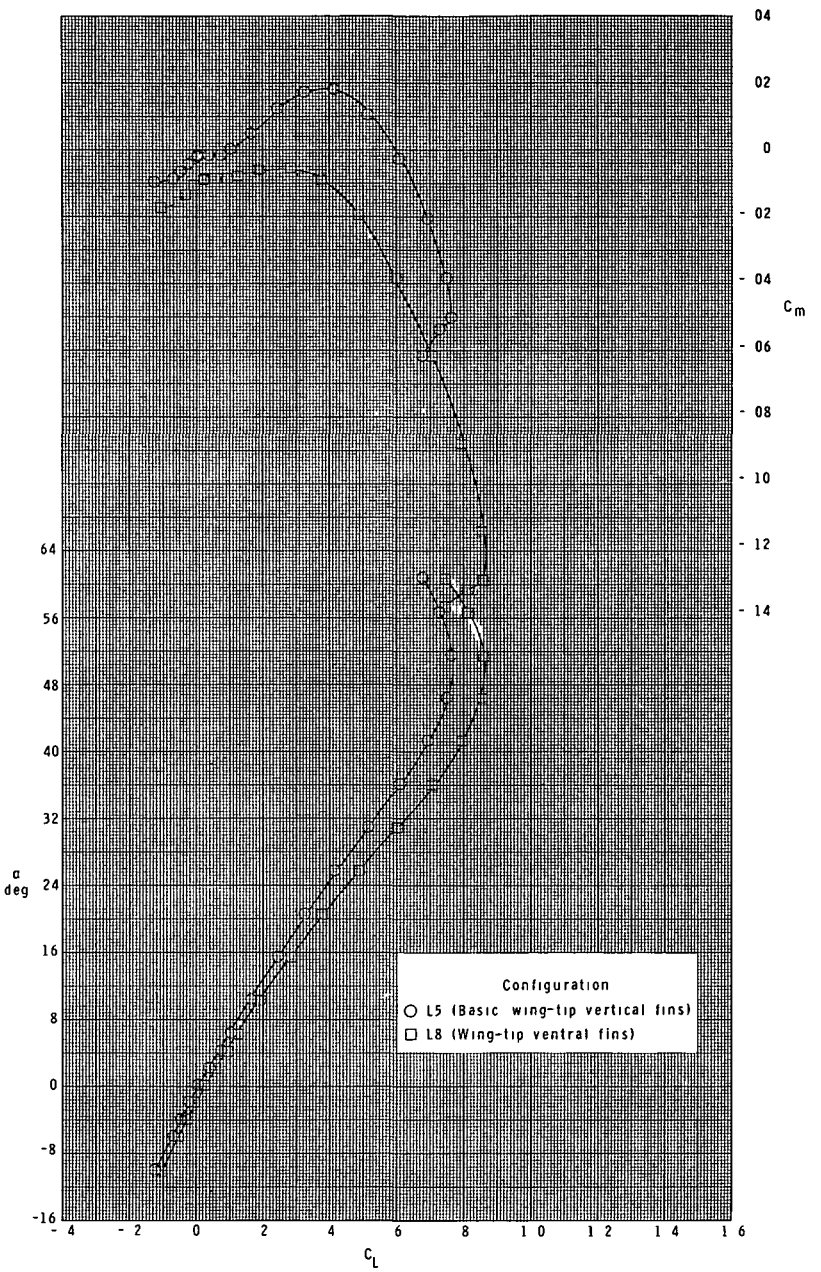

(d) Continued.

Figure 26.- Continued.

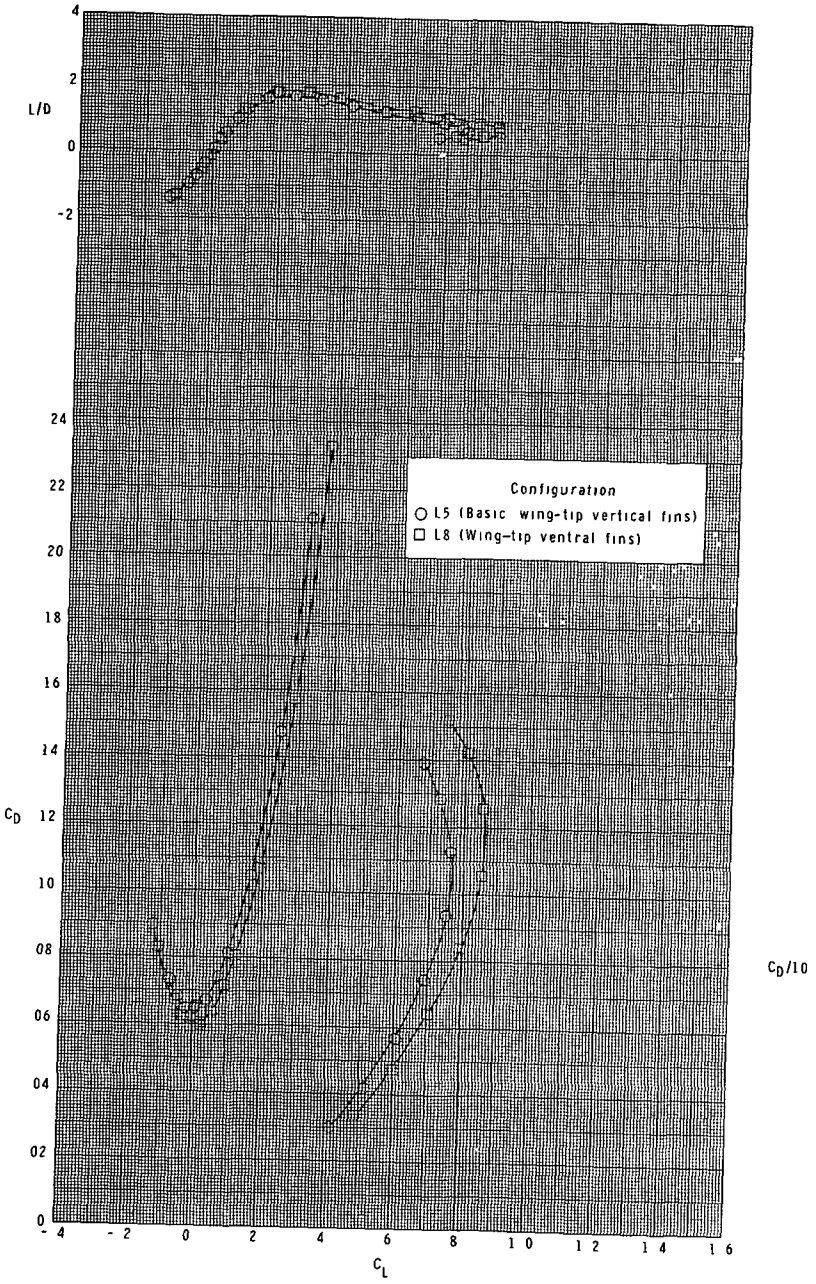

(d) Concluded.

Figure 26.- Concluded.

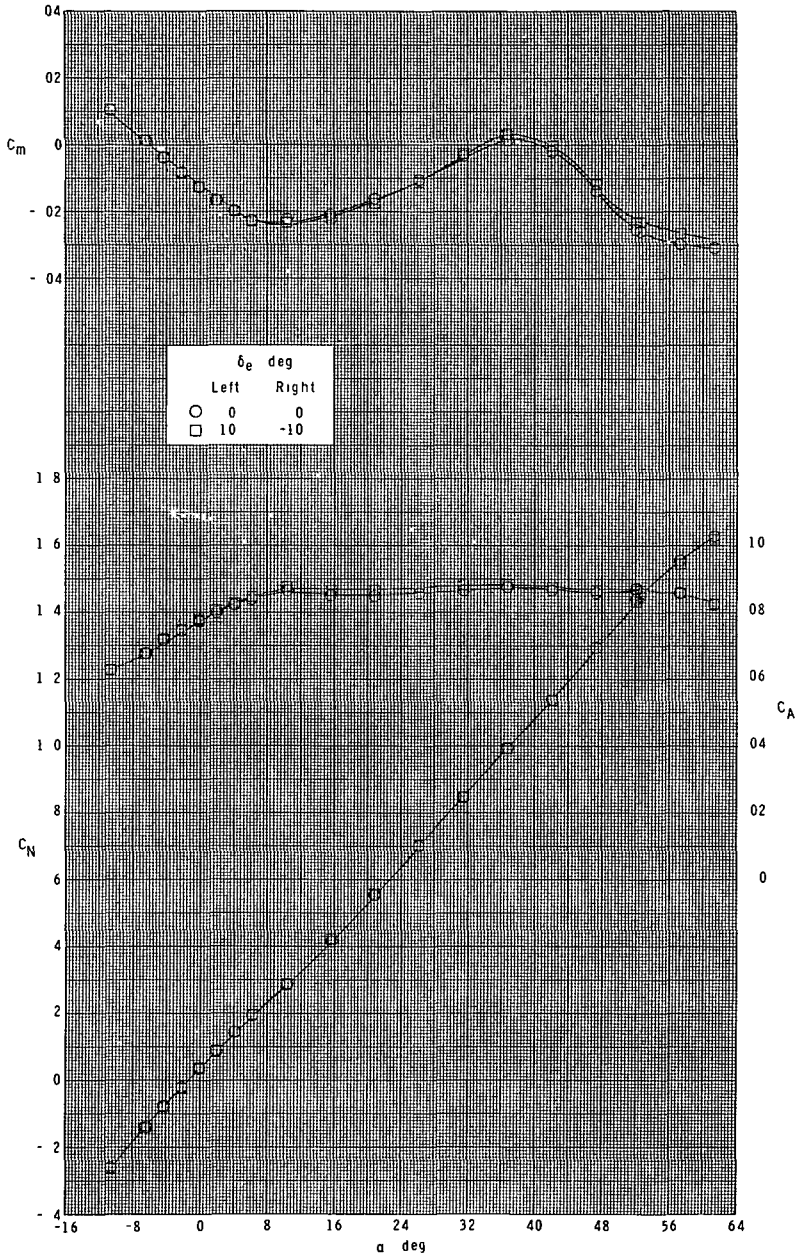

(a) M = 2.30.

Figure 27.- Effect of elevon deflection-in-roll on longitudinal characteristics. Booster configuration.

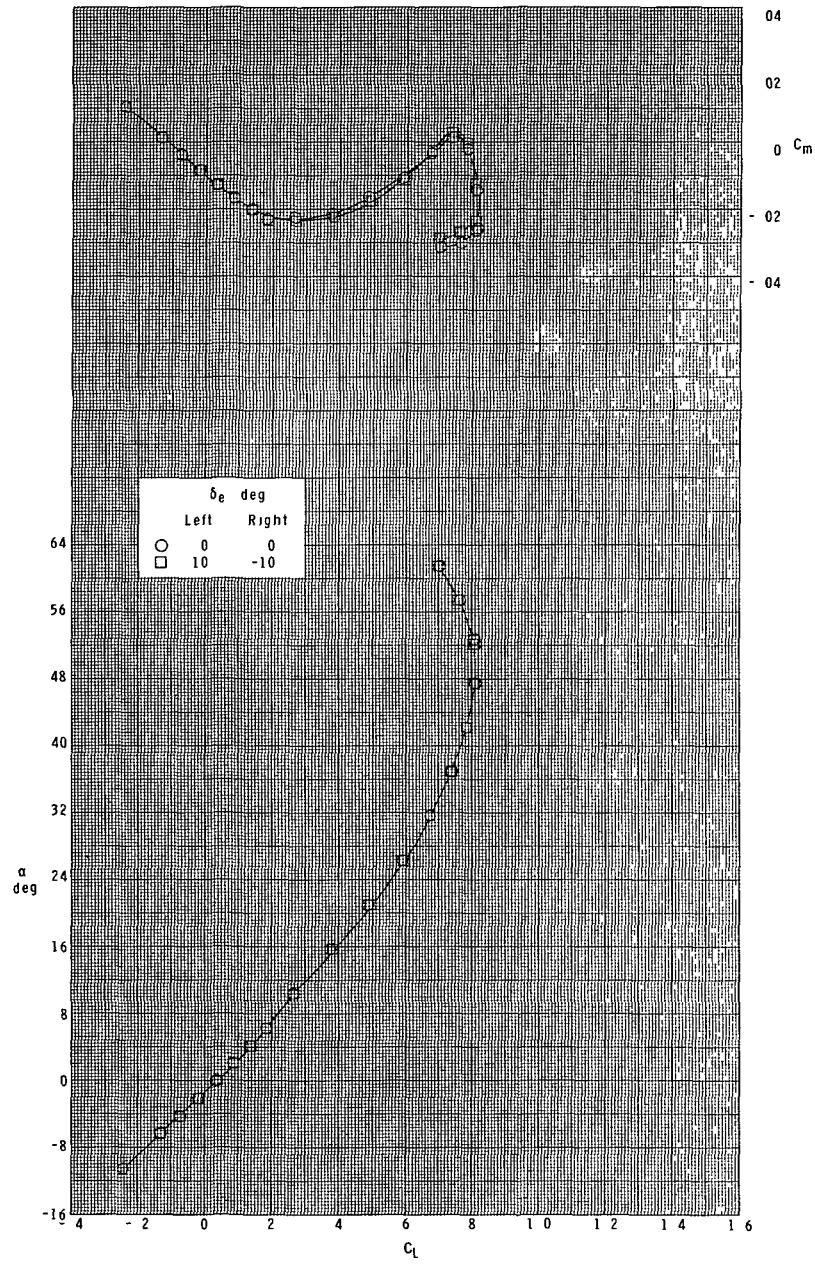

(a) Continued.

Figure 27.- Continued.

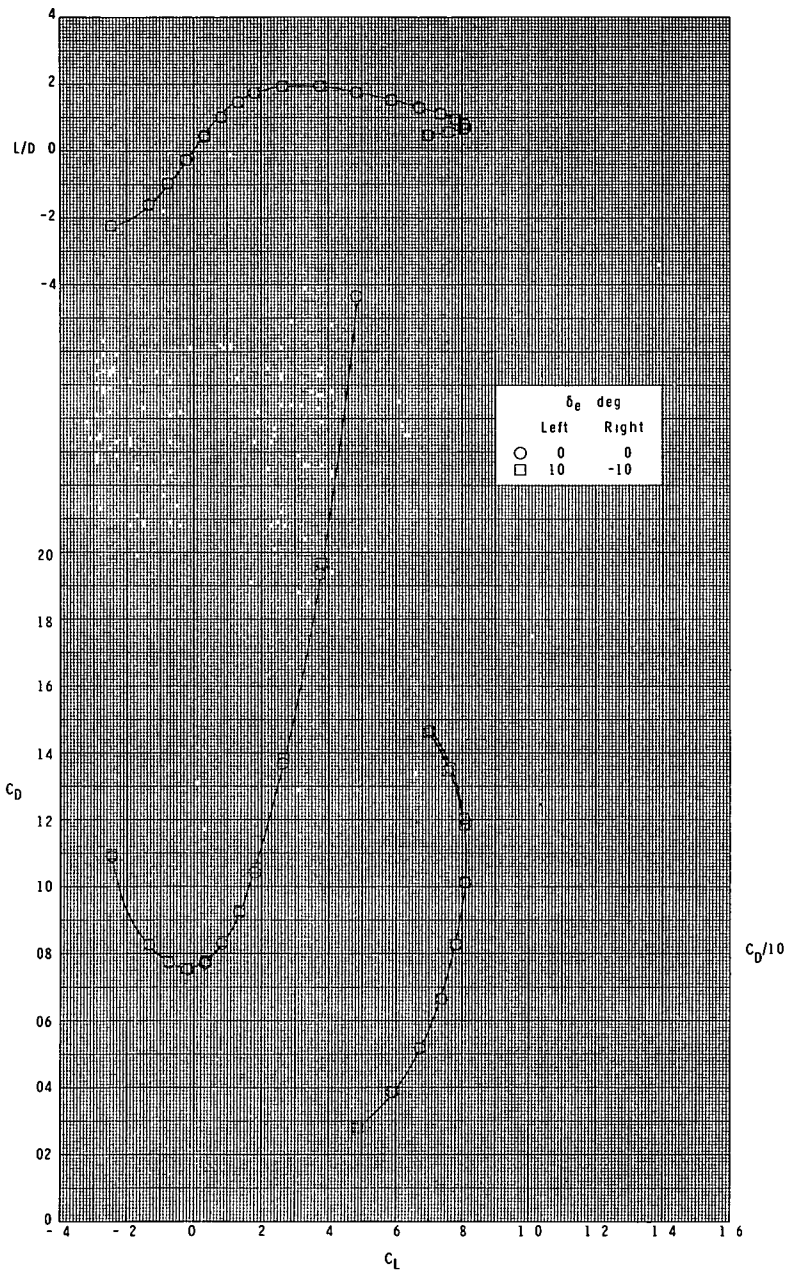

(a) Concluded.

Figure 27.- Continued.

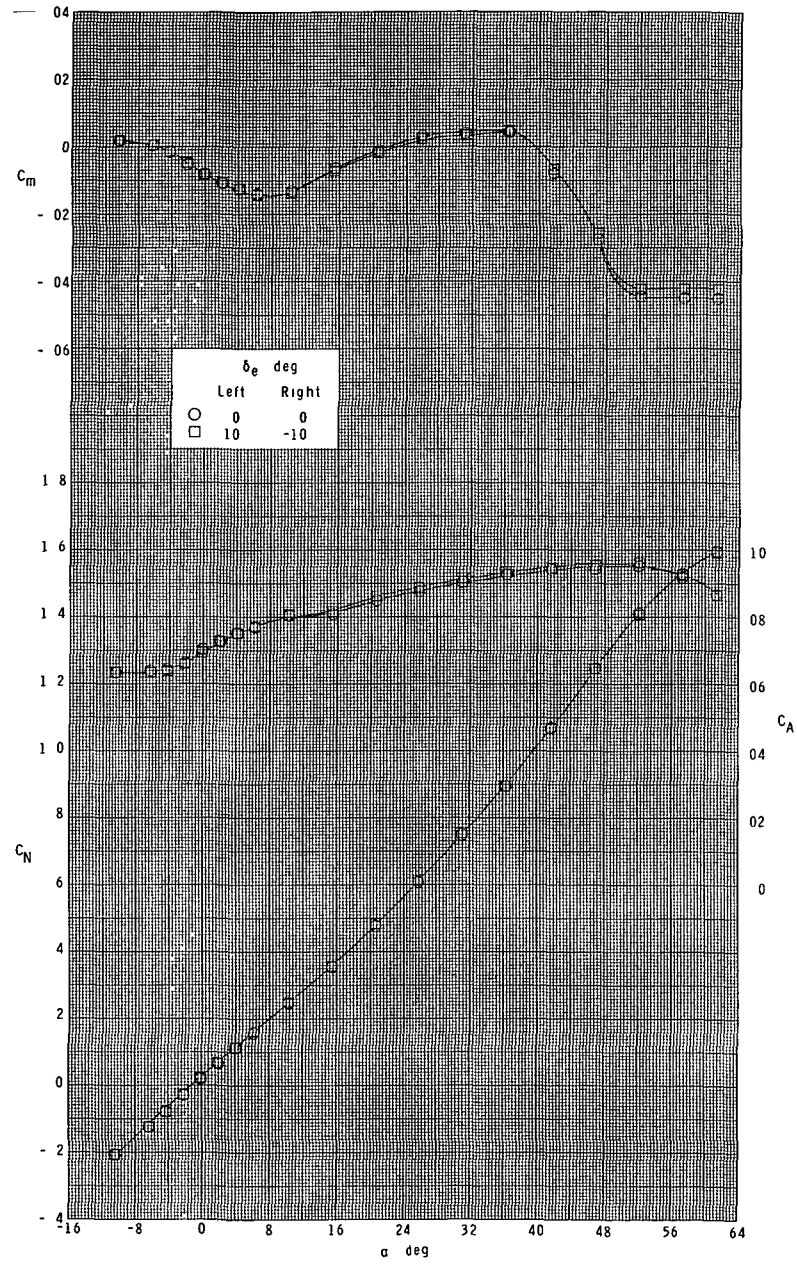

(b) M = 2.96.

Figure 27.- Continued.

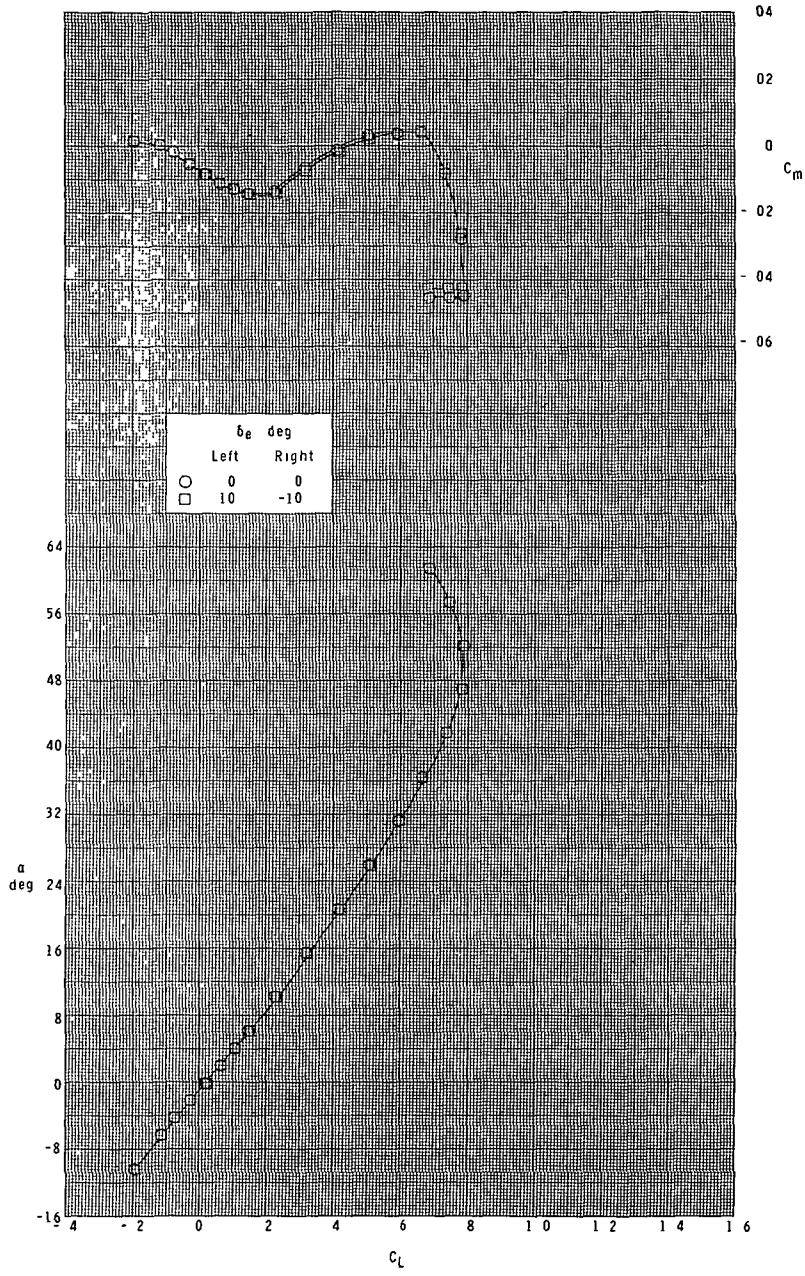

(b) Continued.

Figure 27.- Continued.

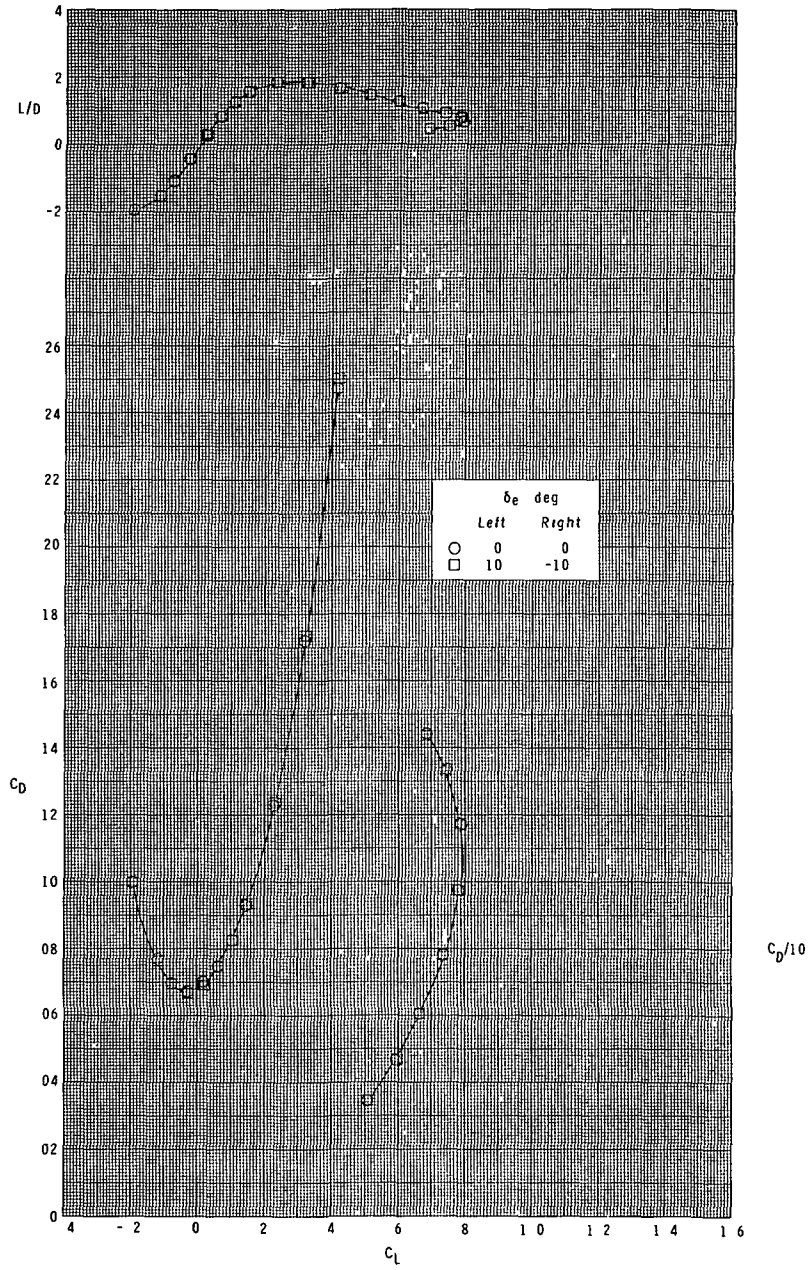

(b) Concluded.

Figure 27.- Continued.

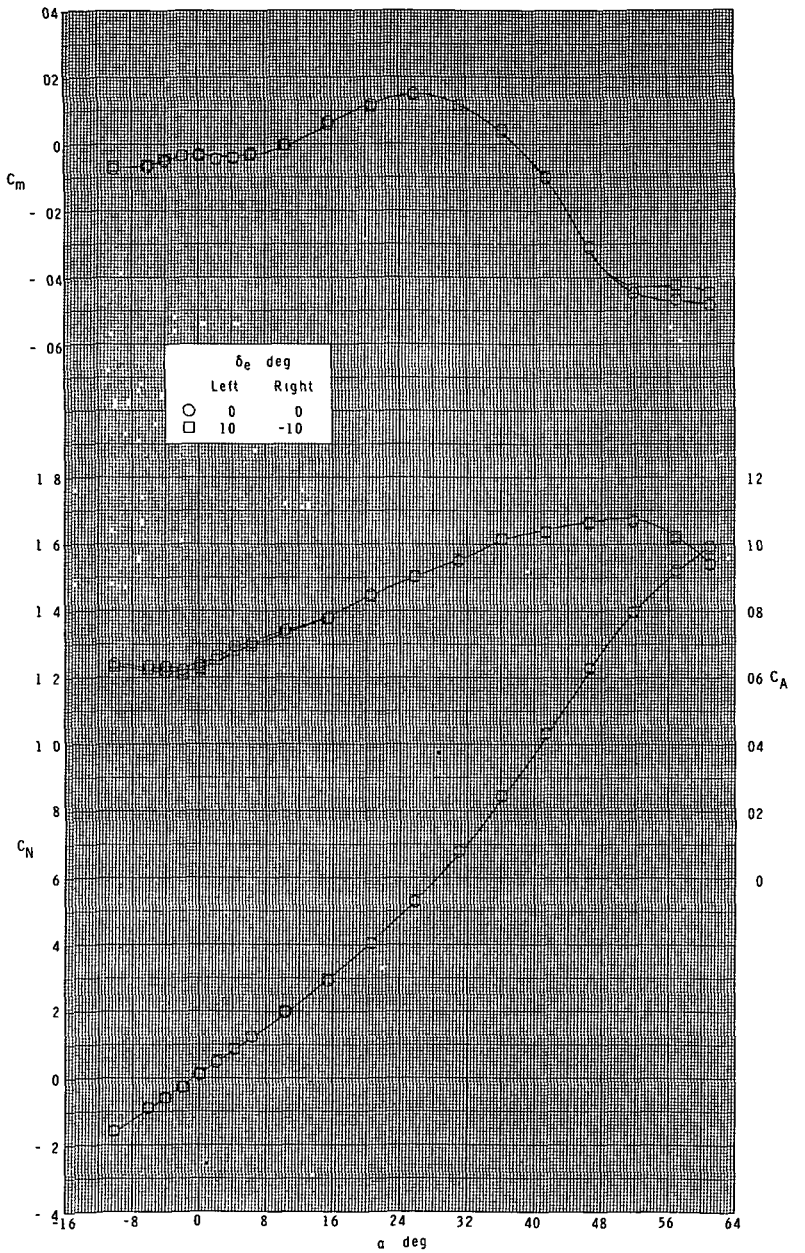

(c) M = 3.95.

Figure 27.- Continued.

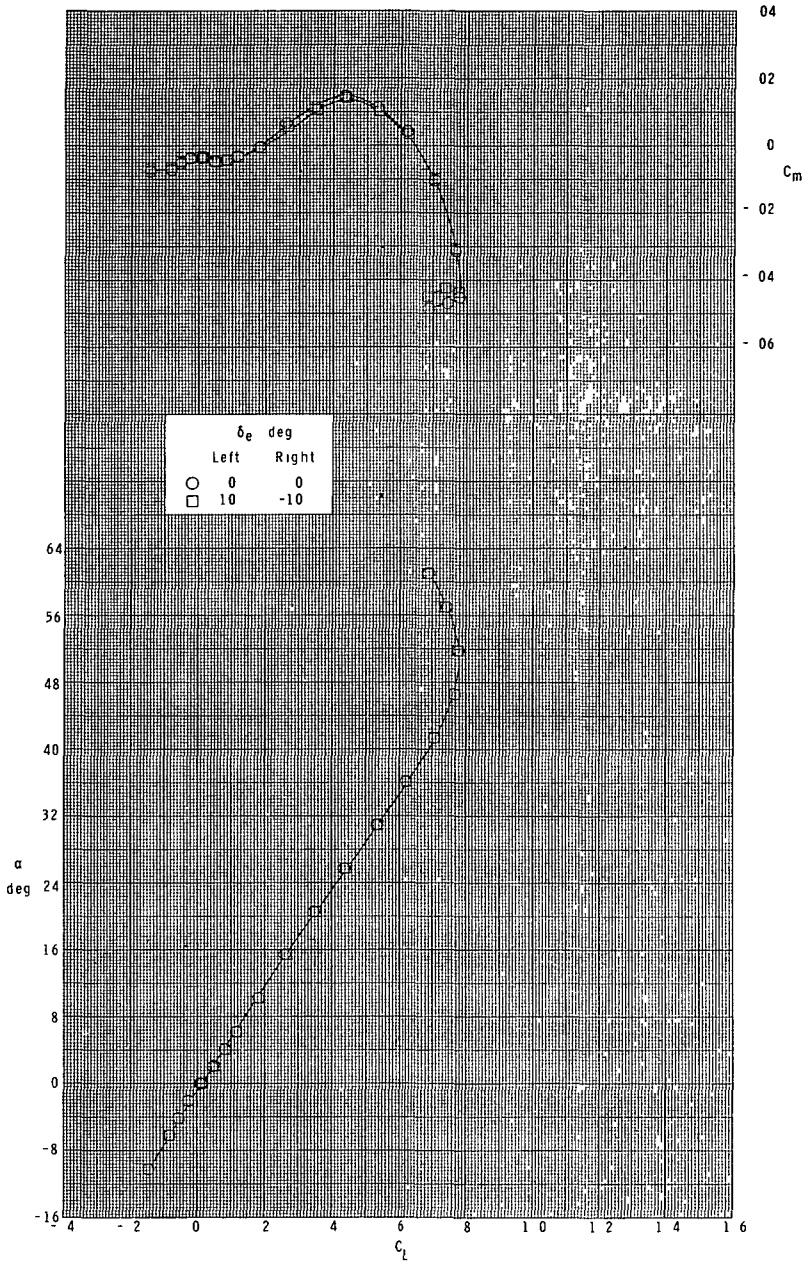

(c) Continued.

Figure 27.- Continued.

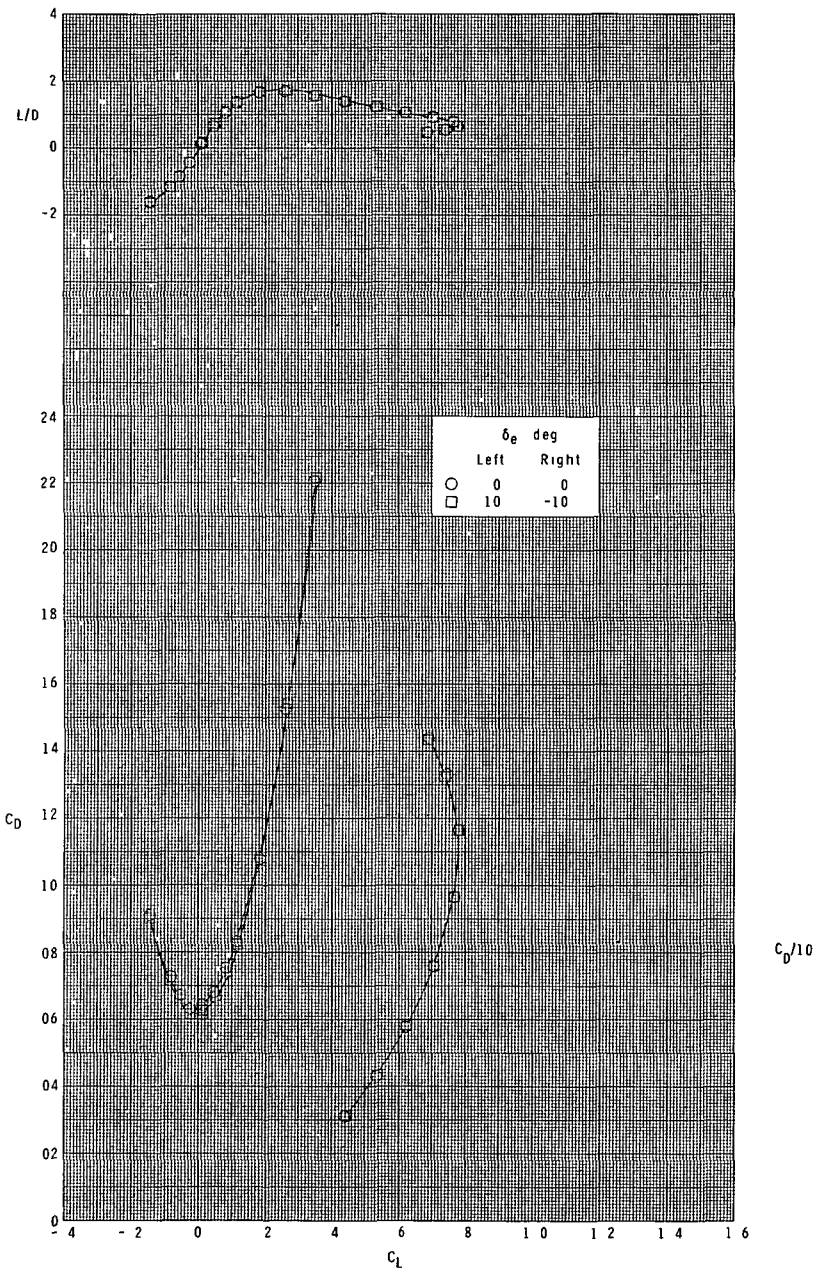

(c) Concluded.

Figure 27.- Continued.

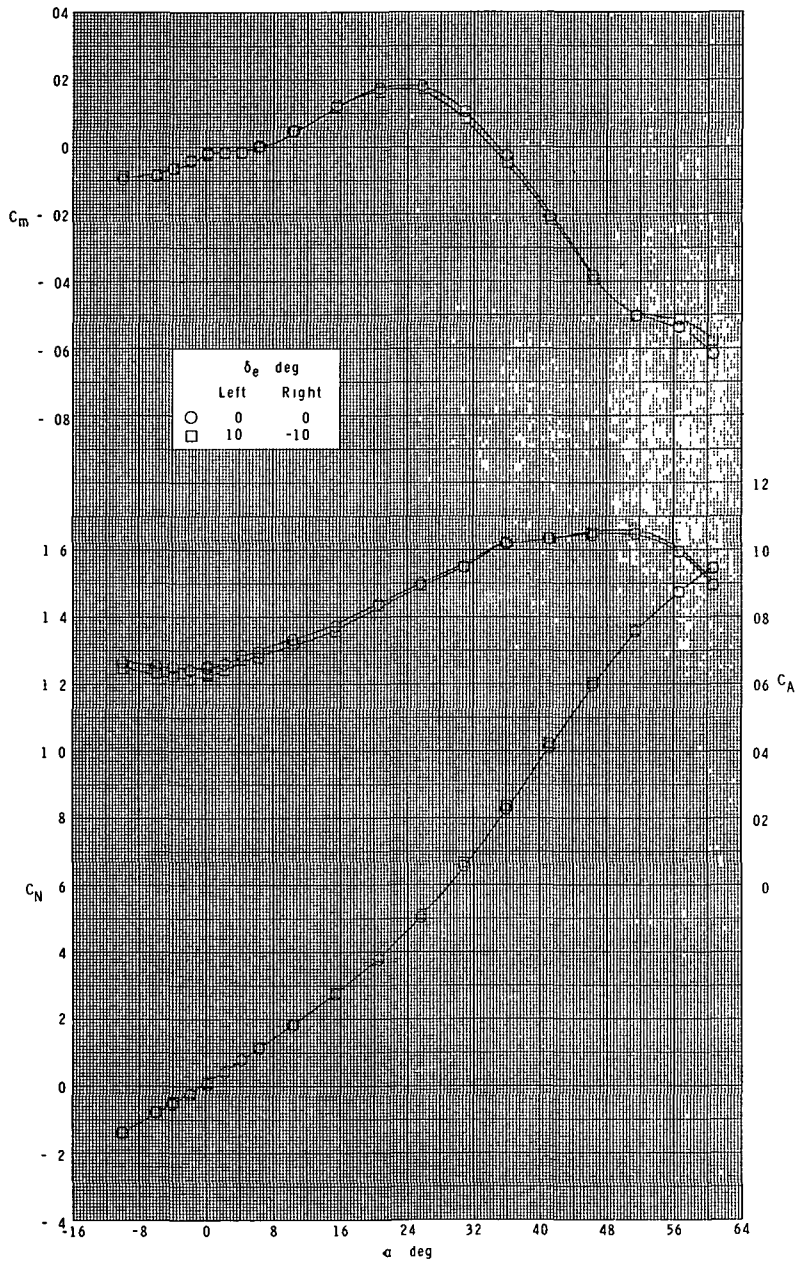

(d) M = 4.60.

Figure 27.- Continued.

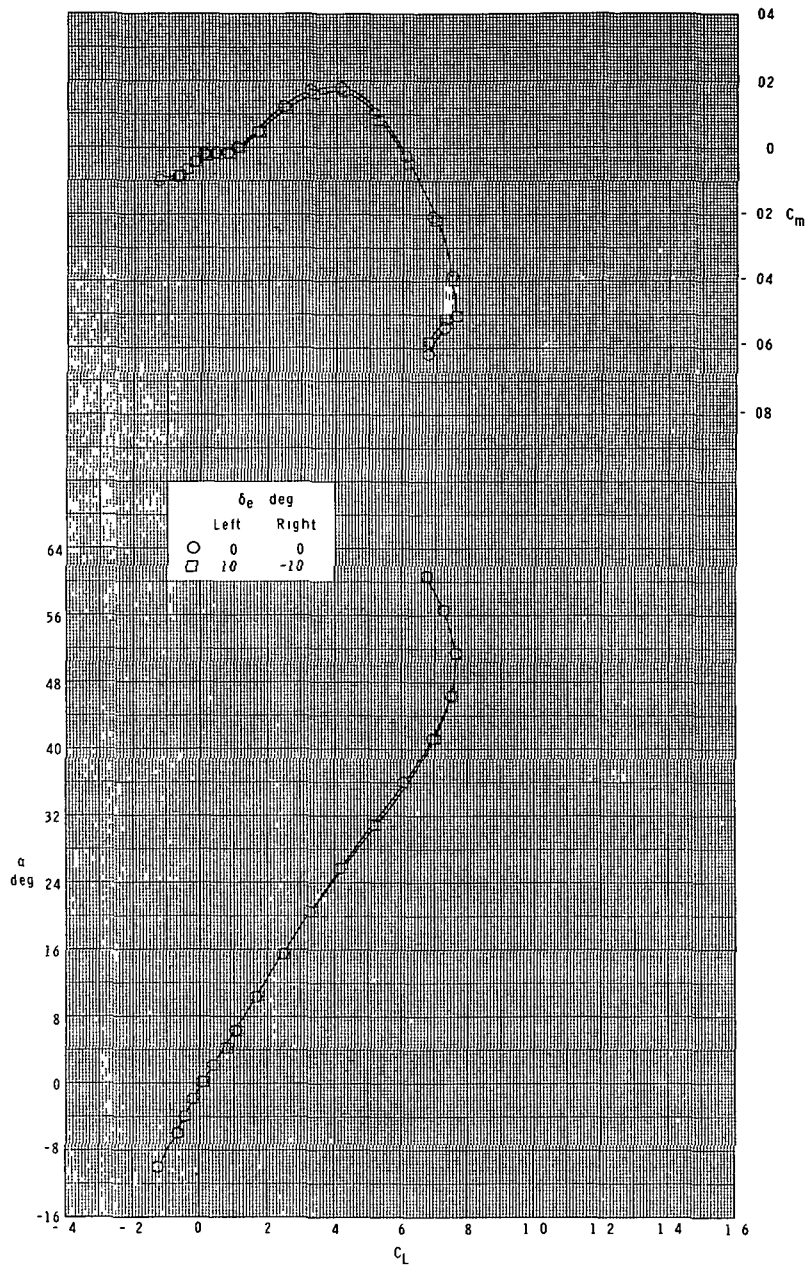

(d) Continued.

Figure 27.- Continued.

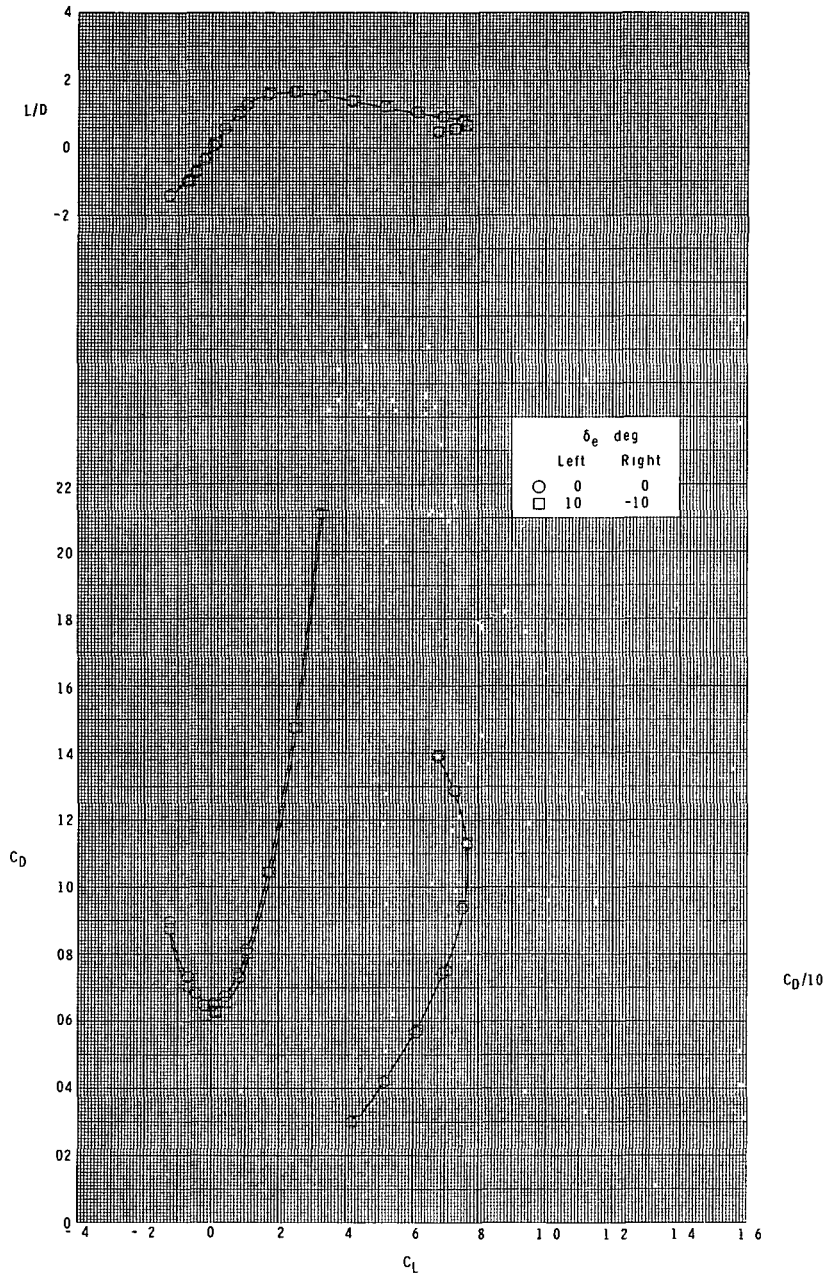

(d) Concluded.

Figure 27.- Concluded.

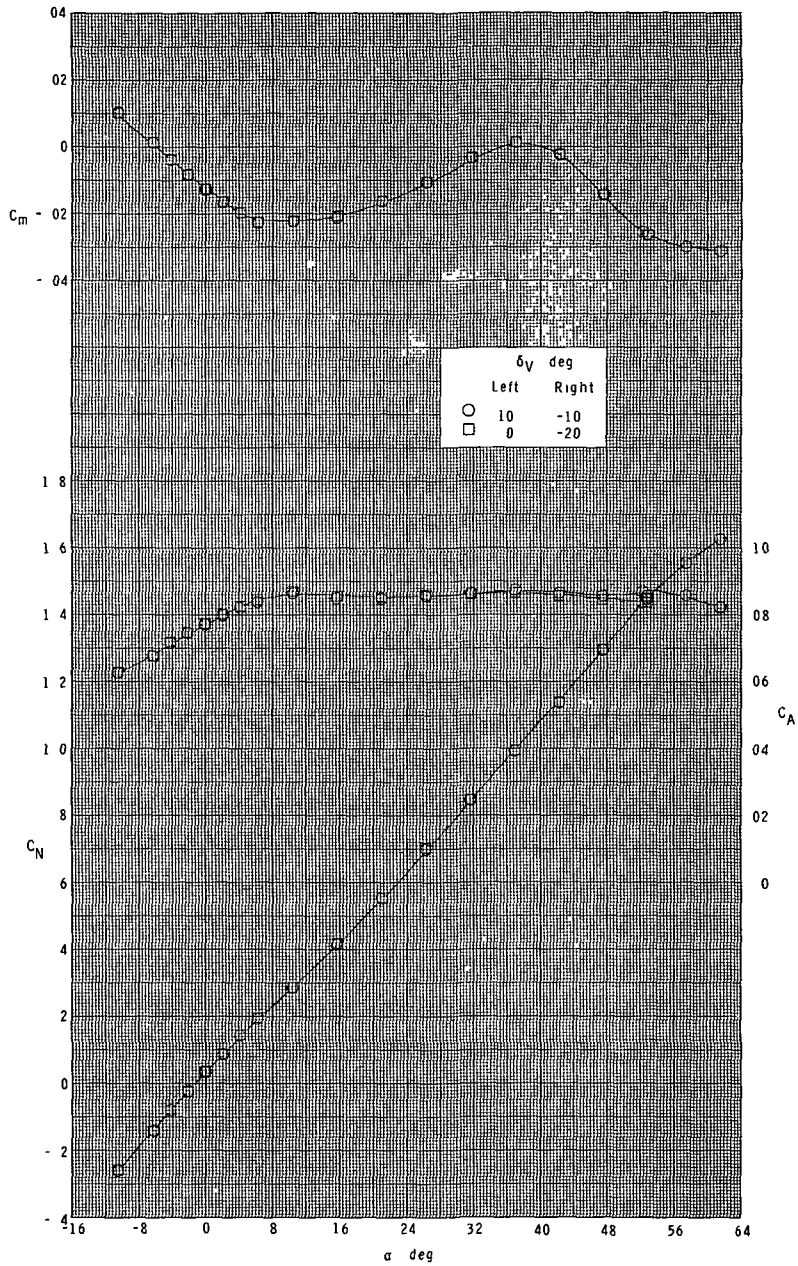

(a) M = 2.30.

Figure 28.- Effect of vertical-fin rudder deflection on longitudinal characteristics. Booster configuration.

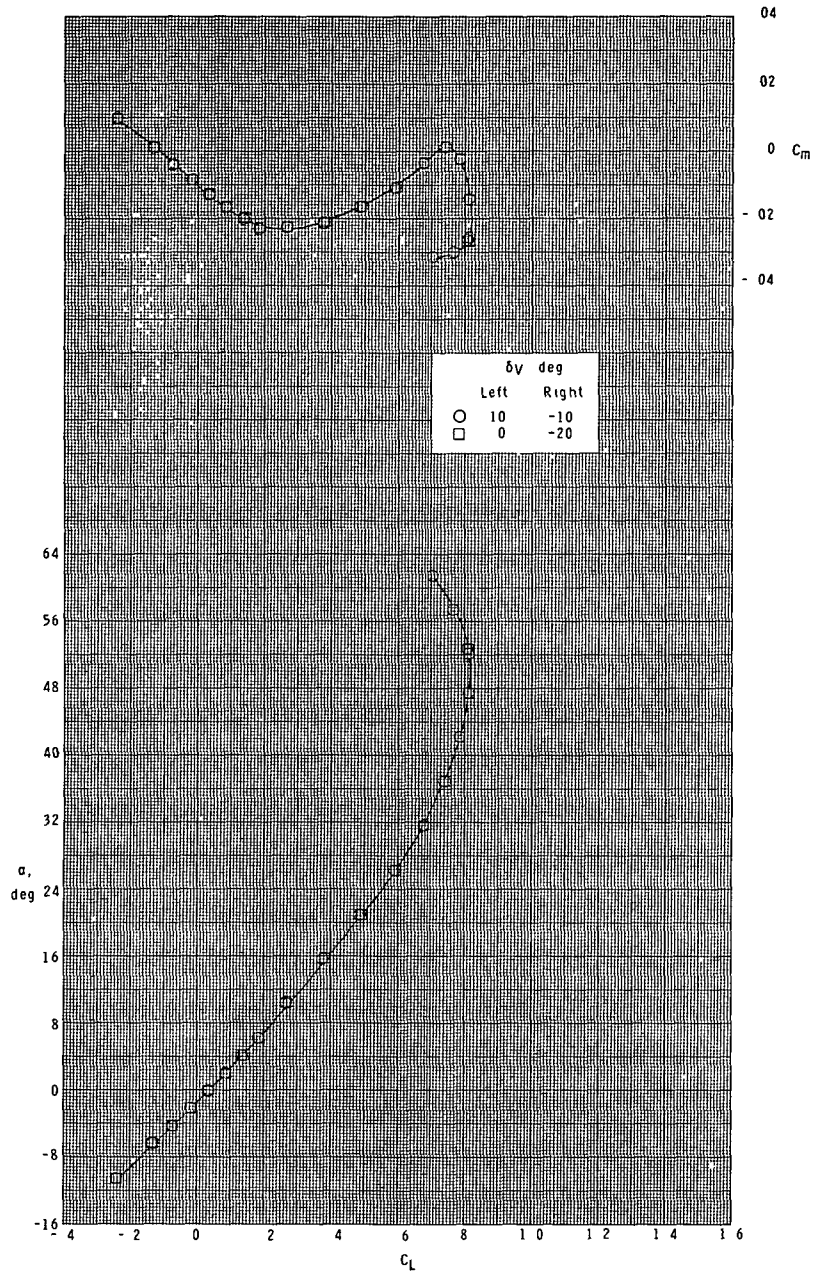

(a) Continued.

Figure 28.- Continued.

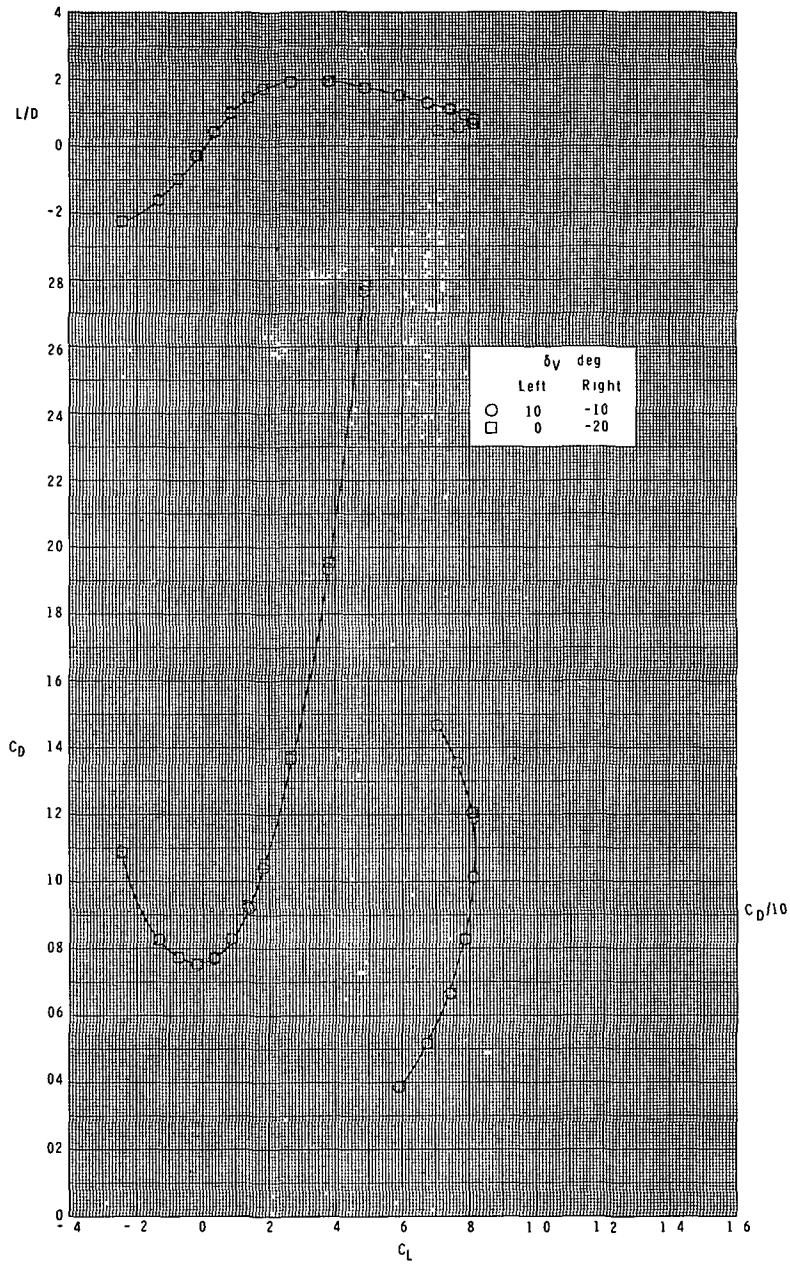

(a) Concluded.

Figure 28 - Continued.

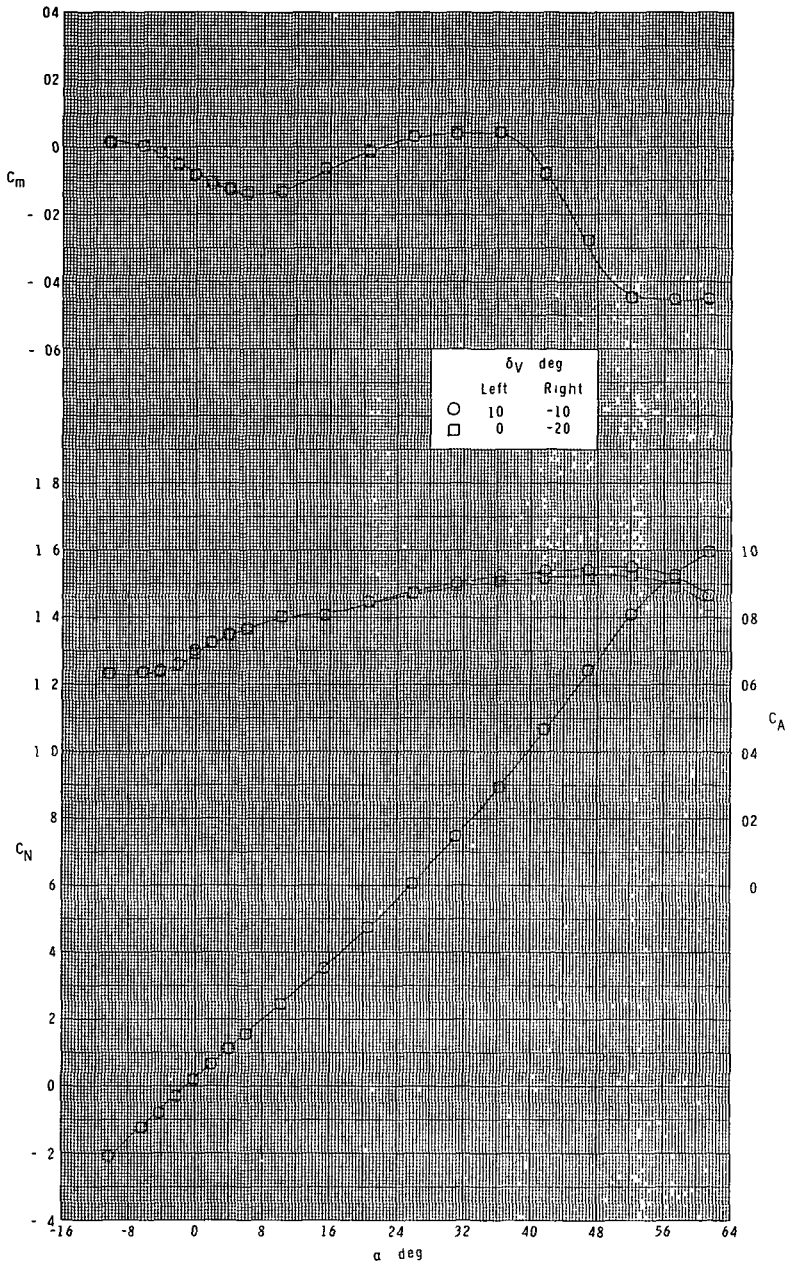

(b) M = 2.96.

Figure 28.- Continued.

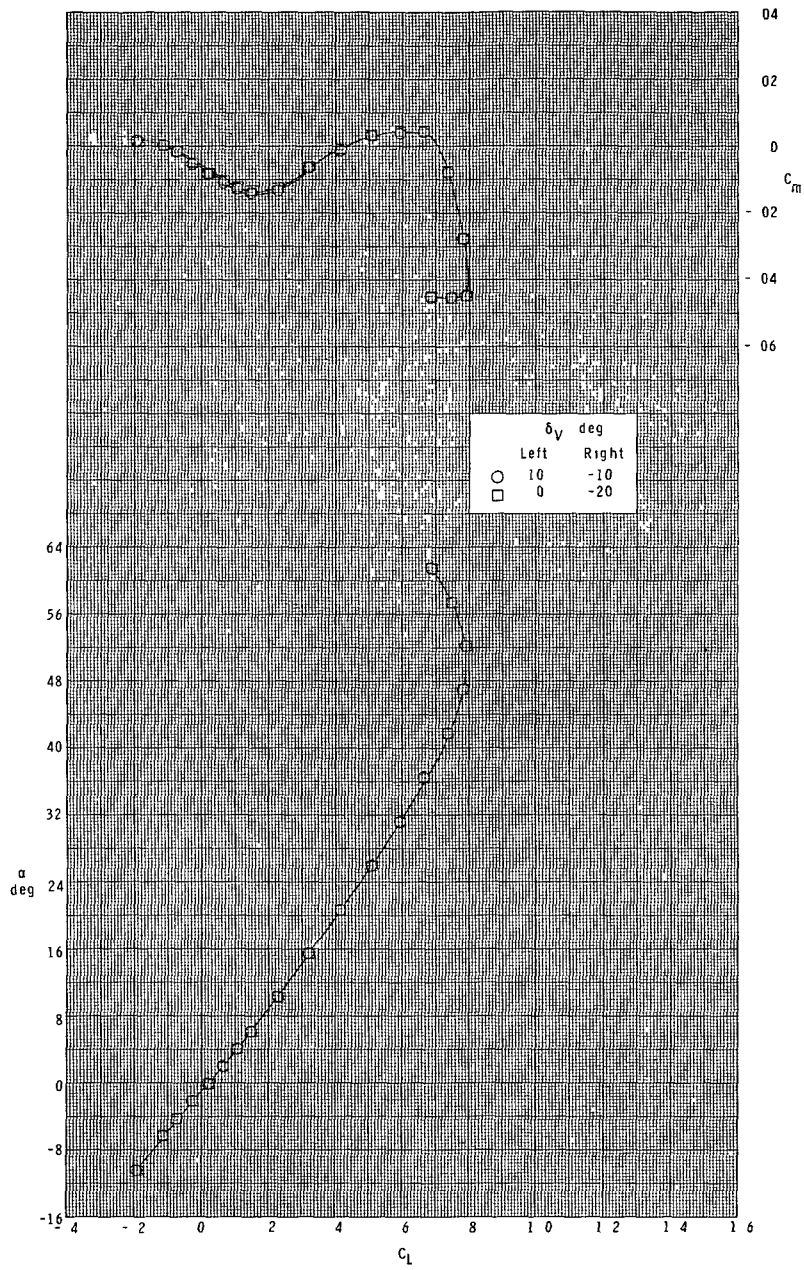

(b) Continued.

Figure 28 - Continued.

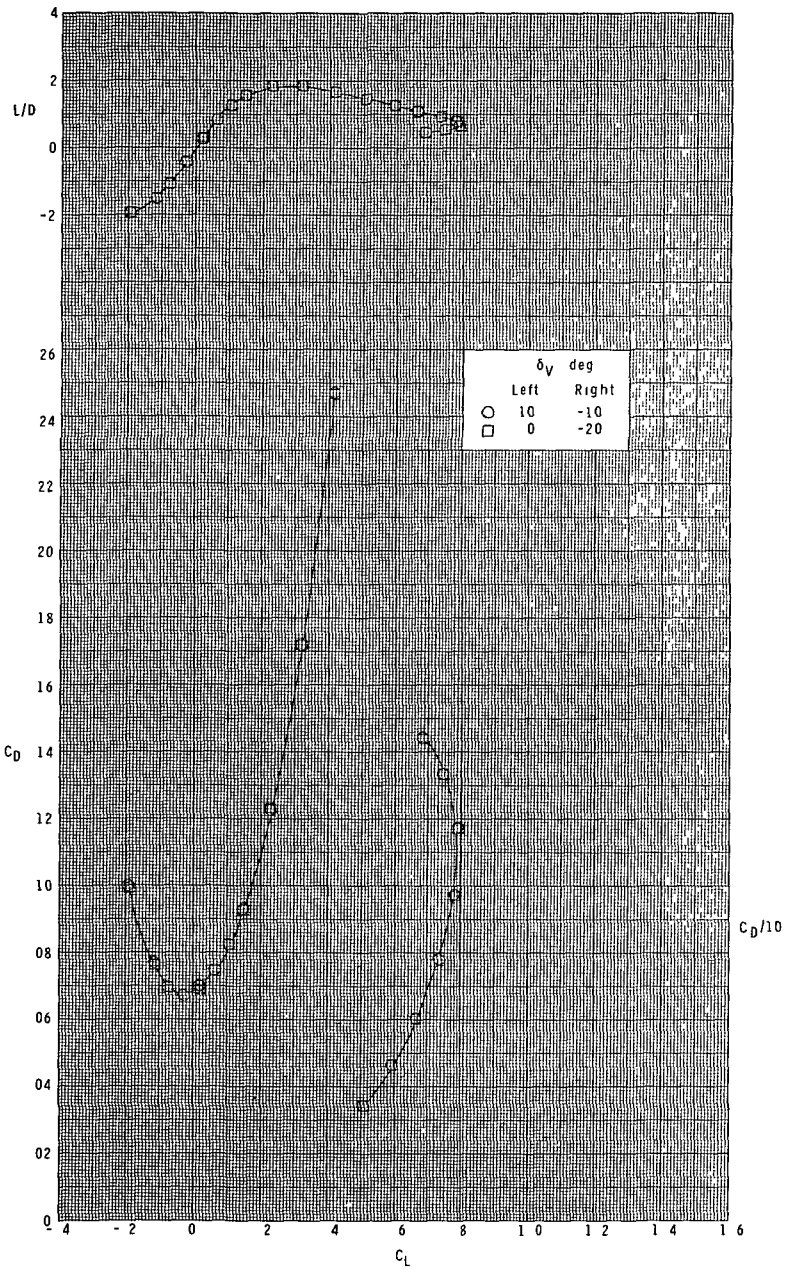

(b) Concluded.

Figure 28.- Continued.

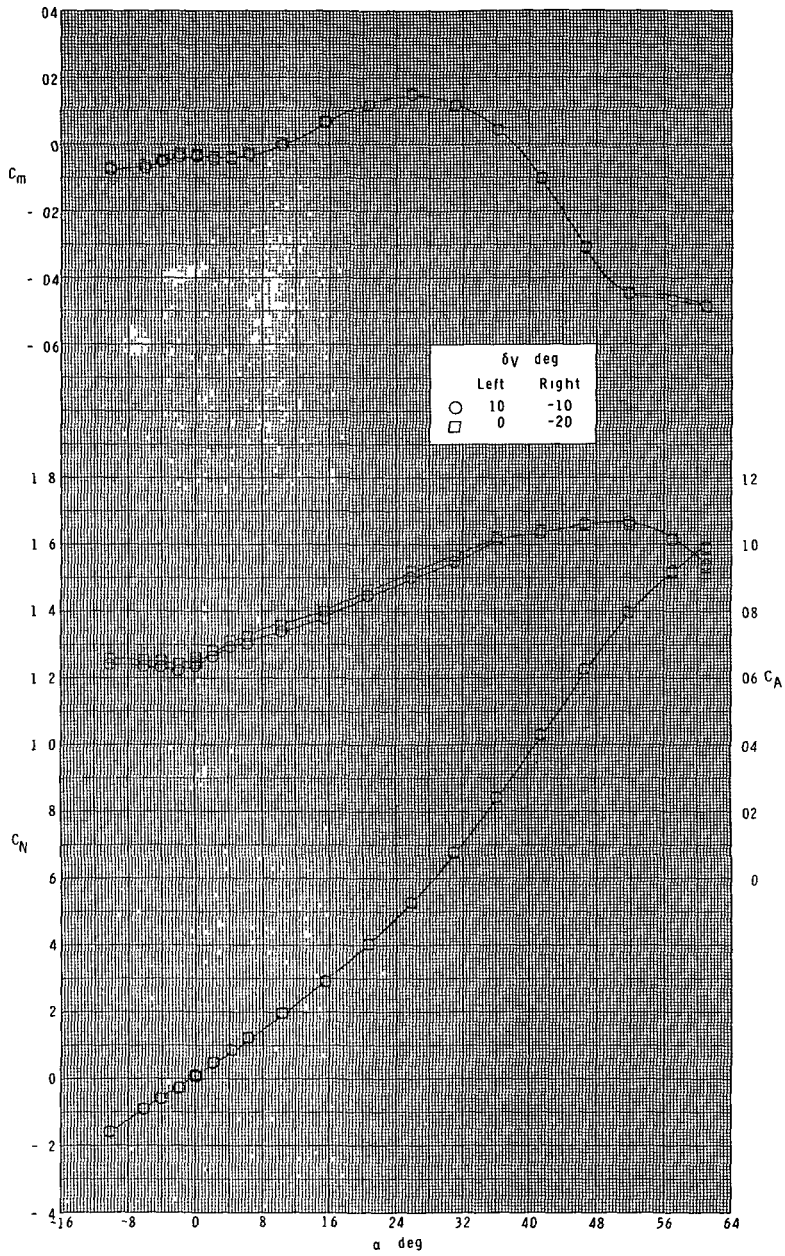

(c) M = 3.95.

Figure 28.- Continued.

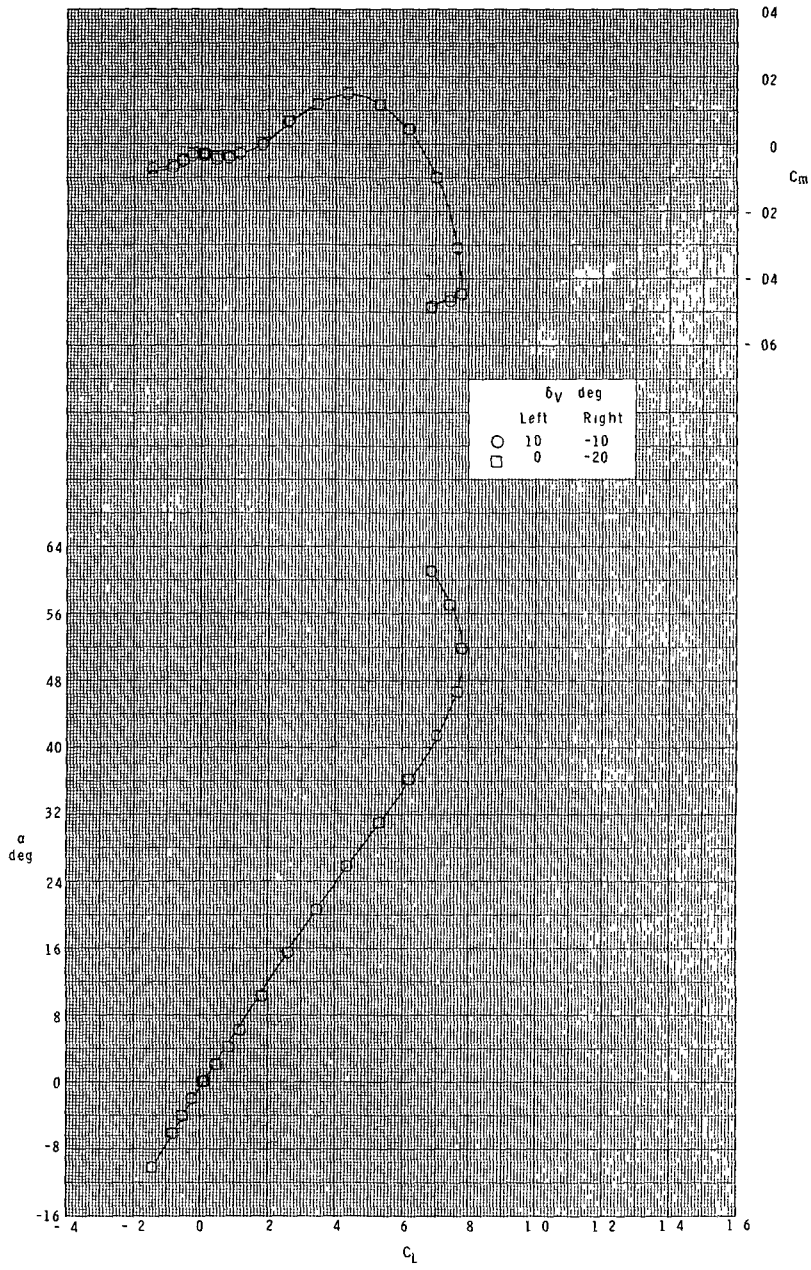

(c) Continued.

Figure 28.- Continued.

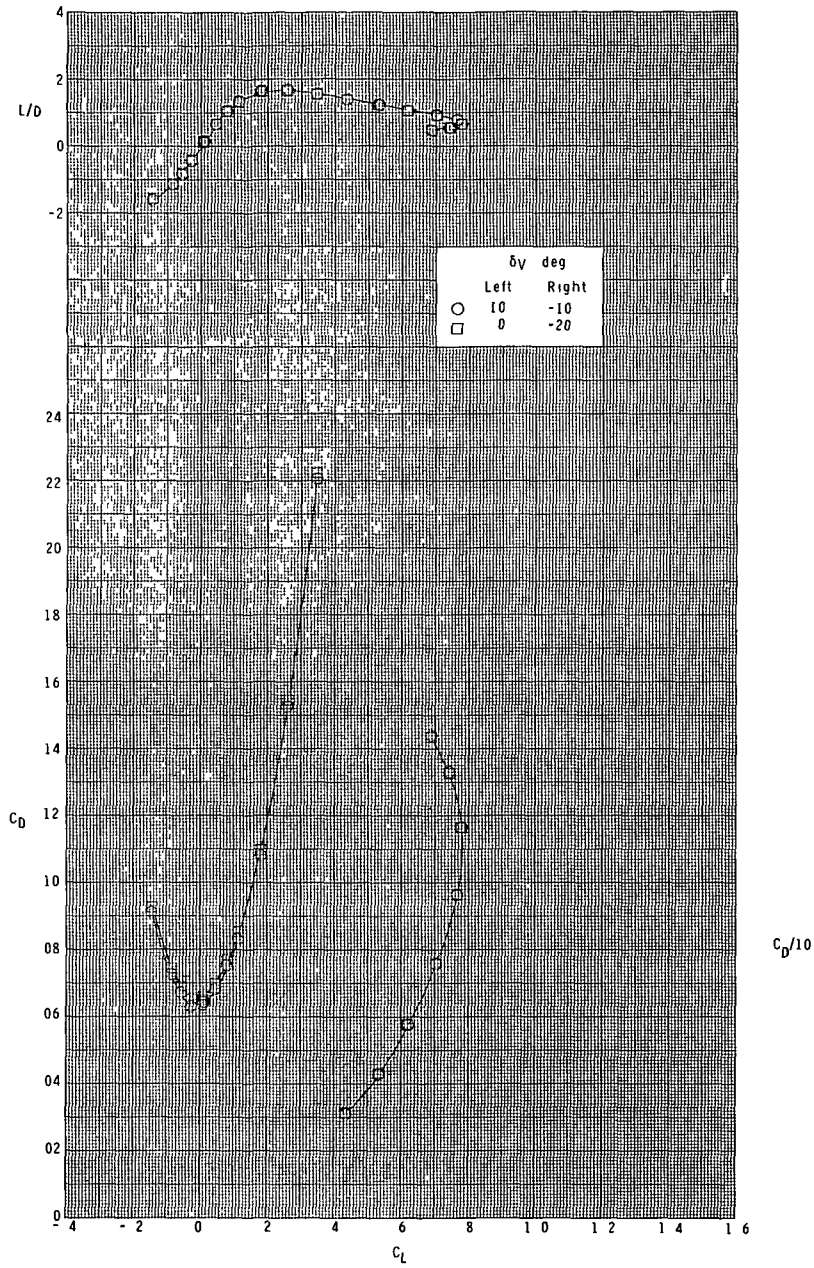

(c) Concluded.

Figure 28.- Continued.

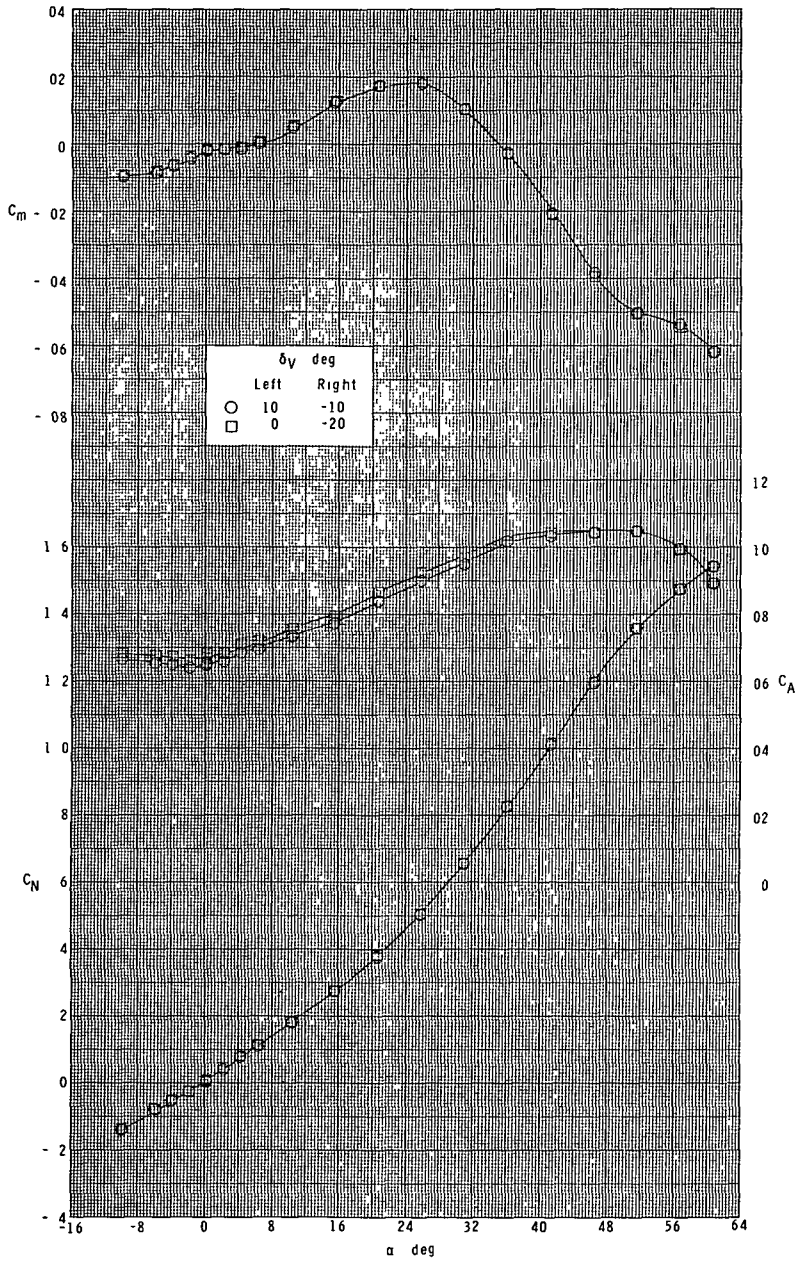

(d) M = 4.60.

Figure 28.- Continued.

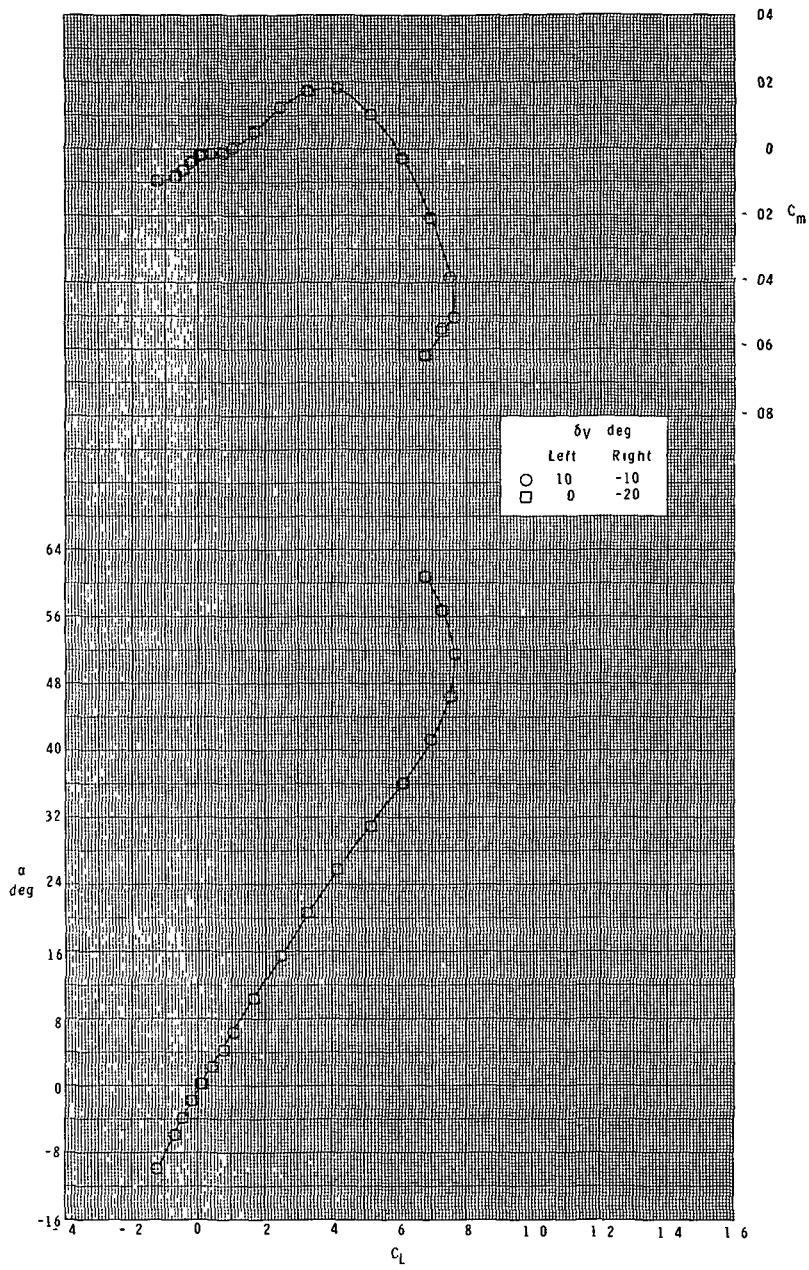

(d) Continued.

Figure 28.- Continued.

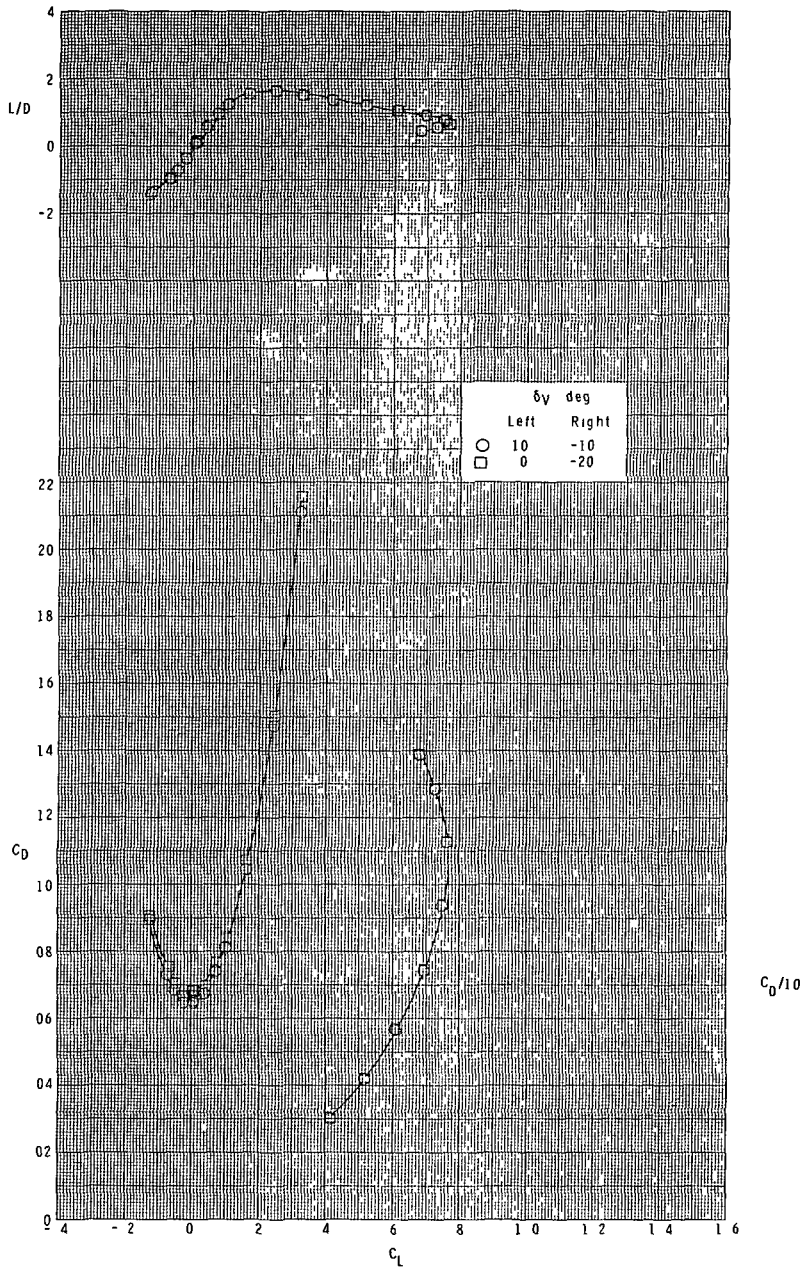

(d) Concluded.

Figure 28.- Concluded.

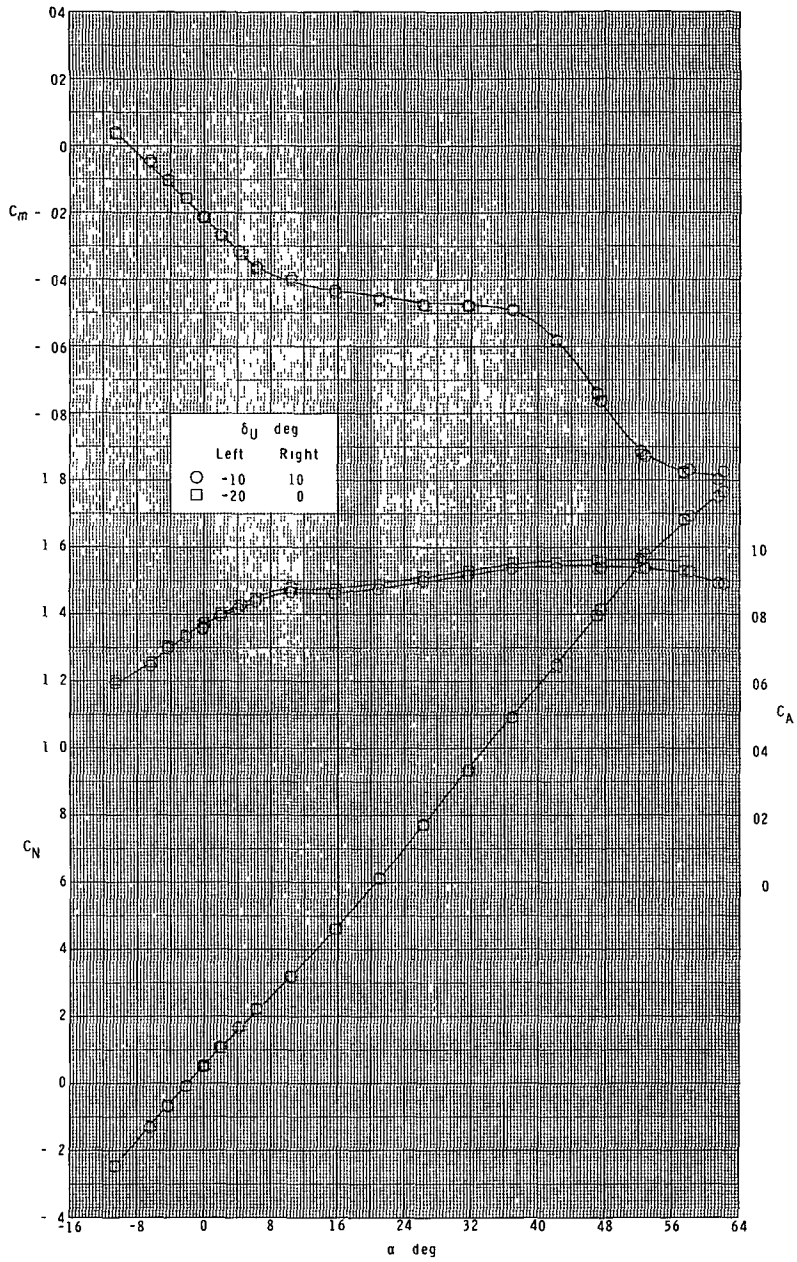

(a) M = 2.30.

Figure 29.- Effect of ventral-fin rudder deflection on longitudinal characteristics. Booster configuration.

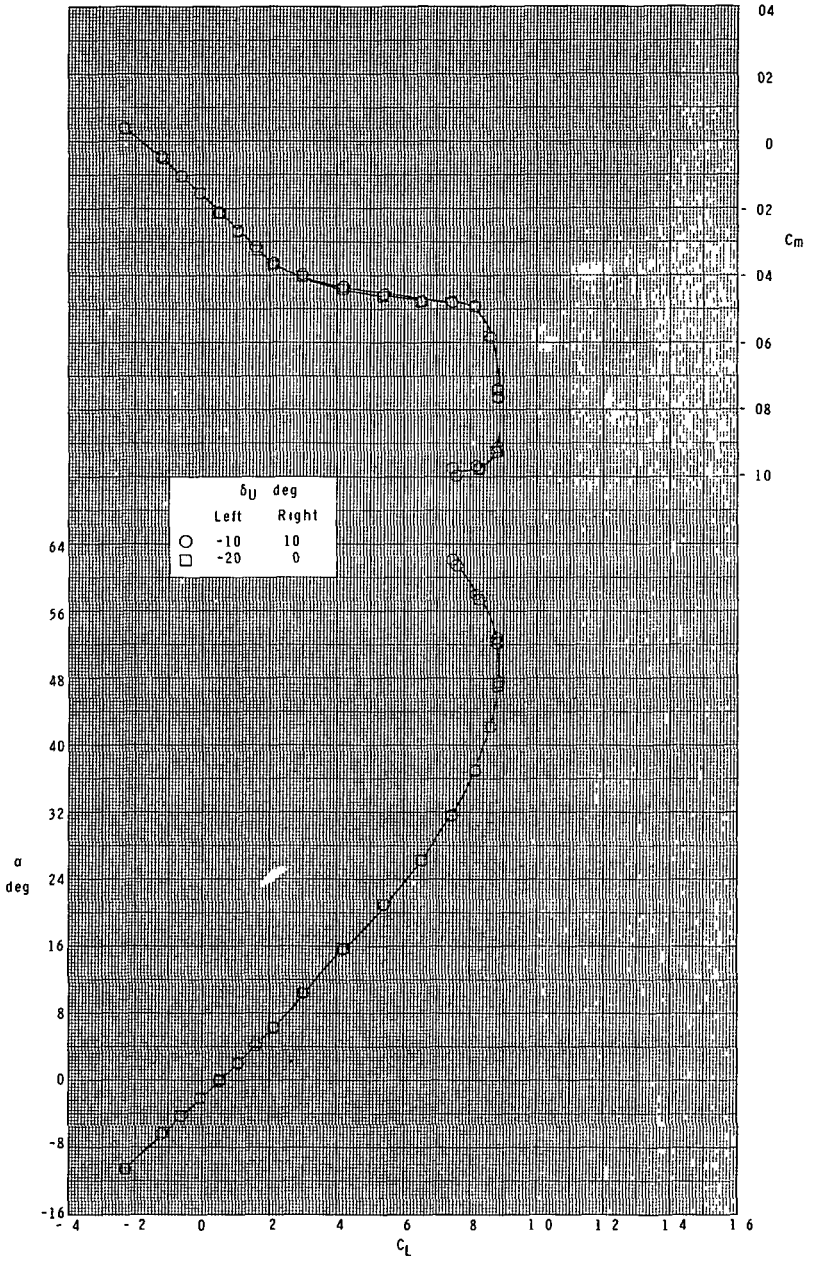

(a) Continued.

Figure 29.- Continued.

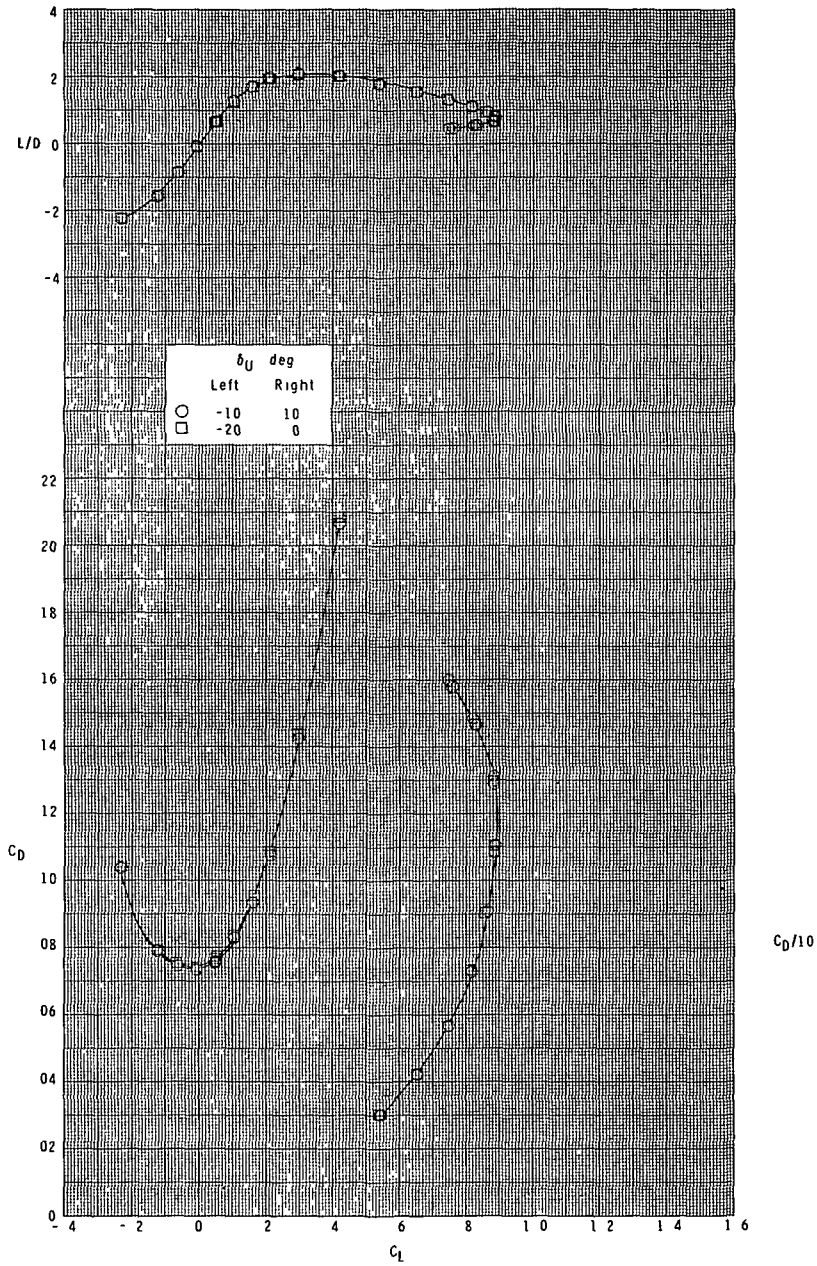

(a) Concluded.

Figure 29.- Continued.

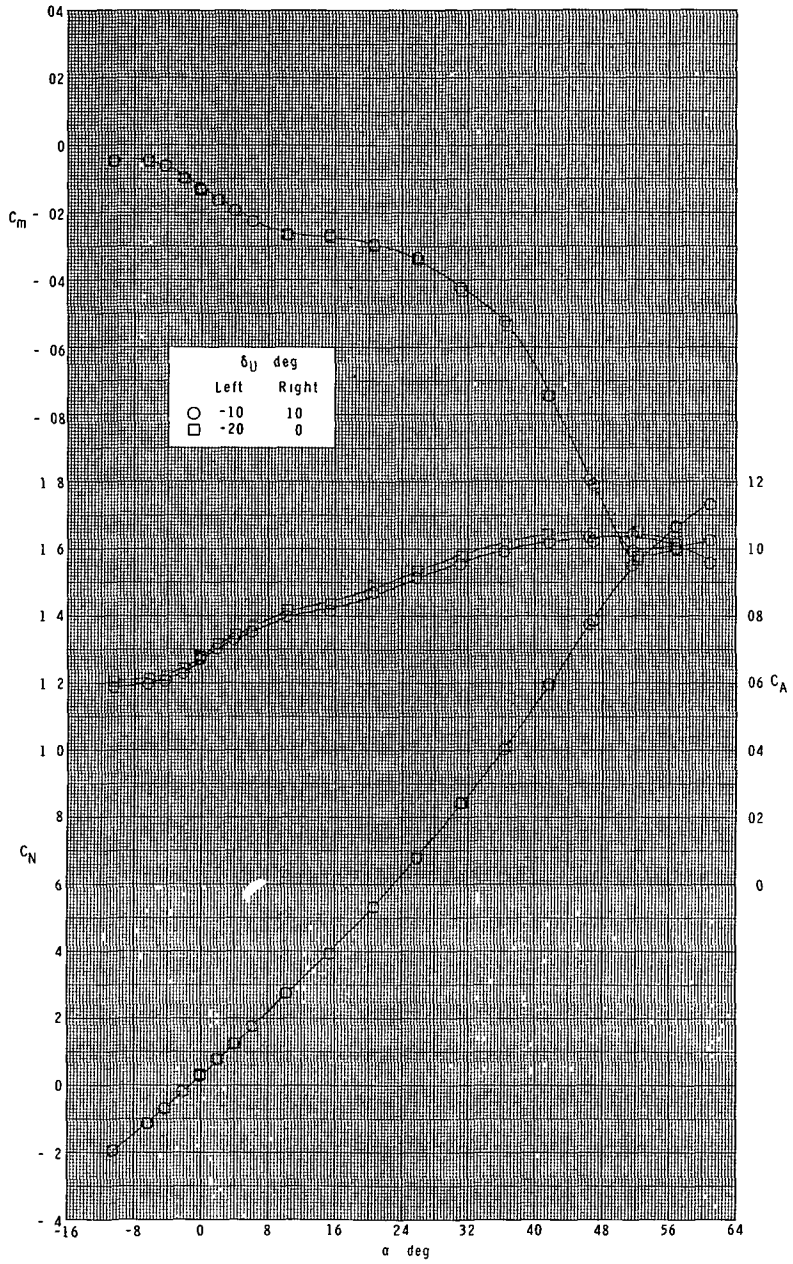

(b) M = 2.96.

Figure 29.- Continued.

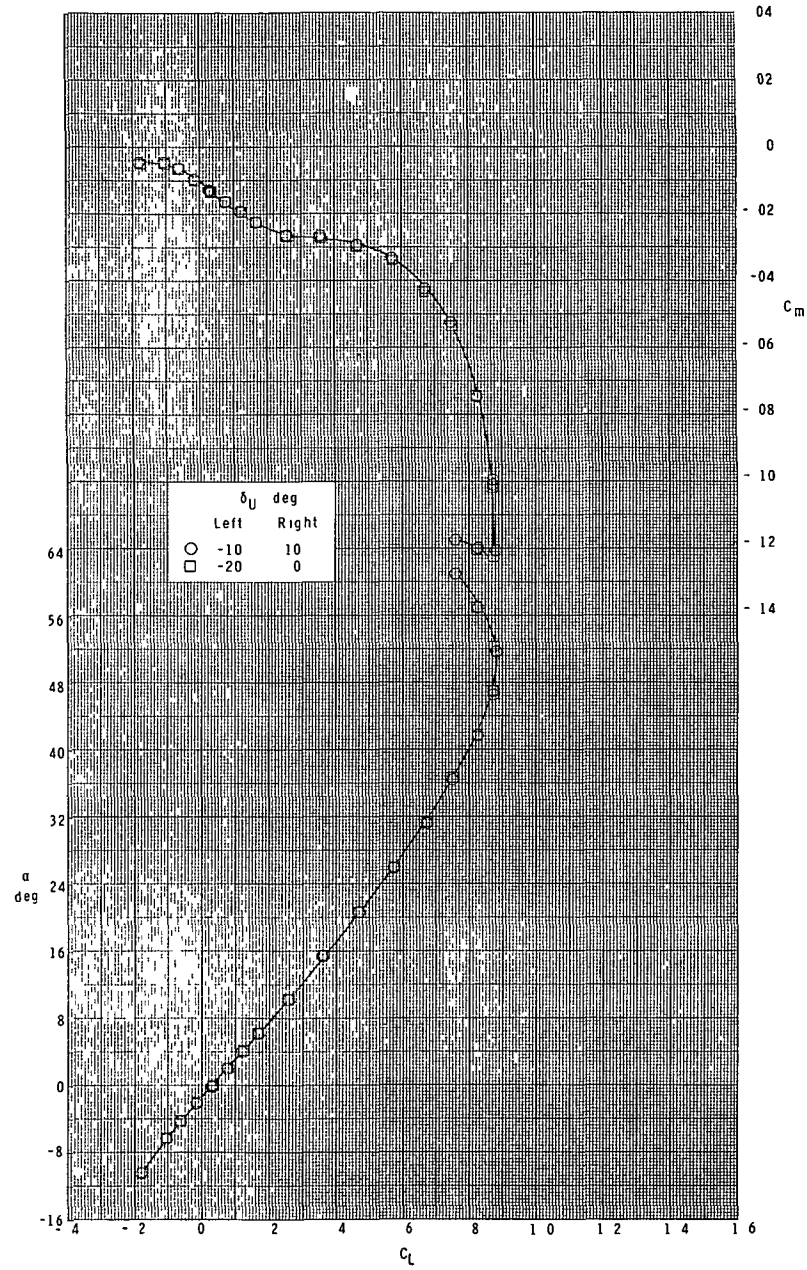

(b) Continued.

Figure 29.- Continued.

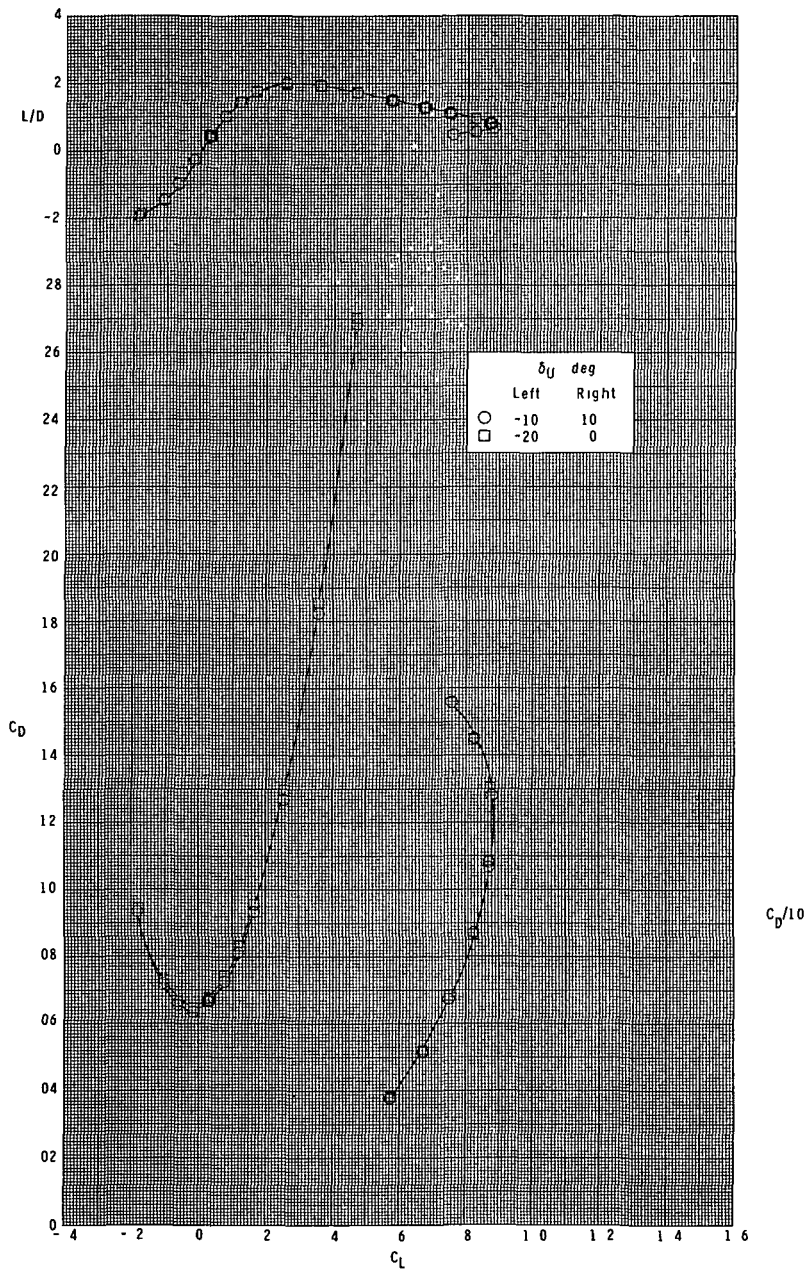

(b) Concluded.

Figure 29.- Continued.

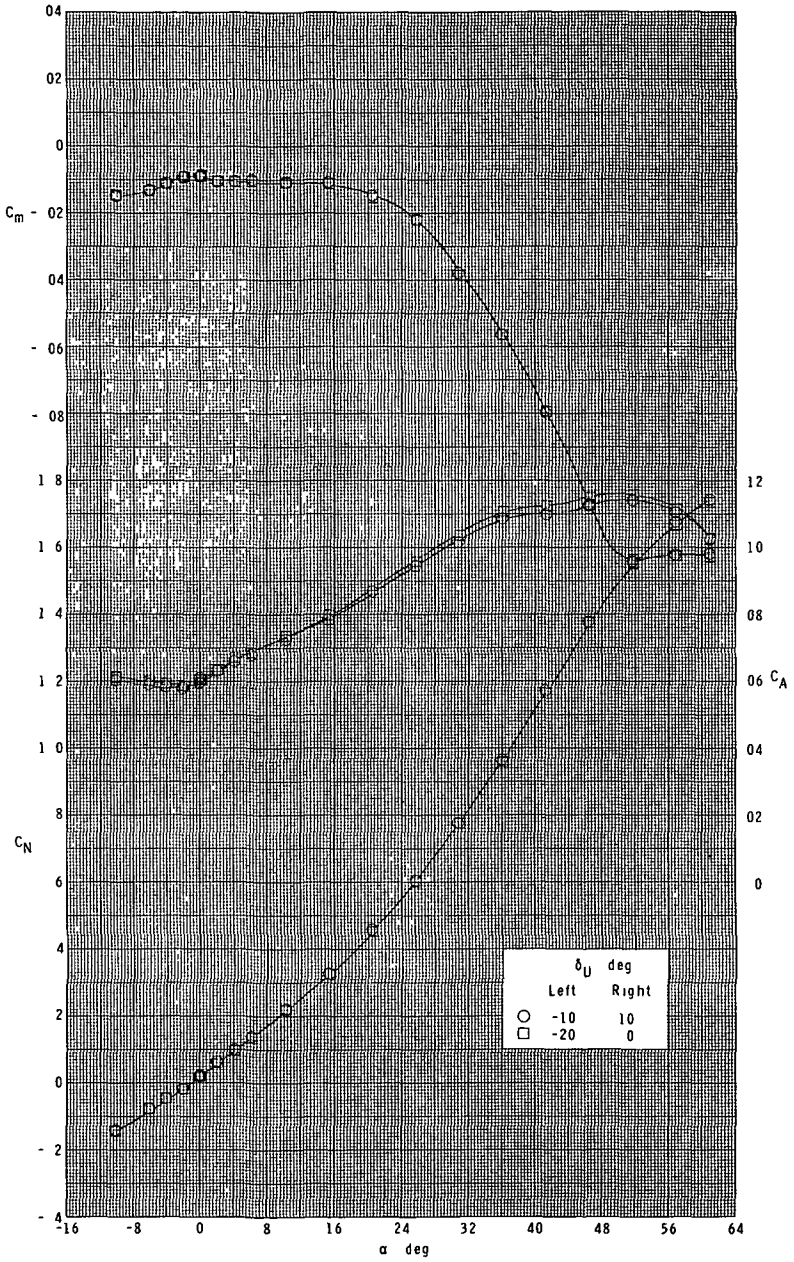

(c) M = 3.95.

Figure 29.- Continued.

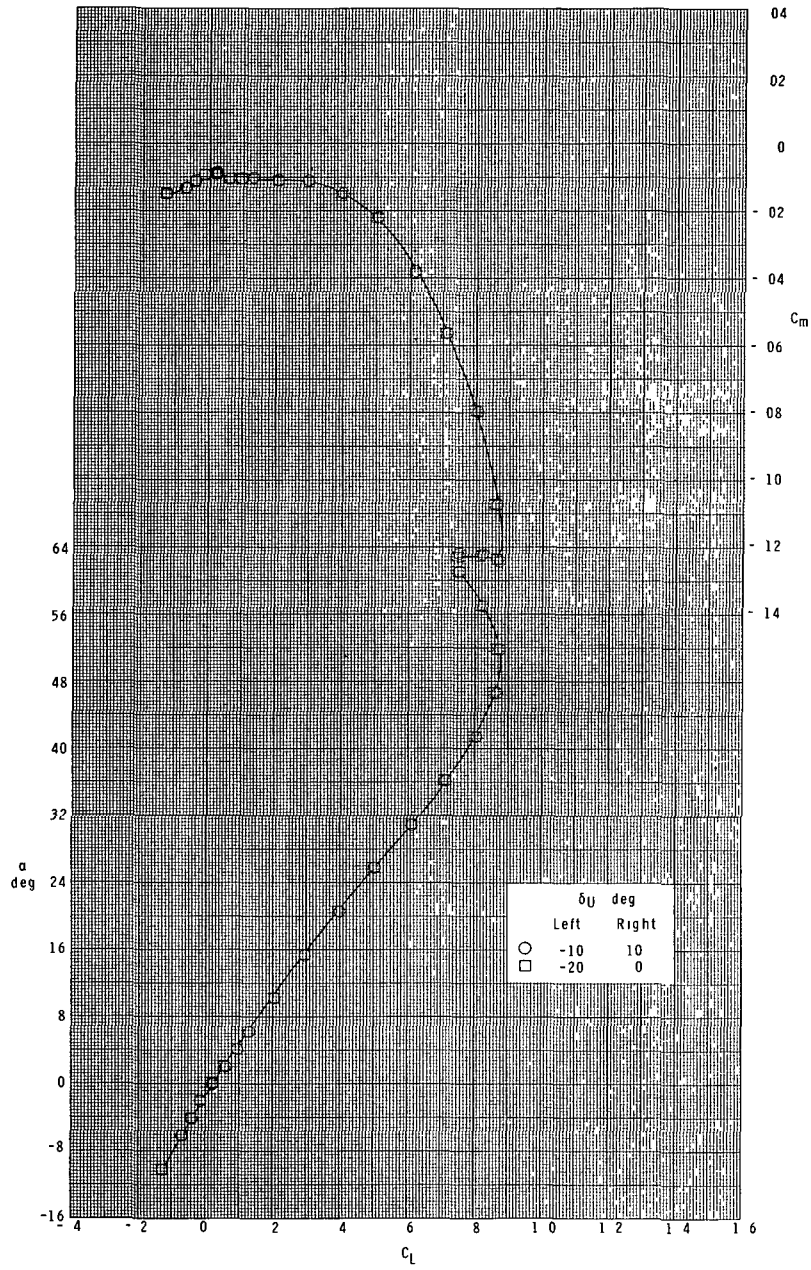

(c) Continued.

Figure 29.- Continued.

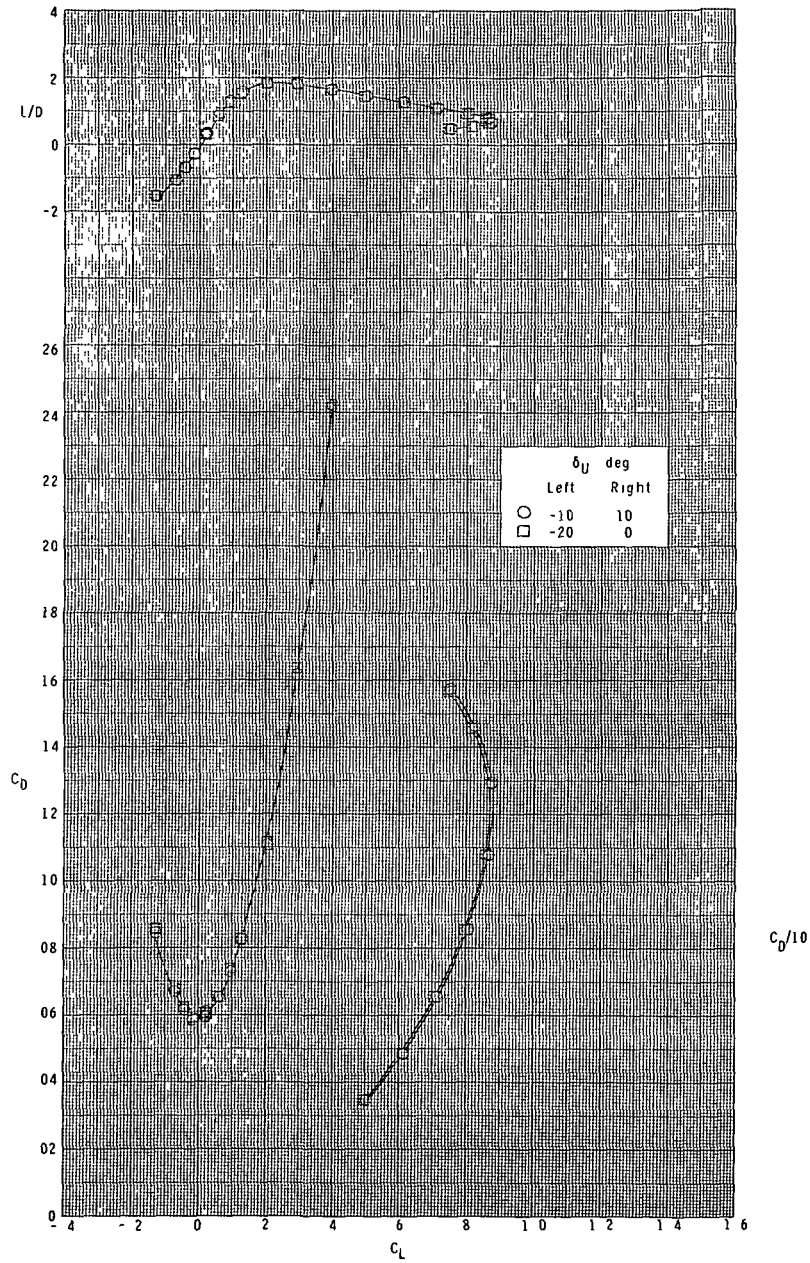

(c) Concluded.

Figure 29.- Continued.

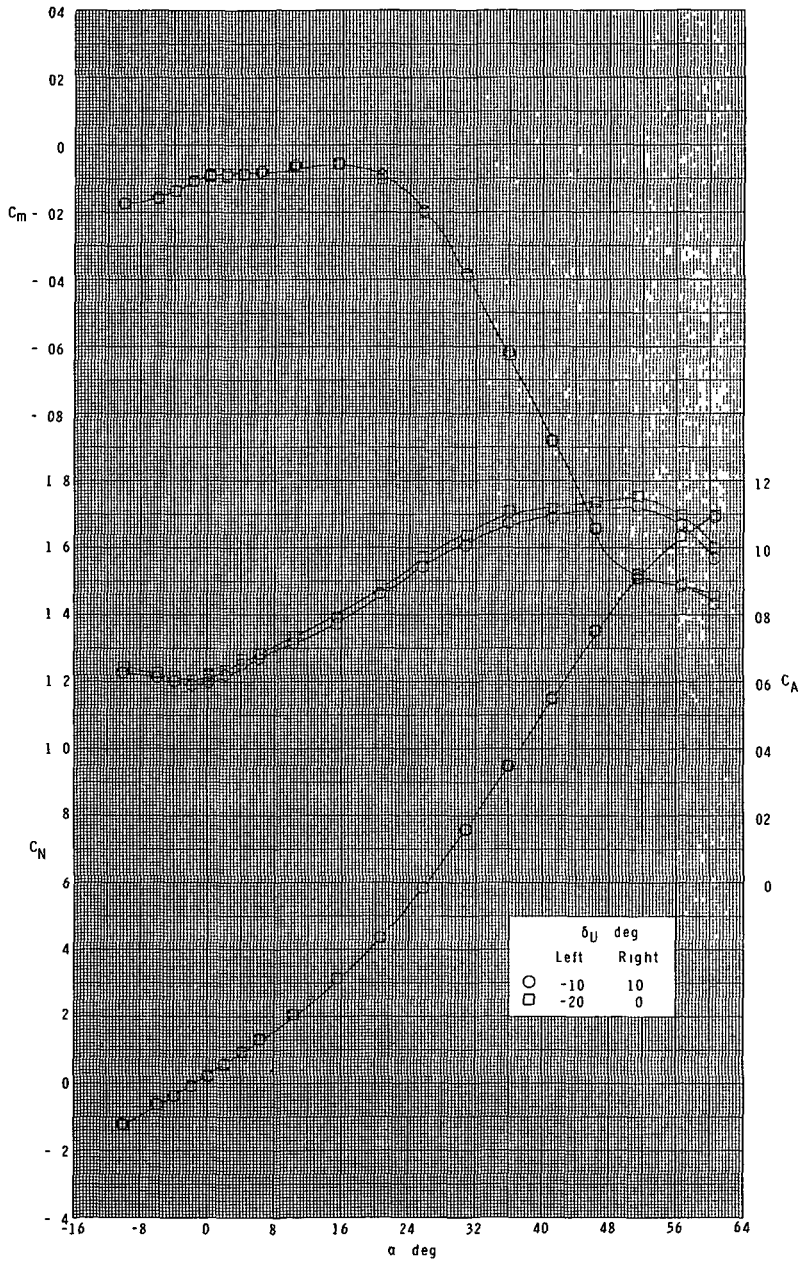

(d) M = 4.60.

Figure 29.- Continued.

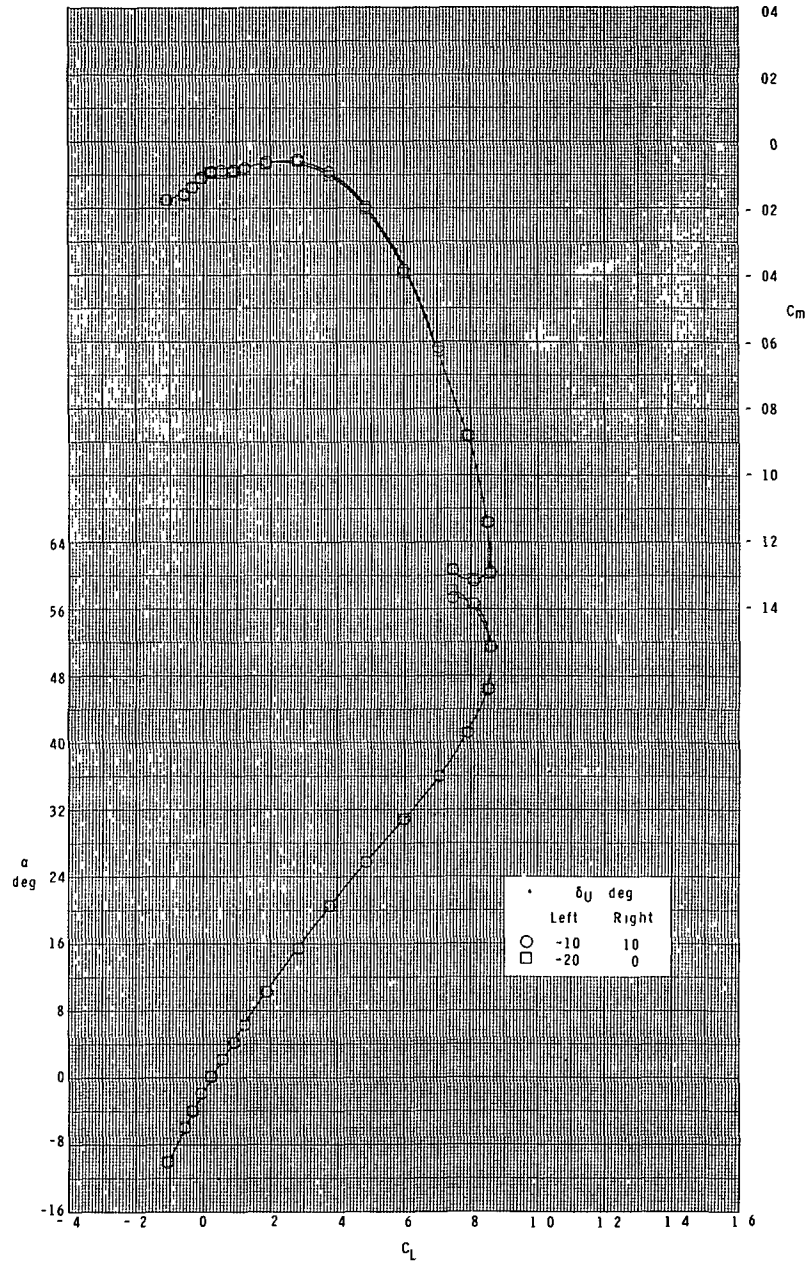

(d) Continued.

Figure 29.- Continued.

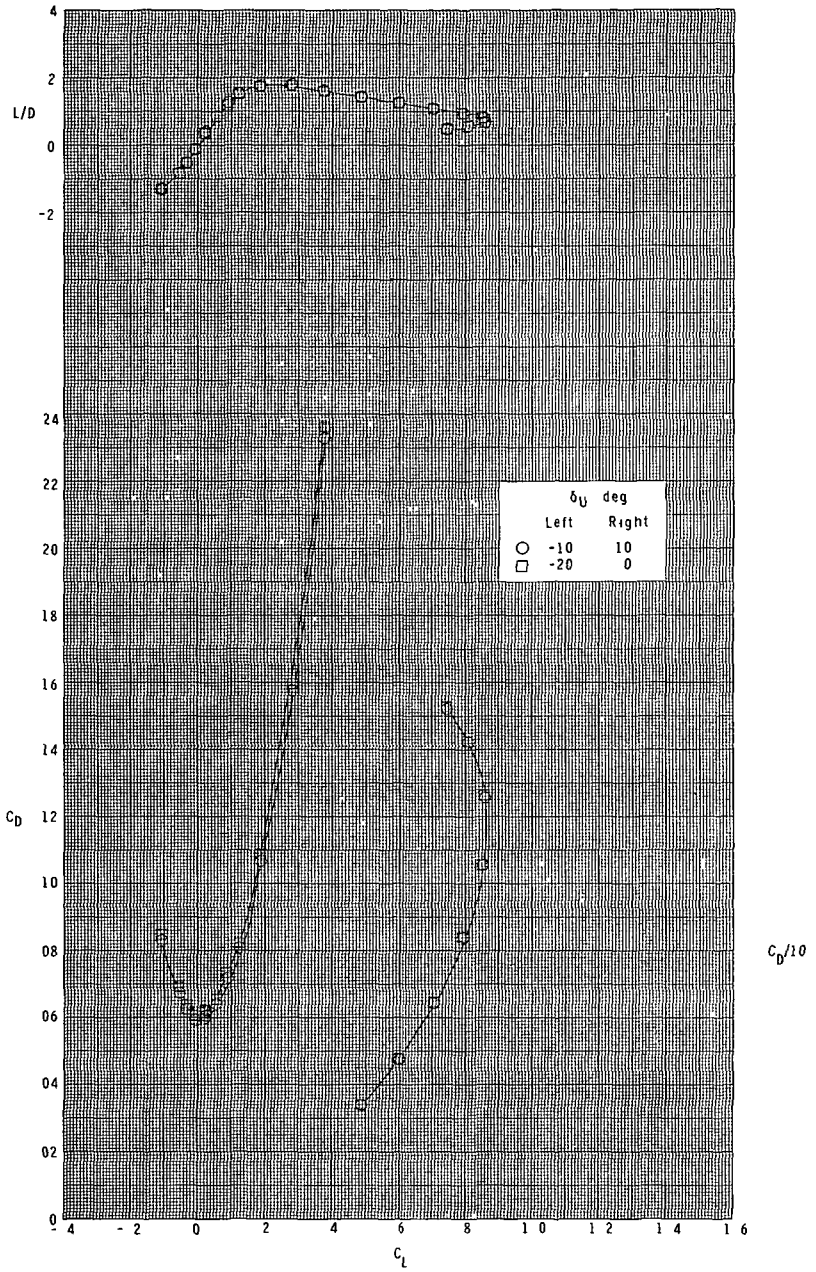

(d) Concluded.

Figure 29.- Concluded.

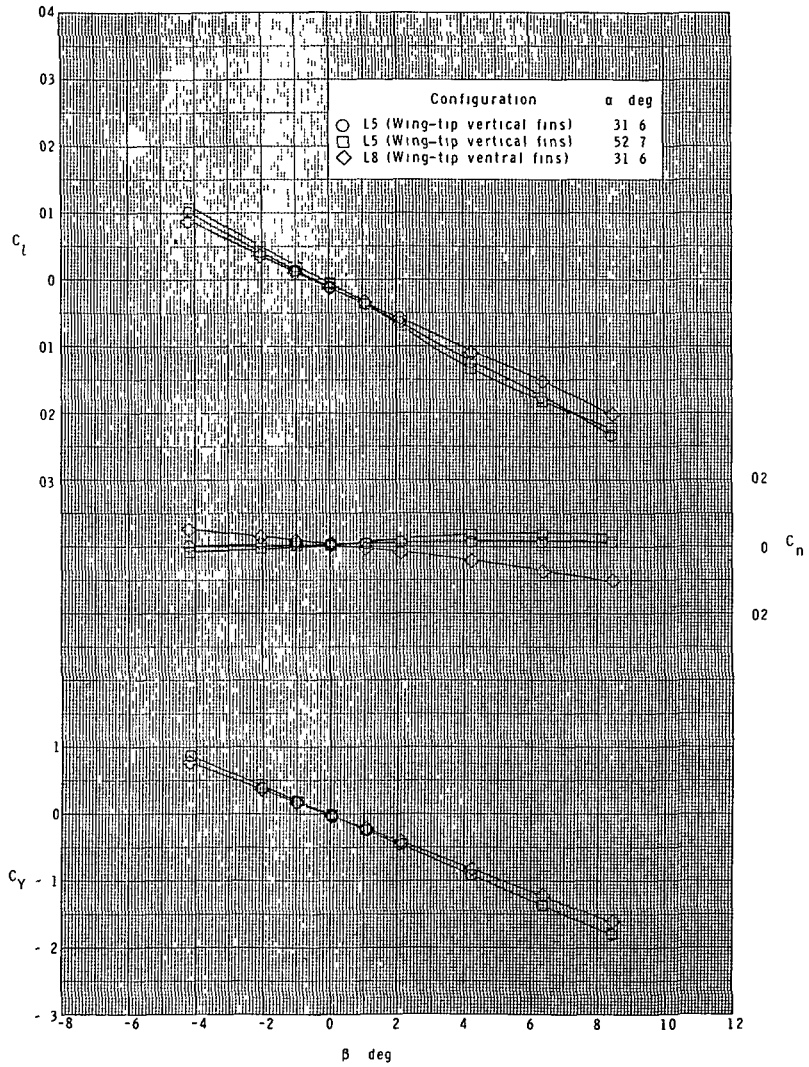

(a) M = 2.30.

Figure 30.- Lateral characteristics in sideslip. Booster configuration.

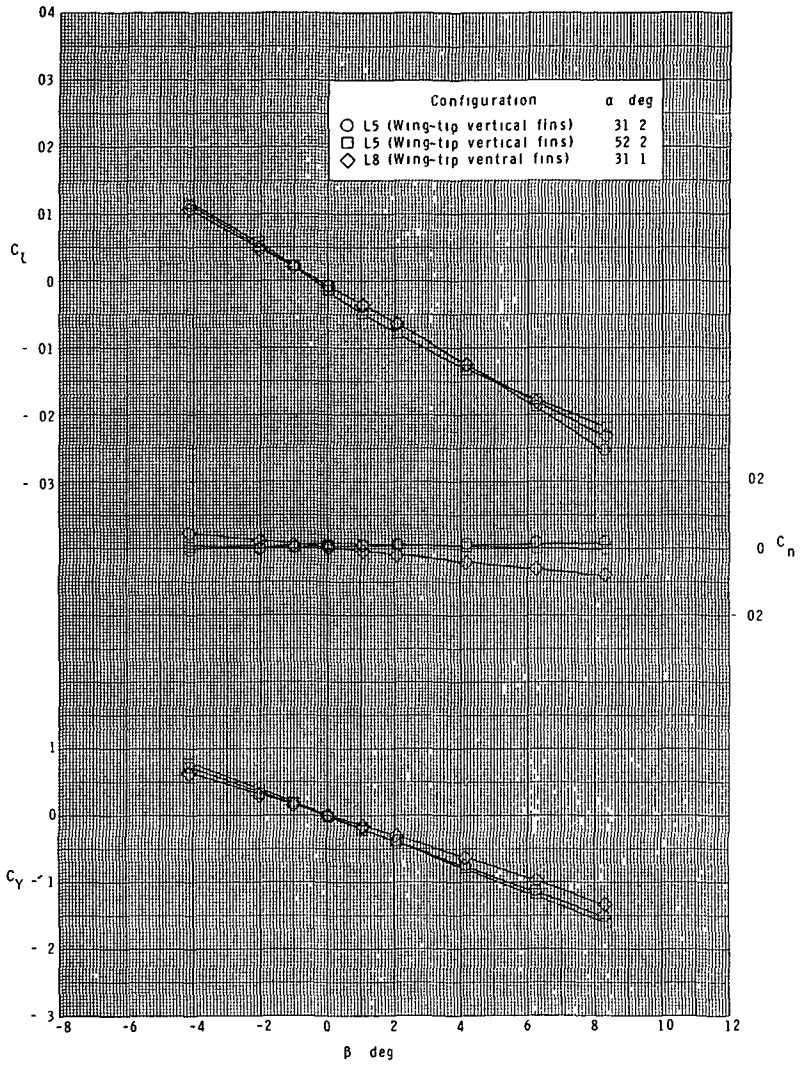

(b) M = 2.96.

Figure 30.- Continued.

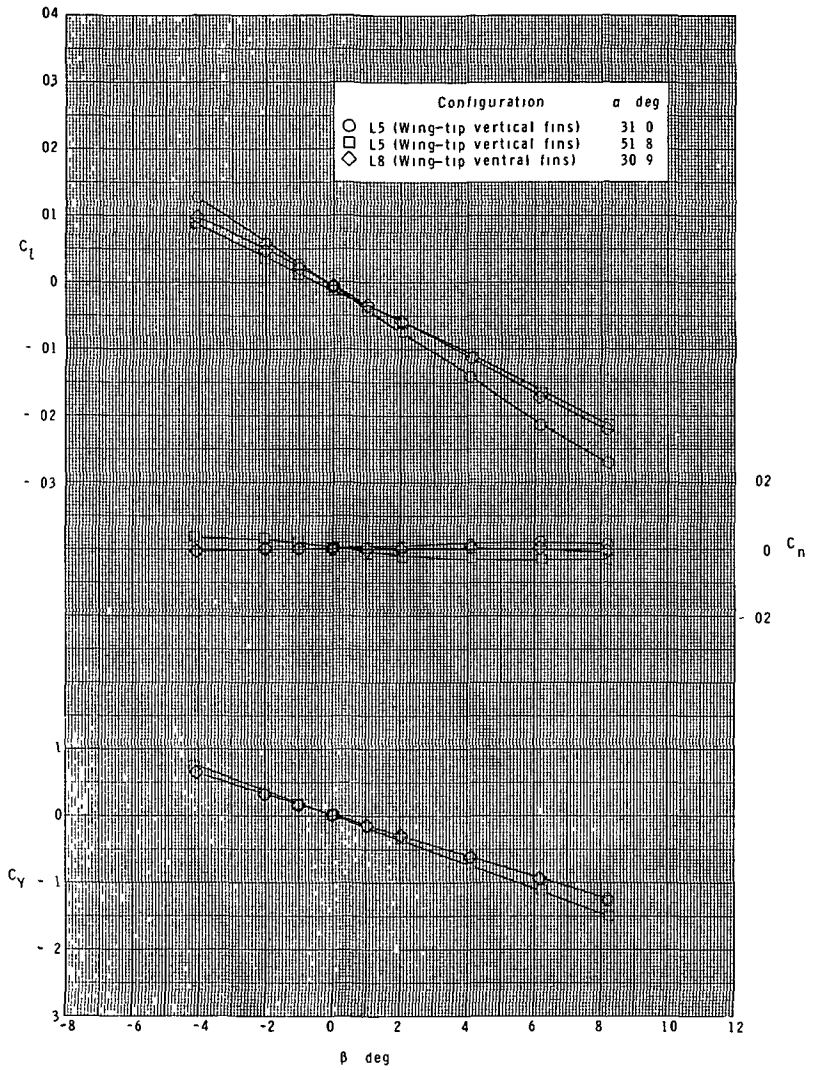

(c) M = 3.95.

Figure 30.- Continued.

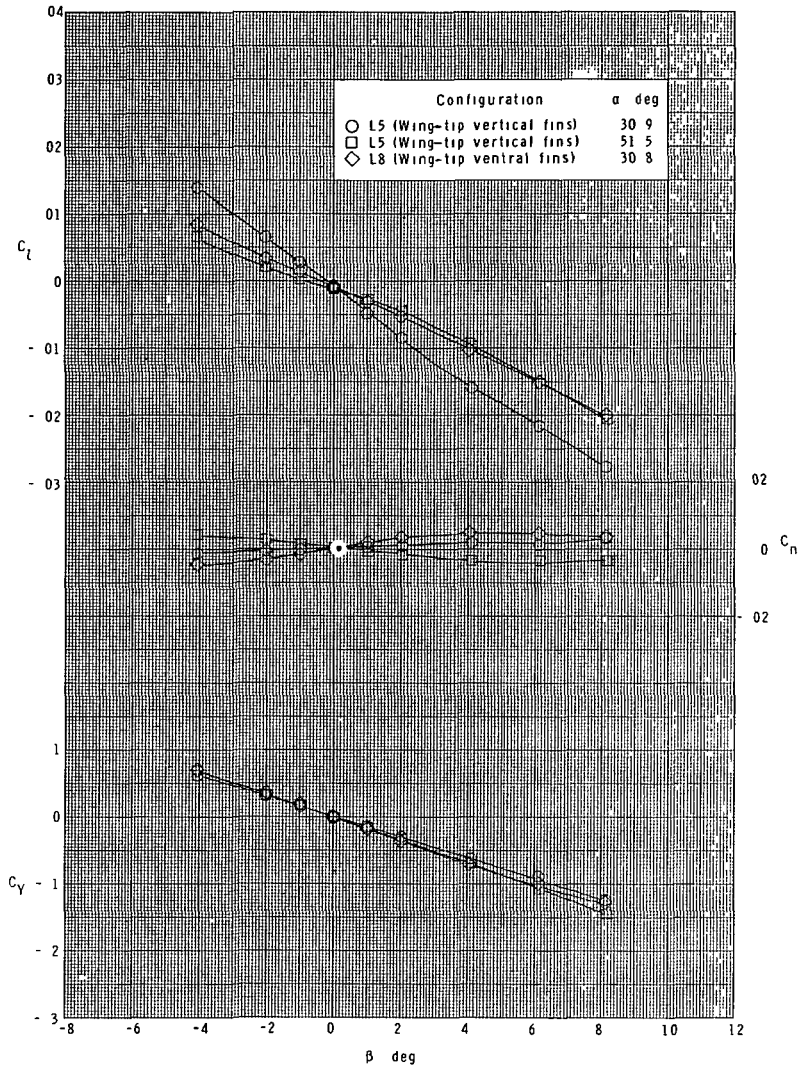

(d) M = 4.60.

Figure 30.- Concluded.

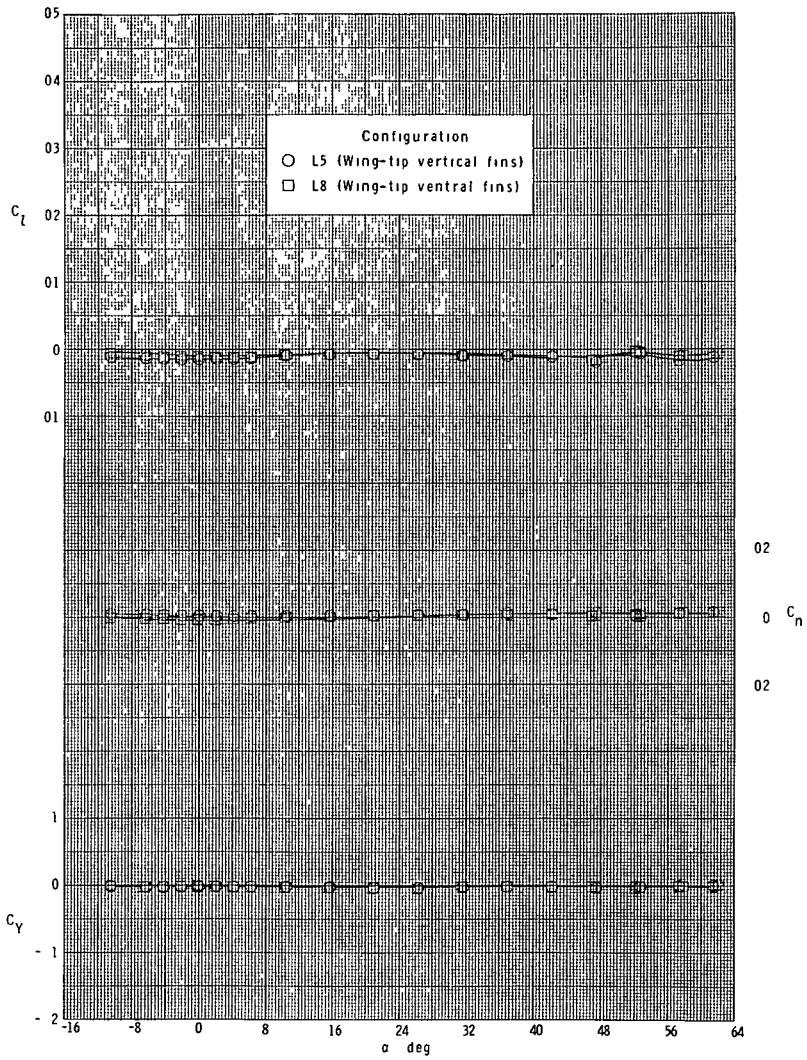

(a) M = 2.30.

Figure 31.- Effect of vertical location of wing-tip fins on lateral characteristics. Booster configuration.

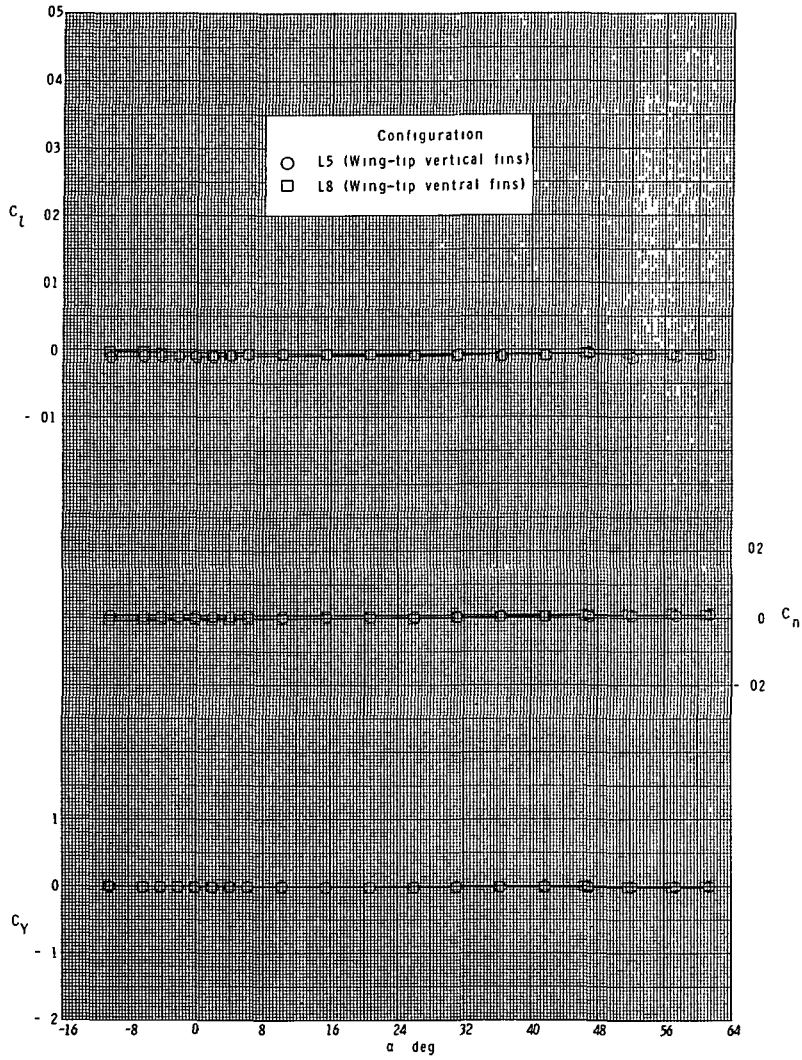

(b) M = 2.96.

Figure 31.- Continued.

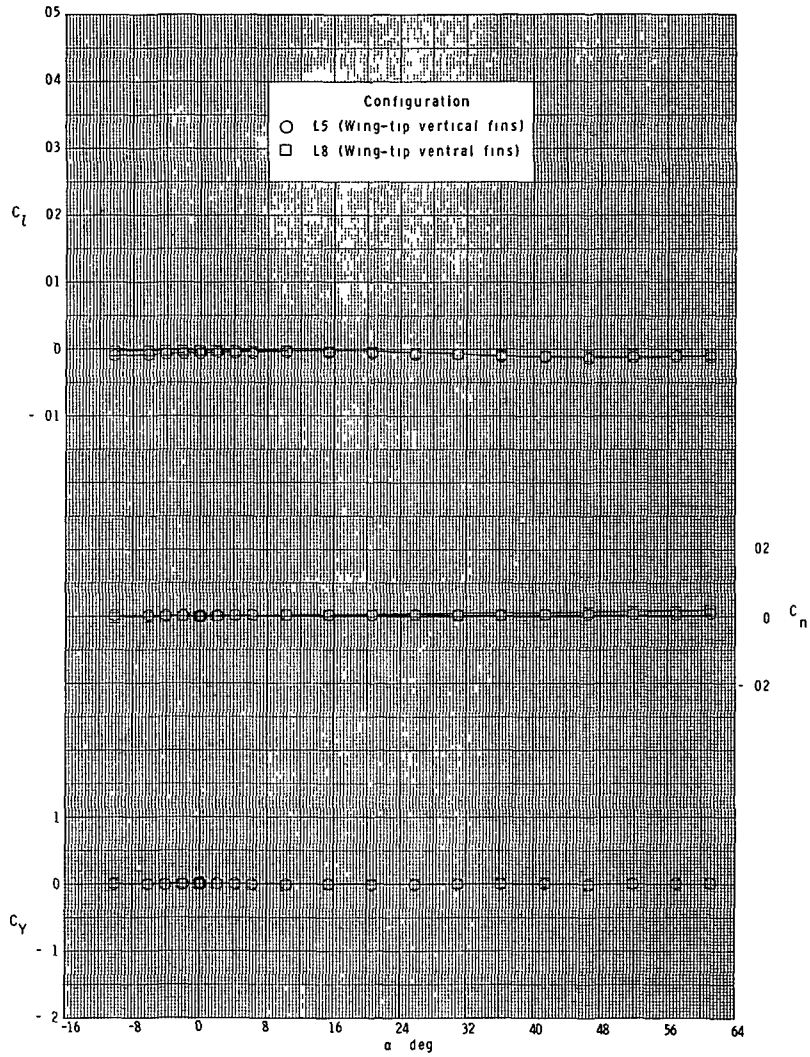

(c) M = 3.95.

Figure 31.- Continued.

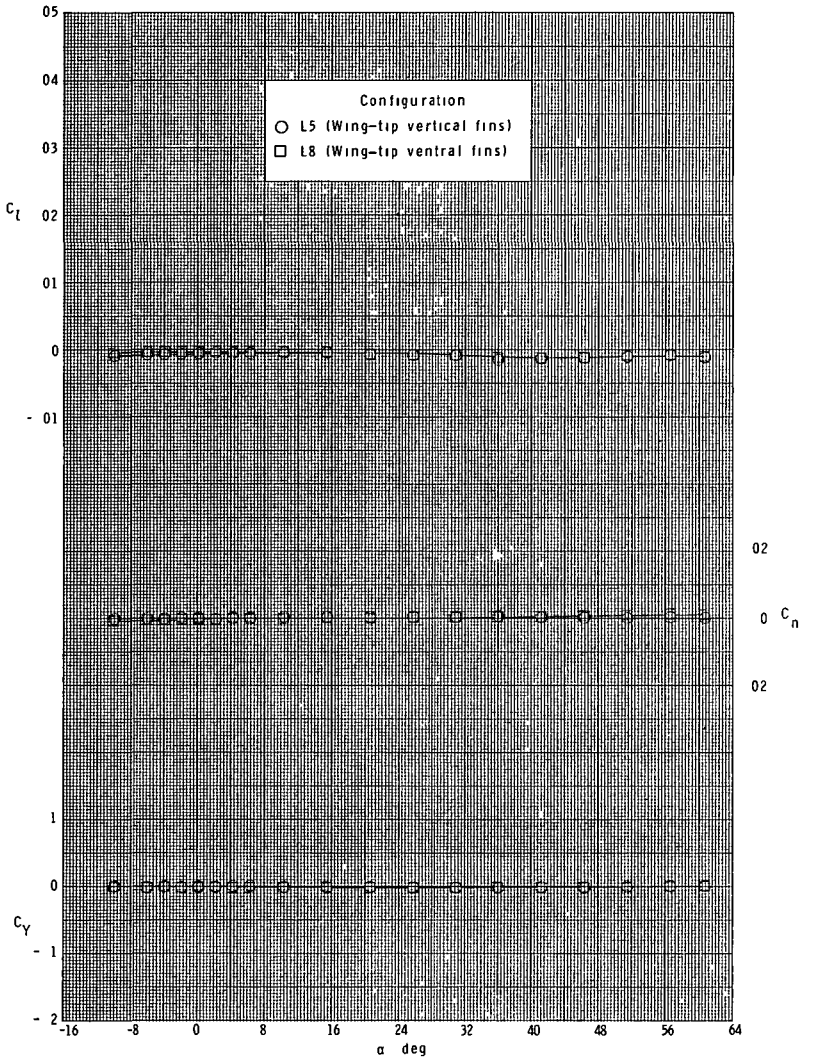

(d) M = 4.60.

Figure 31.- Concluded.

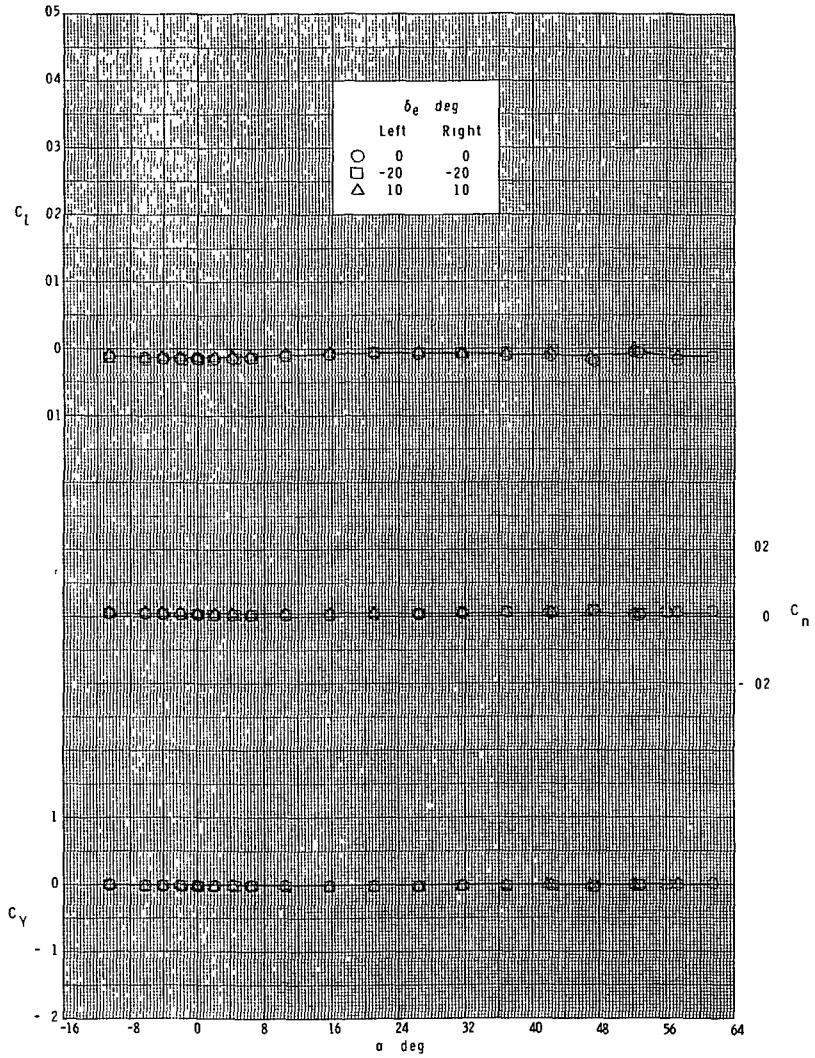

(a) M = 2.30.

Figure 32.- Effect of elevon deflection-in-pitch on lateral characteristics. Booster configuration.

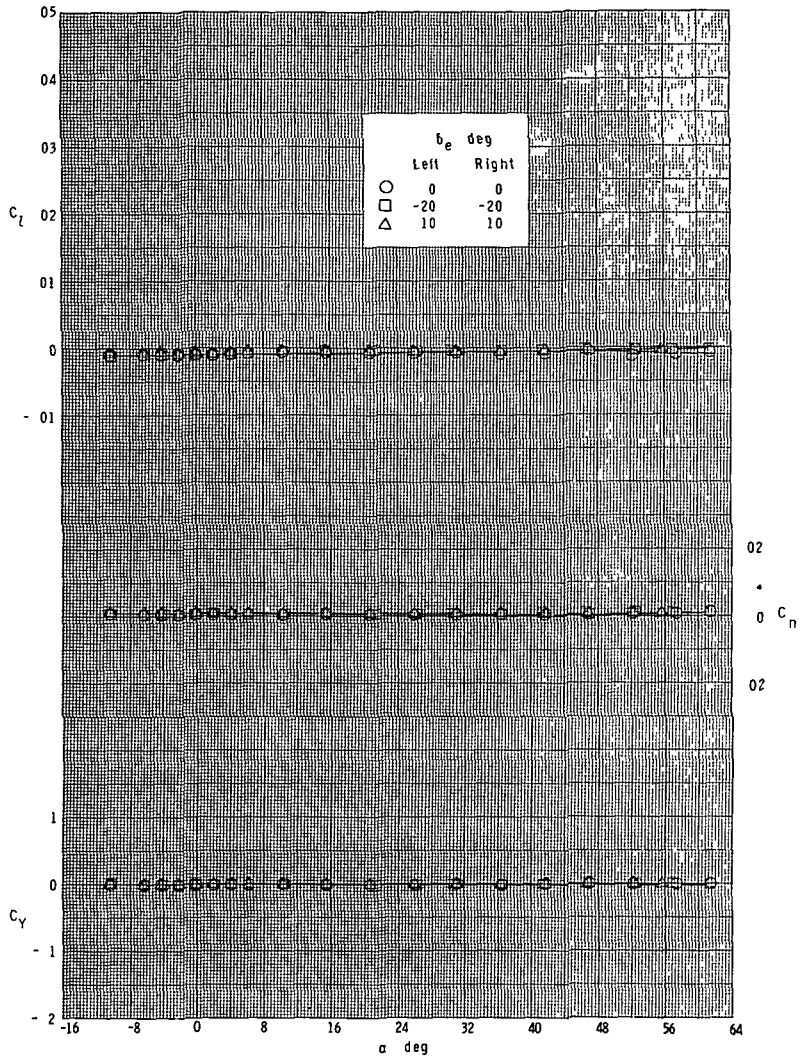

(b) M = 2.96.

Figure 32.- Continued.

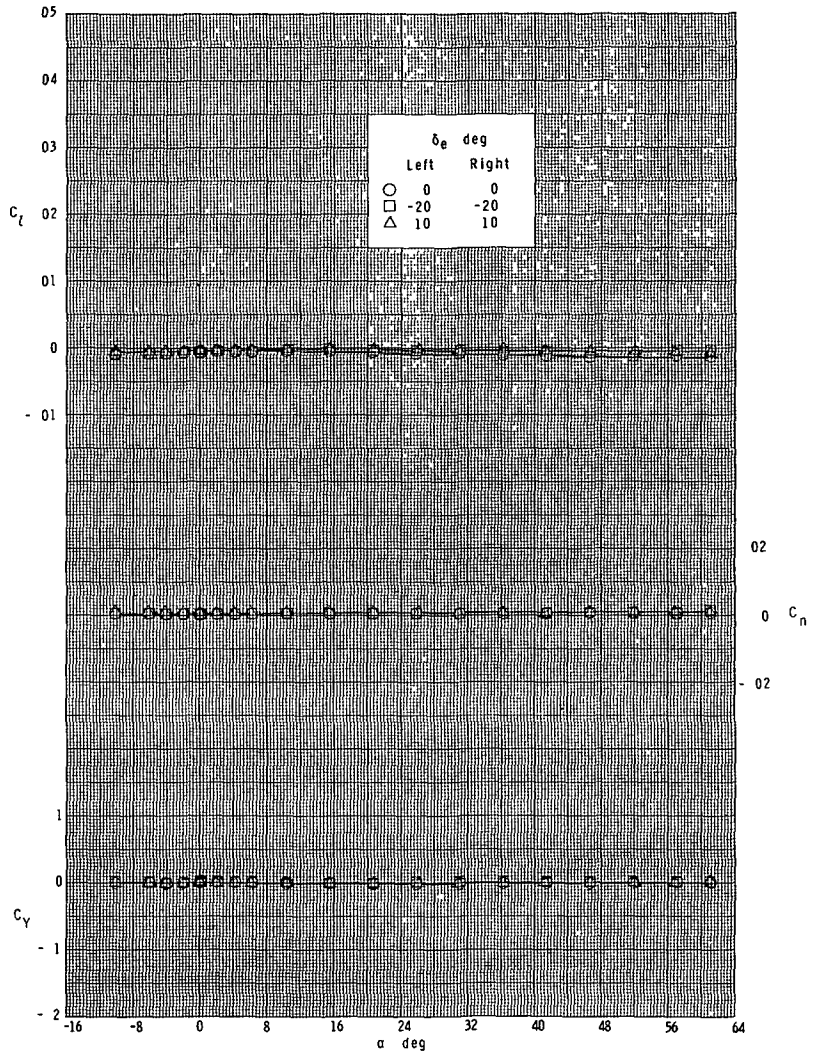

(c) M = 3.95.

Figure 32.- Continued.

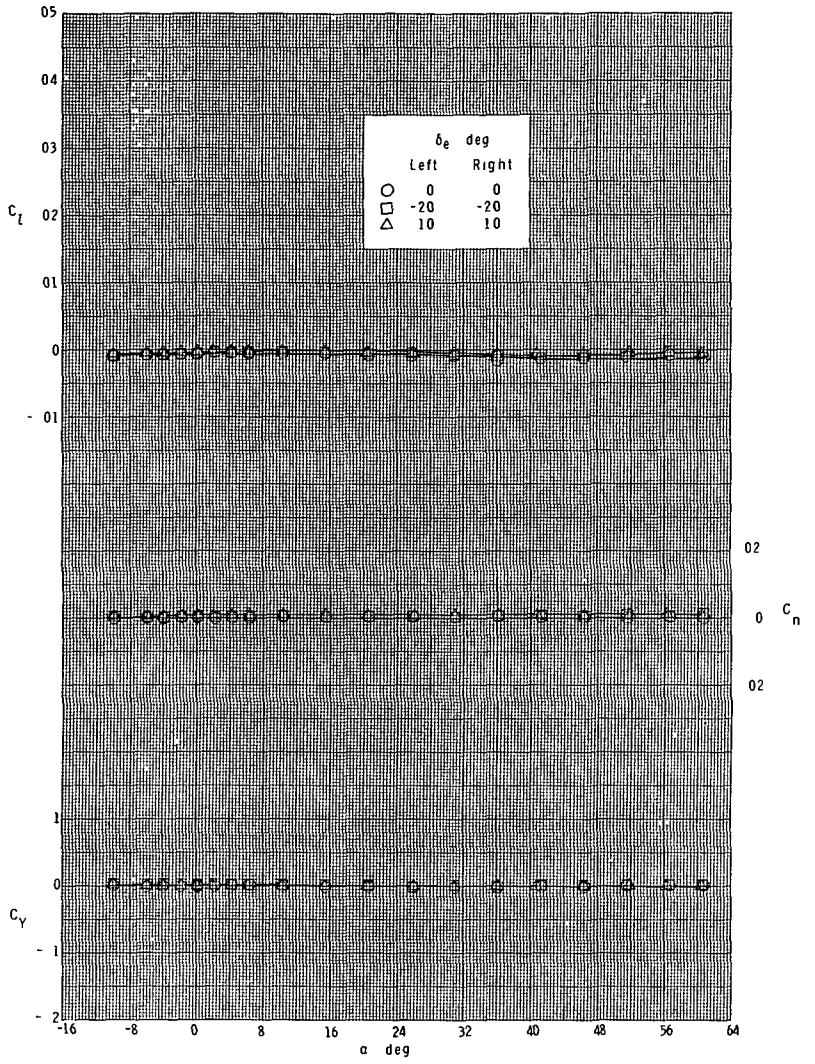

(d) M = 4.60.

Figure 32.- Concluded.

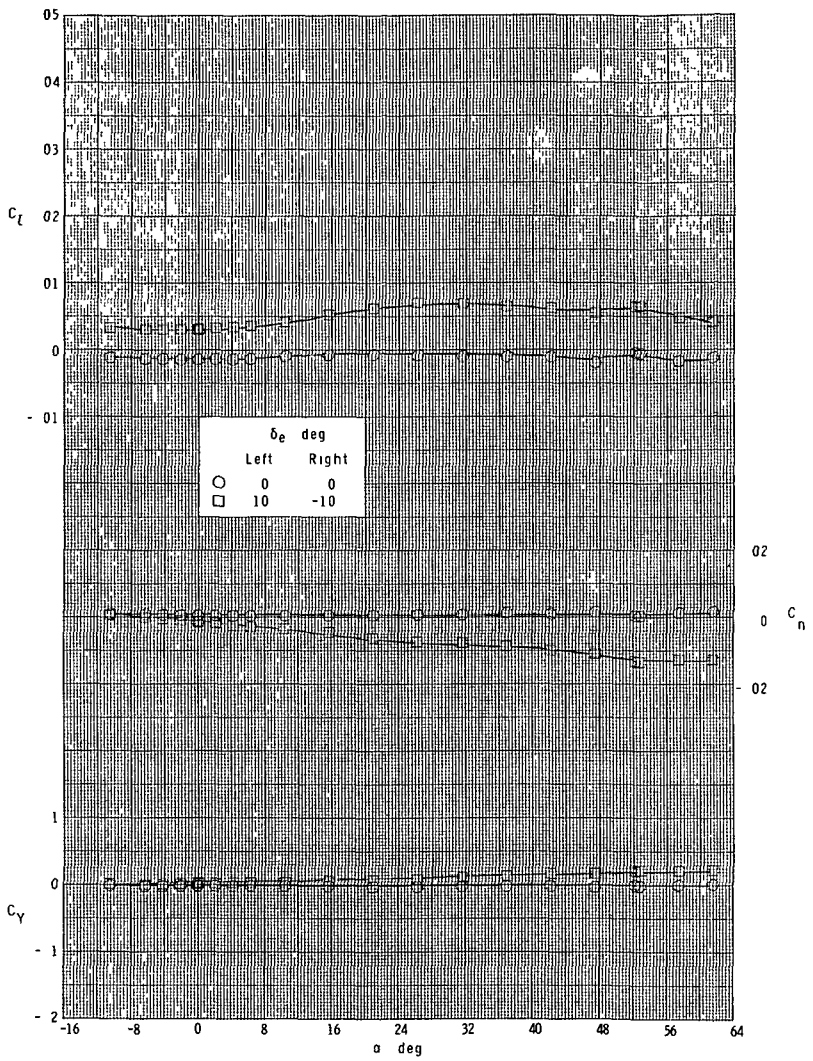

(a) M = 2.30.

Figure 33.- Elevon roll-control effectiveness. Booster configuration.

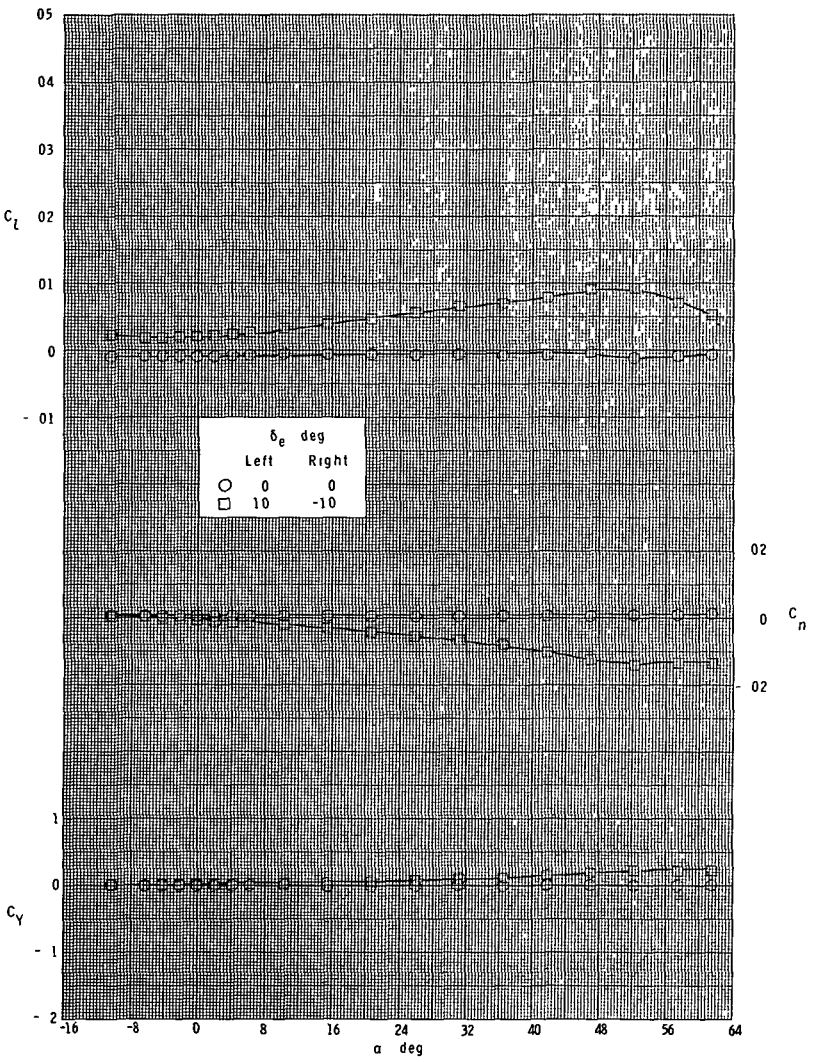

(b) M = 2.96.

Figure 33.- Continued.

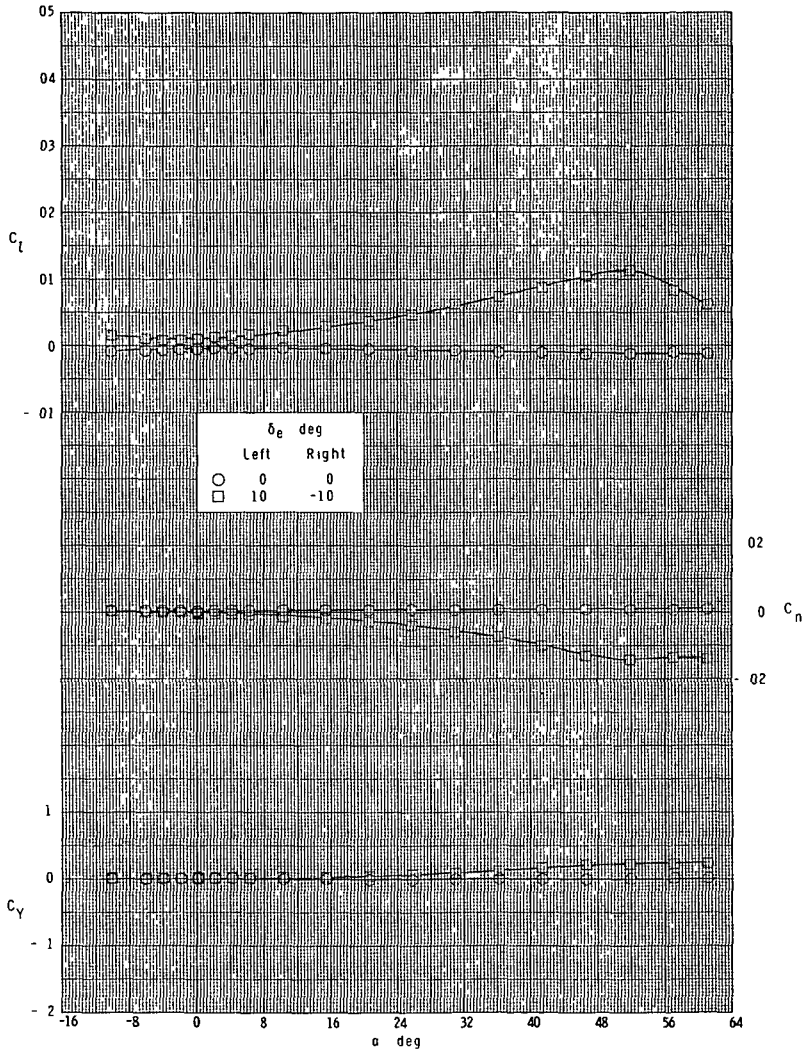

(c) M = 3.95.

Figure 33.- Continued.

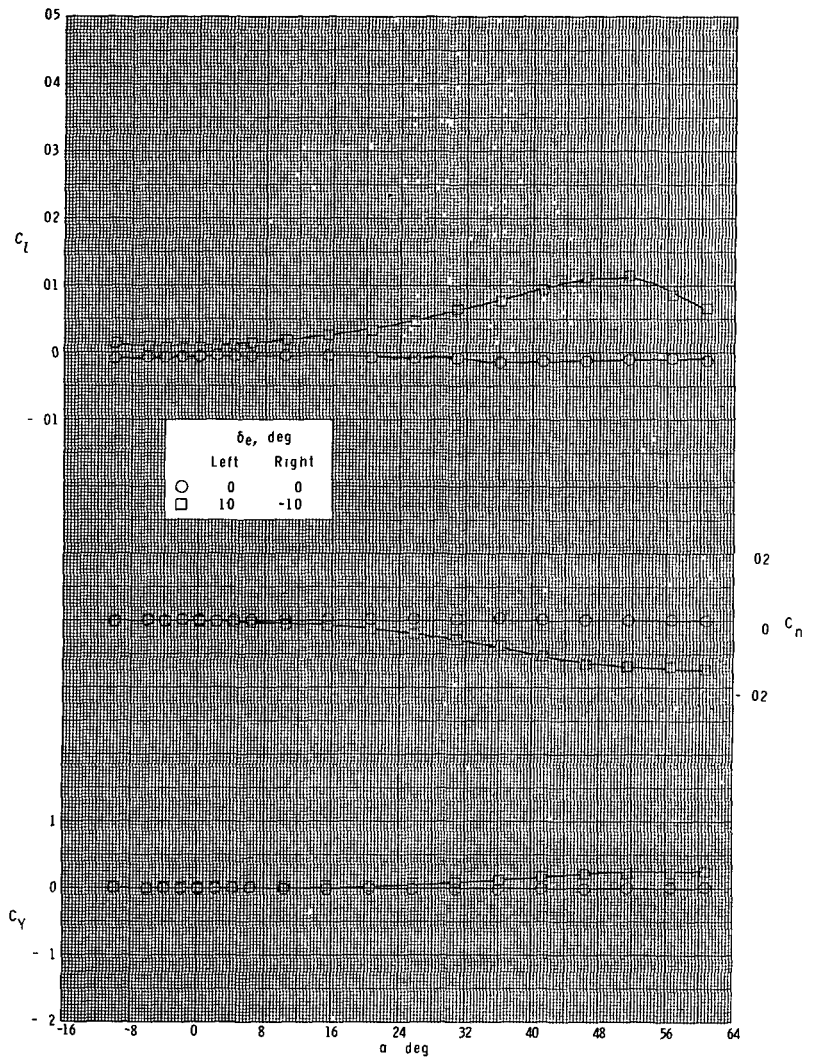

(d) M = 4.60.

Figure 33.- Concluded.

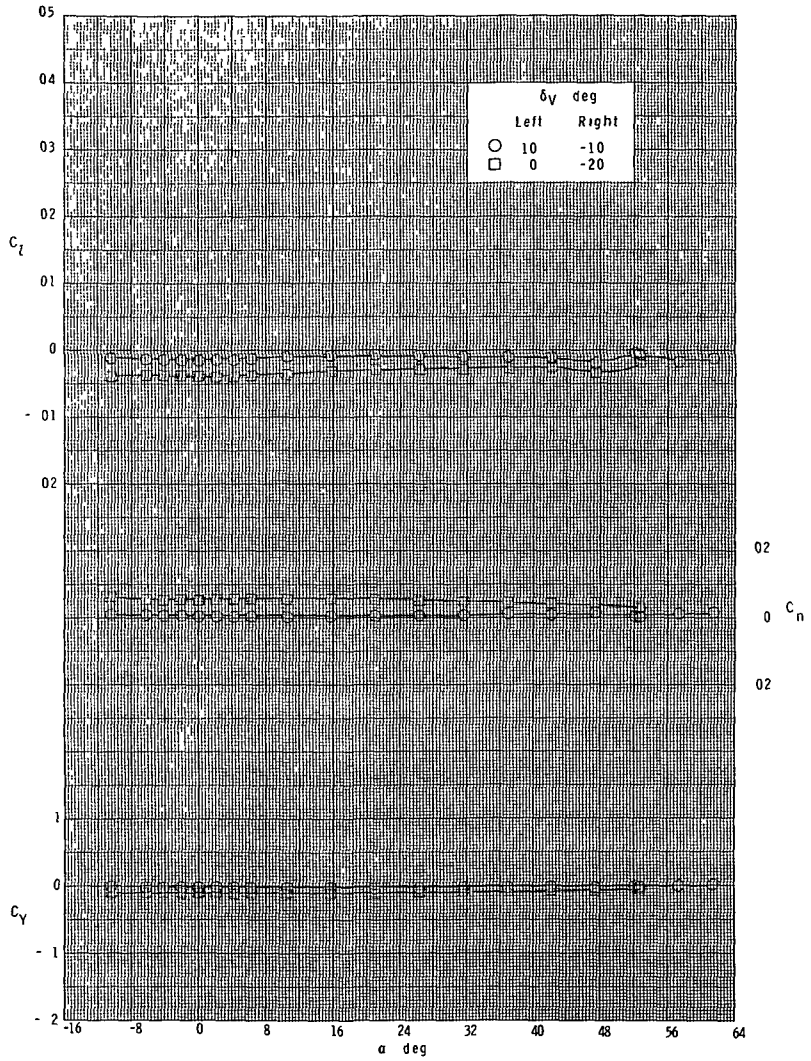

(a) M = 2.30.

Figure 34.- Effect of vertical-fin rudder deflection on lateral characteristics. Booster configuration.

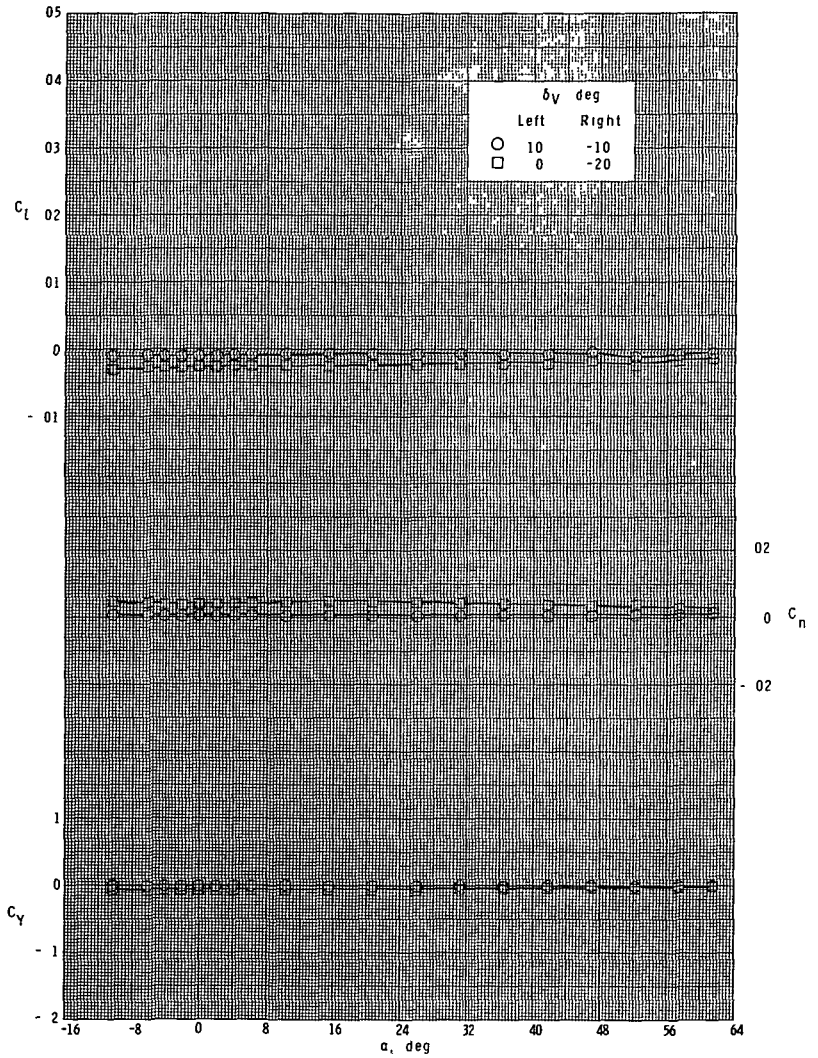

(b) M = 2.96.

Figure 34.- Continued.

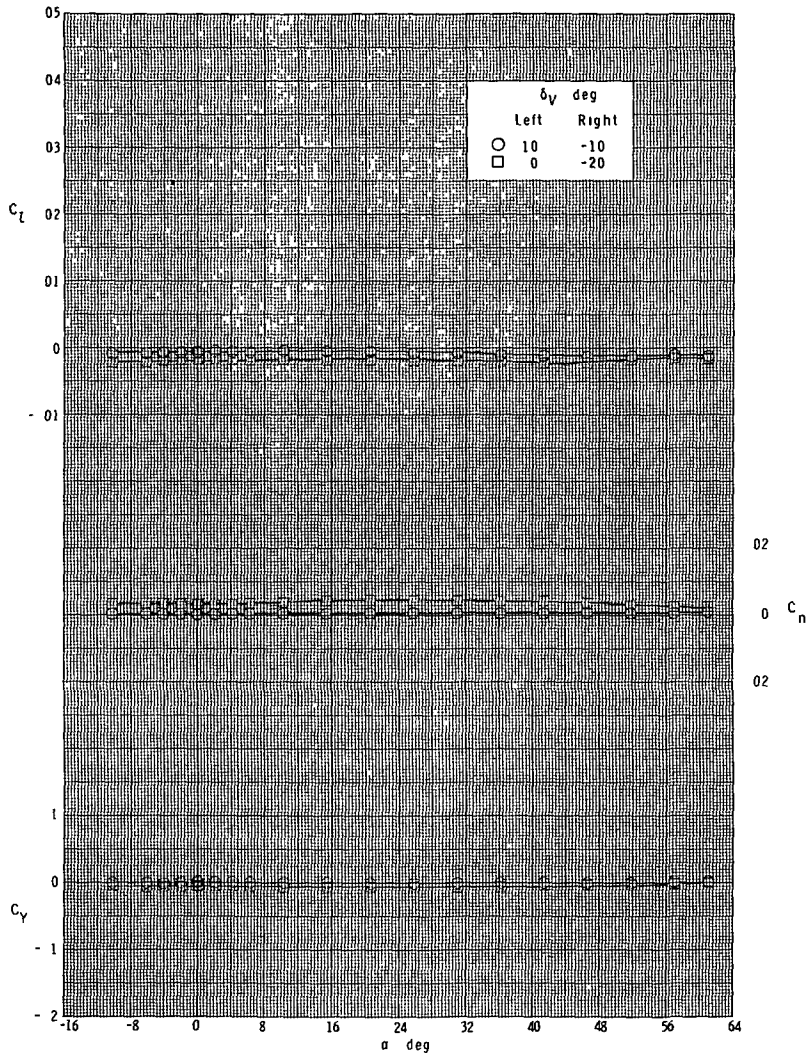

(c) M = 3.95.

Figure 34.- Continued.

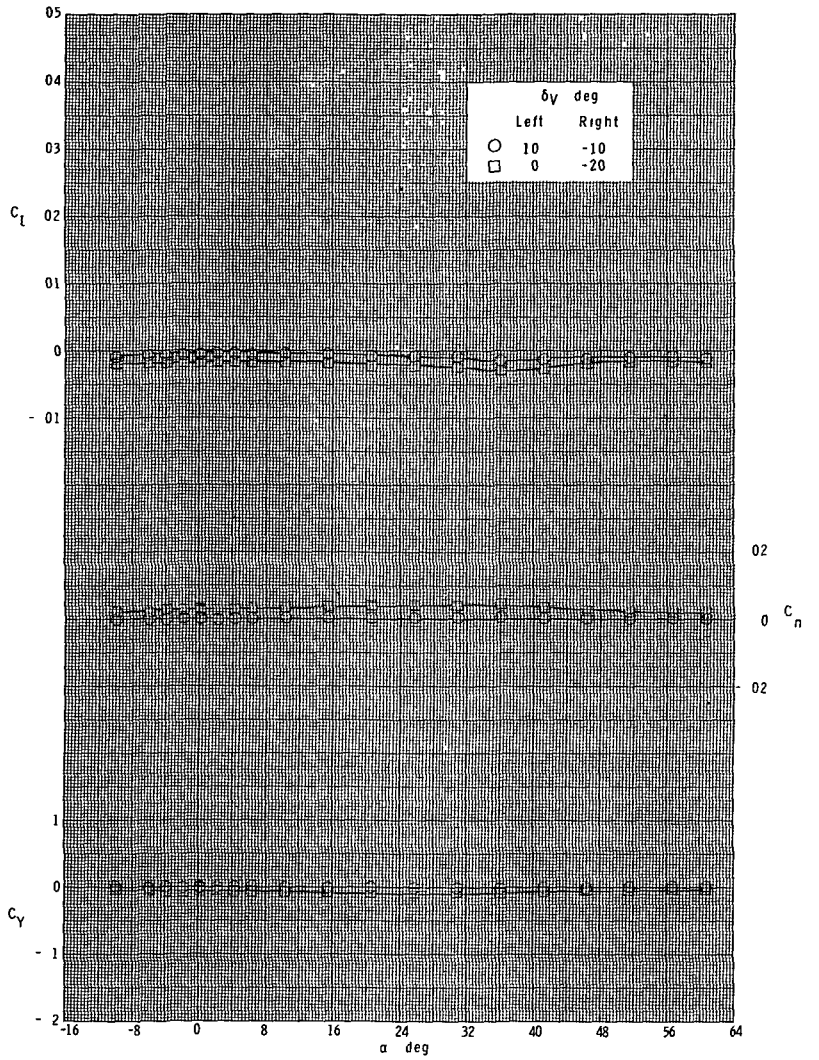

(d) M = 4.60.

Figure 34.- Concluded.

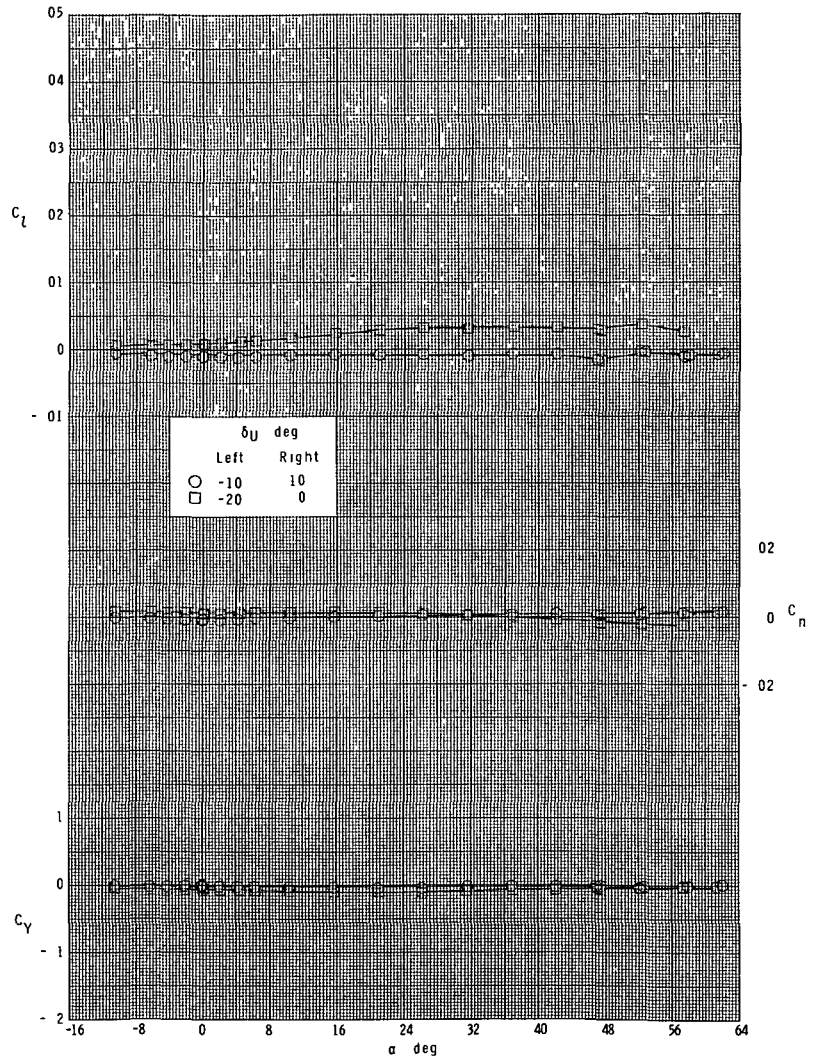

(a) M = 2.30.

Figure 35.- Effect of ventral-fin rudder deflection on lateral characteristics. Booster configuration.

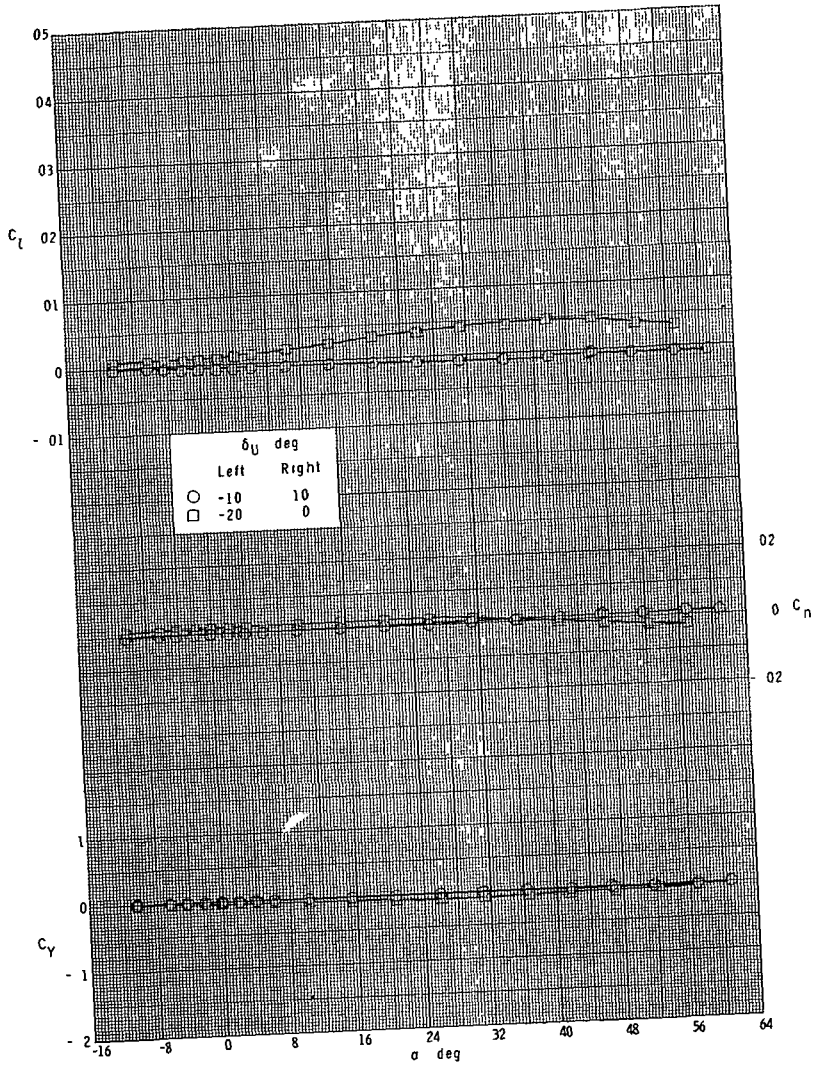

(b) M = 2.96.

Figure 35.- Continued.

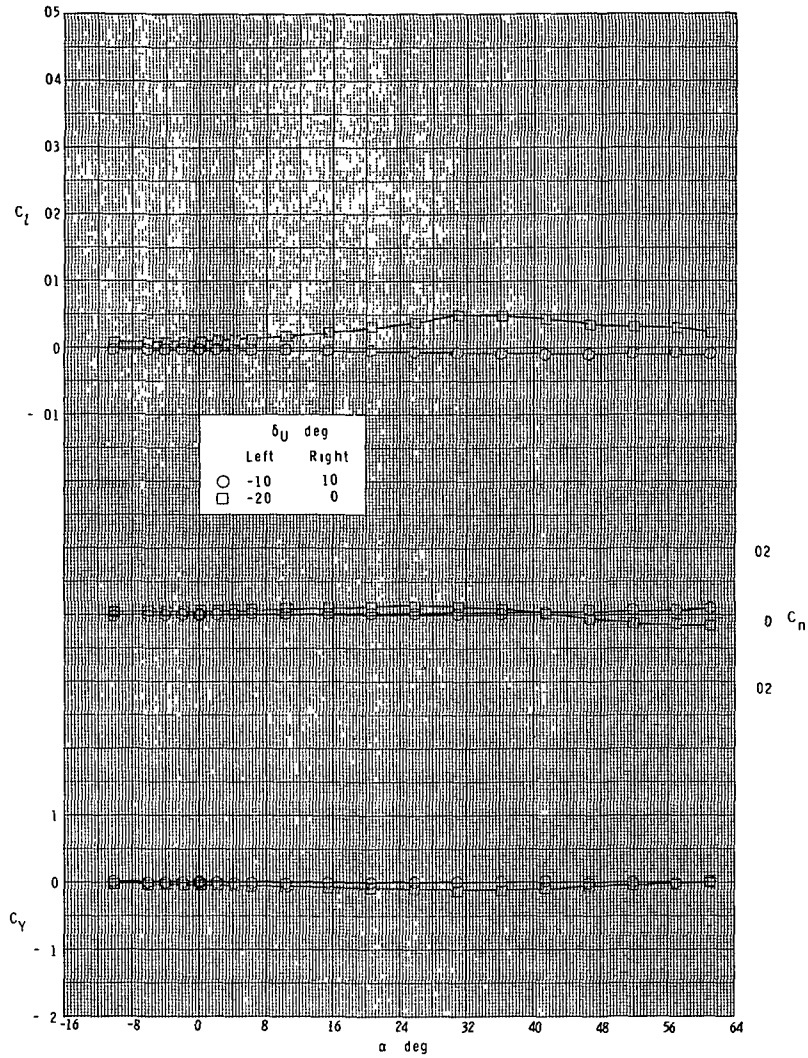

(c) M = 3.95.

Figure 35.- Continued.

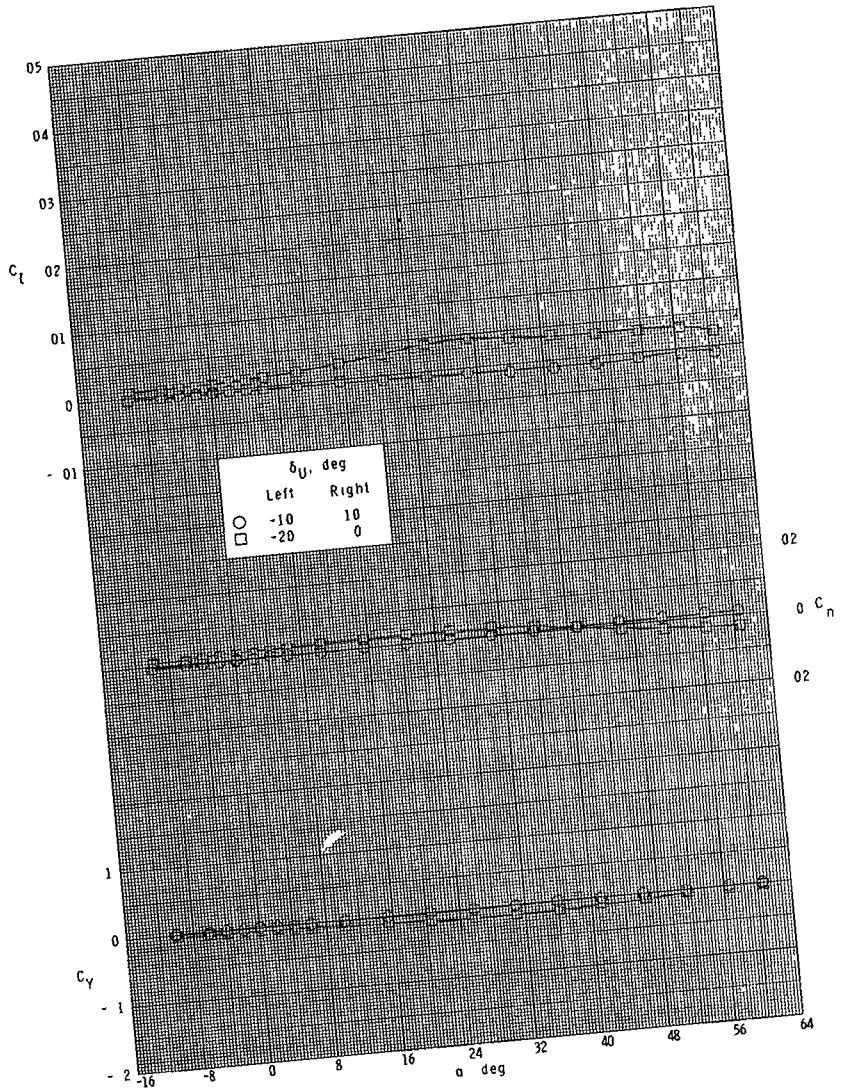

(d) M = 4.60.

Figure 35.- Concluded.

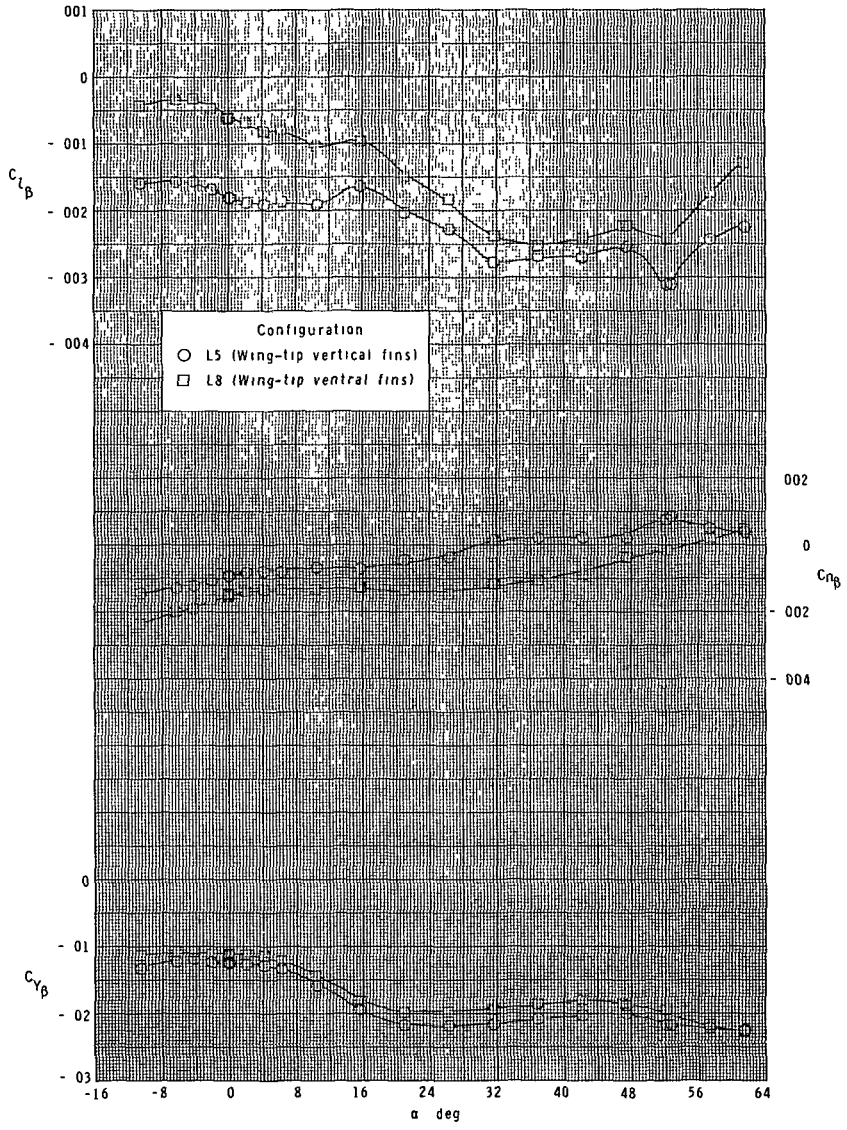

(a) M = 2.30.

Figure 36.- Lateral-stability parameters. Booster configuration.

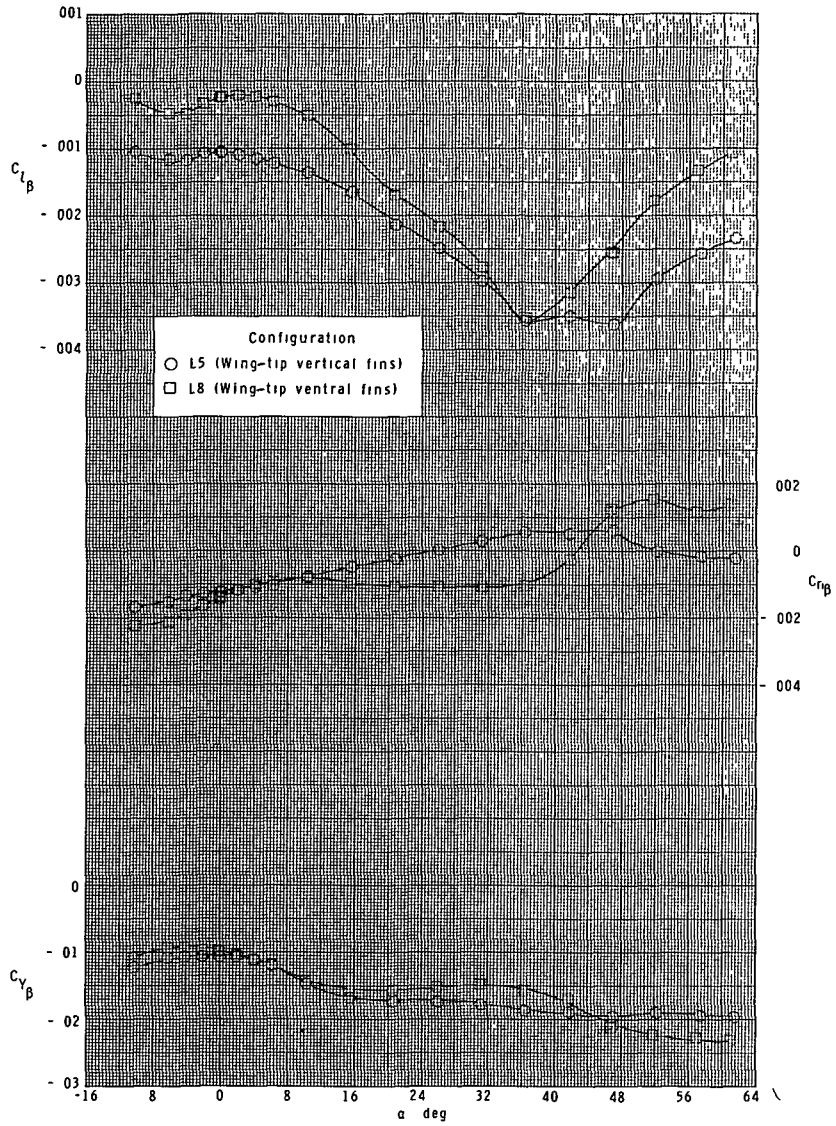

(b) M = 2.96.

Figure 36.- Continued.

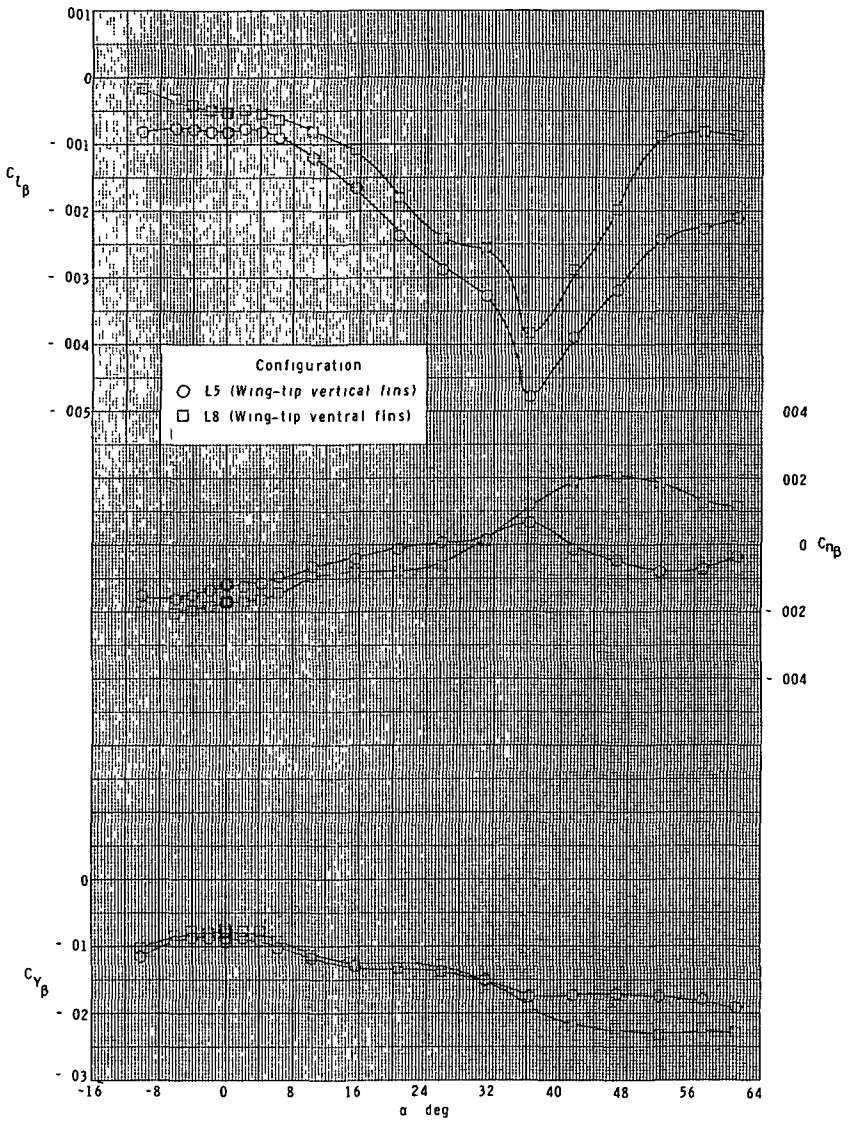

(c) M = 3.95.

Figure 36.- Continued.

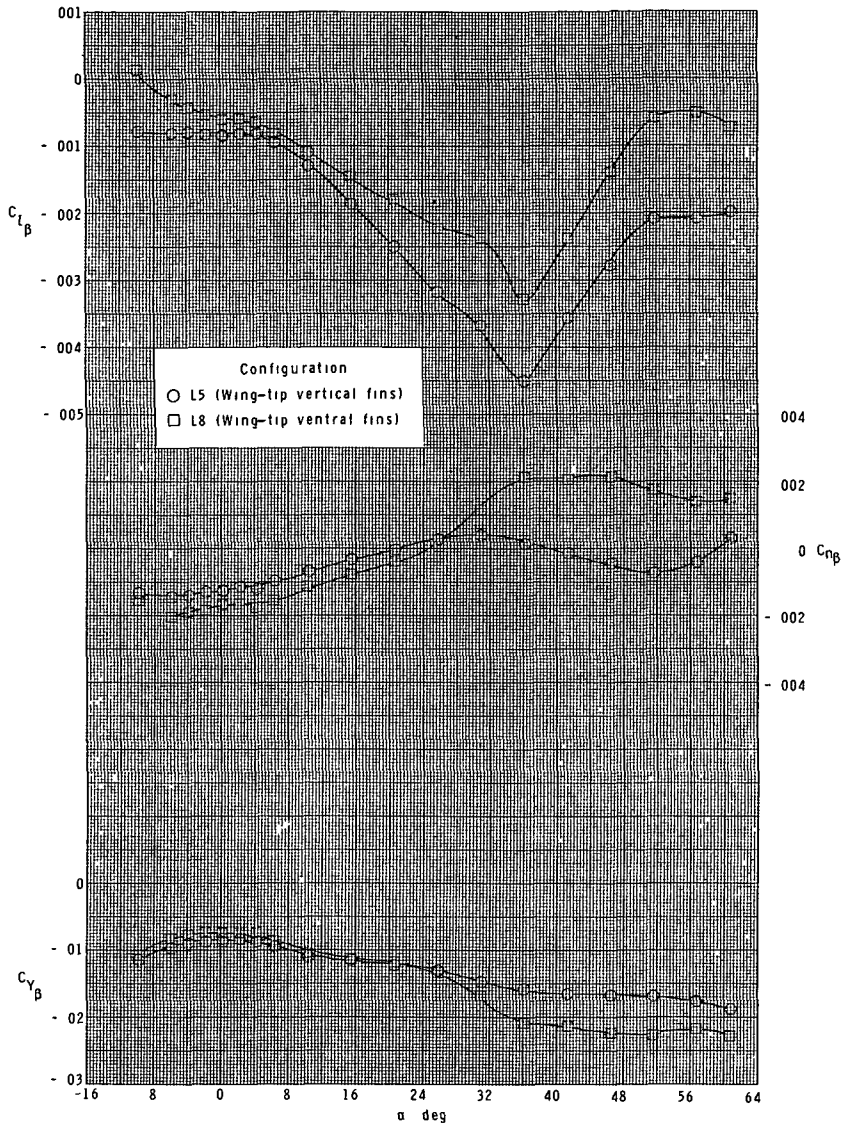

(d) M = 4.60.

Figure 36.- Concluded

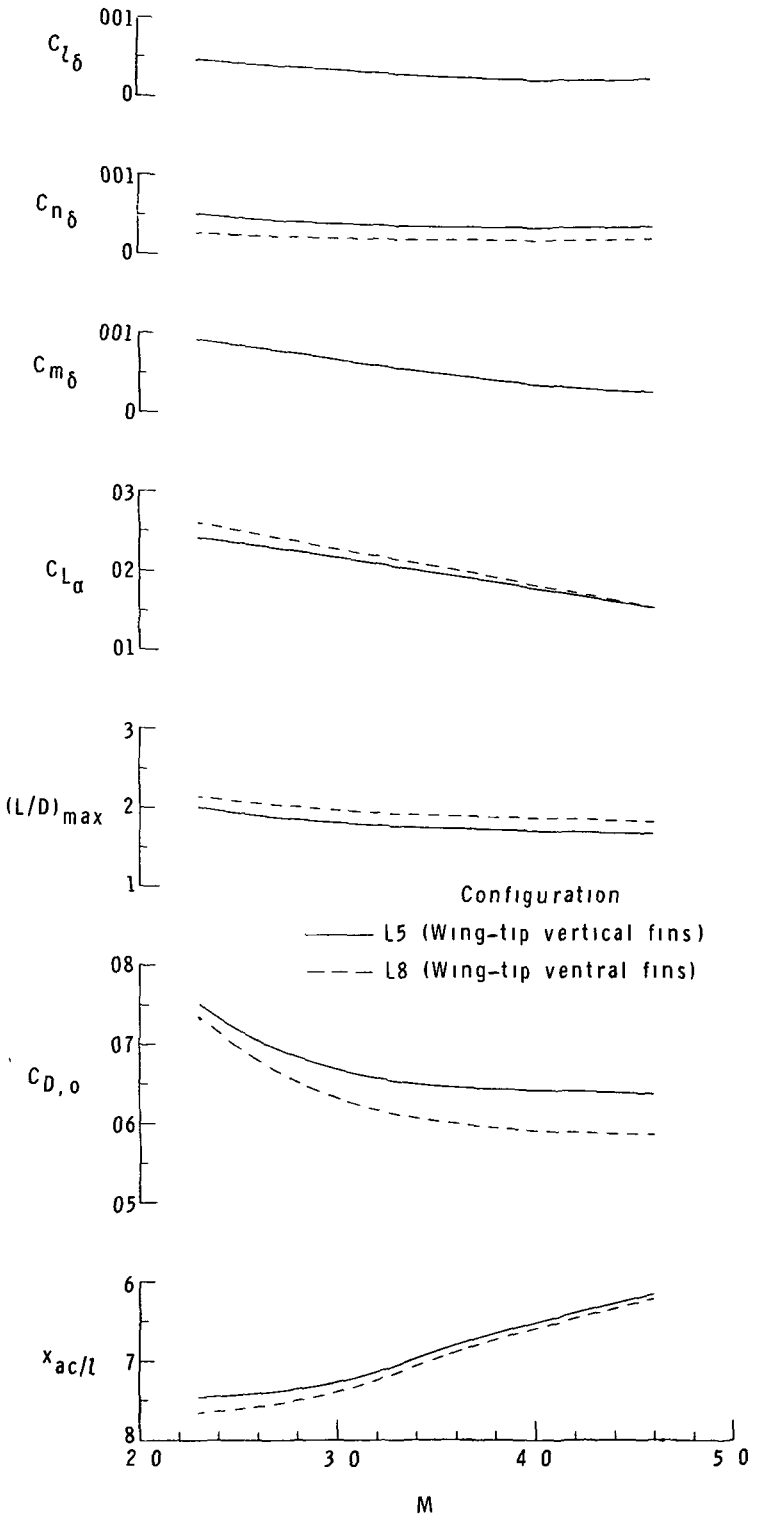

Figure 37.- Summary of characteristics.
Booster configuration.

NATIONAL AERONAUTICS AND SPACE ADMINISTRATION
WASHINGTON, D.C. 20546

OFFICIAL BUSINESS
PENALTY FOR PRIVATE USE $300

FIRST CLASS MAIL

POSTAGE AND FEES PAID
NATIONAL AERONAUTICS AND
SPACE ADMINISTRATION
451

U.S.MAIL

POSTMASTER: If Undeliverable (Section 158 Postal Manual) Do Not Return

"The aeronautical and space activities of the United States shall be conducted so as to contribute . . . to the expansion of human knowledge of phenomena in the atmosphere and space. The Administration shall provide for the widest practicable and appropriate dissemination of information concerning its activities and the results thereof."

—NATIONAL AERONAUTICS AND SPACE ACT OF 1958

NASA SCIENTIFIC AND TECHNICAL PUBLICATIONS

TECHNICAL REPORTS: Scientific and technical information considered important, complete, and a lasting contribution to existing knowledge.

TECHNICAL NOTES: Information less broad in scope but nevertheless of importance as a contribution to existing knowledge.

TECHNICAL MEMORANDUMS: Information receiving limited distribution because of preliminary data, security classification, or other reasons. Also includes conference proceedings with either limited or unlimited distribution.

CONTRACTOR REPORTS: Scientific and technical information generated under a NASA contract or grant and considered an important contribution to existing knowledge.

TECHNICAL TRANSLATIONS: Information published in a foreign language considered to merit NASA distribution in English.

SPECIAL PUBLICATIONS: Information derived from or of value to NASA activities. Publications include final reports of major projects, monographs, data compilations, handbooks, sourcebooks, and special bibliographies.

TECHNOLOGY UTILIZATION PUBLICATIONS: Information on technology used by NASA that may be of particular interest in commercial and other non-aerospace applications. Publications include Tech Briefs, Technology Utilization Reports and Technology Surveys.

Details on the availability of these publications may be obtained from:

SCIENTIFIC AND TECHNICAL INFORMATION OFFICE

NATIONAL AERONAUTICS AND SPACE ADMINISTRATION

Washington, D.C. 20546